

A new species of *Bathypathes* (Cnidaria, Anthozoa, Antipatharia, Schizopathidae) from the Red Sea and its phylogenetic position

Giovanni Chimienti^{1,2}, Tullia Isotta Terraneo³, Silvia Vicario⁴, Fabio Marchese³, Sam J. Purkis^{5,6}, Ameer Abdulla Eweida⁷, Mattie Rodrigue⁸, Francesca Benzoni³

1 Department of Biology, University of Bari Aldo Moro, Bari, Italy **2** CoNISMa, Rome, Italy **3** Red Sea Research Center, Division of Biological and Environmental Science and Engineering, King Abdullah University of Science and Technology, Thuwal, Saudi Arabia **4** University of Milano Bicocca, Milan, Italy **5** Center for Carbonate Research, Department of Marine Geosciences, Rosenstiel School of Marine and Atmospheric Science, University of Miami, Miami, FL 33149, USA **6** Khaled bin Sultan Living Oceans Foundation, Annapolis, U.S.A. **7** Neom, Saudi Arabia **8** OceanX, New York, USA

Corresponding author: Giovanni Chimienti (giovanni.chimienti@uniba.it)

Academic editor: James Reimer | Received 27 December 2021 | Accepted 11 June 2022 | Published 4 August 2022

<https://zoobank.org/5A9FB0AB-B37B-4569-A1F0-16DFB9AE3F7A>

Citation: Chimienti G, Terraneo TI, Vicario S, Marchese F, Purkis SJ, Abdulla Eweida A, Rodrigue M, Benzoni F (2022) A new species of *Bathypathes* (Cnidaria, Anthozoa, Antipatharia, Schizopathidae) from the Red Sea and its phylogenetic position. ZooKeys 1116: 1–22. <https://doi.org/10.3897/zookeys.1116.79846>

Abstract

A black coral, *Bathypathes thermophila* Chimienti, **sp. nov.** is described from the Saudi Arabian coasts of the Gulf of Aqaba and north Red Sea (Neom area) using an integrated taxonomic approach. The morphological distinctiveness of the new species is confirmed by molecular analyses. The species thrives in warm and high salinity waters typical of the Red Sea at bathyal depths. It can form colony aggregations on muddy bottoms with scattered, small hard substrates. Colonies are monopodial, feather-like, and attached to a hard substrate through a thorny basal plate. Pinnules are simple, arranged biserially and alternately, and all the same length (up to approximately 20 cm) except for few, proximal ones. Spines are triangular, laterally compressed, subequal, smooth, and simple or rarely bifurcated. Polyps are elongated transversely, 1.5–2.0 mm in transverse diameter. Large colonies can have one or few branches, whose origin is discussed. The phylogenetic position of *B. thermophila* sp. nov. within the order Antipatharia, recovered using three mitochondrial markers, shows that it is nested within the family Schizopathidae. It is close to species in the genera *Parantipathes*, *Lillipathes*, *Alternatipathes*, and *Umbellapathes* rather than to the other available representatives of the genus *Bathypathes*, as currently defined based on morphology. In agreement with previous findings, our results question the evolutionary significance of morphological characters traditionally used to discriminate Antipatharia at higher taxonomic level.

Keywords

Black corals, *cox1-cox3*, deep sea, *igrN*, *igrW*, Neom, Saudi Arabia

Introduction

Black corals (Cnidaria, Anthozoa, Antipatharia) are ubiquitous to the world's ocean, spanning cold deep to shallow tropical reefs. Traditionally, their description and classification rely on morphological traits, such as the corallum growth form, polyps shape and distribution, number of mesenteries, and size, shape and ornamentation of the skeletal spines (e.g., Opresko 2002; Brugler et al. 2013; Molodtsova and Opresko 2017; Opresko and Molodtsova 2021). With the advent of molecular analyses aiming at the study of phylogenetic relationships and taxa boundaries, several inconsistencies between the phylogenies and the current taxonomy of black corals were revealed. This has led to several Antipatharia families and genera currently recognised as polyphyletic (Brugler et al. 2013; Bo et al. 2018; Barret et al. 2020; Lü et al. 2021). For example, the intergenic spacer between *nad5*-IGR-*nad1* (*igrN*), which is the most variable region of the mitochondrial genome of black corals, in combination with *trnW*-IGR-*nad2* (*igrW*), and the spacer between *cox3* and *cox1* (*cox3-cox1*), have been used to clarify the phylogenetic position and describe new genera and species within the order Antipatharia (Thoma et al. 2009; Brugler et al. 2013; MacIsaac et al. 2013; Horowitz et al. 2020; Opresko and Molodtsova 2021). Moreover, the rRNA internal transcribed spacer region (comprising the 18S, ITS1, ITS2, and 5.8S) has been used in a growing number of publications to elucidate phylogenetic relationships within the families Antipathidae Ehrenberg, 1834, Aphanipathidae Opresko, 2004, and Schizopathidae Brook, 1889 (Lapian et al. 2007; Bo et al. 2018; Barret et al. 2020), as well as in population connectivity studies (Terrana et al. 2021). Finally, the use of next generation sequencing techniques, such as ultra-conserved elements, has recently proven useful in inferring relationships at species level in black corals (Horowitz et al. 2020).

Within the family Schizopathidae, the genus *Bathypathes* Brook, 1889 includes monopodial black corals and currently accounts for 14 valid species (Molodtsova and Opresko 2021; Molodtsova et al. 2022). It occurs in the Pacific, Indian, Atlantic, and Southern oceans, and has been recorded at depths ranging from 102 to 5393 m (Brook 1889; Opresko 2002; Opresko and Molodtsova, 2021; Molodtsova et al. 2022), although its shallowest record (Thomson 1905) is currently considered doubtful. In fact, those of the genus *Bathypathes* are mostly deep-sea species, with few representatives in the mesophotic zone. With deep-sea technologies allowing the exploration of these unseen depths, new *Bathypathes* species have been recently described and, similarly to all the deep-sea antipatharians known thus far, they live in cold waters.

The Red Sea rift is a young ocean basin (Purkis et al. 2012; Augustin et al. 2021) characterised by environmental conditions elsewhere considered extreme for most of the marine fauna. With sea surface temperatures exceeding 32 °C in the summer and deeper

water temperatures always higher than 21 °C (Manasrah et al. 2019), the Red Sea arguably provides some of the warmest natural conditions for marine fauna. The basin represents a distinct biogeographic province located at the periphery of the larger Indo-Pacific region, and it is characterised by strong environmental gradients and high endemism of marine organisms (Di Battista et al. 2016; Berumen et al. 2019). Among Red Sea anthozoans, black corals are poorly known except for few museum records (e.g., Brook 1889; Wagner et al. 2012) and spot information about their reproduction and associated fauna (Richmond and Hunter 1990; Herler 2007). The black coral fauna of the Saudi Arabia Red Sea is virtually unstudied from an integrated systematics point of view. This is particularly true in the scantily explored and rapidly developing Neom area, which includes the northern Red Sea Saudi Arabian coast and islands north of Duba, delimited by a narrow coastal strip rapidly descending down to more than 2000 m depth, and the Saudi coast of the Gulf of Aqaba, a 180 km long and 25 km wide semi-enclosed gulf with a NNE-SSW orientation, an average depth of 800 m and a maximum depth of 1852 m. The 2020 OceanX-Neom Red Sea Expedition allowed to explore and assess the marine resources in Neom territory with the ultimate goal to inform Saudi Arabia national conservation strategies. In this context, and with the overall objective to characterise for the first time the Red Sea black coral diversity, a reference collection of Antipatharia including all observed in situ macro-morphologies was obtained. During the benthic surveys, several colonies of monopodial, feather-like black corals were observed from 195 to 688 m depth. Later, morphological study of the sampled material led to their assignation to the genus *Bathypathes* Brook, 1889 (e.g., Brook 1889; Totton 1923; Opresko 2002; Opresko and Molodtsova (2021), thus representing the first record of this genus in the Red Sea.

This study reports the description of a new species of *Bathypathes* found at bathyal depths in the highly saline and warm waters of the Red Sea, representing the first record for the family Schizopathidae in the basin. In particular, *B. thermophila* sp. nov. from the Neom area is described based on traditional morphological characters, and its phylogenetic position within the order Antipatharia is inferred genetically using three mitochondrial loci and including available representatives of all the seven Antipatharia families. This study demonstrates that (a) *B. thermophila* sp. nov. is a new species of Schizopathidae commonly present in the bathyal zone of the Red Sea; (b) black coral diversity in the basin is still poorly known and species new to taxonomy are likely to occur; and (c) traditional morphological characters used to describe genera and species in the order might be subject to convergent evolution and the taxonomy of the order is in need of revision.

Materials and methods

Sampling and identification

A series of mesophotic and deep-sea explorations were carried out in the Neom area, on the Saudi Arabia coast of the Gulf of Aqaba and northern Red Sea (Fig. 1), from September to November 2020. Sampling occurred during the 2020 OceanX-Neom

Red Sea Expedition, aboard M/V “OceanXplorer”, using an Argus Mariner XL108 remotely operated vehicle (ROV) named “Chimaera”, and two Triton 3300/3 submersibles named “Neptune” and “Nadir”. The ROV equipment included a Kongsberg HiPaP 501 Ultra Short Base Line acoustic tracking systems, and a complex light-cameras apparatus with, among the others, one DSPL Super wide-angle CCD camera for landscape view and one HDTV 1080p F/Z colour camera for detailed observations. Each submersible was equipped with a Sonardyne Ranger Pro 2 system and several light and camera systems including a Wide Angle Red DSMC2 Helium 8k Canon CN-E15.5–47 mm lens and a macro Red DSMC2 Helium 8k Nikon ED 70–180mm F4.5–5.6D. Both ROV and submersibles were also equipped with a CTD probe (RBR Maestro CTD and Sea-Bird SBE 19+, respectively), two parallel-aligned scaling lasers providing 100-mm scale and a Schilling T4 hydraulic manipulator for sampling.

Images of living corals were taken in situ with the cameras mounted on the ROV and/or the submersibles. Five colonies were collected at four different localities (Fig. 1). The apical 10-cm portion of the colonies was preserved in 99% ethanol, while the rest of the corallum was air-dried in the shadow for 24 hours. For each collected specimens, macro- and micro-morphological characters were examined and photographed using a Leica M205 A stereomicroscope equipped with a Leica DMC 5004 camera in the Red Sea Research Center laboratory at King Abdullah University of Science and Technology (**KAUST**). Fragments of stem and pinnules were taken from different parts of the dry samples, hydrated in distilled water, cleaned with gentle rinses in diluted sodium hypochlorite (NaClO), then washed with distilled water and dehydrated in a graded ethanol series (Chimienti et al. 2020). Dehydrated skeletal elements were mounted on stubs, coated with a 5-nm thick layer of iridium using a Quorum Q150T S turbomolecular pumped coater, and imaged using a Thermo Fisher Scientific Quattro S Environmental SEM at KAUST Imaging Core Lab.

Type material is deposited at the National Museum of Natural History (**MNHN**), Paris, France. The paratypes are currently kept at KAUST, Thuwal, Saudi Arabia, and at the Zoological Museum of the University of Bari Aldo Moro (**MUZAC**), Bari, Italy.

DNA extraction, amplification, and sequence analyses

Total genomic DNA was extracted using the DNeasy Blood and Tissue Kit (Qiagen Inc., Hilden, Germany) following the manufacturer’s protocol. DNA quality and quantity was assessed using a NanoDrop 2000 C spectrophotometer (Thermo Fisher Scientific, Wilmington, USA), and polymerase chain reaction (PCR) was used to amplify three genetic markers. In particular, the mitochondrial *igrN* was amplified with the ND5-5’anti10725F-ND1anti11217R primers and the *igrW* with TRPntiF-ND2anti1040R, following Thoma et al. (2009). The primers CO3gen3360F-CO1gen4600R were used for the *cox3-cox1* region following Thoma et al. (2009) and Brugler et al. (2013). All PCRs were carried out in 15 µl reactions using 1X Multiplex PCR Master Mix (Qiagen Inc., Hilden, Germany), purified using Illustra ExoStar (GE Healthcare, Buckinghamshire, UK), and sequenced in forward and reverse direction using an ABI 3730xl

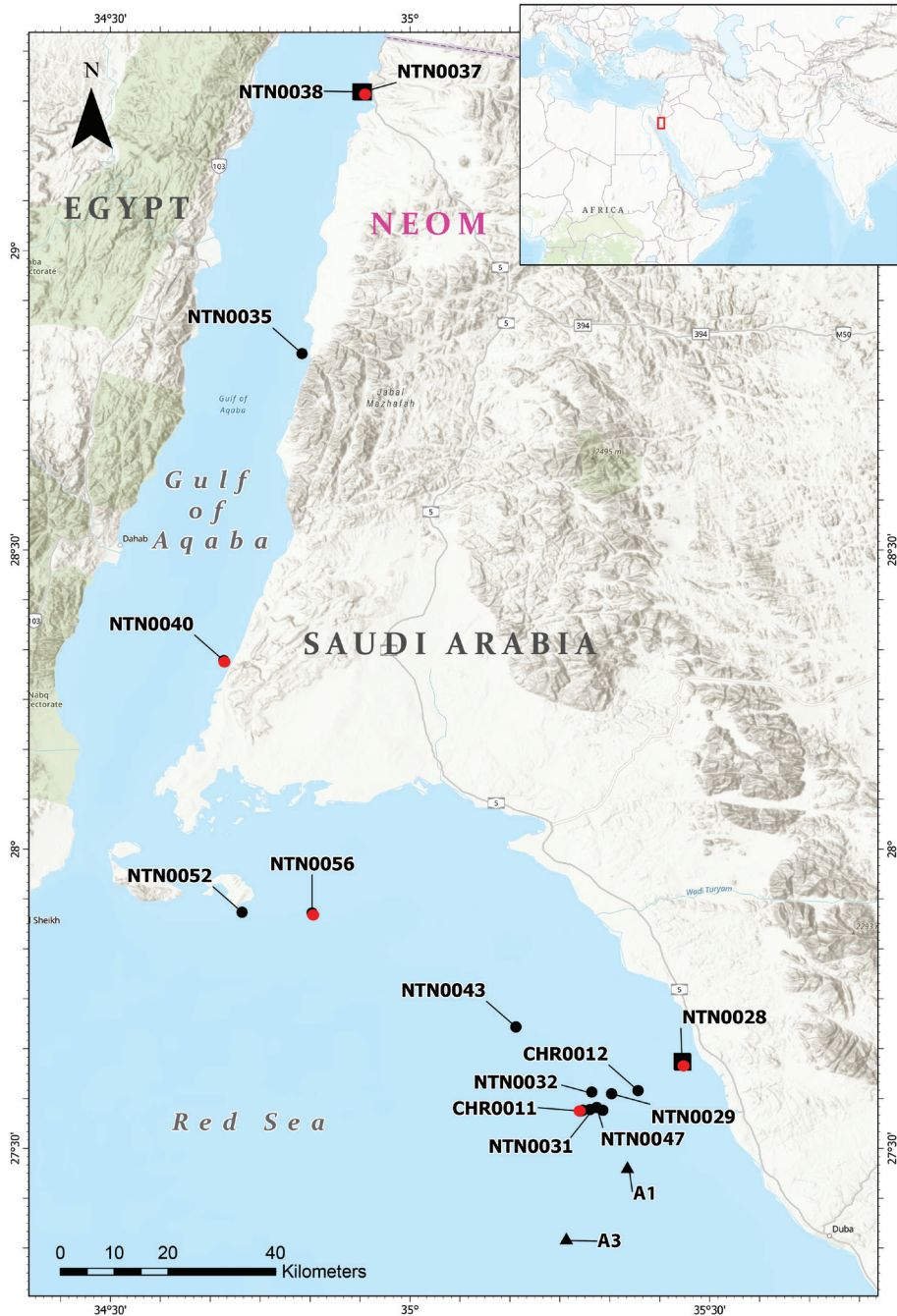


Figure 1. Map of the study area showing the known occurrences of *Bathypathes thermophila* sp. nov. Black dots: observed colonies during the 2020 OceanX-Neom Red Sea Expedition; red dots: sampled colonies; triangles: photographic record by Qurban et al. (2014). Black squares indicate the occurrence of an aggregation of colonies. Codes indicate the submersible (NTN) or remotely operated vehicle (CHR) dives. Coordinates and depth ranges for each dive are reported in Suppl. material 1.

DNA Analyzer (Applied Biosystems, Carlsbad, USA) at KAUST Bioscience Core Lab. Chromatograms of the obtained strands were assembled and edited using Sequencher 5.3 (Gene Codes Corp., Ann Arbor, USA). The sequences generated from this study were deposited in GenBank, and accession codes are available in Suppl. material 2.

Sequences of the genus *Leiopathes* Haime, 1849, representative of Leiopathidae Haeckel, 1896, were downloaded from GenBank and used as outgroup in all phylogenetic reconstructions because of its confirmed sister position to the other families of antipatharians (Barret et al. 2020). Newly produced sequences from this study, as well as 157 sequences (*igrN*), 130 sequences of *igrW*, and 67 sequences of *cox3-cox1* retrieved from GenBank, were aligned using MAFFT 7.130b (Katoh and Standley 2013) with the E-INS-i method. The best substitution model for each marker was calculated using PartitionFinder 2 (Lanfear et al. 2017). A Maximum likelihood (ML) phylogenetic reconstruction was performed using RAxML 2 (Stamatakis 2014) on the online CIPRES server (Miller et al. 2012). The ML analyses were run with multiparametric bootstrap analyses of 1000 bootstrap replicates.

Results

Taxonomy

Order Antipatharia

Family Schizopathidae Brook, 1889

Genus *Bathypathes* Brook, 1889

Bathypathes thermophila Chimienti, sp. nov.

<https://zoobank.org/6D09BCE9-D0B6-4DA0-922A-2324A29380B3>

Figs 2–5

Material examined. *Holotype*: MNHN-IK-2016-45 (Fig. 2), Red Sea, Duba Channel, 27.643801°N, 35.455505°E, 303 m, 9 Oct 2020, *Neptune* submersible (collection code NTN0028-6). *Paratypes*: KAUST-NTN0037-8, Red Sea, off Haql (Gulf of Aqaba), 29.264796°N, 34.920449°E, 278 m, 21 Oct 2020, *Neptune* submersible (collection code NTN0037-8); MUZAC-6665, Red Sea, South of Magna (Gulf of Aqaba), 28.31497°N, 34.68936°E, 323 m, 25 Oct 2020, *Neptune* submersible (collection code NTN0040-2); MUZAC-6666, Red Sea, South Sila Island, 27.562322°N, 35.283313°E, 629 m, 12 Oct 2020, *Chimaera* ROV (collection code CHR0011-2); KAUST-NTN0056-3, Red Sea, off Shusha Island, 27.8933°N, 34.83665°E, 597 m, 7 Nov 2020, *Neptune* submersible (collection code NTN0056-3).

Diagnosis. Colony attached though a basal disk, monopodial, generally unbranched or with a few, random branches, and pinnulate (Figs 2a, b, 3a–e). Stem cylindrical (Fig. 2c), regularly decreasing in diameter from the base to the top. Lower unpinnulated section of the stem (stalk) much shorter than upper pinnulated section.

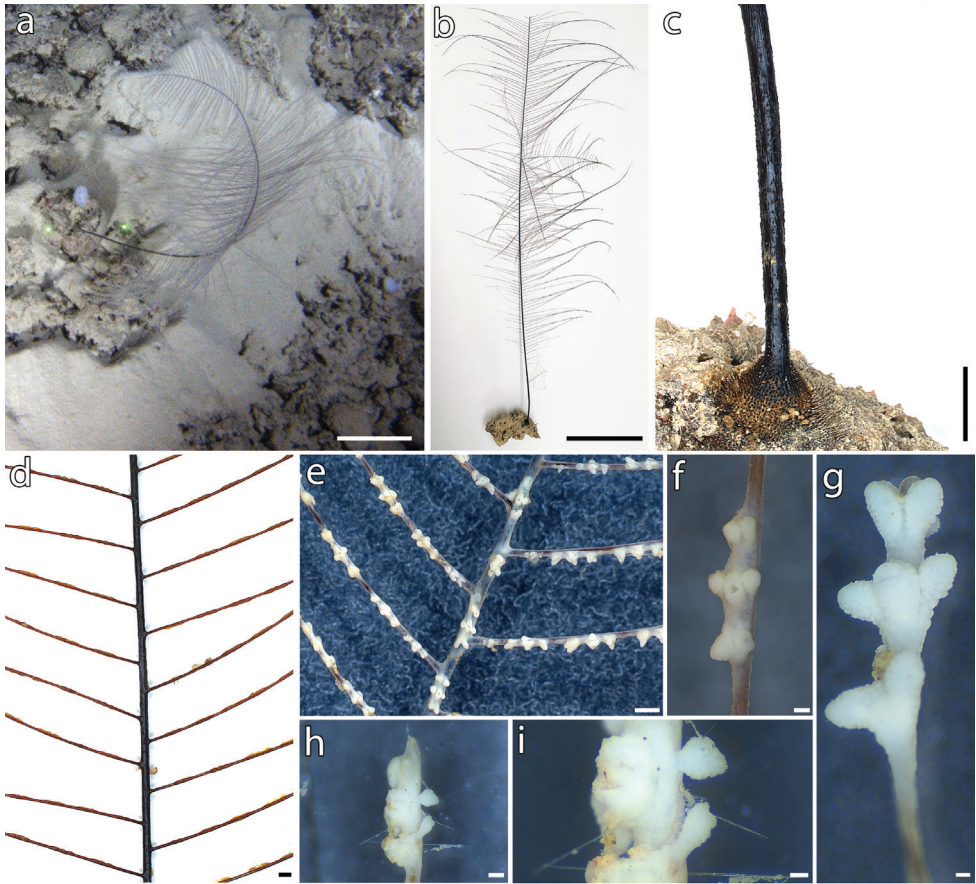


Figure 2. *Bathypathes thermophila* sp. nov., holotype (MNHN-IK-2016-45) **a** colony in situ **b** dry colony **c** base and stem **d** alternate arrangement of pinnules **e** polyps on both stem and pinnules, with **f** detail of a polyp **g** pinnular terminal polyp **h, i** apical polyp of the colony. Scale bars: 10 cm (**a, b**); 5 cm (**c**); 1 mm (**d, e**); 200 μ m (**f, h**); 100 μ m (**g, i**).

Pinnules simple, up to 20 cm long and subequal in length over most of the corallum, except for proximal and distal ones that are shorter. Pinnules arranged alternately in two lateral rows along the stem (Fig. 2d), although one or few couples of pinnules can be occasionally present on the same side (Fig. 3f). Pinnules inclined of 30° in frontal view (Fig. 2d) and oriented slightly forward in the polypar side with respect to the stem. Pinnular basal diameter 0.18–0.40 mm (0.11 in young colonies). Spacing of pinnules on the same side 2.8–4.3 mm (Fig. 2d), with a pinnular density of 12–18 per 3 cm (up to 20 in young colonies), including pinnules on both sides.

Spines on the pinnules smooth, laterally compressed, triangular, acute, simple or rarely bifurcated, 0.015–0.025 mm tall (occasionally down to 0.008 mm or up to 0.028 mm), with polypar spines almost the same size of abpolypar ones or slightly larger. Four or five rows of spines in lateral view, each row bearing from one to three

spines (Fig. 4d–i), with a density of 5–8 spines per mm (considering double or triple spines as one). Rows can be less obvious on some pinnules.

Spines on the stem smooth, laterally compressed, triangular in profile, acute, simple and enlarged at the base, 0.020–0.030 mm tall. Spines uniformly distributed around the stem, arranged in 10–14 longitudinal rows, each one bearing one to three parallel spines (Fig. 4a–c). Spines often random on the proximal stem and near the basal disk. Basal disk with numerous, elongated spines up to 1.2 mm tall.

Polyps present on one side on both pinnules and stem (Fig. 2e), elongated along the transverse axis, 1.5–2.5 mm in transverse diameter (rarely smaller or larger) and 0.5 mm large (Fig. 2f–i). Polyps sharply divided into three regions, with pairs of tentacles 0.5 mm long (contracted polyps) and 0.2–0.3 mm apart, and prominent oral cones. Polyps distance ranging from 0.5 to 2.5 mm, generally 1 mm, with a density of 10–15 polyps per 3 cm.

Description of the holotype. The holotype (MNHN-IK-2016-45) is a complete colony with an intact basal disk and apex. The colony is attached to the subfossil remains of an irregular echinoid encrusted by various small invertebrates. The colony is 74.5 cm long with a stem basal diameter of 1.8 mm. The unpinnulated stalk is 4 cm long. The basal disk is 7 mm in diameter with numerous, erect and acute spines, up to 0.9 mm tall, all over its surface. The pinnules are simple, bilateral and arranged alternately. Although pinnules are quite flexible, some of them are broken off. The longest remaining ones are ~ 20 cm in length with a basal diameter of ~ 0.28–0.40 mm. The number of pinnules on the corallum is 186 on one side and 181 on the other. Some pinnules are missing at the base of the corallum, likely broken and lost during collection with the sampling manipulator. Within each row, the pinnules are spaced 2.8–3.5 mm apart on the apical portion of the corallum, 3.2–3.7 mm on the middle area and 3.4–4.0 mm on the basal one. The resulting pinnular density is 14 per 3 cm (total for both rows) on the proximal portion of the stem to ~ 16–18 per 3 cm in the median and towards the distal end. The central axial canal is 0.31 mm wide on a pinnule 0.42 mm in diameter, and 0.10 mm on a pinnule 0.22 mm in diameter.

The stem is characterised by six or seven rows of spines in lateral view, although in some areas their distribution can be irregular. A single, 4-cm branch is present in the proximal area of the corallum, and a dichotomous ramification is present in the median area (Fig. 3c, d).

Pinnular spines are small, from 0.017 to 0.022 mm tall, and 0.20–0.31 mm apart. Spines can be double or triple, particularly in the proximal portion of pinnules. Bifurcated spines are also present, although not common.

The polyps are 1.5–2.0 mm in transverse diameter, rarely smaller than 1.5 mm. Polyps density is 11–15 polyps per 3 cm on the stem and 11–13 polyps per 3 cm on the pinnules.

Description of the paratypes. The general morphology of the four paratypes analysed is similar to that of the holotype, with a monopodial corallum and pinnules simple, bilateral and arranged alternately. All paratypes have elongated polyps occurring in a single series on one side of the pinnules and of the stem.

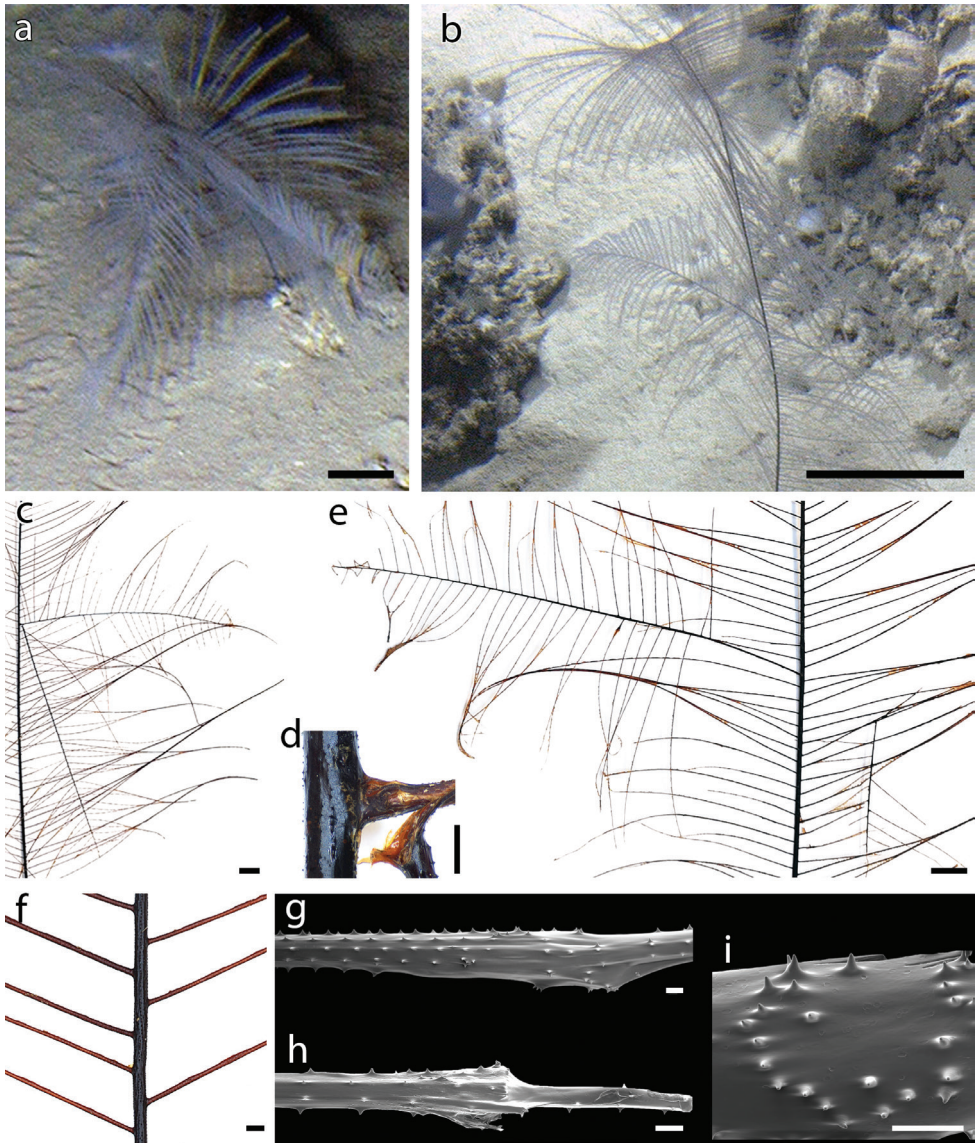


Figure 3. Branching and damages in *Bathypathes thermophila* sp. nov. **a** example of a colony in situ with different branches. Holotype (MNHN-IK-2016-45) **b** ramification observed in situ **c** ramification at the middle of the colony with **d** detail of the ramification. Paratype MUZAC-6665 **e** primary branch (on the left) and secondary branch (on the right) **f** example of two pinnules present on the same side of the stem with respect to the alternate pattern **g** cicatricial nodule on a pinnule **h** narrowing of the pinnular section possibly due to an injury and a subsequent recovery **i** spines arranged irregularly over a skeletal scar. Scale bars: 10 cm (**a, b**); 1 cm (**c, e**); 1 mm (**d, f**); 100 μ m (**g–i**).

Paratype KAUST-NTN0037-8 is a complete colony of 27 cm in length (Fig. 5a, b), with a stem basal diameter of 1 mm. The unpinnulated stalk is 2.8 cm long, while the basal disk is 4 mm in diameter with tall spines, up to 1 mm, erect or curved up-

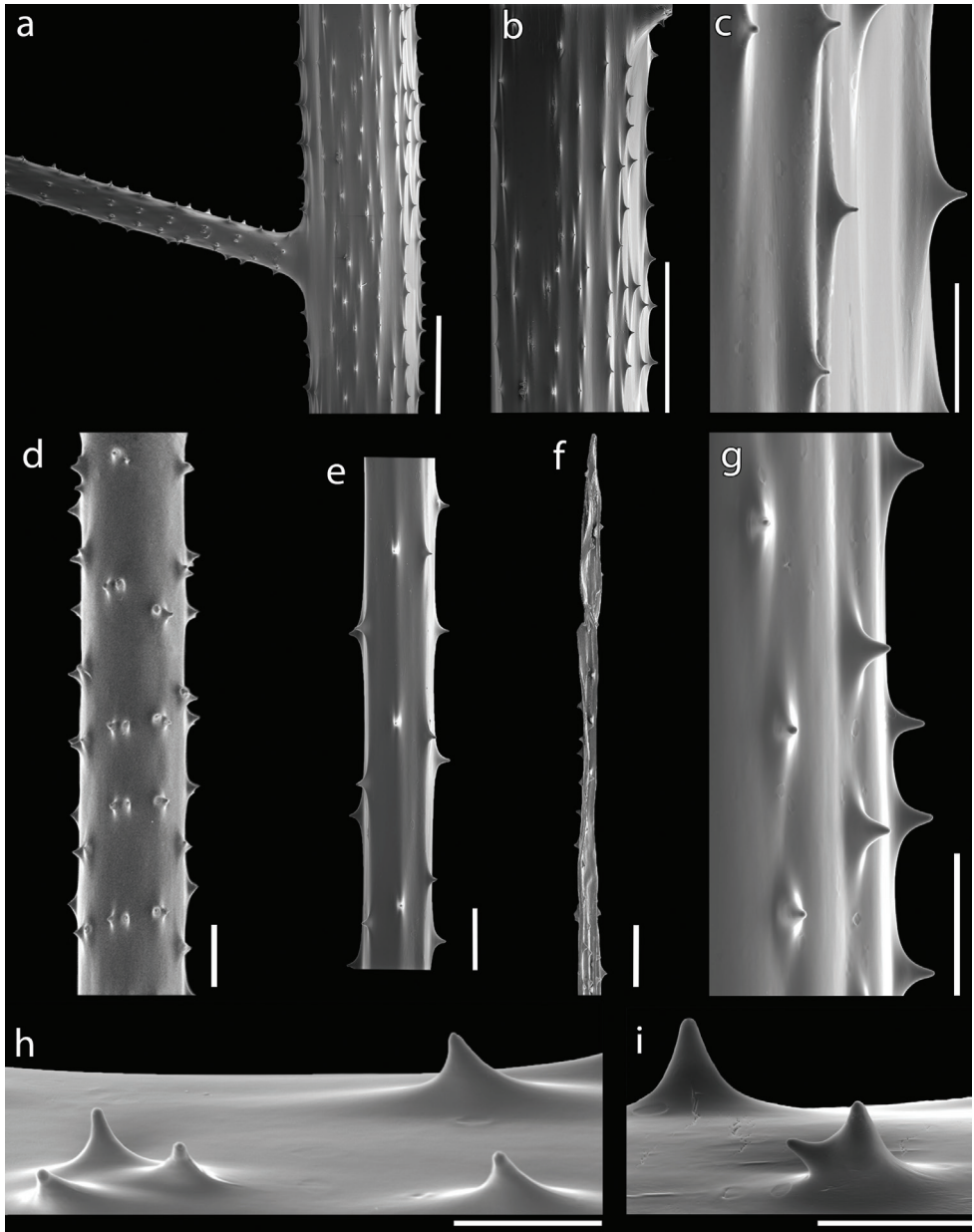


Figure 4. Scanning Electron Microscope of the spines of *Bathypathes thermophila* sp. nov., MNHN-IK-2016-45 (**a–f, h**), MUZAC-6665 (**g, i**) **a** stem and pinnule form the middle portion of the corallum **b** stem from the upper part of the corallum with **c** detail of the spines. Pinnule from the middle portion of the corallum with details of **d** proximal portion **e** distal portion, and **f** terminal portion **g** polypar spines on pinnule **h** row with three polypar spines on a distal pinnule **i** bifurcated polypar spine on pinnule. The right side of vertical skeletal elements and the upper side of horizontal ones is the polypar side. Scale bars: 500 μm (**a, b**); 100 μm (**c–g**); 50 μm (**h, i**).

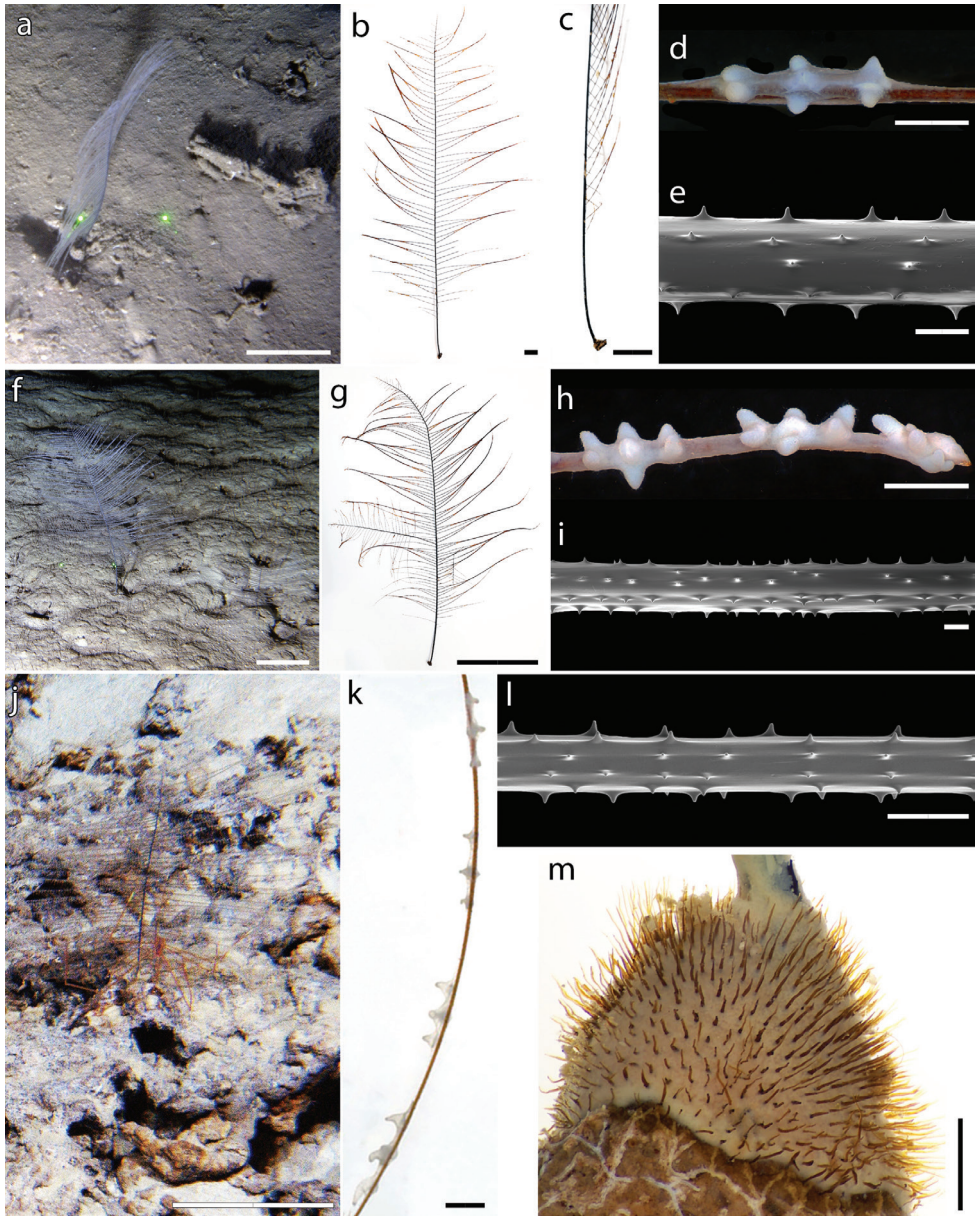


Figure 5. Paratypes of *Bathypathes thermophila* sp. nov. KAUST-NTN0037-8 **a** colony in situ, on a muddy bottom with scattered biogenic hard substrate **b** dry colony in frontal view (polypar side) and in **c** lateral view **d** polyp **e** spines on a proximal pinnule. MUZAC-6665 **f** colony in situ on muddy bottom **g** dry colony in frontal view **h** distal polyps **i** proximal spines on a pinnule from the lower part of the corallum. MUZAC-6666 **j** colony in situ on a hard ground, with a spider crab as epibiont **k** polyps on pinnule **l** spines arrangement on pinnule form the upper part of the corallum **m** base of the colony. Upper side of horizontal skeletal elements is the polypar side. Scale bars: 10 cm (**a**, **f**, **j**); 1 cm (**b**, **c**); 1 mm (**d**, **h**, **k**, **m**); 100 μ m (**e**, **i**, **l**).

wards. The pinnules are up to 9 cm long with a basal diameter of 0.25–0.35 mm and a pinnular density of 14–16 per 3 cm (Fig. 5c). Distance between adjacent pinnules on one side of the stem is 3.3–4.2 mm, except for one couple of pinnules in the median part of the colony that is not alternately arranged. The stem is characterised by six rows of spines in lateral view, although in some areas their distribution is more irregular. Rows are uniformly distributed around the stem, and host spines 0.020–0.028 mm tall. Spines on the pinnules are 0.018–0.022 mm tall, and 0.13–0.20 mm apart (Fig. 5e). Each pinnule bears 4–5 rows of spines in lateral view. Polyps are generally 1.9–2.5 mm in transverse diameter (Fig. 5d), rarely up to 3.0 mm, while young ones can be only 1.3 mm. They are mostly 1 mm apart, although distance can range between 0.8 and 2.3 mm. Density of 10 polyps per 3 cm.

Paratype MUZAC-6665 is a complete colony of 45 cm in length (Fig. 5f, g), with a stem basal diameter of 1.6 mm. The unpinnulated stalk is 3 cm long, while the basal disk is 6.2 mm in diameter with spines up to 1.2 mm tall, erect or curved upwards. Pinnules up to 16 cm long with a basal diameter of 0.30–0.40 mm and a pinnular density of 12–15 per 3 cm. One couple of pinnules at the median and two at the distal part of the stem interrupt the alternate arrangement, being on the same side. A single, primary branch is present on one side of the colony and a single, secondary one on the other side (Fig. 3e). Pinnular spines 0.021–0.028 mm tall, 0.12–0.30 mm apart, and arranged in 4–5 rows in lateral view (Fig. 5i). Spines on the stem arranged in 6–7 rows per side and 0.020–0.030 mm tall. Polyps 2.0–2.5 mm in transverse diameter (occasionally up to 3.0 mm or down to 1.3 mm), with a density of 10–12 polyps per 3 cm (Fig. 5h).

Paratype MUZAC-6666 is a complete colony of 14 cm in length (Fig. 5j), with a stem basal diameter of 0.6 mm. The unpinnulated stalk is 1.6 cm long, while the basal disk is 4 mm in diameter with spines up to 0.8 mm tall (Fig. 5m). The pinnules are up to 7 cm long with a basal diameter of 0.11 mm and a pinnular density of 18–20 per 3 cm. The pinnules are characterised by four or five rows of spines in lateral view, with spines 0.012–0.016 mm tall and 0.10–0.22 mm apart (Fig. 5l). Polyps are 1.5–2.0 mm in transverse diameter, 1.5–2.0 mm apart, with a density of 9–10 polyps per 3 cm (Fig. 5k).

Paratype KAUST-NTN0056-3 is a complete colony 26 cm long, with a stem basal diameter of 0.9 mm. The unpinnulated stalk is 3.0 cm long, while the basal disk is 2.7 mm in diameter with tall spines, erect or curved upwards, up to 0.9 mm tall. Pinnules up to 11 cm long with a basal diameter of 0.18–0.26 mm and a pinnular density of 14–17 per 3 cm. Pinnules are alternate, with adjacent ones spaced 3.2–4.3 mm, except for one, single pair of pinnules present on the same side of the stem, in the median part of the colony. The central axial canal is 0.07 mm in diameter on a pinnule 0.12 mm in diameter. Pinnules with four rows of spines in lateral view, mostly 0.008–0.012 mm tall (some up to 0.018 mm) and 0.10–0.18 mm apart. Stem bearing five rows of spines in lateral view, 0.016–0.020 mm tall. The colony was found dead, without polyps.

Etymology. The species name is derived from the Greek words *thermos* (hot) and *philia* (love, preference for), referring to the occurrence of this species in the rather warm Red Sea waters, especially compared to the water temperatures usually measured in other bodies of water within the same depth range.

Distribution. A colony matching the macro-morphology of *B. thermophila* sp. nov. is shown in Qurban et al. (2014: fig. 3F), where it is reported as an “unidentified sea fan”. It is reported from two areas off Duba (Fig. 1), at 360–720 m depth, extending the known distribution further south from our sampling area. To date, *B. thermophila* sp. nov. is only known from the Gulf of Aqaba and northern Red Sea (Fig. 1), from 195 to 720 m depth.

Habitat and ecology. *Bathypathes thermophila* sp. nov. seems to grow preferentially on scattered hard substrates (e.g., rocks, fresh, fossil or subfossil shells, coral rubble, and subfossil sea urchin tests) surrounded by mud, although it can occur also on rocky bottoms. The holotype (MNHN-IK-2016-45) had settled on a subfossil test of an irregular echinoid, recovered on a sloping rocky substrate covered in a thin muddy layer. The paratypes occurred on muddy bottom with scattered biogenic small substrates (KAUST-NTN0037-8, MUZAC-6665) and on hardground surrounded by mud (MUZAC-6666, KAUST-NTN0056-3).

Water temperature on the seabed was 22 °C, as also reported off Duba by Qurban et al. (2014: fig. 6), indicating that *B. thermophila* sp. nov. lives in relatively warm waters. The species is quite common in the bathyal zone of the Red Sea, where a total of 335 colonies were observed within this study (Suppl. material 1, 2). Aggregations of up to two colonies m⁻² were found at 280–300 m depth in two different areas (Fig. 1, Suppl. material 1), where *B. thermophila* sp. nov. was the only erect organism (Fig. 6a–d). There, it enhances the benthic structural complexity on flat or gently sloping seabed covered by a mud veneer. *B. thermophila* sp. nov. is often used as habitat by crinoids, spider crabs, and other epibionts (Fig. 6c–e).

Comparisons. Within the genus *Bathypathes*, *B. platycaulus* Totton, 1923 and *B. pseudoalternata* Molodtsova, Opresko and Wagner 2022 show alternate subpinnules. The former is characterised by a peculiar broadening of the stem in the middle region, to which the species name refers (Totton 1923), while *B. thermophila* sp. nov. has a cylindrical stem all along the corallum which lacks a flattened region. *Bathypathes thermophila* sp. nov. also differs from *B. platycaulus* in the pinnular rows of spines (four or five per side homogeneously distributed vs. six or seven on one side and four on the other) and in the size of the spines (0.015–0.025 mm vs. 0.040 mm). Finally, the basal diameter of the stem of *B. platycaulus* increases in width in the first 7 cm (from 1.5 mm to 1.75 mm) after which it tapers away gradually up to ~ 0.28 mm at the apex (Totton 1923), being somehow flattered. Conversely, the stem diameter of *B. thermophila* sp. nov. decreases slightly and constantly from the base to the apex.

Bathypathes thermophila sp. nov. differs from *B. pseudoalternata* in having a colony which can bear one or a few branches (vs unbranched), higher pinnular density (12–20 vs. 6–12 pinnules per 3 cm), shorter pinnular spines (0.008–0.028 vs 0.030–0.080 mm) with higher density (5–8 vs. 4–5 spines per mm), smaller polyps (1.5–2.5 vs. 3–5 mm in transverse diameter), and higher density of polyps (10–15 vs. 6–7.5 polyps per 3 cm).

Remarks. Large colonies, approximately higher than 40 cm, can show one or few ramifications (Fig. 3a–e). Despite Opresko and Molodtsova (2021) suggesting that monopodial colonies of *Bathypathes* can have one ramification due to damaging events, skeletal analysis in proximity of the branching in *B. thermophila* sp. nov. colonies did

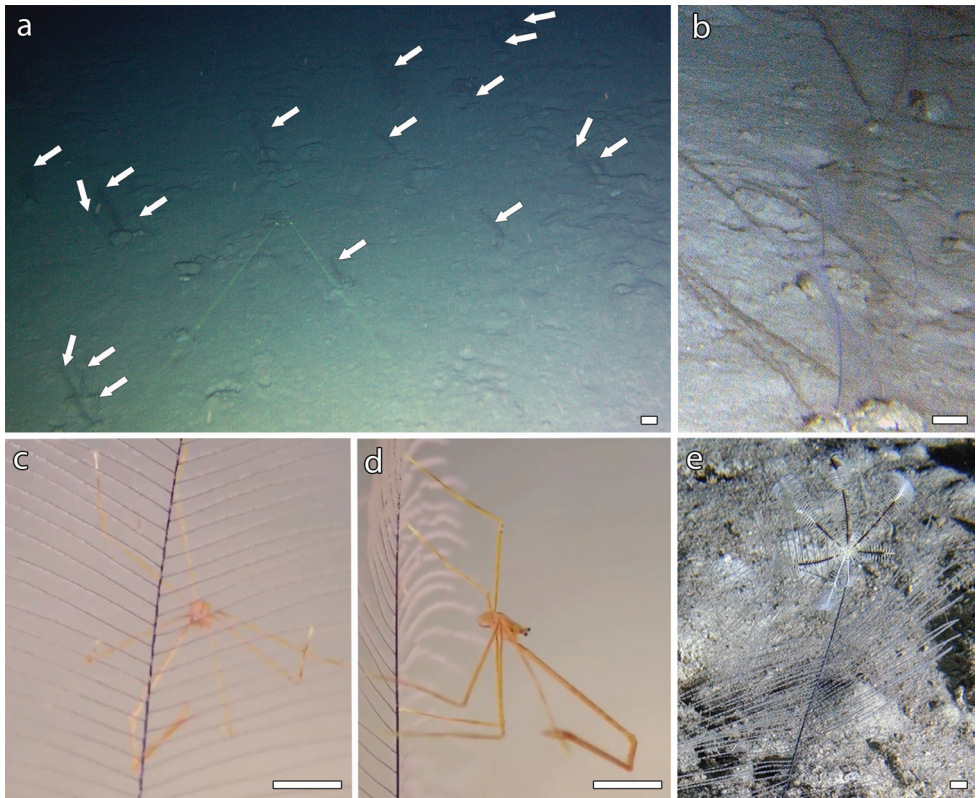


Figure 6. Distribution and associations of *Bathypathes thermophila* sp. nov. **a** aggregations of colonies (white arrows) **b** detail of four co-occurring colonies. Epibionts **c, d** unidentified spider crabs **e** unidentified crinoid. Scale bars: 10 cm (**a, b**); 1 cm (**c–e**).

not reveal signs of past issues, suggesting that occasional branching can be due to the division of a primary polyp. On the contrary, signs of recovery after mechanical damage were observed on the skeletal of *B. thermophila* sp. nov. without the occurrence of ramifications. These signs were evident mostly as a skeletal swelling (Fig. 3g), a chaotic pattern of spines (Fig. 3i), or a drastic narrowing of the pinnular section (Fig. 3h).

Molecular results

A total of four sequences were obtained and analysed for the mitochondrial *igrN* and *igrW*, and *cox3-cox1* region. The final *igrN* alignment consisted of 612 bp, with 60 polymorphic sites, 56 parsimony informative sites, and 72 mutations. The *igrW* alignment consisted of 623 bp, with 93 polymorphic and 69 parsimony-informative sites, and 114 mutations, while the alignment of the *cox3-cox1* was 820 bp long (199 polymorphic and 174 parsimony informative sites, and a total of 250 mutations).

The *igrN* and *igrW* ML topologies are shown in Fig. 7a, b, with ML bootstrap support, while the *cox3-cox1* reconstruction is included in Suppl. material 3.

Bathypathes thermophila sp. nov. is monophyletic, genetically distinct, and molecularly closely related to the available representatives of the genera *Parantipathes* Brook, 1889, *Lillipathes* Opresko, 2002, *Dendropathes* Opresko, 2005, *Saropathes* Opresko, 2002, *Alternatipathes* Molodtsova & Opresko, 2017, and *Umbellapathes* Opresko, 2005 (*igrN*, *igrW*, *cox3-cox1*), all retrieved in the same clade comprising also one sequence of *Schizopathes* Brook, 1889 (*igrN*, *igrW*) and one of *Sibopathes* van Pesch, 1914 (*igrN*, *igrW*). However, the representatives of *Bathypathes* available in the literature and included in our analyses cluster into a separate clade not closely related to the *B. thermophila* sp. nov. clade. Rather, they are closer to representatives of the genera *Stauropathes* Opresko, 2002 and *Telopathes* MacIsaac & Best, 2013 (Fig. 7a, b; Suppl. material 3).

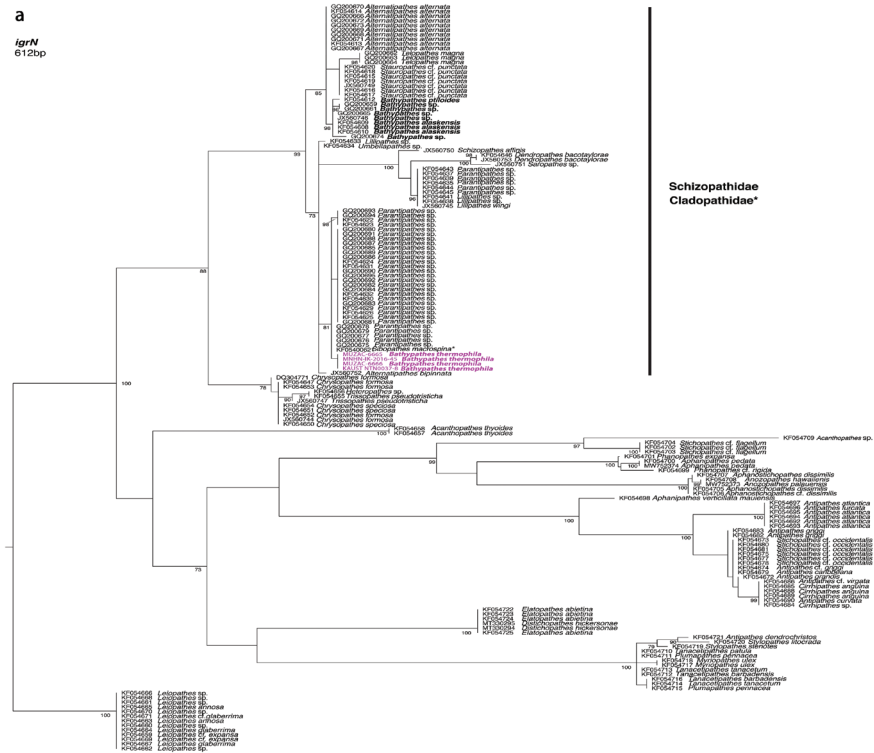
Discussion

Within the Family Schizopathidae, species with a monopodial, unbranched corallum are ascribed to the genera *Bathypathes*, *Schizopathes*, *Abyssopathes* Opresko, 2002, *Saropathes*, *Alternatipathes*, and *Parantipathes*. Our specimens lack the triangular-shaped pinnulated section typical of *Alternatipathes* and *Schizopathes*, the latter also characterised by unattached colonies with a hook-like holdfast for support (Opresko 2002; Molodtsova and Opresko 2017). Moreover, our specimens have only two rows of primary pinnules, simple and lateral, unlike the genera *Abyssopathes* (three rows of pinnules: two lateral and one or more anterior), *Saropathes* (primary pinnules in four rows, with subpinnules) and *Parantipathes* (six or more rows of pinnules) (Opresko 2002).

Based on morphological characters considered diagnostic in black coral taxonomy, we assigned the examined material to the genus *Bathypathes* and described it as a new species. From a molecular point of view, data from three loci, consistently and concordantly placed *B. thermophila* sp. nov. in a clade closely related to the genus *Parantipathes* rather than with the other available sequences of *Bathypathes*. This is relatively unsurprising as previous works already highlighted that the genus *Bathypathes*, as currently defined based on morphological characters, is polyphyletic. For example, rDNA phylogenetic reconstructions showed that *Bathypathes*, comprising representatives of the type species, *B. patula*, clusters with *Stauropathes* (Bo et al. 2018; Lü et al. 2021), and one nuclear sequence of *Bathypathes* sp. (MG023167-YPM IZ 028566) is close to the genus *Telopathes* (Bo et al. 2018; Lü et al. 2021). Given that *Bathypathes*, *Stauropathes* and *Telopathes* also share some morphological similarities, the morphological characters used to distinguish *Bathypathes* from other genera seem to lack evolutionary meaning (Barret et al. 2020) and further analyses are likely to reveal that *B. thermophila* sp. nov. falls within a different genus. Previous phylogenetic reconstructions based on the same mitochondrial regions have included representatives of *B. patula* (e.g., Brugler et al. 2013; Bilewitch and Tracey 2020). However, some of these samples were recently used by Opresko and Molodtsova (2021) to describe a new species within the genus, *B. alaskensis*, while the sequences from others have never been made available online for comparison. While acknowledging the disagreement between morphological and

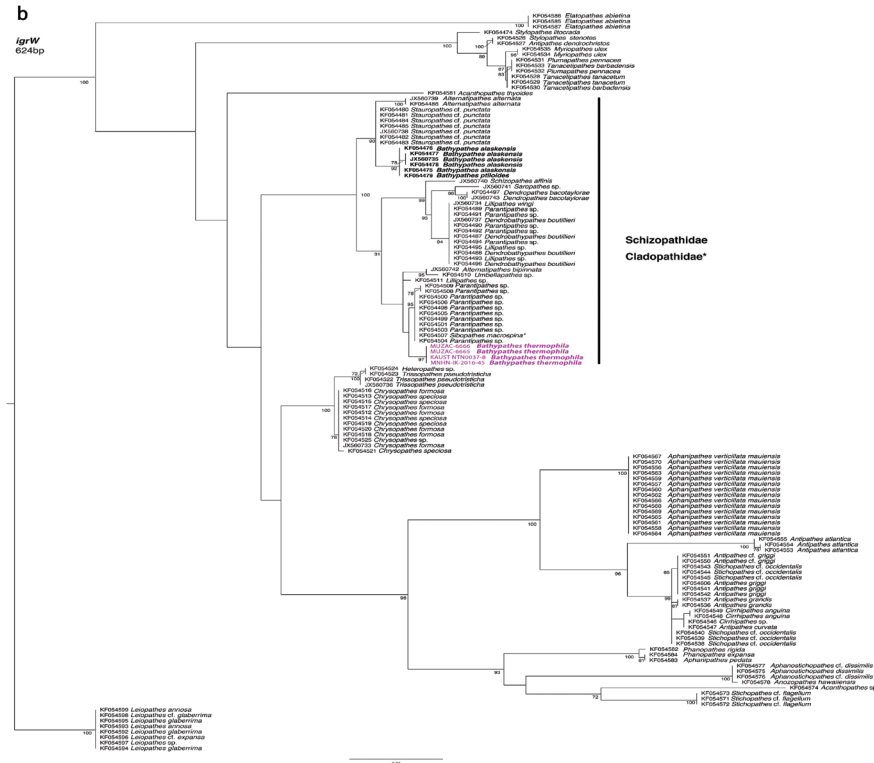
a

igrN
612bp



b

igrW
604bp



genetic assignation of the newly described species, in absence of available sequences of the genus *Bathypathes* type species, we decided to adopt a conservative approach and describe *B. thermophila* as a new species within the genus based on traditional morphological characters, still widely used in Antipatharia descriptions.

The overall ML analyses based on the three loci were mostly concordant and recovered a consistent reconstruction of the phylogenetic relationships within the order Antipatharia, in agreement with previously published molecular findings. The three mitochondrial phylogenetic reconstructions obtained consistently placed *B. thermophila* sp. nov. within a distinct molecular lineage including the sequences of all available representatives of the family Schizopathidae and one representative of the family Cladopathidae Kinoshita, 1910 (*Sibopathes macrospina* Opresko, 1993), with the exception of *cox3-cox1* reconstruction, where no sequences of *Sibopathes* were available (Fig. 7a, b, Suppl. material 3). The inclusion of *S. macrospina* within this molecular lineage is consistent with previous results, since the family Schizopathidae is currently considered polyphyletic only due to the position of *S. macrospina* with the genus *Parantipathes* (Brugler et al. 2013). Other representative genera of the family Cladopathidae (*Trissopathes* Opresko, 2003, *Chrysopathes* Opresko, 2003, *Cladopathes* Brook, 1889, *Heteropathes* Opresko, 2011) are nested in a separate clade. Opresko (1993) already discussed the similarity of skeletal characters between the genera *Parantipathes* and *Sibopathes*, and Brugler et al. (2013) suggested that the morphological characters used to discriminate the latter could be derived. Barret et al. (2020) reconstructed the phylogenetic relationships of black corals on the base of complete mitochondrial genomes, and recovered a concordant topology, with the placement of *S. macrospina* within the Schizopathidae.

Antipatharians are currently largely understudied in the Red Sea, particularly in the mesophotic and aphotic zones. Due to the unique environmental features of this body of water, and its geographic position at the periphery of the greater Indo-Pacific region, a detailed study of Red Sea black corals can greatly contribute to our understanding of the evolution, phylogenetic relationships and biogeography of the whole group, ultimately pushing towards its pending taxonomic revision. Moreover, a reassessment of the morphological characters so far considered informative and diagnostic for black corals taxonomy is needed. In this respect, our molecular reconstructions and their comparison with the observed morphological features represent a first step in this direction and provide a baseline for future works. Future studies of Red Sea black corals will ultimately need to integrate nuclear and Next Generation Sequencing data. Indeed, molecular taxonomy is highlighting similar patterns at different taxonomic levels within the entire order Antipatharia and suggests that a molecular revolution similar to the one which has taken place in the last 20 years for other metazoans in general, and cnidarians in particular, is timely.

Figure 7. RAxML phylogenetic reconstruction of Antipatharia and the position of *Bathypathes thermophila* sp. nov. (in purple) inferred from two molecular loci **a** the mitochondrial intergenic spacer between *nad5-igr-nad1* and **b** the mitochondrial intergenic spacer between *trnW-igr-nad2*. Node values are maximum likelihood bootstrap values (> 70%). The genus *Leiopathes* was selected as outgroup. Sequences highlighted by (*) are representatives of the family Cladopathidae.

Conclusions

Bathypathes thermophila sp. nov. is described for the Neom region in the north Saudi Arabian Red Sea and represents the first black coral species described from the basin, the first record for the family Schizopathidae, as well as the only member of this family known thus far to live in relatively warm waters at certain depths. Considering the unique ecological and geological features of the Red Sea rift and the peculiar coral fauna that has adapted to live there, it is hardly surprising that the first systematic sampling effort to target black corals diversity and distribution led to the discovery of a new species. Indeed, as the study of the Neom reference collection proceeds, more taxa new to science are likely to be discovered. The study of their phylogenetic relationships and distribution, like in the case of *Bathypathes thermophila* sp. nov., will contribute to our knowledge of black corals and, ultimately, to a revision of their current taxonomic framework, increasingly exposed by molecular investigations to be plagued by polyphyly.

Acknowledgements

We warmly thank Neom, and in particular Thamer Habis, Razan Khamis, Peter Mackelworth, Paul Marshall, Justin Mynar, and Giacomo Palavacini for organising, coordinating, and facilitating the Red Sea Expedition in 2020. We would like to thank OceanX and the crew of OceanXplorer for their operational and logistical support for the duration of this expedition. In particular, we would like to acknowledge the ROV and Sub teams for data acquisition, sample collection and support of scientific operations on board OceanXplorer. We would also like to thank OceanX Media, for documenting and communicating this work with the public. We are grateful to Ivan Agerton, on behalf of OceanX Media, for photographs in Fig. 6c and d, Christina Alcon for the support in the DNA extraction and amplification, and Alessandro Genovese for facilitating the use of the SEM at KAUST Imaging Core Lab.

References

- Augustin N, van der Zwan FM, Devey CW, Brandsdóttir B (2021) 13 million years of seafloor spreading throughout the Red Sea Basin. *Nature Communications* 12(1): e2427. <https://doi.org/10.1038/s41467-021-22586-2>
- Barret NJ, Hogam RI, Allcock AL, Molodtsova T, Hopkins K, Wheeler AJ, Yesson C (2020) Phylogenetics and mitogenome organisation in black corals (Anthozoa: Hexacorallia: Antipatharia): An order-wide survey inferred from complete mitochondrial genomes. *Frontiers in Marine Science* 7: e440. <https://doi.org/10.3389/fmars.2020.00440>
- Berumen ML, Arrigoni R, Bouwmeester J, Terraneo TI, Benzoni F (2019) Corals of the Red Sea. In: Voolstra CR, Berumen ML (Eds) *Coral Reefs of the Red Sea*. Springer, Cham, 123–155. https://doi.org/10.1007/978-3-030-05802-9_7

- Bilewitch JP, Tracey D (2020) Protected coral connectivity in New Zealand. Final Report prepared by NIWA for the Conservation Services Programme, Department of Conservation. DOC19306- POP201806. NIWA Client Report 2020222WN: 32. [Available at] <https://www.doc.govt.nz/globalassets/documents/conservation/marine-and-coastal/marine-conservation-services/reports/final-reports/pop2018-06-protected-coral-connectivity-final-report.pdf>
- Bo M, Barucca M, Biscotti MA, Brugler MR, Canapa A, Canese S, Lo Iacono C, Bavestrello G (2018) Phylogenetic relationships of Mediterranean black corals (Cnidaria: Anthozoa: Hexacorallia) and implications for classification within the order Antipatharia. *Invertebrate Systematics* 32(5): 1102–1110. <https://doi.org/10.1071/IS17043>
- Brook G (1889) Report on the Antipatharia. Report on the Scientific Results of the Voyage of the HMS Challenger during the years 1873–1876. *Zoology* 32: 1–222.
- Brugler MR, Opreško DM, France SC (2013) The evolutionary history of the order Antipatharia (Cnidaria: Anthozoa: Hexacorallia) as inferred from mitochondrial and nuclear DNA: implications for black coral taxonomy and systematics. *Journal of the Linnean Society* 169(2): 312–361. <https://doi.org/10.1111/zoj.12060>
- Chimienti G, De Padova D, Mossa M, Mastrototaro F (2020) A mesophotic black coral forest in the Adriatic Sea. *Scientific Reports* 10(1): e8504. <https://doi.org/10.1038/s41598-020-65266-9>
- Di Battista JD, Roberts MB, Bouwmeester J, Bowen BW, Coker DJ, Lozano-Cortes DF, Choat JH, Gaither MR, Hobbs JPA, Khalil MT, Kochzius M, Myers RF, Paulay G, Robitzsch VSN, Saenz-Agudelo P, Salas E, Sinclair-Taylor TH, Toonen RJ, Westneat MW, Williams ST, Berumen ML (2016) A review of contemporary patterns of endemism for shallow water reef fauna in the Red Sea. *Journal of Biogeography* 43(3): 423–439. <https://doi.org/10.1111/jbi.12649>
- Herler J (2007) Microhabitats and ecomorphology of coral- and coral rock-associated gobiid fish (Teleostei: Gobiidae) in the northern Red Sea. *Marine Ecology* 28: 82–94. <https://doi.org/10.1111/j.1439-0485.2007.00165.x>
- Horowitz J, Brugler MR, Bridge TCL, Cowman PF (2020) Morphological and molecular description of a new genus and species of black coral (Cnidaria: Anthozoa: Hexacorallia: Antipatharia: Antipathidae: *Blastopathes*) from Papua New Guinea. *Zootaxa* 3(3): e4821. <https://doi.org/10.11646/zootaxa.4821.3.7>
- Katoh K, Standley DM (2013) MAFFT multiple sequence alignment software version 7: Improvements in performance and usability. *Molecular Biology and Evolution* 30(4): 772–780. <https://doi.org/10.1093/molbev/mst010>
- Lanfear R, Frandsen PB, Wright AM, Senfeld T, Calcott B (2017) PartitionFinder 2: New methods for selecting partitioned models of evolution for molecular and morphological phylogenetic analyses. *Molecular Biology and Evolution* 34(3): 772–773. <https://doi.org/10.1093/molbev/msw260>
- Lapian HFN, Barucca M, Bavestrello G, Biscotti MA, Bo M, Canapa A, Tazioli S, Olmo E (2007) A systematic study of some black corals species (Antipatharia, Hexacorallia) based on rDNA internal transcribed spacers sequences. *Marine Biology* 151(2): 785–792. <https://doi.org/10.1007/s00227-006-0525-8>

- Lü T, Zhan Z, Xu K (2021) Morphology and molecular phylogeny of three black corals (Antipatharia, Schizopathidae) from seamounts in the Western Pacific Ocean, with description of a new species. *Journal of Oceanology and Limnology* 39(5): 1740–1757. <https://doi.org/10.1007/s00343-021-0455-9>
- MacIsaac KG, Best M, Brugler MR, Kenchington EL, Anstey LJ, Jordan T (2013) *Telopathes magna* gen. nov., spec. nov. (Cnidaria: Anthozoa: Antipatharia: Schizopathidae) from deep waters off Atlantic Canada and the first molecular phylogeny of the deep-sea family Schizopathidae. *Zootaxa* 3700(2): 237–258. <https://doi.org/10.11646/zootaxa.3700.2.3>
- Manasrah R, Abu-Hilal A, Rasheed M (2019) Physical and Chemical Properties of Seawater in the Gulf of Aqaba and Red Sea. In: Rasul N, Stewart I (Eds) *Oceanographic and Biological Aspects of the Red Sea*. Springer, Cham, 41–73. https://doi.org/10.1007/978-3-319-99417-8_3
- Miller MA, Pfeiffer W, Schwartz T (2012) The CIPRES science gateway: enabling high-impact science for phylogenetics researchers with limited resources. Proceedings of the 1st Conference of the Extreme Science and Engineering Discovery Environment: Bridging from the extreme to the campus and beyond, Chicago (Illinois, USA), July 2012. Association for Computing Machinery, New York-USA, 1–8. <https://doi.org/10.1145/2335755.2335836>
- Molodtsova T, Opresko D (2017) Black corals (Anthozoa: Antipatharia) of the Clarion-Cliperton Fracture Zone. *Marine Biodiversity* 47(2): 349–365. <https://doi.org/10.1007/s12526-017-0659-6>
- Molodtsova T, Opresko D (2021) World List of Antipatharia. *Bathypathes Brook*, 1889. [Accessed through: World Register of Marine Species at:] <http://www.marinespecies.org/aphia.php?p=taxdetails&id=103304> [accessed on 28 Oct 2021]
- Molodtsova TN, Opresko DM, Wagner D (2022) Description of a new and widely distributed species of *Bathypathes* (Cnidaria: Anthozoa: Antipatharia: Schizopathidae) previously misidentified as *Bathypathes alternata* Brook, 1889. *PeerJ* 10: e12638. <https://doi.org/10.7717/peerj.12638>
- Opresko DM (1993) A new species of *Sibopathes* (Cnidaria: Anthozoa: Antipatharia: Antipathidae) from the Gulf of Mexico. *Proceedings of the Biological Society of Washington* 106(1): 195–203.
- Opresko DM (2002) Revision of the Antipatharia (Cnidaria: Anthozoa), Part II. Schizopathidae. *Zoologische Mededeelingen* 76: 411–442.
- Opresko DM, Molodtsova T (2021) New species of deep-sea Antipatharians from the North Pacific (Cnidaria: Anthozoa: Antipatharia), Part 2. *Zootaxa* 4999(5): 401–422. <https://doi.org/10.11646/zootaxa.4999.5.1>
- Purkis SJ, Harris PM, Ellis J (2012) Patterns of sedimentation in the contemporary Red Sea as an analog for ancient carbonates in rift settings. *Journal of Sedimentary Research* 82(11): 859–870. <https://doi.org/10.2110/jsr.2012.77>
- Qurban MA, Krishnakumar PK, Joydas TV, Manikandan KP, Ashraf TTM, Quadri SI, Wafar M, Qasem A, Cairns SD (2014) In-situ observation of deep water corals in the northern Red Sea waters of Saudi Arabia. *Deep-sea Research. Part I, Oceanographic Research Papers* 89: 35–43. <https://doi.org/10.1016/j.dsr.2014.04.002>

- Richmond RH, Hunter CL (1990) Reproduction and recruitment of corals: Comparisons among the Caribbean, the Tropical Pacific, and the Red Sea. *Marine Ecology Progress Series* 60: 185–203. <https://doi.org/10.3354/meps060185>
- Stamatakis A (2014) RAxML version 8: A tool for phylogenetic analysis and post-analysis of large phylogenies. *Bioinformatics (Oxford, England)* 30(9): 1312–1313. <https://doi.org/10.1093/bioinformatics/btu033>
- Terrana L, Flot JF, Eeckhaut I (2021) ITS1 variation among *Stichopathes* cf. *maldivensis* (Hexacorallia: Antipatharia) whip black corals unveils conspecificity and population connectivity at local and global scales across the Indo-Pacific. *Coral Reefs* 40(2): 521–533. <https://doi.org/10.1007/s00338-020-02049-8>
- Thoma JN, Pante E, Brugler MR, France SC (2009) Deep-sea octocorals and antipatharians show no evidence of seamount-scale endemism in the NW Atlantic. *Marine Ecology Progress Series* 397: 25–35. <https://doi.org/10.3354/meps08318>
- Thomson JA (1905) “Scotia” Collections: Scottish Antarctic Expeditions. Report on the Antipatharians. *Proceedings of the Royal Physical Society of Edinburgh* 16: 76–79.
- Totton AK (1923) Coelenterata, Part III, Antipatharia (and their Cirripede commensals). *British Antarctic (Terra Nova) Expedition, 1910–1913, Natural History Reports. Zoology (Jena, Germany)* 5: 97–120.
- Wagner D, Luck DG, Toonen RJ (2012) The Biology and Ecology of Black Corals (Cnidaria: Anthozoa: Hexacorallia: Antipatharia). *Advances in Marine Biology* 63: 67–132. <https://doi.org/10.1016/B978-0-12-394282-1.00002-8>

Supplementary material I

Table S1

Authors: Giovanni Chimienti, Tullia Isotta Terraneo, Silvia Vicario, Fabio Marchese, Sam J. Purkis, Ameer Abdulla Eweida, Mattie Rodrigue, Francesca Benzoni

Data type: Docx file.

Explanation note: Records of *Bathypathes thermophila* sp. nov. with indication of the dive and the relative gear (CHR: “Chimaera” ROV; NTN: “Neptune” submersible), the geographic coordinates, the depth and the number of colonies observed (N). When several colonies were observed within a transect, coordinates and depth refer to the shallowest and the deepest records.

Copyright notice: This dataset is made available under the Open Database License (<http://opendatacommons.org/licenses/odbl/1.0/>). The Open Database License (ODbL) is a license agreement intended to allow users to freely share, modify, and use this Dataset while maintaining this same freedom for others, provided that the original source and author(s) are credited.

Link: <https://doi.org/10.3897/zookeys.1116.79846.suppl1>

Supplementary material 2

Table S2

Authors: Giovanni Chimienti, Tullia Isotta Terraneo, Silvia Vicario, Fabio Marchese, Sam J. Purkis, Ameer Abdulla Eweida, Mattie Rodrigue, Francesca Benzoni

Data type: Docx file.

Explanation note: Metadata of the samples of *Bathypathes thermophila* sp. nov. considered in this study.

Copyright notice: This dataset is made available under the Open Database License (<http://opendatacommons.org/licenses/odbl/1.0/>). The Open Database License (ODbL) is a license agreement intended to allow users to freely share, modify, and use this Dataset while maintaining this same freedom for others, provided that the original source and author(s) are credited.

Link: <https://doi.org/10.3897/zookeys.1116.79846.suppl2>

Supplementary material 3

Figure S1

Authors: Giovanni Chimienti, Tullia Isotta Terraneo, Silvia Vicario, Fabio Marchese, Sam J. Purkis, Ameer Abdulla Eweida, Mattie Rodrigue, Francesca Benzoni

Data type: Jpg file.

Explanation note: RAxML phylogenetic reconstruction of Antipatharia and the position of *Bathypathes thermophila* sp. nov. (in purple) inferred with a cox3-cox1 reconstruction. Node values are maximum likelihood bootstrap values (> 70%). The genus *Leiopathes* was selected as outgroup. Some of the samples reported as *Alternatipathes alternata* are now doubtful with respect to the recently-described *Bathypathes pseudoalternata*.

Copyright notice: This dataset is made available under the Open Database License (<http://opendatacommons.org/licenses/odbl/1.0/>). The Open Database License (ODbL) is a license agreement intended to allow users to freely share, modify, and use this Dataset while maintaining this same freedom for others, provided that the original source and author(s) are credited.

Link: <https://doi.org/10.3897/zookeys.1116.79846.suppl3>

Catalog of the genus *Cylindrepomus* Blanchard (Coleoptera, Cerambycidae, Dorcaschematini) in the Philippines, with description of a new species from northern Mindanao

Milton Norman D. Medina¹, Melbert James G. Baul², Analyn A. Cabras¹

1 Coleoptera Research Center, University of Mindanao, Davao City, Philippines **2** Human Resources for Health Network, Department of Health Center for Health Development - Northern Mindanao, J.V. Serina Street, Carmen, Cagayan de Oro City, Philippines

Corresponding author: Milton Norman D. Medina (mnd_medina@umindanao.edu.ph)

Academic editor: Francesco Vitali | Received 24 May 2022 | Accepted 19 July 2022 | Published 4 August 2022

<https://zoobank.org/997F8571-0D22-4C83-92C7-F57610409705>

Citation: Medina MND, Baul MJG, Cabras AA (2022) Catalog of the genus *Cylindrepomus* Blanchard (Coleoptera, Cerambycidae, Dorcaschematini) in the Philippines, with description of a new species from northern Mindanao. ZooKeys 1116: 23–32. <https://doi.org/10.3897/zookeys.1116.86906>

Abstract

A catalog of the genus *Cylindrepomus* Blanchard, 1853 in the Philippines, along with the description of a new species from northern Mindanao, is presented. Notes on the ecology, threats, and conservation of the new species are also provided.

Keywords

Beetle, conservation, Davao City, Dorcaschematini, Mindanao, Philippines

Introduction

Cylindrepomus Blanchard, 1853 is a tropical genus of long-horn beetles (Cerambycidae) (type species *Cylindrepomus nigrofasciatus* Blanchard, 1853) distributed within South China, Southeast Asia, and Oceania. They are easily distinguished from other members of Dorcaschematini for having highly punctate, tomentose elytra covered with recumbent hairs, a bulbous and coarsely granulated scape, and 3rd antennomere 2–4 times longer than scape.

There are 14 species and one subspecies of *Cylindrepomus* in the Philippines; all are endemic to the country, with the majority distributed in a specific island or mountain range. There are four species described from Mindanao Island: *Cylindrepomus bivitticollis* Breuning, 1947, *Cylindrepomus elisabethae* Hüddepohl, 1987, *Cylindrepomus peregrinus samarensis* Dillon & Dillon, 1948, and *Cylindrepomus sexlineatus* Schultze, 1934. The most recent addition to the Philippine fauna is *Cylindrepomus nigerrimus* Vives, 2017 from northern Luzon.

The 2022 Philippine Coleopterological Expedition conducted by the Daugavpils University Beetle Research Team and the University of Mindanao Coleoptera Research Center yielded a diverse collection of beetles from different mountain ranges in Mindanao. Included in this collection was the new species of *Cylindrepomus* from northern Mindanao described herein, the fifth species of the genus known from Mindanao Island. An updated catalog of *Cylindrepomus* in the Philippines is included in this paper.

Materials and methods

The new *Cylindrepomus* material was obtained during the 2022 Philippine Coleopterological Expedition through the Erasmus+ Mobility Programme of Daugavpils University in Latvia and the University of Mindanao Coleoptera Research Center, Philippines. The project aimed to document the coleopteran fauna in various mountain ranges in Mindanao, Philippines. The specimens under study were collected using hand nets along riparian fields at an elevation of approximately 600–700 m a.s.l.; specimens were killed with ethyl acetate. The habitat consists of an old-growth secondary forest with relatively high moisture and semi-open foliage allowing daylight to filter through.

Morphological characters were observed under Luxeo 4D and Nikon SMZ745T stereomicroscopes. Habitus images were taken with a Canon EOS 6D digital camera equipped with an MP-E macro lens. All images were then stacked using Helicon Focus and processed using a licensed version of the Photoshop CS6 Portable software.

Measurements of the various body parts follow Yoshitake and Yamasako (2016), with slight modifications concerning body length: **LB** = length of body from antennal support to apices of clothed elytra; **WH** = maximum width across head from the outer margin of a gena to that of another; **LG** = length of gena from upper margin to lower margin; **LL** = length of lower eye lobe from upper margin to lower margin; **WL** = maximum width across lower eye lobe; **LP** = length of pronotum from base to apex along midline; **WP** = maximum width across pronotum; **LE** = length of elytra from level of basal margins to apices of clothed elytra; **WEH** = width of elytra at humeri; / separates different lines on a label; // separates different labels. All measurements are given in millimeters.

Comparative materials and specimens used in this study are deposited in the following institutional collections:

- ANSP** Academy of Natural Sciences of Philadelphia, USA;
- MMCP** Milton Medina Collections, Mindanao, Philippines;
- MTKD** Senckenberg Naturhistorische Sammlungen Dresden, Germany;

- NRM** Naturhistoriska Riksmuseet, Stockholm, Sweden;
SMF Natur-Museum und Forschungs-Institut Senckenberg, Frankfurt am Main, Germany;
UMCRC University of Mindanao Coleoptera Research Center, Mindanao, Philippines;
USNM National Museum of Natural History (Smithsonian), Washington, D.C., USA;
ZSM Zoologische Staatssammlung des Bayerischen Staates München, Germany.

Catalog

Cylindrepomus albomaculatus Breuning, 1947

Arkiv för Zoologi, Uppsala, 39: p. 26; Breuning 1962: p. 417; Hüdepohl 1987: p. 74.
Distribution: Philippines.
Type and depository information: Holotype male, NRM.

Cylindrepomus albosignatus Breuning, 1974

Reichenbachia, Dresden, 15(5): p. 38; Hüdepohl 1987: p. 74.
Distribution: Philippines (Luzon: Panay, Gulasi, Zambales; Visayas: Mt. Macosolon in Capiz Western Visayas; Mindanao: Zamboanga).
Type and depository information: Holotype, MTKD.

Cylindrepomus astyochus Dillon & Dillon, 1948

Transactions of the American Entomological Society, Philadelphia, 73: pp. 258, 262, pl. IX, fig. 14; Breuning 1962: p. 417; Hüdepohl 1987: p. 73.
Distribution: Philippines (Palawan; Visayas, Negros).
Type and depository information: Holotype male, ANSP.

Cylindrepomus atropos Dillon & Dillon, 1948

Transactions of the American Entomological Society, Philadelphia, 73: pp. 257, 260, pl. IX, fig. 17; Breuning 1962: p. 416; Hüdepohl 1987: p. 73; Lingafelter et al. 2014: p. 21; Vives 2017: p. 52.
Distribution: Philippines (Luzon: Apayao; Visayas: Mt. Halcon in Mindoro, Samar).
Type and depository information: Holotype female, USNM.

Cylindrepomus bayanii Hüdepohl, 1987

Entomologische Arbeiten aus dem Museum G. Frey, Tutzing bei München 35/36: pp. 74, 76, fig. 2.
Distribution: Philippines (Romblon).
Type and depository information: Holotype male, ZSM.

***Cylindrepomus bivitticollis* Breuning, 1947**

Arkiv för Zoologi, Uppsala, 39(6): p. 27; Breuning 1962: p. 416; Hüdepohl 1987: p. 74; Vives 2013: p. 72, fig. 12.

Distribution: Philippines (Mindanao: Mt. Kitanglad in Bukidnon).

Type and depository information: Holotype male, NRM.

***Cylindrepomus cicindeloides* Schwarzer, 1926**

Senckenbergiana, Frankfurt am Main, 8: p. 290, pl. 5, fig. 7; Breuning 1940: pp. 528, 537; Breuning 1962: p. 417; Hüdepohl 1987: p. 74.

Distribution: Philippines (Luzon: Mt. Banahao).

Type and depository information: Holotype, SMF.

***Cylindrepomus elisabethae* Hüdepohl, 1987**

Entomologische Arbeiten aus dem Museum G. Frey, Tutzing bei München 35/36: pp. 74–75, fig. 1.

Distribution: Philippines (Mindanao: Tandag Surigao del Sur).

Type and depository information: Holotype female, ZSM.

***Cylindrepomus flavicollis* Breuning, 1947**

Reichenbachia, Dresden, 15(5): pp. 25 ; Breuning 1962: p. 416; Hüdepohl 1987: p. 74.

Distribution: Philippines.

Type and depository information: Holotype male, NRM.

***Cylindrepomus mucronatus* Schwarzer, 1926**

Senckenbergiana, Frankfurt am Main, 8: p. 290, pl. 5, fig. 6 ; Breuning 1940: pp. 528, 537 ; Breuning 1962: p. 416; Hüdepohl 1987: p. 73.

Distribution: Philippines (Luzon: Imugan).

Type and depository information: Holotype male, SMF.

***Cylindrepomus nigerrimus* Vives, 2017**

Les Cahiers Magellanes, 25: p. 52, fig. 10.

Distribution: Philippines, Luzon, Nueva Vizcaya, Dupax del Sur.

Type and depository information: Holotype male, Collection E. Vives, Terrassa, Barcelona, Spain.

***Cylindrepomus peregrinus samarensis* Dillon & Dillon, 1948**

Transactions of the American Entomological Society, Philadelphia, 73: p. 264, pl. IX, fig. 10; Breuning 1962: p. 417; Hüdepohl 1987: p. 74; Lingafelter et al. 2014: p. 297.

Distribution: Philippines (Luzon: Panay; Visayas: Negros, Samar; Mindanao).

Type and depository information: Holotype male, USNM.

***Cylindrepomus rufofemoratus* Breuning, 1947**

Arkiv för Zoologi, Uppsala, 39(6): p. 47; Breuning 1962: p. 418; Hüdepohl 1987: p. 73.

Distribution: Philippines.

Type and depository information: Holotype male, NRM.

***Cylindrepomus sexlineatus* Schultzze, 1934**

The Philippine Journal of Science 53 (3): p. 312, pl. 1, fig. 3; Breuning 1940: pp. 529, 538; Breuning 1947: p. 6; Breuning 1950: p. 527; Breuning 1962: p. 416; Hüdepohl 1987: p. 74.

Distribution: Philippines (Mindanao: Lanao Province).

Type and depository information: Holotype female, MTKD.

Synonyms: *Cylindrepomus sexlineatus* m. *ininterruptus* Breuning, 1950; *Cylindrepomus sexlineatus* m. *reductevittatus* Breuning, 1947.

***Cylindrepomus ysmaeli* Hüdepohl, 1987**

Entomologische Arbeiten aus dem Museum G. Frey, Tutzing bei München 35/36: pp. 74, 77, fig. 3.

Distribution: Philippines (Luzon: Mountain Province).

Type and depository information: Holotype female, ZSM.

Taxonomy***Cylindrepomus ansihagani* Medina & Cabras, sp. nov.**

<https://zoobank.org/AF70CDCE-A5E7-445E-B5B0-FFA2AD50E42E>

Fig. 1A–D

Holotype (Fig. 1), male: PHILIPPINES – Mindanao / Northern Mindanao / Misamis Oriental III.2022 / local collector (MMCP), to be deposited at PNM.

Other material examined. *Cylindrepomus bivitticollis* Breuning, 1947, holotype male, NRM; *C. sexlineatus* Schultzze, 1934, holotype female, MTKD.

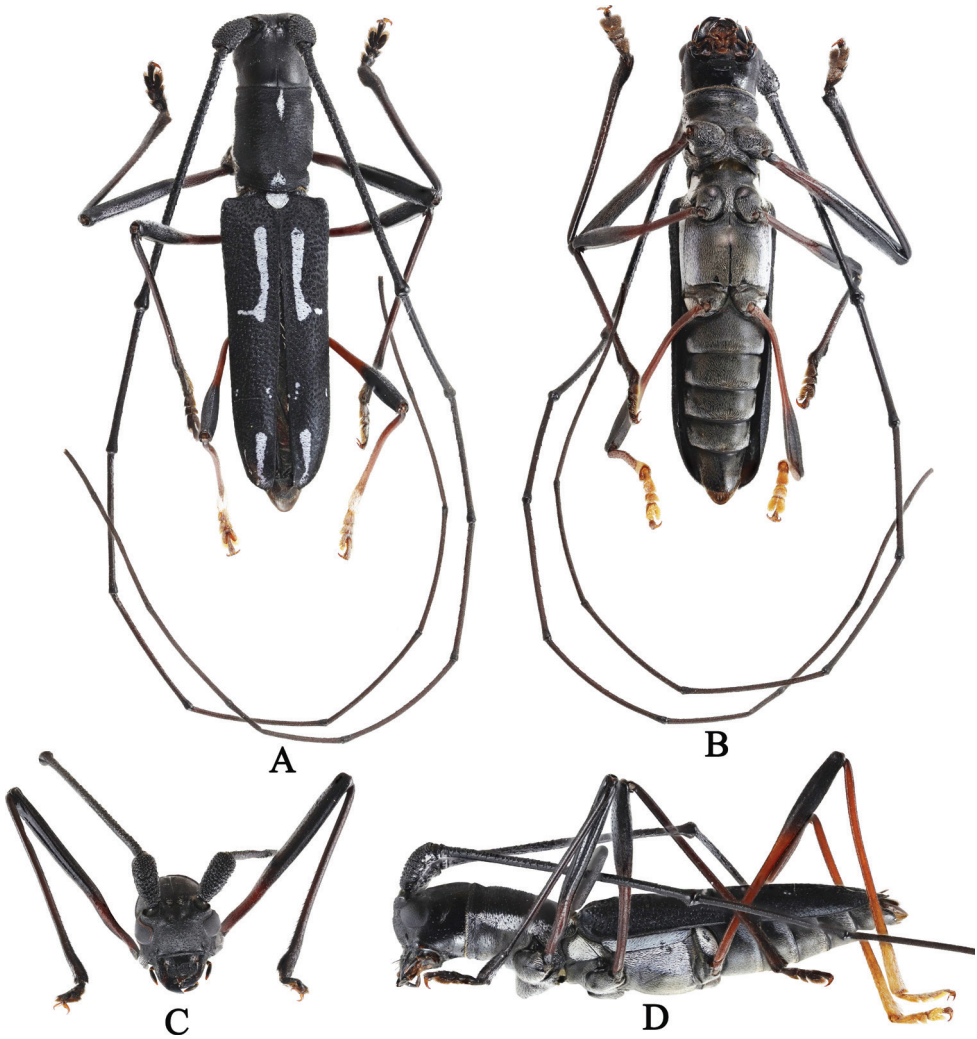


Figure 1. *Cylindrepomus ansihagani* sp. nov. male holotype, habitus **A** dorsal aspect **B** ventral aspect **C** frons **D** lateral aspect.

Description. Male. Dimensions ($n = 1$): LB: 14.0 mm. WH: 2.0 mm. LG: 1.5 mm. LL: 1.0 mm. WL: 1.0 mm. LP: 3.0 mm. WP: 2.0 mm. LE: 8.5 mm. WEH: 3.0 mm.

Teguments generally matt black, pro- and mesotibia reddish-brown near base; metatibia reddish-brown up to apical third; mid tarsus pale brown; hind tibia, tarsus, and claw light brown. Ventral side matt black, tomentose, covered with white recumbent pubescence on prosternum, prothorax, and abdomen.

Head and gena tomentose, covered with black recumbent pubescence; genae with few erect black hairs at the side; vertex with two small bands of white recumbent pubescence. Eyes prominent, black, as long as wide. Antennae long and slender (except scape), more than twice the body length, matt black; scape bulbous, coarsely granulated, with recumbent white setae near base, 2 \times longer than wide; 2nd antennomere wider

than long; 3rd antennomere coarsely granulated, 2× longer than each of antennomeres 4–11; 5th antennomere slightly granulated; antennomeres 6–11 finely granulated.

Pronotum 1.5× wider than long, tomentose, covered with black recumbent hairs; with two narrow bands of white recumbent pubescence, one at the base shaped like an elongated diamond, the other one triangle-shaped and near the margin; apical margin lined with golden setae.

Prosternum tomentose, covered with black recumbent hairs at middle and white recumbent setae at sides. Mesosternum and metasternum tomentose, covered with black and white recumbent setae. Mesepisternum and metepisternum tomentose, covered with white recumbent setae. 1st to 4th abdominal ventrites tomentose, covered with white and black recumbent setae with sparse golden setae at each side; pygidium tomentose, covered with full black recumbent setae, apex lined with golden hairs (Fig. 1B).

Elytra 2.5× longer than wide, with coarse, uniformly aligned punctation; humeri slight recurved; suture and margin raised, slightly truncate along suture; apex lanceolate; with two thick bands of white recumbent pubescence, one at basal third longitudinal with apex expanded laterally, and one near the apex, narrowed toward the tip; a few tiny white spots near suture and margin at apical third. Scutellum tomentose, covered with white recumbent setae, obscuring surface (Fig. 1A).

Coxae tomentose, covered with whitish recumbent hairs; trochanters reddish-brown; tibia armed with two small spines at base (colored black on protibia and mesotibia, pale brown on metatibia). Profemur slightly recurved near base.

Male genitalia (Fig. 2 A–J): Tegmen ~1.5 mm long; lateral lobes slender, ~0.1 mm long and 0.6 mm wide; base with a broad central lobe bearing fine setae; apex bearing numerous golden setae, ~0.2–0.6 mm long. Aedeagus ~2.0 mm long and 0.5 mm wide, slightly recurved and tapering towards apex. Endophallus ~6.0 mm long.

Diagnosis. *Cylindrepomus ansihagani* sp. nov. is distinct from its Mindanao endemic congeners (*C. bivitticollis* and *C. sexlineatus*) in having pronotum with two narrow bands of white recumbent pubescence, one at the base, shaped like an elongated diamond, the other a triangular band of white recumbent pubescence near the margin, while *C. bivitticollis* has pronotum with a complete, pale yellow longitudinal band on each side of the disc and *C. sexlineatus* has pronotum with a yellowish spot on each side at the base.

Etymology. This new species is named after Datu Ramil P. Ansihagan, the tribal chieftain of the Higaunon Tribe, for his efforts in protecting and preserving the remaining forests in Barangay Eureka Gingoog City, Philippines.

Distribution of *Cylindrepomus ansihagani* sp. nov. Philippines: Mindanao: Northern Mindanao, Gingoog City.

Notes on ecology, threats, and conservation of *Cylindrepomus ansihagani* sp. nov. The species is known from a single specimen that was collected during the expedition. The species was collected at an elevation of approximately 1000–1100 m a.s.l. using hand nets along the boundary between an agro-ecosystem and a secondary forest. Most of the trees present are endemic species including but not limited to *Shorea negrosensis* (Red Lauan), *Shorea contorta* (White Lauan), and *Quercus subsericea* (Philippine Ulayan Tree), all of which are native to the Philippines and considered highly valued trees.

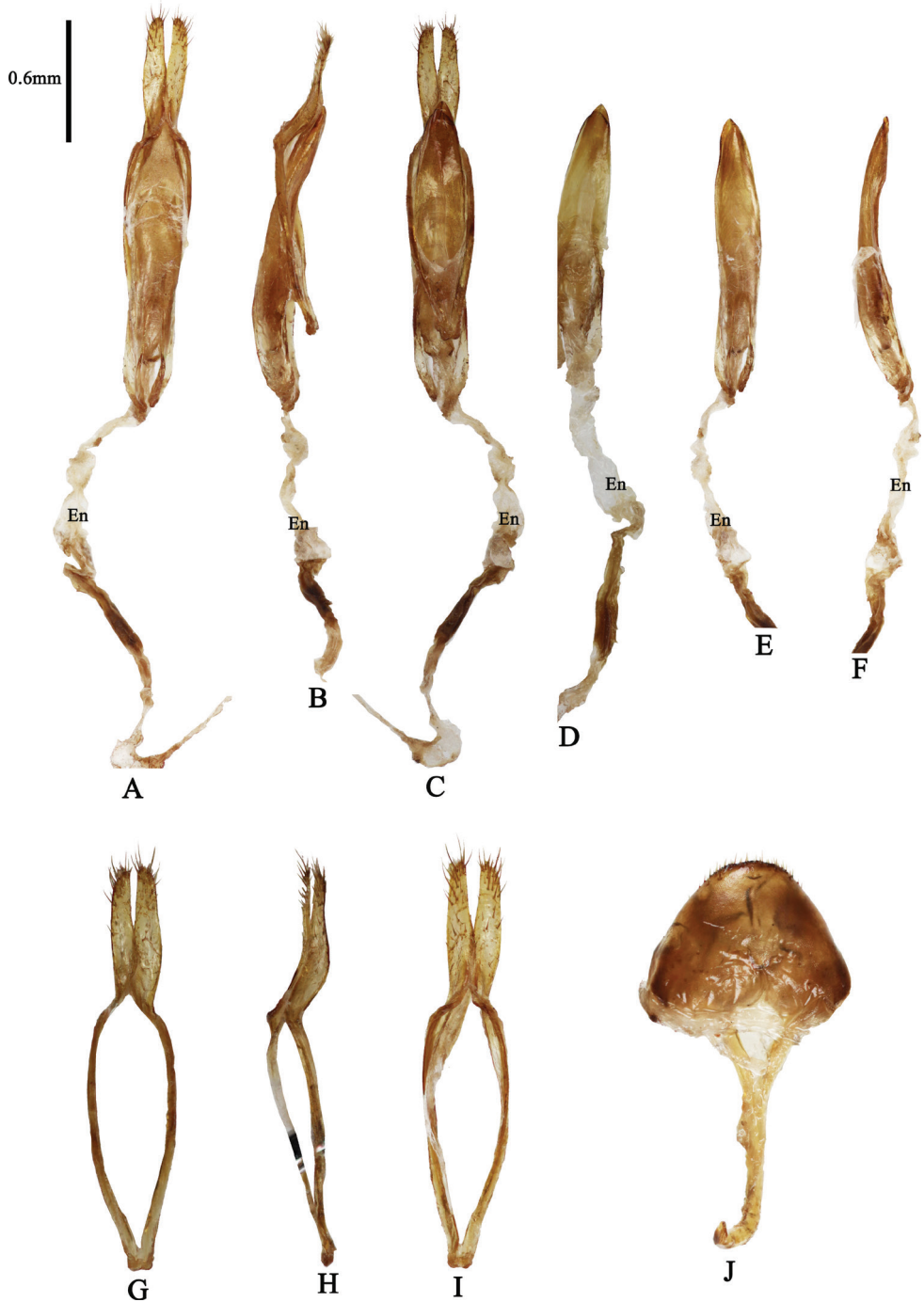


Figure 2. *Cyliindrepomus ansihagani* sp. nov. **A** genitalia, dorsal aspect **B** genitalia, lateral aspect **C** genitalia, ventral aspect **D** aedeagus, ventral aspect **E** aedeagus, dorsal aspect **F** aedeagus, lateral aspect **G** tegmen, dorsal aspect **H** tegmen, lateral aspect **I** tegmen, ventral aspect **J** tergite VIII. Abbreviation: **En** – Endophallus.

The current threat to the species' habitat is the continued conversion of the remaining secondary forests into agricultural lands. Farmers use various chemicals such as pesticides, herbicides, and fungicides that could affect the species' population. There is a need to conduct more expeditions, covering more habitats, to find additional populations of this and other species. Hence, research identifying the exact species distribution, area of occupancy and the species' extent of occurrence is important as a guide in making a future IUCN Red List assessment of this endemic species.

Acknowledgements

Our gratitude to Guillermo P. Torres Jr. for his continued support to the UMCRC. To the ERASMUS+ Mobility Program between UMCRC and DUBC, funded by the European Union. To our local guides: Ricky, Xyrex Quin, Joshua, Jephtha, Gerwen, Jomart, and the entire Higaunon tribe in Baliguihan Gingoog City. To Alex Anichtchenko, Anastasija Vasiljeva, Felix Landim, and Dexter Patalita. To our good friend Arvids Barsevskis for the wonderful scientific collaboration throughout the years. To Mattias Forshage for the warm assistance during the first and third authors' visit at Naturhistoriska Riksmuseet Stockholm Sweden. Thanks to Larry Bezark and Xavier Gouverneur for the important comments and suggestions. Special thanks to Francesco Vitali for the guidance and fruitful discussions on improving this work.

References

- Breuning S (1940) Études sur les Lamiaires (Coléop. Cerambycidae). Neuvième Tribu: Dorcaschematini Thoms. *Novitates Entomologicae*, 3^{ème} supplément (67–71): 527–568. [figs 522–582]
- Breuning S (1950) Lamiaires nouveaux de la collection Lepesme. *Longicornia* I: 511–535. [8 figs. Paul Lechevalier, Paris]
- Breuning S (1962) Catalogue des Lamiaires du Monde (Col. Cerim.). Verlag des Museums G. Frey, Tutzing bei München, 6 August 1962, 387–459.
- Breuning S von (1947) Nouvelles formes de longicornes du Musée de Stockholm. *Arkiv för Zoologi*, Uppsala, 39, A, 6: 1–68.
- Hüdepohl KE (1987) Die philippinischen Arten der Gattung *Cylindrepomus* Blanchard (Cerambycidae, Lamiinae, Dorcaschematini). *Entomologische Arbeiten aus dem Museum G. Frey Tutzing bei München* 35/36: 73–79.
- Lingafelter SW, Nearn EH, Tavakilian GL, Monné MA, Biondi M (2014) Longhorned Wood-boring Beetles (Coleoptera: Cerambycidae and Disteniidae) Primary Types of the Smithsonian Institution. Smithsonian Institution Scholarly Press, Washington D.C., [v–xviii +] 1–390. [187 figs., ISBN: 978-1-935623-40-3]
- Yoshitake H, Yamasako J (2016) A new *Doliops* (Coleoptera, Cerambycidae) from Bohol Island, the Philippines. *Japanese Journal of Systematic Entomology* 22(1): 1–5.

Vives E (2013) New or interesting Cerambycidae from the Philippines (Part VII) (Coleoptera, Cerambycidae). *Les Cahiers Magellanes* (NS) 11: 62–75. [15 figs]

Vives E (2017) New or interesting Cerambycidae from the Philippines (Part XV) (Coleoptera, Cerambycidae, Lamiinae). *Les Cahiers Magellanes* 25: 46–65.

Supplementary material I

Figure S1

Authors: Milton Norman D. Medina, Melbert James G. Baul, Analyn A. Cabras

Data type: COL (jpg, image)

Explanation note: A catalog of the genus *Cylindrepomus* Blanchard, 1853 in the Philippines with description of a new species from Northern Mindanao is presented.

Notes on the ecology, threats, and conservation of the new species is also provided.

Copyright notice: This dataset is made available under the Open Database License (<http://opendatacommons.org/licenses/odbl/1.0/>). The Open Database License (ODbL) is a license agreement intended to allow users to freely share, modify, and use this Dataset while maintaining this same freedom for others, provided that the original source and author(s) are credited.

Link: <https://doi.org/10.3897/zookeys.1116.86906.suppl1>

Notes on spotted-elytron species of *Gallerucida* Motschulsky with the description of six new species from China (Coleoptera, Chrysomelidae, Galerucinae)

Si-yuan Xu^{1,2}, Rui-E Nie^{1,3}, Xing-ke Yang^{1,4}

1 Key Laboratory of Zoological Systematics and Evolution, Institute of Zoology, Chinese Academy of Sciences, 1 Beichen West Road, Chaoyang District, Beijing 100101, China **2** University of Chinese Academy of Sciences, No. 19(A) Yuquan Road, Shijingshan District, Beijing, 100049, China **3** Anhui Provincial Key Laboratory of the Conservation and Exploitation of Biological Resources, College of Life Sciences, Anhui Normal University, Wuhu, 241000, China **4** Guangdong Key Laboratory of Animal Conservation and Resource Utilization, Guangdong Public Laboratory of Wild Animal Conservation and Utilization, Guangdong Institute of Applied Biological Resources, Guangzhou 510260, China

Corresponding authors: Rui-E Nie (niere2021@ahnu.edu.cn), Xing-ke Yang (yangxk@ioz.ac.cn)

Academic editor: Astrid Eben | Received 29 April 2022 | Accepted 8 June 2022 | Published 4 August 2022

<https://zoobank.org/17267ADE-DEB4-4936-8A2A-CB9670FF6CA2>

Citation: Xu S-y, Nie R-E, Yang X-K (2022) Notes on spotted-elytron species of *Gallerucida* Motschulsky with the description of six new species from China (Coleoptera, Chrysomelidae, Galerucinae). ZooKeys 1116: 33–55. <https://doi.org/10.3897/zookeys.1116.85987>

Abstract

In this study, fifteen species of *Gallerucida* Motschulsky, 1860 (Coleoptera: Chrysomelidae: Galerucinae), with spotted elytra, from China are reviewed, including one new record: *G. balyi* (Duvivier, 1885), six new species: *G. fortispina* Xu & Yang, **sp. nov.**, *G. levifasciata* Xu & Nie, **sp. nov.**, *G. nigrovittata* Xu & Yang, **sp. nov.**, *G. octodecimpunctata* Xu & Yang, **sp. nov.**, *G. piceusfasciata* Xu & Yang, **sp. nov.**, *G. rufipectoralis* Xu & Nie, **sp. nov.**, and *Aplosonyx gansuica* (Chen, 1942), **comb. nov.** is removed from genus *Gallerucida*. A key to the spotted-elytron species of *Gallerucida* from China is given as well as habitus photographs of the related species and *Aplosonyx gansuica* **comb. nov.** and photographs of the aedeagus of each new species.

Keywords

Coleoptera, Chrysomelidae, Galerucinae, *Gallerucida*, new species

Introduction

Gallerucida Motschulsky, with 81 species described so far, is one of the largest genera in Galerucinae (Coleoptera: Chrysomelidae). All known species are distributed in the Palearctic region and Oriental region, of which 64 species are recorded in China (Yang et al. 2015). Larvae and adults feed on leaves, and some species are severe pests of commercial crops.

Due to the rich species diversity of *Gallerucida* in China, in this study we focus on the spotted-elytron species of *Gallerucida* from China, but this group, comprising 14 species, may not be a natural group. We describe six new species and record one new species from China, give habitus and aedeagus images and a key to species from China.

Materials and methods

The specimens were examined with an Olympus SZ61 microscope. Abdomens and aedeagus of each species were dissected using the following procedure: for dried or ethanol preserved specimens, the abdomen was separated and transferred to a vial containing 10% KOH which was heated in a boiling water bath for 20–25 min. The abdomen was moved to a clean cavity slide and the abdomen pressed with the back of a dissecting needle to extrude and separate the aedeagus. The abdomen and aedeagus were then washed with distilled water and carefully moved using fine forceps to another cavity slide containing glycerin for examination.

Habitus images were taken using a Canon EOS 5DSR digital camera, equipped with MP-E 65 mm f/2.8 lens. Illumination was by flash, and each photo was taken by a macro slide system.

Aedeagus images were taken using a Nikon D610 digital camera, linking a Zeiss microscope, with 5× objective lens. A cable shutter release was used to prevent the camera from shaking. The depth of field was determined by different sizes of the aedeagus. Helicon Focus 6 (<http://www.heliconsoft.com/heliconsoft-products/helicon-focus>) stacked full depth of images. Adobe Photoshop CC (<https://www.photoshop.com>) edited images and resulted output.

The label data were translated into English from the original Chinese. Accurate labelling data for all type specimens of species: A slash (/) divides the date into different lines of a label. A double slash (//) separates the data of different labels. Type specimens of the six new species are deposited in the Institute of Zoology, Chinese Academy of Sciences, Beijing, China (**IZAS**). Abbreviations used in the paper are **TL**: type locality and **TD**: type depository.

Specimens studied herein are deposited at the following institutes and collections:

- ISNB** Institut Royal des Sciences naturelles de Belgique, Bruxelles, Belgium;
IZAS Institute of Zoology, Chinese Academy of Sciences, Beijing, China;

- MNHN** Museum national d'Histoire naturelle, Paris, France;
NHMB Naturhistorisches Museum, Basel, Switzerland;
NHMUK The Natural History Museum, London, UK;
SDEI Senckenberg Deutsches Entomologisches Institut, Müncheberg, Germany.

Taxonomy

Genus *Gallerucida* Motschulsky

Gallerucida Motschulsky, 1861: 24. Type species: *Gallerucida bifasciata* Motschulsky, 1861, designated by Weise 1924.

Eustetha Baly, 1861: 296. Type species: *Eustetha flaviventris* Baly, 1861, by original designation. Synonymized by Chûjô 1962: 147.

Melospila Baly, 1861: 297. Type species: *Melospila nigromaculata* Baly, 1861, by monotypy and original designation. Synonymized by Chapuis 1875: 227.

Hylaspes Baly, 1865: 436. Type species: *Hylaspes longicornis* Baly, 1865, by monotypy and original designation. Synonymized by Gressitt and Kimoto 1963: 717.

Gallerucida: Chapuis 1875: 224, 227. error or emendation for *Gallerucida* Motschulsky, 1861: 24.

Stethidea Baly, 1890: 13. Type species: *Doryida balyi* Duvivier, 1885, by monotypy and original designation. Synonymized by Kimoto 1989: 234.

Coptomesa Weise, 1912: 91. Type species: *Gallerucida (Coptomesa) maculata* Weise, 1912, by monotypy. Synonymized by Kimoto 1965: 398.

Distribution. Palaearctic region, Oriental region.

Key to the spotted-elytron species of *Gallerucida* from China

- | | | |
|---|--|---|
| 1 | Pronotum black or atropurpureus (dark purple)..... | 2 |
| – | Pronotum not as above | 8 |
| 2 | Pronotum atropurpureus | 3 |
| – | Pronotum black | 4 |
| 3 | From scutellum to middle area of elytra with an irregular brown band, after middle with 5 small brownish spots, arranged in two rows as 4:1 | |
| | <i>G. levifasciata</i> sp. nov. | |
| – | Basal area of elytra with one atropurpureus oval spot adjacent to the scutellum, middle area of elytra with a transverse atropurpureus stripe and subapically with an atropurpureus spot | |
| | <i>G. ornatipennis</i> (Duviver, 1885) | |
| 4 | Antennae black | 5 |
| – | Antennae not black | 6 |

- 5 Elytra yellowish brown, with a round black spot adjacent to the scutellum, middle area of elytra with a transverse black stripe followed by 4 black spots, arranged two rows as 3:1 *G. bifasciata* Motschulsky, 1860
- Elytra black, with two oblique transverse yellow stripes..... *G. tenuefasciata* Fairmaire, 1888
- 6 Ventral surface totally black, elytra with three wide subparallel transverse atropurpureus stripes and a rounded atropurpureus spot near apex..... *G. rubrozonata* Fairmaire, 1889
- Ventral surface totally brown or only ventral surface of the thorax black 7
- 7 Ventral surface of thorax black, after middle of elytra with a transverse black stripe..... *G. nigrovittata* sp. nov.
- Ventral surface of thorax and abdomen totally brown *G. nigropicta* Fairmaire, 1888
- 8 Pronotum and ventral surface dark green *G. piceusfasciata* sp. nov.
- Pronotum not dark green..... 9
- 9 Pronotum with black spots 10
- Pronotum without spots 11
- 10 Antennae brown except four basal segments orange *G. octodecimpunctata* sp. nov.
- Antennae yellow *G. balyi* (Duvivier, 1885)
- 11 Pronotum yellow, ventral surface yellowish brown 12
- Pronotum reddish brown, ventral surface black..... 13
- 12 Head black *G. fortispina* sp. nov.
- Head yellow or reddish brown *G. sauteri* Chûjô, 1938
- 13 Elytra yellow, middle area with a transverse black stripe *G. tricolor* Gressitt & Kimoto, 1963
- Elytra yellowish brown, basal area with a slim black stripe, subapically with a wide transverse black stripe *G. rufipectoralis* sp. nov.

***Gallerucida balyi* (Duvivier, 1885) (new record)**

Fig. 43

Doryida balyi Duvivier, 1885: 394. TL Malaysia: Malacca; TD ISNB

Stethidea fulva Laboissière, 1931: 135

Stethidea maculata Laboissière, 1931: 133 (nec *Galerucida maculata* Weise, 1912)

Stethidea oranta Laboissière, 1932: 132 (nom. nov. for *Stethidea maculata* Laboissière, nec Weise)

Gallerucida balyi: Kimoto, 1989: 234.

Type material. Paratype: labels: V. Laboissière vid., 1939 / *Stethidea* / *Balyi* Duviv. / Type // sec. Weise, Col. Cat. / Junk (78), 1924, p143: / *Stethidea* / *Balyi* Duv. // cf. Stett. Ent. Zeitung. / XVI, 1885, p.394 // Type // det. Duvivier. / *Doryida* / *balyi* Du-

viv. // Type // Collect. / Duvivier. (ISNB). **Syntype:** labels: *Doryida / balyi* / Duvivier / halacca. // SYN-TYPE. // 37 // Baly coll. (NHMUK).

Other material examined. 1♂, CHINA, Guangxi, Longzhou, Sanlian, 350 m, 13-VI-2000, Wen-Zhu Li, leg. (IZAS).

Distribution. China: Guangxi. India; Myanmar; Thailand; Laos; Vietnam; Malaysia: Malacca.

Gallerucida bifasciata Motschulsky, 1861

Fig. 44

Gallerucida bifasciata Motschulsky, 1861: 24. TL Japan; TD MNHN.

Melospila nigromaculata Baly, 1861: 297. Synonymized by Kimoto 1965: 399.

Melospila consociata Baly, 1874: 184. Synonymized by Ogloblin 1936: 354.

Gallerucida nigrofasciata Baly, 1879: 453. Synonymized by Gressitt and Kimoto 1963: 722.

Gallerucida nigrita Chûjô, 1935: 168. Synonymized by Kimoto 1966: 34.

Gallerucida bifasciata nigromaculata Takizawa, 1980: 73. Synonymized by Takizawa 1985: 10.

Type material. **Syntype:** labels: *Gallerucida / bifasciata* / Motch. / Type / Japonia // Ex-Musaeo / E. Harold. (MNHN).

Other material examined (115 spec.). CHINA: **Heilongjiang:** 1♀, Heilongjiang, Jingpo Hu, 6-IX-1970, unknown, leg.; 3♂♂, Heilongjiang, Harbin Shi, (20-22)-VI-1955, unknown, leg.; **Jinlin:** 2♀♀, 1♂, Jilin, Linjiang, 14-V-1955, unknown, leg.; **Liaoning:** 1♂, Liaoning, Qianshan, 15-V-1955, unknown, leg.; 1♂, Liaoning, Qingyuan, 3-VI-1955, unknown, leg.; **Gansu:** 3♀♀, 5♂♂, Gansu, Huixian, Yuguan, 23-V-1981, unknown, leg.; **Hebei:** 2♂♂, Hebei, Wuling Mountain, Shizigou [Zishigou], 500 m, 2-VI-1981, Pei-Yu Yu, leg.; 1♂, Hebei, Yu Xian, Longquanguan, 3-VIII-1998, Ai-Min Shi et al., leg.; 1♂, Hebei, Wuling Mountain, 1200–1800 m, 5-VII-1963, Sheng-Qiao Jiang, leg.; **Shaanxi:** 2♀♀, 1♂, Shaanxi, Hua Mountain, 9-VI-1936, unknown, leg.; 1♂, 1♀, Shaanxi, Hua Mountain, 1670 m, 29-V-1963, Jin-Long Mao, leg.; 1♂, Shaanxi, Hua Mountain, 1000 m, 10-VII-1972, Shu-Yong Wang, leg.; 1♀, 1♂, Shaanxi, Ningxia Xian, Shibazhang, 1150 m, 28-VI-1999, De-Cheng Yuan, leg.; **Henan:** 1♀, Henan, Luanchuan, Longyuwan, 1000–1400 m, 12-VII-1996, Wan-Zhi Cai, leg.; 2♀♀, Henan, Jigong Mountain, 18-VII-1960, unknown, leg.; 1♂, Henan, Jigong Mountain, 8-VI-1982, unknown, leg.; 1♀, Henan, Jigong Mountain, 8-VI-1982, unknown, leg.; 1♂, Henan, Luoyang, 18-VI-1936, unknown, leg.; **Jiangsu:** 2♂♂, Jiangsu, Nanjing, 6-V-1936, unknown, leg.; 1♂, Jiangsu, Nanjing, 22-VI-1923, unknown, leg.; **Anhui:** 1♀, Anhui, Jinzhai Xian, Baojiawo, Linchang, 524.5 m, 1-VIII-2021, Zheng-Yu Zhao, leg.; **Zhejiang:** 1♀, Zhejiang, Mogan Mountain, 8-V-1935, unknown, leg.; 3♂♂, Zhejiang, Tianmu Mountain, 300–900 m, 24-VI-1957, unknown, leg.; 1♀, Zhejiang, Anji Xian, Longwang Mountain, 450 m, 16-V-1996, Hong Wu, leg.; 1♀, Zhejiang,

Anji Xian, Longwang Mountain, 500 m, 17-V-1996, Hong Wu, leg.; 1♀, Zhejiang, Anji Xian, Longwang Mountain, 500 m, 12-VI-1996, Xing-Ke Yang, leg.; 1♂, Zhejiang, Hangzhou Shi, 12-VI-1954, unknown, leg.; **Hubei**: 1♂, Hubei, Badong, Sanxia, Linchang, 180 m, 27-VI-1993, Wen-Zhu Li, leg.; 2♀♀, Hubei, Zigui Xian, Maoping, 80 m, 28-IV-1994, Jian Yao, leg.; 1♀, Hubei, Zigui Xian, Jiulingtou, 110 m, 1-V-1994, You-Wei Zhang, leg.; 1♀, Hubei, Xingshan, Xiakou, 140 m, 2-V-1994, You-Wei Zhang, leg.; 1♂, Hubei, Badong, Dongxiangkou, 100 m, 14-V-1994, Wen-Zhu Li, leg.; 1♂, Hubei, Zigui Xian, Maoping, 170 m, 28-IV-1994, Wen-Zhu Li, leg.; 7♀♀, 1♂, Hubei, Zigui Xian, Jiulingtou, 100 m, 13-VI-1993, Wen-Zhu Li, leg.; **Jiangxi**: 1♀, Jiangxi, Yishouyuanqian, 9-V-1959, unknown, leg.; **Hunan**: 1♂, Hunan, Yongshun, Shanmuhe, Linchang, 500 m, 7-VIII-1988, Liu Hong, leg.; 1♀, Hunan, Yongshun, Shanmuhe, Linchang, 600 m, 6-VIII-1988, Shu-Yong Wang, leg.; 1♂, Hunan, Nanyue, 1300 m, VII-1963, unknown, leg.; 1♀, Hunan, Zhangjiajie, 16-VII-1988, Yong-Kun Li, leg.; **Fujian**: 1♀, Fujian, Jianyang, Huangkeng, 290–320 m, 2-IV-1960, Fu-Ji Pu, leg.; 1♀, Fujian, Jianyang, Huangkeng, 290–320 m, 6-IV-1960, Fu-Ji Pu, leg.; 1♀, Fujian, Jianyang, Huangkeng, 290 m, 27-III-1960, Sheng-Qiao Jiang, leg.; 1♀, Fujian, Jianyang, Huangkeng, Guilin, 290–400 m, 5-IV-1960, Sheng-Qiao Jiang, leg.; 1♀, Fujian, Jianyang, Huangkeng, Guilin, 290–400 m, 5-IV-1960, Sheng-Qiao Jiang, leg.; 1♀, Fujian, Jianyang, Huangkeng, Guilin, 290 m, 10-IV-1960, Sheng-Qiao Jiang, leg.; 1♂, Fujian, Jianyang, Huangkeng, 290–320 m, 6-IV-1960, Fu-Ji Pu, leg.; 1♂, Fujian, Jianyang, Huangkeng, 290 m, 2-IV-1960, Fu-Ji Pu, leg.; 1♂, Fujian, Jianyang, Huangkeng, Aotou, 950 m, 3-VI-1960, Sheng-Qiao Jiang, leg.; 1♂, Fujian, Jianyang, Huangkeng, Guilin, 290–320 m, 14-IV-1960, Fu-Ji Pu leg.; 1♀, 2♂♂, Fujian, Jianyang, Huangkeng, Guilin, 290 m, 11-IV-1960, Sheng-Qiao Jiang, leg.; **Guangxi**: 2♀♀, 1♂, Guangxi, Guilin, 150 m, 20-V-1963, Yong-Shan Shi, leg.; 1♀, 2♂♂, Guangxi, Longsheng, Sanmen, 300 m, 31-V-1963, leg.; 5♀♀, 6♂♂, Guangxi, Guilin, 150 m, 20-V-1963, Yong-Shan Shi, leg.; 2♀♀, Guangxi, Luoxiang, 200 m, 15-V-1985, Xue-Zhong Zhang, leg.; **Sichuan**: 1♀, Sichuan, Emei Mountain, Baogوسي, 3-VI-1957, Ke-Ren Huang, leg.; 1♀, Sichuan, Emei Mountain, 580 m, 24-VI-1955, Tian-rong Huang, leg.; 1♂, Sichuan, Emei Mountain, 580–650 m, 20-VI-1955, Bing-rong Ou, leg.; 1♀, 4♂♂, Sichuan, Emei Mountain, 580 m, 24-VI-1955, Tian-rong Huang, leg.; 2♂♂, Sichuan, Guan Xian, 700–1000 m, 29-IV-1963, Xue-Zhong Zhang, leg.; 1♂, Sichuan, Xichang, Zhaojue, 2100 m, VI-1998, Rong-Hua Guo, leg.; **Guizhou**: 1♀, Guizhou, Leishan, Taojiang, 1000 m, 5-VII-1988, Long-Long Yang, leg.; 1♂, Guizhou, Leishan, Taojiang, 950 m, 7-VII-1988, Xing-Ke Yang, leg.; 1♀, Guizhou, Huaxi, 20-IV-1948, unknown, leg.; 1♀, Guizhou, Maolan, Xiaoaqikong, 30-V-1998, Liang-Zhang Song, leg.; **Yunnan**: 1♂, Yunnan, Zhenxiong Xian, 1850 m, Jia-Hua Zhen, 11-V-1980, leg. (all IZAS).

Distribution. China: Heilongjiang, Jilin, Liaoning, Gansu, Hebei, Shaanxi, Henan, Jiangsu, Anhui, Zhejiang, Hubei, Jiangxi, Hunan, Fujian, Taiwan, Guangxi, Sichuan, Guizhou, Yunnan.

Host plants. *Reynoutria japonica*, *Fagopyrum esculentum*, *Rumex acetosa*, *Polygonum* sp., *Prunus persica*, *Rheum officinale*, *Polygonum multiflorum*, *Spiraea salicifolia*.

***Gallerucida nigropicta* Fairmaire, 1888**

Fig. 45

Gallerucida nigropicta Fairmaire, 1888: 40. **TL** China: Yunnan; **TD** MNHN.*Eustetha nigropuncta* Fairmaire, 1889: 79. Synonymized by Gressitt and Kimoto 1963: 727.*Gallerucida nigropicta fulvicollis* Laboissière, 1934: 119. Synonymized by Gressitt and Kimoto 1963: 727.*Gallerucida nigropuncta*: Ogloblin 1936: 362, 442.*Gallerucida nigropicta*: Gressitt and Kimoto 1963: 727.**Type material. Syntypes:** labels: CHINA, Yunnan // *Gallerucida / nigropicta / Fairm.* // Ex-Musaeo / L. Fairmaire / 1893. (MNHN).; CHINA, Yunnan // Ex-Musaeo / L. Fairmaire / 1893. (MNHN).**Other material examined (2 spec.).** CHINA: **Guizhou:** 1♂, Guizhou, Guiyang, VI-VII-1981; **Yunnan:** 1♂, Yunnan, Yanjin, Lijiang, Yulong Xueshan, 14-VIII-1979, Ling zuo-pei, leg. (all IZAS).**Distribution.** China: Gansu, Hubei, Sichuan, Guizhou, Yunnan.**Host plant.** *Debregeasia* sp.***Gallerucida ornatipennis* (Duviver, 1885)**

Fig. 46

Hylaspes? Ornatipennis Duviver, 1885: 397. **TL** China; **TD** ISNB.*Eustetha annulipennis* Fairmaire, 1889: 79. Synonymized by Weise 1922: 93.*Eustetha varians* Allard, 1891: 233. Synonymized by Kimoto 1989: 238.*Gallerucida ornatipennis*: Weise 1924: 141.*Gallerucida ornatipennis* var. *decolora* Laboissière, 1934: 120. Synonymized by Wilcox 1971: 205.*Gallerucida ornatipennis* var. *violacea* Laboissière, 1934: 120. Synonymized by Wilcox 1971: 205.*Gallerucida ornatipennis* ab. *Inornana* Mader, 1938: 57. Synonymized by Wilcox 1971: 205.*Gallerucida ornatipennis* ab. *Aeneicollis* Mader, 1938: 57. Synonymized by Laboissière 1940: 23 (= var. *violacea* Laboissière, 1934: 120).*Gallerucida ornatipennis*: Gressitt and Kimoto 1963: 728.**Other material examined (43 spec.).** CHINA: **Guangxi:** 1♂, Guangxi, Linyun Xian, Shali, 28-VIII-1980, unknown, leg.; **Sichuan:** 1♀, Sichuan, Emei Mountain, 10-VI-1955, Ke-Ren Huang & Yin-Tao Jin, leg.; 1♀, Sichuan, Emei Mountain, 760 m, 23-VI-1955, Jin-Hua Li, leg.; 1♀, Sichuan, Emei Mountain, Baoguozi, 550–750 m, 22-VI-1957, You-Cai Lu, leg.; 1♀, Sichuan, Emei Mountain, Qinyinge, 800–1000 m, 22-IV-1957, Ke-Ren Huang, leg.; 1♂, Sichuan, Emei Mountain, 29-VI-1955, Ke-Ren Huang, leg.; 1♂, Sichuan, Emei Mountain, 580–1100 m, 21-VI-1955, Yun-Zhen Zi, leg.; 1♂, Sichuan, Emei Mountain, 580–650 m, 20-VI-1955, Zhong-Lin Ge, leg.; 1♂, Sichuan, Xichang

Xian, 1600 m, 24-IX-1960, Xu-Wu Meng, leg.; **Guizhou**: 2♀♀, Guizhou, Guiyang, Huaxi, 1000 m, 3-VII-2006, De-Yan Ge, leg.; **Yunnan**: 1♀, Yunnan, Fengqing Xian, 1500 m, 2-VII-1980, unknown, leg.; 1♀, Yunnan, Jingdong Xian, 1170 m, 28-VI-1956, Krejanovsky, leg.; 1♀, Yunnan, Jingdong Xian, Dongjiafen, 1250 m, 26-VI-1956, Krejanovsky, leg.; 1♀, Yunnan, Jinping Xian, Mengla, 370 m, 22-IV-1956, Ke-Ren Huang et al., leg.; 1♀, Yunnan, Lunan Yizu Zizhixian, Shilin, 1700 m, 9-VII-1956, Krejanovsky, leg.; 1♀, Yunnan, Qiubei Xian, 1320 m, 12-VII-1979, Wen-Zheng Hu, leg.; 1♂, Yunnan, Jingdong Xian, 1170 m, 27-V-1956, Krejanovsky, leg.; 1♂, Yunnan, Jingdong Xian, 1170 m, 27-V-1956, Krejanovsky, leg.; 1♂, Yunnan, Jingdong Xian, 1170 m, 2-VII-1956, Wei Zhang, leg.; 1♂, Yunnan, Jingdong Xian, 1170 m, 7-VI-1956, Wei Zhang, leg.; 1♂, Yunnan, Jingdong Xian, Dongjiafen, 1250 m, 30-V-1956, Krejanovsky, leg.; 1♂, Yunnan, Jingdong Xian, Dongjiafen, 1250 m, 6-VI-1956, Wei Zhang, leg.; 1♂, Yunnan, Lu Shui, Laowo, 1670 m, 25-VI-1981, Xue-Zhong Zhang, leg.; 1♂, Yunnan, Lunan Yizu Zizhixian, Shilin, 1700 m, 9-VII-1956, Krejanovsky, leg.; 1♂, Yunnan, Wenshan Xian, 18-VII-1958, unknown, leg.; 2♀♀, Yunnan, Jingdong Xian, 1170 m, 4-VII-1956, Krejanovsky, leg.; 2♀♀, Yunnan, Laowo, 1670 m, 25-VI-1981, Shu-Yong Wang, leg.; 2♂♂, Yunnan, Jingdong Xian, Dongjiafen, 1250 m, 5-VI-1956, Krejanovsky, leg.; 2♂♂, Yunnan, Lunan Yizu Zizhixian, Shilin, 1700 m, 9-VII-1956, Krejanovsky leg.; 3♀♀, 6♂♂, Yunnan, Baoshan Xian to Yongping Xian, 28-V-1955, Tian-Rong Huang, leg. (all IZAS).

Distribution. China: Guangxi, Sichuan, Guizhou, Yunnan.

Gallerucida rubrozonata Fairmaire, 1889

Fig. 47

Gallerucida rubrozonata Fairmaire, 1889: 75, 79. **TL** China: Sichuan; **TD** MNHN.

Gallerucida rubrozonata ab. *Atronotata* Fairmaire, 1889: 76. Synonymized by Laboisière 1926: 53.

Gallerucida rubrozonata: Gressitt and Kimoto 1963: 731, fig. 188b.

Type material. **Syntype**: labels: 701 // MUS. HIST. NAT. / A. DAVID / Moupin (Thibet), 1871 // *Gallerucida rubrozonata* Fairm. // Type // Syntype // Syntype // *Gallerucida l rubrozonata* Fairmaire, 1889. (MNHN EC12240).

Other material examined (7 spec.). CHINA: **Yunnan**: 1♂, Yunnan, Lijiang, 18-V-1974, leg.; **Sichuan**: 1♀, Sichuan, Emei Mountain, Jiulaodong, 1800–1900 m, 19-VIII-1957, Zong-Yuan Wang, leg.; 1♀, Sichuan, Emei Mountain, Jiulaodong, 1780 m, 18-VIII-1957, You-Cai Lu, leg.; 1♀, Sichuan, Emei Mountain, Xixiangchi, 1800–2000 m, 8-IX-1957, Ke-Ren Huang, leg.; 1♀, Sichuan, Emei Mountain, Jiulaodong, 1800–2000 m, 17-VIII-1957, You-Cai Lu, leg.; 1♀, Sichuan, Emei Mountain, Xixiangchi, 1800–2000 m, 22-V-1957, You-Cai Lu, leg.; 1♀, Sichuan, Emei Mountain, Qinyingge, 800–1000 m, 30-V-1957, You-Cai Lu, leg. (all IZAS).

Distribution. China: Sichuan, Yunnan (new record).

***Gallerucida sauteri* Chûjô, 1938**

Fig. 48

Gallerucida sauteri Chûjô, 1938: 141. **TL** China: Taiwan; **TD** SDEI.*Gallerucida quadraticollis* Takizawa, 1978: 127. Synonymized by Kimoto and Chu 1996: 92.**Type material. Syntypes.** labels: CHINA, Kankau (Koshun) / Formosa (Taiwan) / H. Sauter V. 1912 // Syntypus // *Gallerucida sauteri* / Chûjô / Det. M. Chûjô // DEI Münchenberg / Col - 09173 / Paralectotypus // *Gallerucida sauteri* / Chûjô, 1938 / des. C. -F. Lee, 2017. (SDEI #303336).; CHINA, Koshun / Formosa (Taiwan) / H. Sauter / VIII. 18 // *Gallerucida sauteri* / Chûjô / Det. M. Chûjô // DEI Münchenberg / Col - 09172 // Paralectotypus // *Gallerucida sauteri* / Chûjô, 1938 / des. C. -F. Lee, 2017. (SDEI #303335).**Distribution.** China: Taiwan.**Host plant.** *Tetrastigma formosanum*.***Gallerucida tenuefasciata* Fairmaire, 1888**

Fig. 49

Gallerucida tenuefasciata Fairmaire, 1888: 40. **TL** China: Yunnan; **TD** MNHN.*Gallerucida potanini* Ogloblin, 1936: 358, 442, 445, fig. Synonymized by Gressitt and Kimoto 1963: 734.*Gallerucida tenuefasciata*: Gressitt and Kimoto 1963: 734, fig. 188c.**Type material. Syntype:** labels: CHINA, Yunnan // *Gallerucida tenuefasciata* / Fairm. // Ex-Musaeo / L. Fairmaire / 1893. (MNHN).**Distribution.** China: Sichuan, Yunnan.***Gallerucida tricolor* Gressitt & Kimoto, 1963**

Fig. 50

Gallerucida tricolor Gressitt & Kimoto, 1963: 736, fig. **TL** China: Yunnan; **TD** NHMB.**Type material. holotype:** labels: CHINA, prov. Yunnan. / Vallis flumin. / Soling-ho. // Holotype ♂ / *Gallerucida tricolor* / Gressitt & Kimoto // Museum Frey / Tutzing // *Gallerucida* / sp. nov. 2 / *tricolor* Hole 161 / Det. S. Kimoto. (NHMB)**Other material examined.** CHINA: **Yunnan:** 1♂, Yunnan, Liusheng, Liude, 2400 m, 18-VIII-1984, Shu-Yong Wang, leg. (IZAS).**Distribution.** China: Yunnan.

Description of new species

Gallerucida fortispina Xu & Yang, sp. nov.

<https://zoobank.org/19F245F1-6963-4917-BDEF-A70E0AA8FE26>

Figs 1–7

Type material. Holotype. CHINA: ♂, Guangxi, Nape, Nongxin / 1000 m / 12-IV-1998, Chao-Dong Zhu, leg. (IZAS).

Paratypes. CHINA: 1♂, Guangxi, Nape, Beidou / 550 m / 12-IV-1998, Chun-Sheng Wu, leg.; 1♂, Guangxi, Nape, Beidou / 550 m / 10-IV-1998, Chao-Dong Zhu, leg.; 1♂, Guangxi, Nape, Beidou / 550 m / 10-IV-1998, Tian-Shan Li, leg. (all IZAS).

Description. Length 7.5–8.0 mm, width 4.0–5.0 mm ($n = 4$, including holotype). Holotype length 7.5 mm, width 4.0 mm

Male: Body oval. General color (Figs 1–3) light yellow; first three segments of antennae yellowish brown, rest brown; head and scutellum black; basal area and apical area of elytra with black bands, epipleura and suture dark brown; meso- and metasternum, abdomen brown except apical of anterior metasternal process light yellow; femora light yellow, tibiae and tarsi brown.

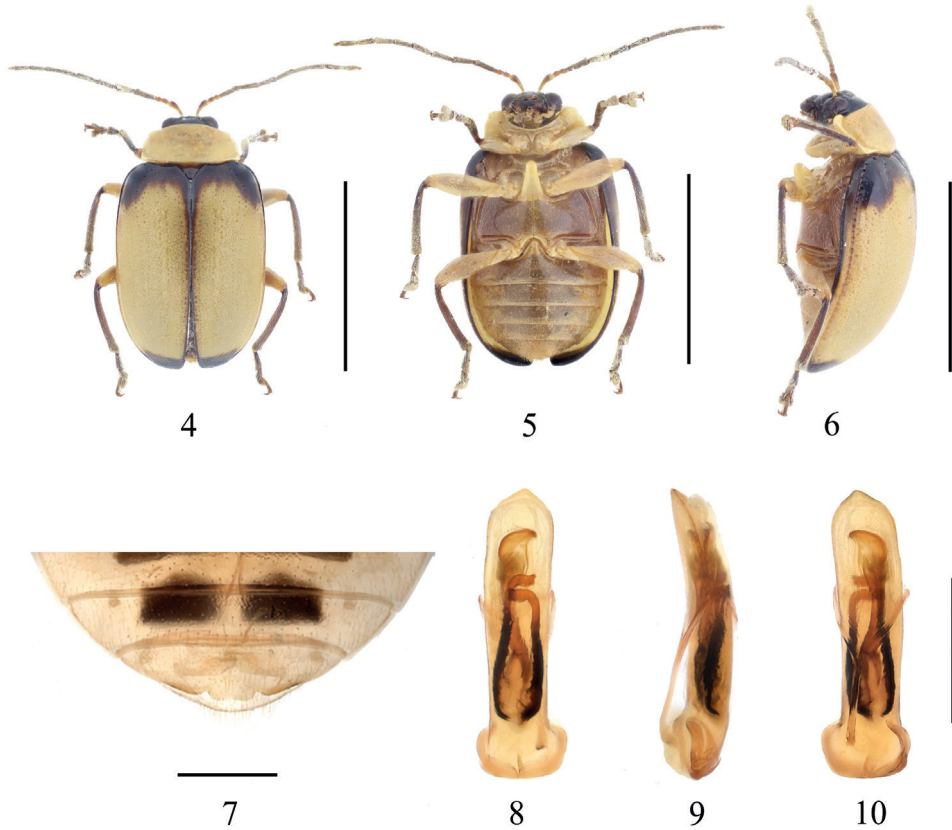
Head distinctly narrower than prothorax; occiput slightly convex, with sparsely punctures; frontoclypeus surface smooth; frontal tubercle developed, triangular. Antennae longer than 1/2 length of elytra, basal three segments moderately shiny, from 4th segment, covered with fine pale hairs; length ratios of antennomeres I–V 1.0: 0.3: 0.3: 1.1: 0.9, in length 3rd and 2nd segment subequal, 4th segment longest, 5th–11th segment subequal. Pronotum transverse, ~ 2.5 × as broad as long; lateral margin subparallel, anterior margin concave, anterior corner indistinct, basal margin convex; disc area impunctate, middle area with a transverse shallow depression. Anterior metasternal process extending obviously beyond the front edge of the meso-coxal cavities, surface smooth. Scutellum triangular, smooth and impunctate. Elytra 1.5 × as long as broad, lateral margin after half evenly narrowing; disc slightly convex, with fine regular punctures, space between punctures larger than the diameter of puncture; epipleura surface smooth. Last sternite of male with distinct trilobite concavities, middle lobate wave-like (Fig. 4).

Aedeagus almost parallel-sided from base to apex in dorsal view, apex obtuse angled, slightly curved towards ventral side; internal sclerites strong (Figs 5–7), median longitudinal sclerite almost reaching apex of aedeagus, with apex enlarged; a pair of lateral longitudinal sclerites, converging apically.

Derivatio nominis. The specific epithet *fortispina* is formed from the Latin adjective *fortis* (strong) and the Latin noun *spina* (spine); it refers to the endophallic sclerite complex.

Distribution. China: Guangxi.

Diagnosis. *Gallerucida fortispina* closely resembles *G. sauteri* Chùjō, but the former has a larger body size, black head, light yellow impunctate pronotum, irregularly punctate elytra, light yellow femora, and metasternal process exceeding mesosternum.



Figures 1–7. *Gallerucida fortispina* sp. nov. **1** dorsal view (paratype) **2** ventral view (paratype) **3** lateral view (paratype) **4** ventral view of 5th ventrite, male (holotype) **5** aedeagus, dorsal view (holotype) **6** ditto, lateral view (holotype) **7** ditto, ventral view (holotype). Scale bars: 5 mm (**1–3**); 1 mm (**4–7**).

***Gallerucida levifasciata* Xu & Nie, sp. nov.**

<https://zoobank.org/8835C446-57D1-4A27-99F9-6DE40573E9D6>

Figs 8–14

Type material. Holotype. CHINA: ♂, Gansu, Gannan / 1992 // unknown, leg. (IZAS).

Paratype. CHINA: 1♂, Gansu, Gannan / 1992 // unknown, leg. (IZAS).

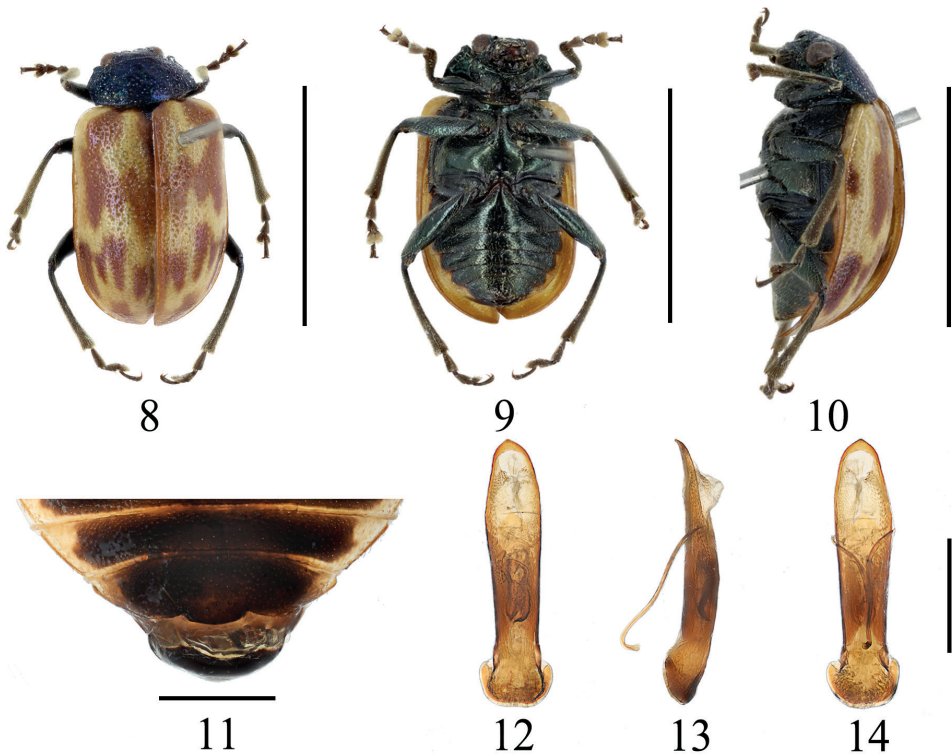
Description. Length 5.5–6.0 mm, width 3.0–3.5 mm ($n = 2$, including holotype). Holotype length 5.5 mm, width 3.0 mm.

Male: Body oval and colorful (Figs 8–10). First three segments of antennae light reddish brown, 4th segment brown, remaining segments lost; head, pronotum and scutellum atropurpureus with metallic luster; elytra and epipleura yellowish brown, elytra with an irregular brown band from scutellum to middle area, and five brown spots after middle distributed in two rows, first row arranged four slight slim brown strips, second row arranged one round brown spot reaching elytron apical area; suture

brown; body ventral surface and femora dark green; apical area of anterior metasternal process, tibiae and tarsi dark brown.

Head distinctly narrower than prothorax; occiput concave, with strong sparsely punctures; frontoclypeus triangular, slightly convex, with punctures; frontal tubercle developed. Antennae (only basal four segments remain) basal three segments moderately shiny, 4th segment covered with fine pale hairs; length ratios of segments I–IV 1.0: 0.3: 0.3: 1.7. Pronotum transverse, ~ 2.3 × as broad as long, lateral margin rounded, anterior margin concave, anterior corner indistinct, basal margin convex, disc area with densely strong punctures. Anterior metasternal process reach apex of the mesocoxal cavities, with punctures. Scutellum triangular, slightly rounded apically, with sparsely punctures. Elytra subparallel-sided, 1.6 × as long as broad; disc slightly convex, two types of irregular punctures in elytra: space between smaller punctures smaller than diameter of puncture, epipleura surface smooth. Last sternite of male with distinctly light trilobite concavities (Fig. 11).

Aedeagus slight broadened in middle area in dorsal view, apex obtuse angled, slightly curved towards ventral side; internal sclerites (Figs 12–14): a pair of lateral sclerites shorter and converging in apical area in dorsal view.



Figures 8–14 *Gallerucida levifasciata* sp. nov. (holotype) **8** dorsal view **9** ventral view **10** lateral view **11** ventral view of 5th ventrite, male **12** aedeagus, dorsal view **13** ditto, lateral view **14** ditto, ventral view. Scale bars: 5 mm (**8–10**); 1 mm (**11–14**).

Derivatio nominis. The specific epithet *levifasciata* is formed from the Latin adjectives *levis* (meaning light) and *fasciata* (banded); named for the irregular light brown band on the elytra adjacent to the scutellum.

Distribution. China: Gansu.

Diagnosis. *Gallerucida levifasciata* closely resembles *G. bifasciata* Motschulsky, but it can be distinguished from the latter by: ventral surface color, scutellum with punctures and elytra with two types of large and small irregular punctures; *G. levifasciata* is also similar to *G. piceufasciata* sp. nov., but the latter has a yellow metasternal process apically and basal abdominal sternite.

***Gallerucida nigrovittata* Xu & Yang, sp. nov.**

<https://zoobank.org/7823DBE0-689D-4441-981D-A7891E8B21C2>

Figs 15–21

Type material. Holotype. CHINA: ♂, Yunnan, Jinping, He-tou-zhai, 2000 m / 10-V-1956 / Ke-Ren Huang et al., leg. (IZAS).

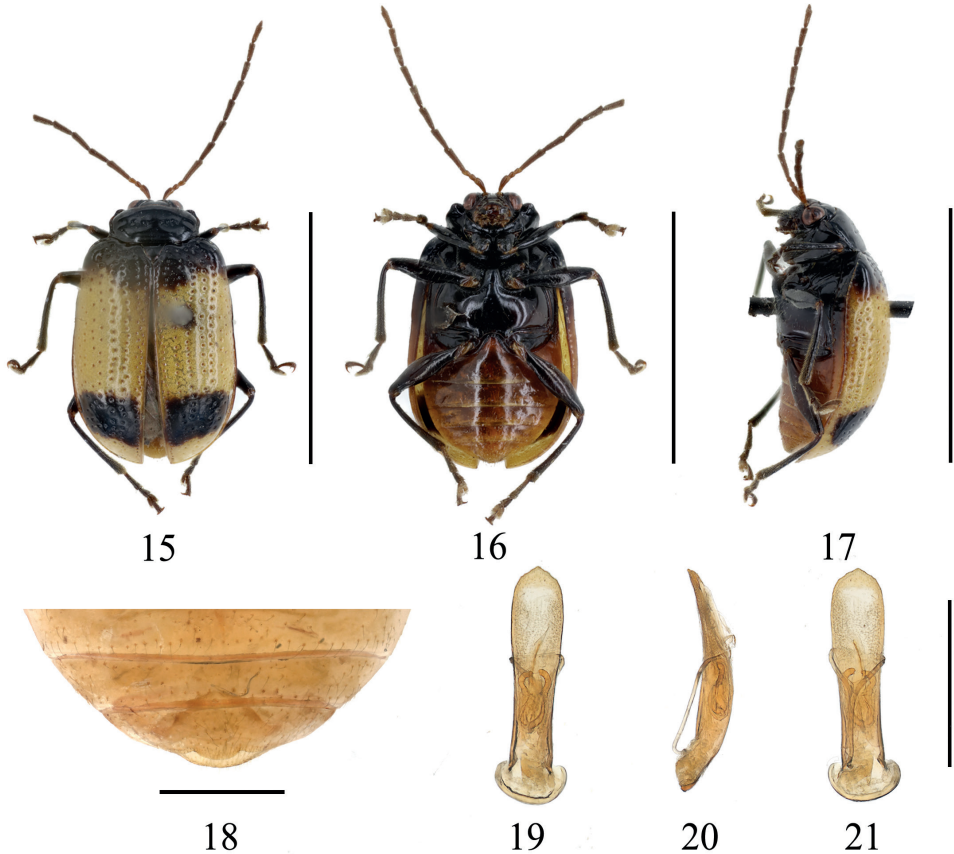
Paratype. CHINA: 3♂♂, Yunnan, Jinping, He-tou-zhai, 2000 m / 10-V-1956 / Ke-Ren Huang et al., leg. (all IZAS).

Description. Length 5.0–5.5 mm, width 3.0–3.5 mm. ($n = 4$, including holotype). Holotype length 5.3 mm, width 3.3 mm.

Male: Body oval. General color (Figs 15–17) black; antennae brown; elytra yellow, basal and subapical area of each elytron with transverse black stripe; 1/3 of epipleura black, rest yellow-brown; meso- and meta- sternum brown or black; ventral surface of abdomen reddish brown; tibiae and tarsi brown or black.

Head narrower than prothorax; occiput distinctly concave, with sparse faint punctures; frontoclypeus surface smooth; frontal tubercle developed, nearly square. Antennae longer than 1/2 length of elytron, basal three segments moderately shiny, from 4th segment, covered with fine pale hairs; length ratios of antennomeres I–V, 1.0: 0.5: 0.5: 2.0: 1.6, 3rd segment and 2nd segment subequal, 4th segment longest, 5th–11th segments subequal. Pronotum transverse, $\sim 2.2 \times$ as broad as long, lateral margin rounded, after middle slight narrow, anterior margin concave, anterior corner distinct, basal margin convex, disc area with a pair of distinct transverse depressions with strong punctures; anterior metasternal process reaching apex of mesocoxal cavities, surface smooth. Scutellum triangular, impunctate. Elytra subparallel-sided, $1.4 \times$ as long as broad, disc slightly convex, with regular punctures, space between punctures larger than diameter of puncture, moderately punctured in rows, ~ 14 rows across central portion. Last sternite of male with slight trilobite concavities (Fig. 18).

Aedeagus slightly broadened in the apical area of dorsal view, apex forming distinct obtuse angle, curved slightly towards ventral side; internal sclerites (Figs 19–21): median sclerite longitudinal, slim in apex, reaching to 2/3 length of aedeagus, a pair of lateral longitudinal sclerites, convergent apically.



Figures 15–21. *Gallerucida nigrovittata* sp. nov. **15** dorsal view (holotype) **16** ventral view (holotype) **17** lateral view (holotype) **18** ventral view of 5th ventrite, male (paratype) **19** aedeagus, dorsal view (paratype) **20** ditto, lateral view (paratype) **21** ditto, ventral view (paratype). Scale bars: 5 mm (**15–17**); 1 mm (**18–21**).

Derivatio nominis. The specific epithet *nigrovittata*, is formed from the Latin adjective *niger* (black) and the Latin adjective *vittata* (banded) referring to the transverse subapical black stripe on the elytron.

Distribution. China: Yunnan.

Diagnosis. *Gallerucida nigrovittata* closely resembles *G. sauteri* Chûjô, but the former differs in having a black pronotum, brown or blackish brown antennae, brown or black meso- and meta- sternum and reddish brown abdomen.

***Gallerucida octodecimpunctata* Xu & Yang, sp. nov.**

<https://zoobank.org/651A3EAF-B572-49B0-9E12-E7DC4DC15681>

Figs 22–28

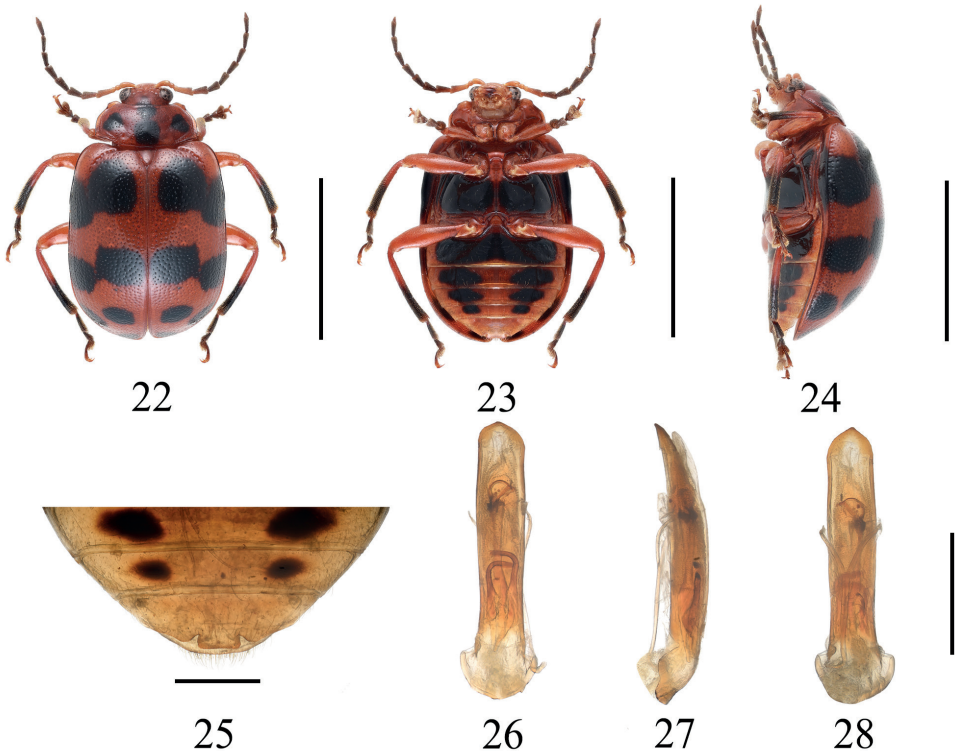
Type material. Holotype. CHINA: ♂, Yunnan, Xishuangbanna, Menglun / 550 m // 15-VII-1959 / Fa-Cai Zhang, leg. (IZAS).

Paratype. CHINA: 1♂, Yunnan, Yiwuzhen / 650 m // 26-VII-1956 / Fa-Cai Zhang leg. (IZAS)

Description. Holotype. Length 7.0 mm, width 4.0 mm.

Male: Body oval. General color (Figs 22–24) red; basal four segments of antennae orange, the rest brown; occiput with a black spot near anterior margin of pronotum; pronotum with four black spots: middle area of disc with two adjacent longitudinal black spots, each side with one round black spot, respectively; elytra with seven rounded black spots, distributed in four rows, arrangement for 2: 2: 2: 1, last one situated at apical area; middle area of epipleura black, rest red; meso - meta sternum black, anterior metasternal process dark red, ventral surface of each visible abdomen except the last one with two black spots; 1/2 of tibiae and tarsi black.

Head distinctly narrower than prothorax, occiput concave, with faintly punctures; frontoclypeus surface smooth; frontal tubercle developed, square. Antennae shorter than 1/2 length of elytra, basal three segments moderately shiny, from 4th segment, covered with short pale hairs; length ratios of antennomeres I–V, 1.0: 0.4: 0.3: 1.2: 1.1, 3rd segment slightly shorter than 2nd segment in length, 5th -11th segments subequal,



Figures 22–28. *Gallerucida octodecimpunctata* sp. nov. **22** dorsal view (paratype) **23** ventral view (paratype) **24** lateral view (paratype) **25** ventral view of 5th ventrite, male (paratype) **26** aedeagus, dorsal view (holotype) **27** ditto, lateral view (holotype) **28** ditto, ventral view (holotype). Scale bars: 5 mm (**22–24**); 1 mm (**25–28**).

the last segment longest. Pronotum transverse, $\sim 2.4 \times$ as broad as long, lateral margin rounded, anterior margin concave, anterior corner indistinct, basal margin convex, disc area with uniformly distributed fine punctures, near lateral margin with shallow inclined depression. Anterior metasternal process reaching apex of mesocoxal cavities, surface smooth, apex square. Scutellum triangular, impunctate. Elytra subparallel-sided, $1.6 \times$ as long as broad, disc slightly convex, disc with uniformly distributed fine punctures, space between punctures larger than the diameter of puncture. Last sternite of male with distinctly trilobite concavities (Fig. 25).

Aedeagus almost parallel-sided from base to apex in dorsal view, apex obtusely angled, slightly curved towards ventral side; internal sclerites (Figs 26–28): median sclerite longitudinal, extending almost to apex of aedeagus, with apex enlarged; a pair of lateral longitudinal sclerites, $\frac{1}{2}$ length of median sclerite, convergent apically.

Derivatio nominis. The specific epithet *octodecimpunctata*, comes from the Latin numeral, *octodecim-* (eighteen) and Latin adjective *punctata* (spotted); it refers to eighteen black spots on the pronotum (4) and elytra (14).

Distribution. China: Guangxi.

Diagnosis. This species is similar to *Gallerucida balyi* (Duvivier), but *G. octodecimpunctata* has brown antennae except the basal segments orange, red femora and black distal $\frac{1}{2}$ of tibiae, while *G. balyi* has antennae total yellowish brown and femora and tibiae yellow.

***Gallerucida piceusfasciata* Xu & Yang, sp. nov.**

<https://zoobank.org/B4EB5AC0-AC8F-41EA-B6BF-C339D4AD58D4>

Figs 29–35

Type material. Holotype. CHINA: ♂, Sichuan, Badan / 19-X-1979 // unknown, leg. (IZAS).

Paratype. CHINA: ♀, Sichuan, Badan / 19-X-1979 // unknown, leg. (IZAS; destroyed).

Description. Length 6.5–6.8 mm, width 3.8 mm ($n = 2$, including holotype). Holotype length 6.8 mm, width 3.8 mm

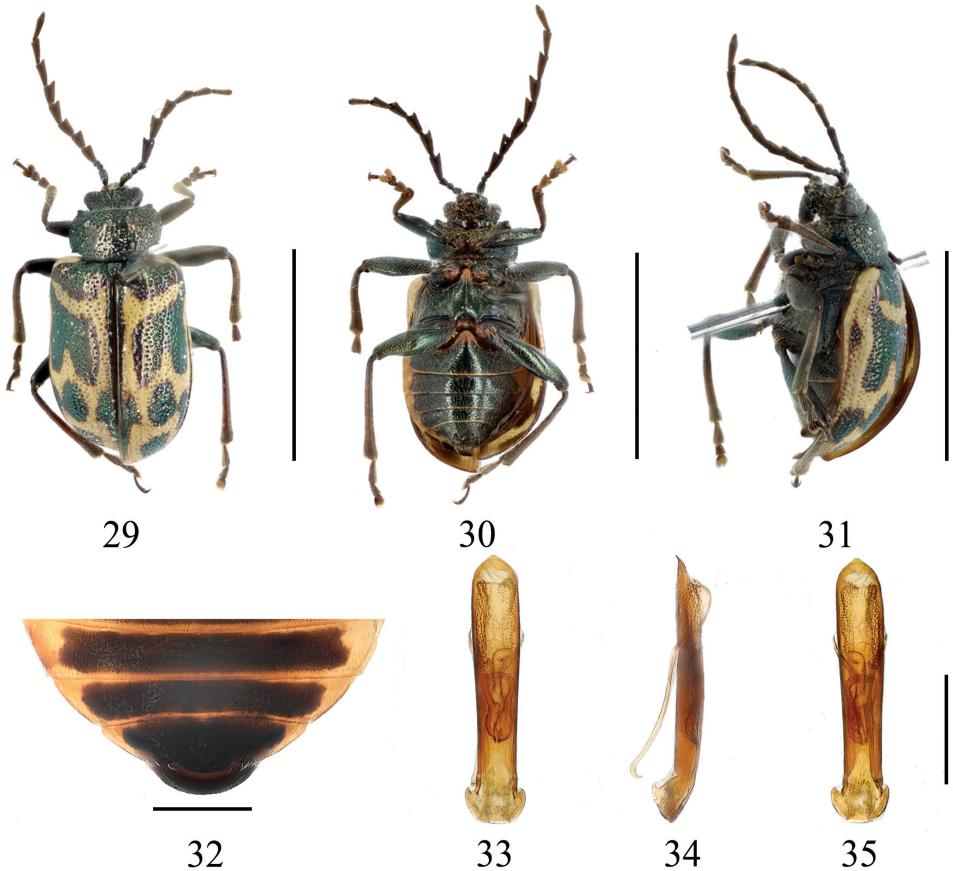
Male: Body oval. General color (Figs 29–31) generally dark green with metallic luster; first three segments of antennae dark green, rest brown; elytra with four pairs of yellow stripes, one pair at elytron humerus, second pair transverse stripe with vertical extension located in $\frac{1}{3}$ elytron, near suture, third pair at middle area forming irregular waved stripes, last pair subapical forming a circle; epipleuron yellow; apical of anterior metasternal process and first visible abdomen sternite yellowish brown; tibiae and tarsi brown.

Head distinctly narrower than prothorax, occiput and frontoclypeus with strong punctures and distinct hairs, frontal tubercle developed. Antennae reaching $\frac{1}{2}$ length of elytron, basal three segments with long hairs, remaining segments covered with short pale hairs; length ratios of antennomeres I–V, 1.0: 0.5: 0.5: 1.6: 1.5, 3rd and 2nd segment subequal in length, length from 4th segment decreased gradually. Pronotum transverse, $\sim 1.8 \times$ as broad as long, lateral margin rounded, anterior margin concave

with dense setae, anterior corner distinct, basal margin convex, posterior corner distinct, disc area with densely strong punctures. Anterior metasternal process not reaching apex of mesocoxal cavities, surface smooth, sides with hairs. Scutellum triangular, rounded apically, with faint punctures. Elytra subparallel-sided, $1.4 \times$ as long as broad, disc slightly convex, with irregular punctures in two sizes, space between smaller punctures little larger the diameter of punctures, space between larger punctures smaller the diameter of punctures. Last sternite of male with shallow trilobite concavities (Fig. 32).

Aedeagus almost parallel-sided from base to apex in dorsal view, apex obtuse angled, slightly curved towards ventral side; internal sclerites (Figs 33–35): median sclerite longitudinal, slight longer than lateral sclerites in length, apically bending; a pair of lateral sclerites close to each other at apical area.

Derivatio nominis. The specific epithet *piceusfasciata*, is formed from the Latin adjectives, *piceus* (dark green) and *fasciata* (banded); referring to the elytra being general dark green with yellow bands.



Figures 29–35. *Gallerucida piceusfasciata* sp. nov. (holotype) **29** dorsal view **30** ventral view **31** lateral view **32** ventral view of 5th ventrite, male **33** aedeagus, dorsal view **34** ditto, lateral view **35** ditto, ventral view. Scale bars: 5 mm (**29–31**); 1 mm (**32–35**).

Distribution. China: Sichuan.

Diagnosis. This species is similar to *Gallerucida bifasciata* Motschulsky. The main differences are the following: *G. piceusfasciata* has subequal 2nd and 3rd antennal segments, sparsely punctured scutellum, and two types of large and small irregular punctures on the elytra.

***Gallerucida rufipectoralis* Xu & Nie, sp. nov.**

<https://zoobank.org/59B59699-ABBD-4DE1-B5E2-F1524C4131CA>

Figs 36–42

Type material. Holotype. CHINA: ♂, Yunnan, Lushui / Laochuang, 2430 m // 19-VI-1981 / Shu-Yong Wang, leg. (IZAS).

Paratypes. CHINA: 3♂♂, Yunnan, Lushui / Laochuang, 2430 m // 19-VI-1981 / Shu-Yong Wang, leg.; 1♂, Yunnan, Yunlongxian / Zhibenshan, 2250 m // 21-VI-1981 / Shu-Yong Wang, leg.; 1♂, Yunnan, Yunlongxian / Zhibenshan, 2550 m // 22-VI-1981 / Shu-Yong Wang, leg.; 1♂, Yunnan, Yunlongxian / Zhibenshan, 2550 m // 22-VI-1981 / Su-Bai Liao, leg. (all IZAS).

Description. Length 5.0–5.5 mm, width 3.0–4.0 mm ($n = 7$, including holotype). Holotype length 5.3 mm, width 3.1 mm.

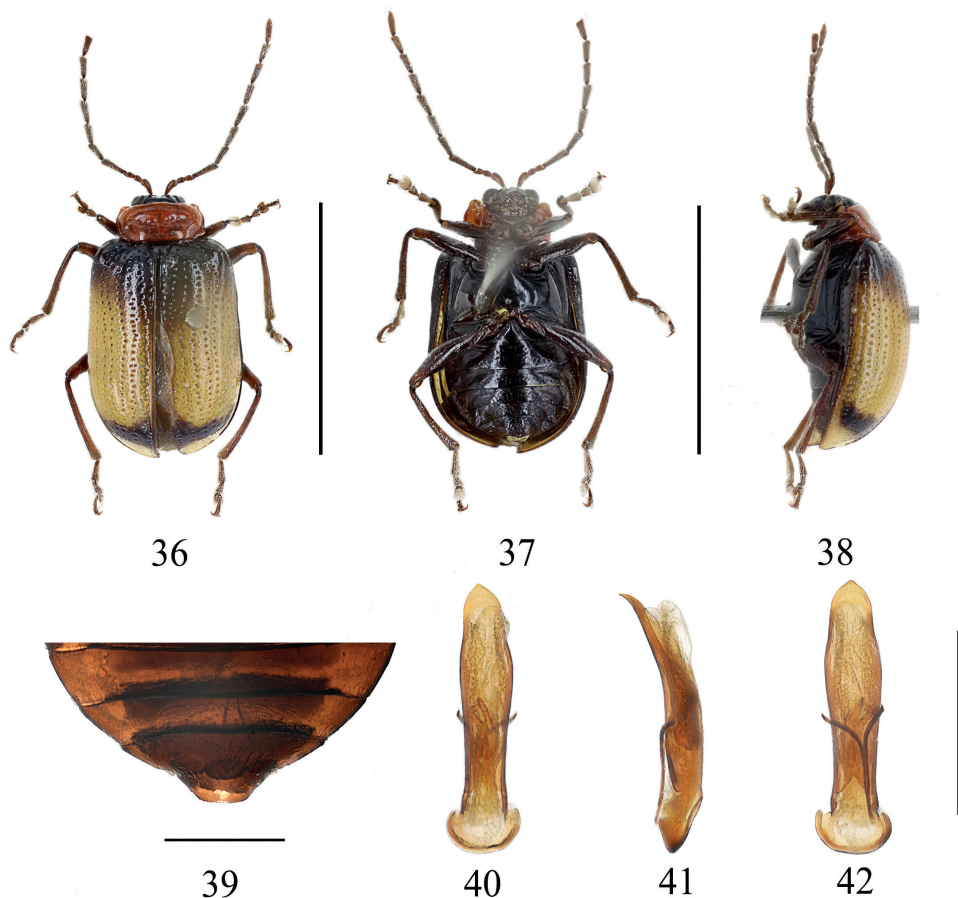
Male: Body oval. General color (Figs 36–38) black; the first three antennal segments light reddish brown, rest brown; pronotum reddish brown; elytra yellowish brown, basal area of elytra with a gradually blurred black band, subapically with a transverse black stripe; epipleura black; femora dark brown, tibiae and tarsi brown.

Head distinctly narrower than prothorax, occiput sparsely punctures, with a transverse depression; frontoclypeus slightly convex, triangular, with sparsely punctures; frontal tubercle developed, rounded. Antennae longer than 1/2 length of elytron, basal three segments moderately shiny, from 4th segment, covered with fine pale hairs; length ratios of antennomeres I–V, 1.0: 0.5: 0.5: 1.6: 1.2, 3rd and 2nd segment subequal in length, 4th segment longest, 5th–11th segments subequal. Pronotum transverse, approximately twice as broad as long, lateral margin subparallel, anterior margin concave, anterior corner indistinct, basal margin convex, disc area with sparse strong punctures and two shallow transverse depressions. Anterior metasternal process not reaching apex of mesocoxal cavities, surface with punctures. Scutellum triangular, surface smooth. Elytra subparallel-sided, 1.6 × as long as broad, disc slightly convex, with regular punctures in nearly 18 rows, space between punctures larger than the diameter of puncture. Last sternite of male with shallow trilobite concavities (Fig. 39).

Aedeagus expanded at 1/2 and 2/3 distance between base to apex, apex sharp in dorsal view, distinctly curved towards ventral side; internal sclerites (Figs 40–42), a pair of sclerites bending apically.

Derivatio nominis. The specific epithet *rufipectoralis*, is formed from the Latin adjectives *rufus* (red) and *pectoralis* (thorax) referring to the pronotum reddish brown.

Distribution. China: Yunnan.



Figures 36–42. *Gallerucida rufispectoralis* sp. nov. **36** dorsal view (holotype) **37** ventral view (holotype) **38** lateral view (holotype) **39** ventral view of 5th ventrite, male (paratype) **40** aedeagus, dorsal view (paratype) **41** ditto, lateral view (paratype) **42** ditto, ventral view (paratype). Scale bars: 5 mm (**36–38**); 1 mm (**39–42**).

Diagnosis. *Gallerucida rufispectoralis* closely resembles *G. sauteri* Chûjô, but the former has dark brown femora, black head and ventral surface, subequal 3rd and 2nd segments of the antennae, and punctured pronotum depression.

***Aplosonyx gansuica* (Chen, 1942), comb. nov.**

Fig. 51

Gallerucida gansuica Chen, 1942: 38. TL China: Gansu; TD IZAS.

Gallerucida gansuica: Gressitt and Kimoto 1963: 724, fig. 188a.

Type material. **Holotype:** labels: CHINA, Gansu / 18-V-1919 // Holotype // IOZ 215680 // *Gallerucida gansuica* / Chen S-H. (IZAS).

Distribution. China: Gansu, Hubei, Sichuan, Guizhou.



43



44



45



46



47



48



49



50



51

Figures 43–51. Habitus. **43** *G. baby* (Paratype, ISNB) **44** *G. bifasciata* (Syntype, MNHN) **45** *G. nigropicta* (Syntype, MNHN) **46** *G. ornatipennis* (identified species) **47** *G. rubrozonata* (Syntype, MNHN) **48** *G. sauteri* (Syntype, SDEI) **49** *G. tenuifasciata* (Syntype, MNHN) **50** *G. tricolor* (Holotype, NHMB) **51** *Aplosonyx ganuica* (Holotype, IZAS). Scale bars: 1 mm.

Acknowledgements

We acknowledge Valérie A. Lemaître and Michael D. Webb (the Natural History Museum, UK) for checking the English and giving useful comments. We thank the Institute of Zoology for providing the specimens. Special thanks to Jan Bezděk (Mendel University, Czech Republic), Antoine Mantilleri (Muséum national d'Histoire Naturelle, France), Christoph Germann (Naturhistorisches Museum, Switzerland), Julien Lalanne (Institut Royal des Sciences naturelles de Belgique, Belgium) and Mandy Schröter (Senckenberg Deutsches Entomologisches Institut, Germany) for providing habitus photographs of some types of *Gallerucida*; Pol Limbourg (Institut Royal des Sciences naturelles de Belgique, Belgium) and Marianna Simões (Senckenberg Deutsches Entomologisches Institut, Germany) for helping to search specimen information, thanks to Michael F. Geiser (the Natural History Museum, UK) for access to borrow types and specimens deposited in the NHMUK. This research was supported by grants from the Biological Resources Program, Chinese Academy of Sciences (No. KFJ-BRP-017-26), the National Science Foundation of China (no. 32170443 and 31772496), and partly by GDAS Special Project of Science and Technology Development (no. 2018GDA-SCX-0107, 2020GDASYL-20200102021, and 2020GDASYL-20200301003). Project of Biological Resources Survey in Wuyishan National Park (HXQT2020120701), the National Science & Technology Fundamental Resources Investigation Program of China (Nos. 2019FY100400, 2019FY101800), the Second Tibetan Plateau Scientific Expedition and Research Program (STEP) (No. 2019QZKK05010101).

References

- Allard E (1891) Collection d'insectes formée dans l'Indo-chine par M. Pavie consul de France au Cambodge. Coléoptères: Phytophages. *Nouvelles Archives du Muséum d'Histoire Naturelle* 3(3): 229–234.
- Baly JS (1861) Descriptions of new Genera and Species of Phytophaga. *Journal of Entomology* 1–2[1860–1862]: 275–302.
- Baly JS (1865) Descriptions of new genera and species of phytophagous. *Transactions of the Entomological Society London* 2(3)[1864–1866]: 427–440. <https://doi.org/10.1111/j.1365-2311.1864.tb00115.x>
- Baly JS (1874) Catalogue of the phytophagous Coleoptera of Japan, with descriptions of the species new to science. *The Transactions of the Entomological Society of London* 1874(2): 161–217. <https://doi.org/10.1111/j.1365-2311.1874.tb00164.x>
- Baly JS (1879) List of the phytophagous Coleoptera collected in Assam by A. W. Chennell, Esp., with notes and descriptions of the uncharacterized genera and species. *Cistula Entomologica* 2: 435–465.
- Baly JS (1890) Descriptions of two new genera and of some uncharacterized species of Gallerucinae. *Entomologist's Monthly Magazine* 26: 12–14.

- Chapuis F (1875) Famille des Phytophages. In: Lacordaire Th, Chapuis F (Eds) Histoire Naturelle des Insectes, Genera des coléoptères ou exposé méthodique et critique de tous les genres proposés jusqu'ici dans cet order d'insectes. Tome onzième. Librairie Enclopédique de Roret, Paris, 420 pp.
- Chen SH (1942) Galerucinae nouveaux de la faune chinoise. Notes d'Entomologie Chinoise 9: 9–67.
- Chûjô M (1935) H. Sauter's. Formosa-Ausbeute: Subfamily Galerucinae (Coleoptera: Chrysomelidae). Arbeiten über Morphologische und Taxonomische Entomologie 2: 160–174.
- Duvivier A (1885) Phytophages exotiques. Entomologische Zeitung (Stettin) 46: 385–400.
- Fairmaire L (1888) Coléoptères de l'intérieur de la Chine (Suite.). Annales de la Société Entomologique de Belgique 32: 7–46.
- Fairmaire L (1889) Coléoptères de l'intérieur de la Chine. 5^e partie. Annales de la Société Entomologique de France 6(9): 5–84.
- Gressitt JL, Kimoto S (1963) The Chrysomelidae (Coleopt.) of China and Korea. Part II. Pacific Insects Monograph 1B: 301–1026.
- Kimoto S (1965) The Chrysomelidae of Japan and the Ryukyu Islands, VII. Subfamily Galerucinae II. Journal of the Faculty of Agriculture, Kyushu University 13(3): 369–400. <https://doi.org/10.5109/22728>
- Kimoto S (1966) A list of the chrysomelid specimens of Taiwan preserved in the Zoological Museum, Berlin. Esakia 5: 21–38. <https://doi.org/10.5109/2351>
- Kimoto S (1989) Chrysomelidae (Coleoptera) of Thailand, Cambodia, Laos and Vietnam. 4. Galerucinae. Esakia 27: 1–241. <https://doi.org/10.5109/2511>
- Laboissière V (1926) Supplement au Catalogus Coleopterorum, Pars 78 (Galerucinae), de Weise J. Precede de remarques sur la classification des Galerucini. Encyclopédie Entomologique I (B) 1925/1926: 38–62.
- Laboissière V (1934) Coléoptères galérucines nouveaux ou peu connus de la faune indo-malaise. Annales de l'Association des Naturalistes de Levallois-Perret 21[1932–1934]: 109–137.
- Laboissière V (1940) Observations sur les Galerucinae des collections du Musée royal d'Histoire naturelle de Belgique et Mémoires de la Société Royale des Sciences de Liège 3(1), xiii + 740 pp (1845); 5, vi + 890 pp (1848).
- Mader L (1938) Neue Coleopteren aus China und Japan nebst Notizen. Entomologisches Nachrichtenblatt 12: 40–61.
- Motschulsky V de (1861) Insects du Japon. Études Entomologiques 9: 22–27.
- Ogloblin DA (1936) Chrysomelidae, Galerucinae. Faune de l'USSR, Insectes Coléoptères 26 (1): [xiv +] 455 pp.
- Takizawa H (1978) Notes on Taiwanese Chrysomelidae. 1. Kontyû 46(1): 123–134.
- Takizawa H (1980) Notes on Korea Chrysomelidae. Nature & Life 19: 67–79.
- Takizawa H (1985) Notes on Korea Chrysomelidae, part 2. Nature & Life 19: 1–18.
- Weise J (1912) Beitrag zur Kenntnis der Chrysomeliden. Archiv für Naturgeschichte 78A(2): 76–98.
- Weise J (1922) Chrysomeliden der Indo-Malayischen Region. Tijdschrift voor Entomologie 65: 39–130.

- Weise J (1924) Chrysomelidae: 13. Galerucinae. In: Schenkling S (Eds) Coleopterorum Catalogus, Pars 78. W. Junk, Berlin, 225 pp.
- Wilcox JA (1971) Chrysomelidae: Galerucinae (Oidini, Galerucini, Metacyclini, Sermlylini). In: Wilcox JA (Eds) Coleopterorum Catalogus Supplementa. Pars 78(1), 2nd Edn. W. Junk, The Netherlands, 200 pp.
- Yang XK, Ge SQ, Nie RE, Ruan YY, Li WZ (2015) Chinese Leaf Beetles. Science Press, Beijing, 500 pp.

Traces of past reintroduction in genetic diversity: The case of the Balkan chamois (Mammalia, Artiodactyla)

Andrea Rezić¹, Toni Safner^{2,3}, Laura Iacolina^{1,4,5}, Elena Bužan^{4,6}, Nikica Šprem¹

1 University of Zagreb, Faculty of Agriculture, Department of Fisheries, Apiculture, Wildlife Management and Special Zoology, Svetošimunska c. 25, 10000, Zagreb, Croatia **2** University of Zagreb, Faculty of Agriculture, Department of Plant Breeding, Genetics and Biometrics, Svetošimunska c. 25, 10000, Zagreb, Croatia **3** Centre of Excellence for Biodiversity and Molecular Plant Breeding (CoE CroP-BioDiv), Svetošimunska c. 25, 10000, Zagreb, Croatia **4** University of Primorska, Faculty of Mathematics, Natural Sciences and Information Technologies, Department of Biodiversity, Glagoljaška 8, 6000, Koper, Slovenia **5** Aalborg University, Department of Chemistry and Bioscience, Section of Biology and Environmental Science, Fredrik Bajers Vej 7H, 9220 Aalborg East, Denmark **6** Faculty of Environmental Protection, Trg mladosti 2, 3320, Velenje, Slovenia

Corresponding author: Andrea Rezić (arezic@agr.hr)

Academic editor: Jesus Maldonado | Received 29 March 2022 | Accepted 20 July 2022 | Published 4 August 2022

<https://zoobank.org/C44362F1-DFAC-40A4-9C01-35E71B74FDA1>

Citation: Rezić A, Safner T, Iacolina L, Buzan E, Šprem N (2022) Traces of past reintroduction in genetic diversity: the case of the Balkan chamois (Mammalia, Artiodactyla). ZooKeys 1116: 57–70. <https://doi.org/10.3897/zookeys.1116.84577>

Abstract

The translocation of wild animal species became a common practice worldwide to re-establish local populations threatened with extinction. Archaeological data confirm that chamois once lived in the Biokovo Mountain but, prior to their reintroduction in the 1960s, there was no written evidence of their recent existence in the area. The population was reintroduced in the period 1964–1969, when 48 individuals of Balkan chamois from the neighbouring mountains in Bosnia and Herzegovina were released. The main objective of this study was to determine the accuracy of the existing historical data on the origin of the Balkan chamois population from the Biokovo Mountain and to assess the genetic diversity and population structure of the source and translocated populations 56 years after reintroduction. Sixteen microsatellite loci were used to analyse the genetic structure of three source chamois populations from Prenj, Čvrsnica and Čabulja Mountains and from Biokovo Mountain. Both STRUCTURE and GENELAND analyses showed a clear separation of the reintroduced population on Biokovo from Prenj's chamois and considerable genetic similarity between the Biokovo population and the Čvrsnica-Čabulja population. This suggests that the current genetic composition of the Biokovo population does not derive exclusively from

Prenj, as suggested by the available literature and personal interviews, but also from Čvrsnica and Čabulja. GENELAND analysis recognised the Balkan chamois from Prenj as a separate cluster, distinct from the populations of Čvrsnica and Čabulja. Our results thus highlight the need to implement genetic monitoring of both reintroduced and source populations of endangered Balkan chamois to inform sustainable management and conservation strategies in order to maximise the chances of population persistence.

Keywords

Biokovo, genetic structure, microsatellite, Prenj, translocation

Introduction

The reintroduction and translocation of wild species for various purposes became a common practice worldwide and was used as a conservation tool for rescuing and re-establishing extirpated populations (Cullingham and Moehrenschrager 2013). Northern chamois (*Rupicapra rupicapra* L.) is one of the examples of successfully translocated species (Apollonio et al. 2014) in many areas of Europe (Crestanello et al. 2009; Martínková et al. 2012; Šprem and Buzan 2016), but also on other continents such as South America (Corlatti et al. 2011) and New Zealand (Christie 1964). Past translocations of chamois left a genetic signature in recent populations which can be now used for reconstructing undocumented events (Crestanello et al. 2009).

Today's populations of the Northern chamois in northern Dinaric Mountains in Croatia are descendants of successfully translocated individuals captured on mountain areas in Bosnia and Herzegovina (*Rupicapra rupicapra balcanica*) and Slovenia (*Rupicapra rupicapra rupicapra*) (Apollonio et al. 2014; Šprem and Buzan 2016). Since different subspecies were involved in past reintroduction efforts, a contact zone was formed on the northern Velebit Mountains where these subspecies hybridise (Šprem and Buzan 2016).

The Balkan chamois (*Rupicapra rupicapra balcanica*) is one of the seven recognised subspecies of the Northern chamois. It is found both in the mountainous regions of Croatia and in the mountain ranges of the eight other countries of the Balkan Peninsula, from north to south: Bosnia and Herzegovina, Serbia, Montenegro, Kosovo, North Macedonia, Albania, Bulgaria, and Greece. The lack of continuity of these habitats and overhunting in the post-Neolithic period have severely fragmented the subspecies' present distribution (Corlatti et al. 2022). In addition to low colonisation rates and reduced gene flow between isolated populations, which may lead to genetic differentiation due to the inbreeding effect and loss of allelic variants, the Balkan chamois is threatened by poaching (Papaioannou and Kati 2007), habitat change (Kavčić et al. 2019), unsustainable hunting (Šprem and Buzan 2016) and by the introduction of Alpine chamois subspecies (Iacolina et al. 2019). As a conservation measure, the Balkan chamois is listed in Annexes II and IV of the European Union Habitats Directive 92/43/EEC (OJ L 206, 22.7.1992) and in Appendix III of the Bern Convention (OJ L 38, 10.2.1982). The Balkan chamois is one of the most poorly studied subspecies of Northern chamois and

knowledge on the genetic diversity and structure of the Balkan chamois population is limited and restricted to regional-local studies (Markov et al. 2016; Šprem and Buzan 2016; Papaioannou et al. 2019; Rezić et al. 2022).

The genetic structure of the Balkan chamois population on the Biokovo has been studied only by Šprem and Buzan (2016), and few other ecological studies have included this population in a population density estimation (Kavčić et al. 2021a) and rutting behaviour (Kavčić et al. 2021b). The study of phylogenetic relationships in Šprem and Buzan (2016) revealed the existence of endemic Balkan haplotypes in the Prenj and Biokovo Mountains and a genetic richness of the historically viable Prenj population comparable to Alpine chamois studied in Buzan et al. (2013) from the south-eastern Alps. The paleontological findings in the Baba cave, which are more than ten thousand years old, confirm that chamois once lived in Biokovo (Šabić 2011) but, before the reintroduction in the 1960s, there was no written evidence of the recent existence of chamois in this area. According to historical records, the chamois on Biokovo Mt. are descendants of individuals translocated from the “Prenj” hunting district in Bosnia and Herzegovina established in 1961 (Rapaić and Kunovac 2020) which included both Prenj and Čvrsnica massifs. This hunting district had, at that time, stable and numerous chamois populations and was used for many reintroduction programmes in the Balkans (Rapaić and Kunovac 2020). The reintroduction of chamois on Biokovo Mt. was the result of the planned introduction on this area by the Union of Hunting Association, the municipality of Makarska and the Union of Hunting Association of Imotski, mainly with the aim of increasing the population size for hunting purposes (Šabić 2011). Prior to the reintroduction from the “Prenj” hunting district, assessment of the suitability of the Biokovo habitat was made and, after a positive evaluation, a first release of 7 individuals (3 males and 4 females) took place on 1 November 1964 (Šabić 2014). A total of 48 chamois was successfully reintroduced in the period between 1 November 1964 and 23 October 1969 (Šabić 2014). The success of the reintroduction of the Balkan chamois in the Biokovo Mt. is reflected by the latest population size estimate (Kavčić et al. 2021a), according to which this area is now inhabited by at least 600 individuals.

The main objective of this study was to determine the accuracy of historical data on the origin of chamois in Biokovo, and to assess and document the genetic status of both the source and translocated populations, 56 years after reintroduction, by using microsatellite markers.

Materials and methods

Ethical statement

All samples used in this study were from hunted (regular hunting activities approved by the competent Ministry of Agriculture of the Republic of Croatia within the annual game management plans) and from remains of naturally dead animals (samples from Bosnia and Herzegovina).

Population sampling

We collected 20 samples from Biokovo and 29 samples from three areas which serve as source populations for reintroduction and possible recent recolonisation (Preanj, Čvrsnica, and Čabulja Mountains). Details of sampling locations are given in Fig. 1 and Table 1. The samples were collected between 2017 and 2020. After collection, the samples were preserved in 96% ethanol, delivered and stored at $-80\text{ }^{\circ}\text{C}$ in the Laboratory of molecular ecology, University of Primorska.

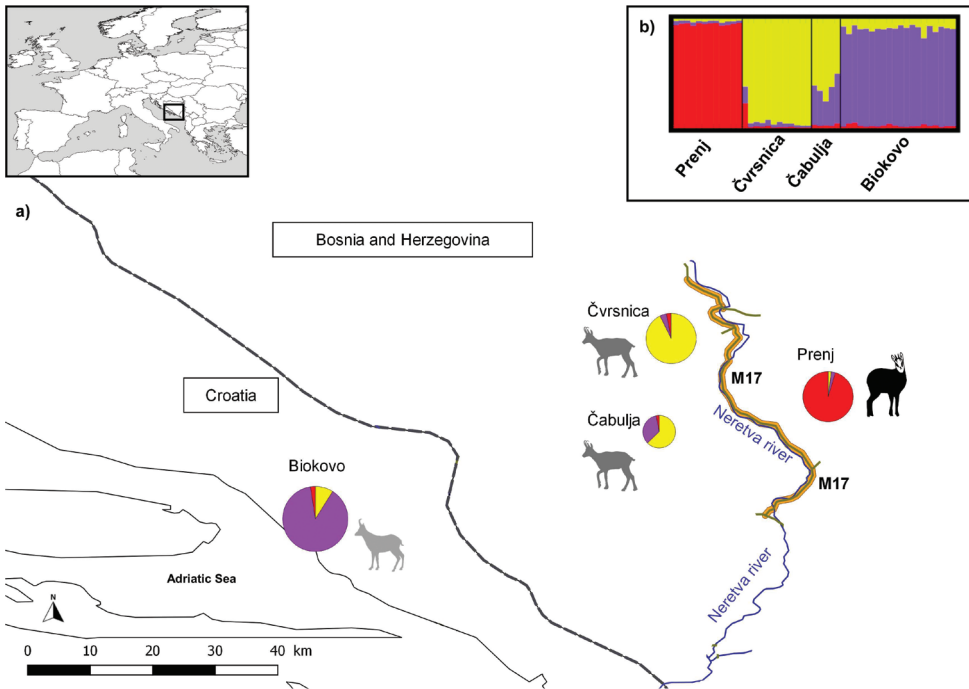


Figure 1. Results of the analysis of sixteen microsatellite loci in four Balkan chamois populations **a** geographical representation of results from STRUCTURE and GENELAND software. The pie charts show the results from STRUCTURE for $K = 3$. The different colours of the pie charts represent the proportions of each ancestral genotype per individual q (in %) in each of the four predefined Balkan chamois populations. The size of the pie charts indicates the number of samples collected at each location. The different shapes and colours of the chamois silhouettes represent the results of the spatial analysis under uncorrelated frequency model performed in GENELAND. The three spatial clusters are shown, while the assignment to the fourth ghost cluster was not shown because no individuals were assigned to it (see text for details). The dashed line indicates the national border, while the state road M17 in Bosnia and Herzegovina is marked with an orange line. The green lines represent connections with other main roads. The course of the river Neretva is marked by a blue line **b** genetic structure of the 49 Balkan chamois individuals analysed, shown as a bar plot from STRUCTURE at $K = 3$. Each vertical bar represents an individual, and the percentage of each colour corresponds to the percentage of the respective ancestral genotype. The studied populations are separated by a black line.

Table 1. Genetic diversity of four Balkan chamois populations assessed using sixteen microsatellite loci.

Population locality/ country	<i>N</i>	H_o (SD)	H_e (SD)	HWE	F_{IS} (IC 95%)	<i>A</i>	<i>AR</i>	N_{pr}	N_e (IC 95%)
Prenj 43°32'03"N, 17°54'12"E/BIH	12	0.636 (0.274)	0.637 (0.150)	0.013*	0.046 (-0.147–0.116)	4.500	2.517	11	10.500 (6.500–18.600)
Čvrsnica 43°38'18"N, 17°38'30"E/BIH	12	0.552 (0.287)	0.536 (0.206)	0.011 ^{NS}	0.014 (-0.131–0.038)	3.937	2.223	3	7.700 (4.100–13.600)
Čabulja 43°29'11"N, 17°37'20"E/BIH	5	0.575 (0.251)	0.535 (0.187)	0.913 ^{NS}	0.059 (-0.415–0.089)	3.375	2.376	2	–
Biokovo 43°19'47"N, 17°63'05"E/HRV	20	0.584 (0.132)	0.597 (0.138)	0.389 ^{NS}	0.048 (-0.050–0.084)	4.625	2.356	6	57.200 (28.600–371.800)

BIH – Bosnia and Herzegovina, HRV – Croatia; *N* – number of samples; H_o – observed heterozygosity; H_e – expected heterozygosity; SD – standard deviation; F_{IS} – inbreeding coefficient; IC 95% – 95% Confidence Interval; HWE – Hardy-Weinberg equilibrium (after Bonferroni adjustment *p* values: ^{NS} – non-significant value; * – significant at *p* < 0.05); *A* – average number of alleles; *AR* – allelic richness; N_{pr} – number of private alleles; N_e – effective population size and its confidence interval estimated with the chi-square (i.e., parametric).

DNA extraction and microsatellite amplification

We extracted DNA from tissue samples (*N* = 49) using the commercial peqGOLD Tissue DNA Mini Kit (PEQLAB Biotechnologie GmbH) following the manufacturer's protocol in a final volume of 150 µL. DNA concentrations were measured with Qubit dsDNA BR Assay Kit (Invitrogen BR Assay Kit, Carlsbad, CA, USA) on a 3.0 Qubit Fluorimeter (Life Technologies, Carlsbad, CA, USA). Sixteen microsatellites were amplified using PCR multiplex sets previously investigated in studies with chamois (Zemanová et al. 2011; Buzan et al. 2013; Šprem and Buzan 2016; see Suppl. material 1: Table S1). The PCR protocol described in Rezić et al. (2022) was used for amplification of microsatellite regions. Genotyping errors were assessed by re-genotyping of ten randomly chosen individuals from the final data set and comparing these genotypes to the initial ones. Fragment analysis was performed on an ABI 3130 Genetic Analyzer (Applied Biosystems) using the GeneScan LIZ500 (-250) Size Standard (Applied Biosystems). Microsatellite genotypes were analysed using Gene Mapper v. 4.0 software (Applied Biosystems).

Microsatellite data analysis

We used the Expectation-Maximization (EM) algorithm implemented in FREENA (Chapuis and Estoup 2007) to estimate null allele frequencies for each microsatellite locus, as they can cause significant heterozygote deficit and population deviation from Hardy-Weinberg equilibrium (HWE). Values of null allele frequency greater than *r* ≥ 0.20 were reported (see Suppl. material 1: Table S2). FREENA software was also used to calculate global F_{ST} values and F_{ST} values for each pair of analysed populations, both with and without the use of the excluding null alleles (ENA) correction method, as described in Chapuis and Estoup (2007). The Wilcoxon Two Sample test was used to compare the corrected F_{ST} values with the original F_{ST} values and to test the signifi-

cance of null alleles in the analyses. The Wilcoxon Two Sample test was performed in R ver. 4.0.5 package stats (R Core Team 2020).

We considered each sampling location as a separate population due to limited dispersal of subspecies between mountain ranges (see Table 1). The exact probability test for each locus and population was used to test the deviation of the observed genotype frequency from HWE using the Markov chain method with 10,000 dememorisation steps, 500 batches and 10,000 subsequent iterations in GENEPOP ver. 4.7.2 (Rousset 2008). The same test, based on a Markov chain method implemented in Genepop, was used to analyse pairwise linkage disequilibrium (LD) between all pairs of loci in all populations. A sequential Bonferroni procedure (Holm 1979) was applied to correct for the effect of multiple comparison tests by using the adjust p -values function implemented in R ver. 4.0.5 package stats.

GENETIX ver. 4.05.2 (Belkhir et al. 1996–2004) was used to calculate the mean number of alleles, observed (H_O) and expected (H_E ; Nei 1978) heterozygosity for each locus in all populations, and the inbreeding coefficient (F_{IS}) and its confidence intervals. The number of private alleles was estimated using the GENALEX ver. 6.502 (Peakall and Smouse 2012). We estimated allele richness in each population using the rarefaction procedure implemented in FSTAT ver. 2.9.3.2 (Goudet 2001). The same software was used to analyse the level of genetic differentiation between sampling populations (pairwise F_{ST}) and calculate their respective p -values using 1000 permutations.

The Bayesian clustering program STRUCTURE ver. 2.3.4. (Pritchard et al. 2000) was used to estimate the most likely number of ancestral genotypes (K) within the entire sample, and to estimate the proportions of each ancestral genotype in Balkan chamois individuals. We ran the analysis allowing for admixture and correlated allele frequency with ten independent runs for each K between 1 and 7 with a burn-in 500,000 steps followed by 10^5 Markov chain Monte Carlo (MCMC) iterations. The results of the repeated runs for each value of K were combined with the Greedy algorithm in CLUMPP v. 1.1.2 (Jakobsson and Rosenberg 2007), and the summary outputs were visualised with DISTRUCT v. 1.1 (Rosenberg 2004). To estimate the most likely K , we applied the ad hoc summary statistic ΔK developed by Evanno et al. (2005). STRUCTURE HARVESTER (Earl and vonHoldt 2012) was used to compare the average estimates of the likelihood of the data, $\ln[\Pr(X|K)]$ for each value of K . The same software was used to generate graphs for the mean log posterior probability of the data (mean \pm SD).

The modal proportions of ancestral genotypes for each individual in each sampled area from the run with the highest log-likelihoods was plotted on a map using QGIS ver. 2.18.21 (QGIS Development Team 2018). We estimated the effective population size (N_e) using the linkage disequilibrium-based method (Hill 1981; Waples 2006; Waples and Do 2010) implemented in NeESTIMATOR V2 (Do et al. 2014). Rare alleles below an allele frequency of 0.02 were excluded (as recommended by Waples and Do 2010). The effective population size for Čabulja Mt. was not calculated due to the small sample size.

The robustness of the results of STRUCTURE was estimated by analysing the same data with the spatial Bayesian clustering model implemented in GENELAND

software (Guillot et al. 2005a). Although there are several Bayesian clustering methods that perform spatial analysis of genetic data, GENELAND was chosen because it provides the most accurate estimates of true genetic structure (Safner et al. 2011). We followed the recommendations of Guillot et al. (2005a) to set up the analysis. The algorithm was run in two steps. In the first step, the algorithm was run ten times to infer K under the uncorrelated frequency model, with the parameter indicating the degree of uncertainty of the spatial coordinates set to 10. The MCMC iterations were set to 10^6 with a thinning of 100. The number of populations was set from $K = 1$ to $K = 5$. The maximum number of nuclei in the Poisson-Voronoi tessellation was set to 300. After determining the number of population clusters in the first step, we ran the algorithm setting K to this number and leaving the other parameters as in the first step.

Results and discussion

The sixteen microsatellite loci yielded a total of 95 alleles, which varied between 2 (for locus ETH10 and SR-CRSP-6) and 10 (for locus BM1258) with an average value of 5.937 alleles per locus (see Suppl. material 1: Table S1).

The values of null allele frequencies were low for most analysed loci, except for loci ETH10, SY434, TGLA53, and SR-CRSP-6, whose frequencies were estimated to be $r \geq 0.20$ (see Suppl. material 1: Table S2). The presence of null alleles was found in all three populations from Bosnia and Herzegovina. The various factors caused by natural population mechanisms, such as disassortative mating, bottleneck, fluctuations in population size, can cause heterozygote deficit that can be interpreted as false positive presence of null alleles (Dąbrowski et al. 2014), which led to the decision to retain all analysed loci.

The Prenj population deviated from Hardy-Weinberg equilibrium (HWE) but the deviation was significant at the 0.05 level only for locus SY434 after applying sequential Bonferroni adjustment (Table 1). This may be a consequence of the recent severe bottleneck in this population, which was previously stable. Gafić and Džeko (2009) noted that the population of Balkan chamois in the Prenj hunting district, which included both the Prenj and Čvrsnica massifs, was approximately 4,000 individuals in 1966, but due to the civil war in the 1990s, the population was greatly reduced by illegal hunting, with up to 95% of the population lost. Since no deviation from HWE was observed at this locus in other populations, we retained it in all subsequent analyses. After applying the sequential Bonferroni correction to the linkage disequilibrium results, no significant value was observed.

The Prenj population had the highest values of observed (0.636) and expected (0.637) heterozygosity, and allelic richness (2.517). A similar pattern was recorded in the study of Šprem and Buzan (2016) where the Prenj population had the highest values of allelic richness, observed, and expected heterozygosity and significantly deviated from HWE. In the Šprem and Buzan (2016) study, the Biokovo population had the lowest allelic richness. The observed number of alleles (A) varied from 3.375 in the

Čabulja population to 4.625 in the Biokovo population. All populations had private alleles (N_p) and the highest number of private alleles (11) was observed in the Prenj population from Bosnia and Herzegovina (Table 1).

Effective population size was estimated for three sampled sites, excluding the Čabulja population due to small sample size (Table 1). Čvrsnica had the lowest results for N_e , although very similar to those estimated for Prenj. The higher estimates for the Biokovo population should be taken with caution, considering our results suggest the presence of multiple funding sources. Additionally, Do et al. (2014) showed that microsatellite loci could lead to a slight upward bias for the linkage disequilibrium method when the critical value is set to $p = 0.02$.

The lowest F_{ST} value was found between Čvrsnica and Čabulja ($F_{ST} = 0.024$), while the highest and significant F_{ST} value (0.084) was observed between two neighbouring populations from Bosnia and Herzegovina (Prenj and Čvrsnica; Table 2). The global F_{ST} values were 0.067 ($CI = 0.031–0.108$) without using the correction method and 0.071 ($CI = 0.038–0.112$) with the ENA correction method for null alleles. The Wilcoxon Two Sample test showed no significant differences between the corrected and original F_{ST} values ($p = 0.734$), indicating that the presence of putative null alleles did not affect the analysis (see Suppl. material 1: Fig. S1).

The algorithm developed by Evanno et al. (2005) identified $K = 3$ as the optimal number of ancestral genotypes detected by STRUCTURE analysis for four analysed populations and detected another peak at $K = 5$ suggesting a possible further genetic structure subdivision within the populations (see Suppl. material 1: Fig. S2). According to STRUCTURE results, populations from Prenj, Čvrsnica, and Biokovo had high proportions of genomes from a single ancestral genotype ($q \geq 0.88$ in all three populations), which for Prenj differ from Čvrsnica and Biokovo, while in the population from Čabulja the highest proportion of same ancestral genotype as in Čvrsnica was lower ($q = 0.63$; Fig. 1a). The difference in genetic composition between Balkan chamois from Prenj and other populations is likely due to a barrier to gene flow between the studied populations, but also probably a consequence of recent bottleneck effect, due to extirpation of chamois during the Balkan civil war (Frković 2008) and population local adaptation. Čvrsnica, Čabulja, and Prenj Mts. are restricted to habitat patches, particularly by the steep river canyon of Neretva, which might lead to their fine-scale fragmentation. The Neretva River, one of the largest rivers in the eastern part of the Adriatic Basin, separates the Prenj Mt. from the Čvrsnica and Čabulja Mts. and forms the official border between the “Čvrsnica” and “Prenj” game reserves (Jurić 1998). Landscape features of the Neretva River valley, as well as the adjacent road M17, built

Table 2. Pairwise F_{ST} values between four studied populations of Balkan chamois.

Populations	Čvrsnica	Čabulja	Biokovo
Prenj	0.084*	0.047 ^{NS}	0.074*
Čvrsnica		0.024 ^{NS}	0.072*
Čabulja			0.027 ^{NS}

p values: ^{NS} – non – significant value; * – significant at $p < 0.05$.

as a part of the European Route E73, can act as effective barriers for the species natural dispersal, and hinder gene exchange between the studied populations (Soglia et al. 2010; Buzan et al. 2013). Additionally, the population decline in the last Balkan civil war could have contributed by isolating small groups of chamois to restricted habitat patches, although geographically very close to each other. Individual proportions of ancestral genotypes assigned by STRUCTURE support the higher levels of admixture in Čabulja when compared to the other populations (Fig. 1b). According to the q values, only one individual from Čabulja had a q value above the threshold of 0.75 sharing similar genotype as individuals from the Čvrstica population, while all others had admixed genotype ($q < 0.70$). One individual from Čvrstica stood out from the others with a $q = 0.23$ proportion of ancestral genotype that was present mostly in Prenj population. As previously mentioned, natural migration between individuals from Prenj and Čvrstica is currently unlikely, due to the presence of barriers, however this might not have been the case before the construction of the road infrastructure. STRUCTURE indicated that the reintroduced Balkan chamois population in the Biokovo Mt. is genetically more similar to the population from Čabulja, suggesting that the reintroduced individuals in the Biokovo Mt. may originate from this area, as well as from Čvrstica, whereas animals translocated from Prenj did not leave detectable genetic signatures. According to Jurić (1998), 992 individuals of Balkan chamois were counted in the Čvrstica hunting ground which also includes the territories of the neighbouring Čabulja Mt. It is possible that populations Čvrstica and Čabulja were connected in the past and formed a single population, as can be inferred from the results of STRUCTURE. Due to the civil war in the Balkans in the 1990s and continued illegal hunting and poaching, this single population has dwindled in numbers and become fragmented and isolated in the high mountain habitats (statements of local people). The divergence between Prenj and Biokovo from Čvrstica and Čabulja populations may be due to the historical founder effect and more recent genetic drift due to isolation, and local adaptation. Despite decades of long unsustainable hunting, predation, poaching and natural events (Šprem and Buzan 2016) the inbreeding levels in the analysed populations are still moderate. The results of genetic composition of Biokovo population can influence population viability through time and it is very important to monitor genetic parameters of the reintroduced population to prevent a loss of genetic diversity due to inbreeding and genetic drift (DeMay et al. 2017).

To improve the previous analyses, the spatial context of individuals was taken into consideration and tested with GENELAND. This analysis revealed a similar pattern of clustering of individuals as STRUCTURE, but suggested an additional fourth spatial cluster along the MCMC chain (see Suppl. material 1: Fig. S3). GENELAND detected two spatial clusters among the three analysed populations in Bosnia and Herzegovina, while one spatial cluster corresponded to the population in Biokovo (Fig. 1). The distinction between Prenj and Biokovo was also detected by Šprem and Buzan (2016), who used the BAPs algorithm for spatial clustering of groups and showed the separation of the Balkan chamois population of the Prenj Mt. from the Biokovo Mt. population. The fourth cluster revealed by

GENELAND spatial model was a so-called “ghost cluster” (Frantz et al. 2009) since no individual was assigned to it. Ghost clusters are not uncommon but are still a poorly understood phenomenon that can be caused by a heterogeneous distribution of samples (Aziz et al. 2018). It is possible that all the clusters identified by GENELAND represent a true genetic subdivision, but the degree of differentiation between them was too low for the clustering to be consistent (Frantz et al. 2009). Another possibility is that the GENELAND model might overestimate the number of genetic clusters when analysing populations which are affected by isolation by distance (Frantz et al. 2009).

Future studies will need to incorporate non-invasive genetic sampling, telemetry and behavioural patterns to confirm possible migration and gene flow between these populations. In the available literature there is no indication of the exact location where the animals released on Biokovo were caught. It is only known that the individuals came from the Prenj hunting district, which included two game reserves called “Čvrsnica” and “Prenj” (established in 1893 by the Austro-Hungarian Empire) and which were declared protected areas (Rapačić and Kunovac 2020). Jurić (1998) stated in his master’s thesis that the translocation of Balkan chamois from the game reserve “Čvrsnica” began in 1962 and lasted until 1970. During this period, a total of 101 Balkan chamois was translocated to different areas in the Balkans, but the author did not write any additional information about the location where the animals were caught or the places where they were translocated. It is not yet known whether these data exist. Therefore, it is very important to establish standards for documenting and monitoring species translocation projects.

Conclusions

Non-invasive monitoring of genetic parameters of both reintroduced and source populations of endangered Balkan chamois, together with demographic monitoring, is crucial for sustainable management practices and improving conservation strategies to maximise the chances of population persistence. Our genetic diversity results show that the Balkan chamois population from Biokovo can serve as a potential source for future translocations, especially to the source habitats, Čvrsnica and Čabulja, that are currently threatened by loss of genetic diversity due to unsustainable hunting and poaching, leading to inbreeding and genetic drift.

Acknowledgments

We thank Luca Corlatti for permission to use his drawing (the silhouettes of the chamois yearling). This work was supported by the Croatian Science Foundation [grant number IP 2016-06-5751] and the ResBios European Union’s Horizon 2020 Research and Innovation Program [grant number 872146].

References

- Apollonio M, Scandura M, Šprem N (2014) Reintroductions as a Management tool for European Ungulates. In: Putman R, Apollonio M (Eds) Behaviour and Management of European Ungulates. Whittles Publishing, Dunbeath, Caithness, 46–77.
- Aziz MA, Smith O, Barlow A, Tollington S, Islam Md A (2018) Do rivers influence fine-scale population genetic structure of tigers in the Sundarbans? *Conservation Genetics* 19(5): 1137–1151. <https://doi.org/10.1007/s10592-018-1084-5>
- Belkhir K, Borsa P, Chikhi L, Raufaste N, Bonhomme F (1996-2004) GENETIX 4.05, logiciel sous Windows TM pour la génétique des populations. Laboratoire Génome, Populations, Interactions, CNRS UMR 5000, Université de Montpellier II, Montpellier (France). <http://www.genetix.univmontp2.fr/genetix/intro.htm>
- Buzan VE, Bryja J, Zemanová B, Kryštufek B (2013) Population genetics of chamois in the contact zone between the Alps and the Dinaric Mountains: Uncovering the role of habitat fragmentation and past management. *Conservation Genetics* 14(2): 401–412. <https://doi.org/10.1007/s10592-013-0469-8>
- Chapuis MP, Estoup A (2007) Microsatellite null alleles and estimation of population differentiation. *Molecular Biology and Evolution* 24(3): 621–631. <https://doi.org/10.1093/molbev/msl191>
- Christie AHC (1964) A note on the chamois in New Zealand. *Proceedings (MDPI)* 11: 32–36. <http://www.jstor.org/stable/24061467> [New Zealand Ecological Society]
- Corlatti L, Lorenzini R, Lovari S (2011) The conservation of the chamois *Rupicapra* spp. *Mammal Review* 41(2): 163–174. <https://doi.org/10.1111/j.1365-2907.2011.00187.x>
- Corlatti L, Iacolina L, Safner T, Apollonio M, Buzan E, Ferretti F, Hammer S, Herrero J, Rossi L, Serrano E, Arnal MC, Brivio F, Chirichella R, Cotza A, Espunyes J, Fernández de Luco D, Gačić D, Grassi L, Grignolio S, Hauffe HC, Kavčić K, Kinser A, Lioce F, Malagnino A, Miller C, Pokorný B, Reiner R, Rezić A, Stipoljev S, Tešija T, Yankov Y, Zwijacz-Kozica T, Šprem N (2022) Past, present, and future of chamois science. *Wildlife Biology* 01025(4). <https://doi.org/10.1002/wlb3.01025>
- Crestanello B, Pecchioli E, Vernesi C, Mona S, Martínková N, Janiga M, Hauffe HC, Bertorelle G (2009) The genetic impact of translocations and habitat fragmentation in chamois (*Rupicapra*) spp. *The Journal of Heredity* 100(6): 691–708. <https://doi.org/10.1093/jhered/esp053>
- Cullingham CI, Moehrenschrager A (2013) Temporal analysis of genetic structure to assess population dynamics of reintroduced swift foxes. *Conservation Biology* 27(6): 1389–1398. <https://doi.org/10.1111/cobi.12122>
- Dąbrowski MJ, Pilot M, Kruczyk M, Żmihorski M, Umer HM, Gliwicz J (2014) Reliability assessment of null allele detection: Inconsistencies between and within different methods. *Molecular Ecology Resources* 14(2): 361–373. <https://doi.org/10.1111/1755-0998.12177>
- DeMay SM, Becker PA, Rachlow JL, Waits LP (2017) genetic monitoring of an endangered species recovery: Demographic and genetic trends for reintroduced pygmy rabbits (*Brachylagus idahoensis*). *Journal of Mammalogy* 98(2): 350–364. <https://doi.org/10.1093/jmammal/gyw197>

- Do C, Waples RS, Peel D, Macbeth GM, Tillett BJ, Ovenden JR (2014) NeEstimator V2: Re-implementation of software for the estimation of contemporary effective population size (N_e) from genetic data. *Molecular Ecology Resources* 14(1): 209–214. <https://doi.org/10.1111/1755-0998.12157>
- Earl DA, vonHoldt BM (2012) STRUCTURE HARVESTER: A website and program for visualizing STRUCTURE output and implementing the Evanno method. *Conservation Genetics Resources* 4(2): 359–361. <https://doi.org/10.1007/s12686-011-9548-7>
- Evanno G, Regnaut S, Goudet J (2005) Detecting the number of clusters of individuals using the software STRUCTURE: A simulation study. *Molecular Ecology* 14(8): 2611–2620. <https://doi.org/10.1111/j.1365-294X.2005.02553.x>
- Frantz AC, Cellina S, Krier A, Schley L, Burke T (2009) Using spatial Bayesian methods to determine the genetic structure of a continuously distributed population: Clusters or isolation by distance? *Journal of Applied Ecology* 46(2): 493–505. <https://doi.org/10.1111/j.1365-2664.2008.01606.x>
- Frković A (2008) Reintroduction of chamois in Northern Velebit. *Sumarski List* 11–12: 543–550. [In Croatian with English summary.]
- Gafić M, Džeko Š (2009) *Prenj*. Turistička zajednica Kantona Sarajevo, Sarajevo, Bosnia and Herzegovina. [In Bosnian.]
- Goudet J (2001) FSTAT. A program for Windows to estimate and test gene diversities and fixation indices. Version 2.9.4. www.unil.ch/izea/software/fstat.html
- Guillot G, Estoup A, Mortier F, Cosson JF (2005a) A spatial statistical model for landscape genetics. *Genetics* 170(3): 1261–1280. <https://doi.org/10.1534/genetics.104.033803>
- Hill WG (1981) Estimation of effective population size from data on linkage disequilibrium. *Genetical Research Cambridge* 38(3): 209–216. <https://doi.org/10.1017/S0016672300020553>
- Holm S (1979) A simple sequentially rejective multiple test procedure. *Scandinavian Journal of Statistics* 6: 65–70.
- Iacolina L, Corlatti L, Buzan E, Safner T, Šprem N (2019) Hybridisation in European ungulates: An overview of the current status, causes, and consequences. *Mammal Review* 49(1): 45–59. <https://doi.org/10.1111/mam.12140>
- Jakobsson M, Rosenberg NA (2007) CLUMPP: A cluster matching and permutation program for dealing with label switching and multimodality in analysis of population structure. *Bioinformatics (Oxford, England)* 23(14): 1801–1806. <https://doi.org/10.1093/bioinformatics/btm233>
- Jurić I (1998) *Revitalizacija lovno – turističkog područja “Čvrsnica”*. Master Thesis, University of Zagreb, Zagreb, Croatia. [in Croatian]
- Kavčić K, Ugarković D, Šabić B, Krupec I, Malnar J, Šprem N (2019) Forest succession as a possible factor on chamois population density: Biokovo Mountain as case study. In: Mioč B, Širić I (Eds) *Proceedings, 54th Croatian & 14th International Symposium on Agriculture*. University of Zagreb Faculty of Agriculture, Zagreb, 378–383.
- Kavčić K, Palencia P, Apollonio M, Vicente J, Šprem N (2021a) Random encounter model to estimate density of mountain-dwelling ungulate. *European Journal of Wildlife Research* 67(5): e87. <https://doi.org/10.1007/s10344-021-01530-1>

- Kavčić K, Apollonio M, Corlatti L, Šprem N (2021b) Rutting behavior of male Balkan chamois. *Mammalian Biology* 101(6): 895–905. <https://doi.org/10.1007/s42991-021-00141-2>
- Markov G, Zhelev P, Ben Slimen H, Suchentrunk F (2016) Population genetic data pertinent to the conservation of Bulgarian chamois (*Rupicapra rupicapra balcanica*). *Conservation Genetics* 17(1): 155–164. <https://doi.org/10.1007/s10592-015-0768-3>
- Martínková N, Zemanová B, Kranz A, Giménez MD, Hájková P (2012) Chamois introductions to Central Europe and New Zealand. *Folia Zoologica* 61(3–4): 239–245. <https://doi.org/10.25225/fozo.v61.i3.a8.2012>
- Nei M (1978) Estimation of average heterozygosity and genetic distance from a small number of individuals. *Genetics* 89(3): 583–590. <https://doi.org/10.1093/genetics/89.3.583>
- Papaioannou H, Kati V (2007) Current status of the Balkan chamois (*Rupicapra rupicapra balcanica*) in Greece: Implications for conservation. *Belgian Journal of Zoology* 137: 33–39.
- Papaioannou H, Fernández M, Pérez T, Domínguez A (2019) Genetic variability and population structure of chamois in Greece (*Rupicapra rupicapra balcanica*). *Conservation Genetics* 20(4): 939–945. <https://doi.org/10.1007/s10592-019-01177-1>
- Peakall R, Smouse PE (2012) GenAlEx 6.5: Genetic analysis in Excel. Population genetic software for teaching and research - an update. *Bioinformatics* 28(19): 2537–2539. <https://doi.org/10.1093/bioinformatics/bts460>
- Pritchard JK, Stephens M, Donnelly P (2000) Inference of population structure using multilocus genotype data. *Genetics* 155(2): 945–959. <https://doi.org/10.1093/genetics/155.2.945>
- QGIS Development Team (2018) QGIS Geographic Information System. Open Source Geospatial Foundation Project. <http://qgis.osgeo.org>
- R Core Team (2020) R: A language and environment for statistical computing. R Foundation for Statistical Computing, Vienna, Austria. <https://www.R-project.org/>
- Rapačić Ž, Kunovac S (2020) Translocation of chamois – the greatest achievement in history of Bosnia-Herzegovina game management. *Nase Sume* 17: 35–49.
- Rezić A, Iacolina L, Bužan E, Safner T, Bego F, Gačić D, Maletić V, Markov G, Milošević D, Papaioannou H, Šprem N (2022). The Balkan chamois, an archipelago or a peninsula? Insights from nuclear and mitochondrial DNA. *Conservation Genetics* 23: 527–539. <https://doi.org/10.1007/s10592-022-01434-w>
- Rosenberg NA (2004) DISTRUCT: A program for the graphical display of population structure. *Molecular Ecology Notes* 4(1): 137–138. <https://doi.org/10.1046/j.1471-8286.2003.00566.x>
- Rousset F (2008) GENEPOP '007: A complete re-implementation of the GENEPOP software for Windows and Linux. *Molecular Ecology Resources* 8(1): 103–106. <https://doi.org/10.1111/j.1471-8286.2007.01931.x>
- Šabić FV (2011) Chamois in the Nature Park Biokovo. In: Protrka K, Škrabić H, Srzić S (Eds) Book of abstracts. Scientific and professional meeting “Biokovo at the turn of the millennium - the development of Nature Park in the 21st century”, Makarska (Croatia), November 2011. Public institution “Nature Park Biokovo”, Makarska, 16 pp.
- Šabić FV (2014) Pedeseta obljetnica naseljavanja divokoza na masiv planine Biokova. Kratki osvrt o provedenim planovima i radnjama te postignuim rezultatima u proteklih 50 godina. *Sumarski List* 9–10: 505–508. [in Croatian]

- Safner T, Miller MP, McRae BH, Fortin MJ, Manel S (2011) Comparison of Bayesian clustering and edge detection methods for inferring boundaries in landscape genetics. *International Journal of Molecular Sciences* 12(2): 865–889. <https://doi.org/10.3390/ijms12020865>
- Soglia D, Rossi L, Cauvin E, Citterio C, Ferroglio E, Maione S, Meneguz PG, Spalenza V, Rasero R, Sacchi P (2010) Population genetic structure of Alpine chamois (*Rupicapra r. rupicapra*) in the Italian Alps. *European Journal of Wildlife Research* 56(6): 845–854. <https://doi.org/10.1007/s10344-010-0382-0>
- Šprem N, Buzan E (2016) The genetic impact of chamois management in the Dinarides. *The Journal of Wildlife Management* 80(5): 783–793. <https://doi.org/10.1002/jwmg.21081>
- Waples RS (2006) A bias correction for estimates of effective population size based on linkage disequilibrium at unlinked gene loci. *Conservation Genetics* 7(2): 167–184. <https://doi.org/10.1007/s10592-005-9100-y>
- Waples RS, Do C (2010) Linkage disequilibrium estimates of contemporary Ne using highly variable genetic markers: A largely untapped resource for applied conservation and evolution. *Evolutionary Applications* 3(3): 244–262. <https://doi.org/10.1111/j.1752-4571.2009.00104.x>
- Zemanová B, Hájková P, Bryja J, Zima Jr J, Hájková A, Zima J (2011) Development of multiplex microsatellite sets for non-invasive population genetic study of the endangered Tatra chamois. *Folia Zoologica* 60(1): 70–80. <https://doi.org/10.25225/fozo.v60.i1.a11.2011>

Supplementary material I

Tables and figures

Authors: Andrea Rezić, Toni Safner, Laura Iacolina, Elena Bužan, Nikica Šprem

Data type: Population genetics.

Explanation note: **Table S1**. Information about microsatellite primer sequences used for the analysis of Balkan chamois population genetics. **Table S2**. Locus/population matrix containing null alleles identified by the FreeNA software. Null allele frequencies were estimated using the EM algorithm. Frequencies with values higher than $r \geq 0.20$ were indicated. **Figure S1**. The comparison of two groups of F_{ST} values (original pairwise F_{ST} values and ENA-corrected pairwise F_{ST} values) using the Wilcoxon Two Sample test. **Figure S2**. Evanno method (Evanno et al. 2005) for selecting the representative number of clusters (K). **Figure S3**. Number of clusters along the MCMC chain for spatial analysis performed with the GENELAND software.

Copyright notice: This dataset is made available under the Open Database License (<http://opendatacommons.org/licenses/odbl/1.0/>). The Open Database License (ODbL) is a license agreement intended to allow users to freely share, modify, and use this Dataset while maintaining this same freedom for others, provided that the original source and author(s) are credited.

Link: <https://doi.org/10.3897/zookeys.1116.84577.suppl1>

A new species of the long-tailed wasp genus *Eurobracon* Ashmead (Hymenoptera, Braconidae, Braconinae) from Java, Indonesia, is described and the type species redescribed

Donald L. J. Quicke¹, Dian Gafar², Kyohei Watanabe³, Buntika A. Butcher¹

1 Integrative Ecology Laboratory, Department of Biology, Faculty of Science Chulalongkorn University, Bangkok 10330, Thailand **2** Bandung, West Java, Indonesia **3** Kanagawa Prefectural Museum of Natural History, Iryuda 499, Odawara, Kanagawa 250-0031, Japan

Corresponding author: Buntika A. Butcher (buntika.a@chula.ac.th)

Academic editor: Kees van Achterberg | Received 30 March 2022 | Accepted 3 May 2022 | Published 5 August 2022

<http://zoobank.org/9F5E5B88-E192-4A73-9D85-728FC7CAB44F>

Citation: Quicke DLJ, Gafar D, Watanabe K, Butcher BA (2022) A new species of the long-tailed wasp genus *Eurobracon* Ashmead (Hymenoptera, Braconidae, Braconinae) from Java, Indonesia, is described and the type species redescribed. ZooKeys 1116: 71–83. <https://doi.org/10.3897/zookeys.1116.84593>

Abstract

A new species, *Eurobracon bhaskarai* Quicke, **sp. nov.**, from West Java, Indonesia, is described, illustrated and differentiated from other members of the genus. It is closely related to the type species of the genus, *E. yokahamae* Dalla Torre, 1898, which is known from China, India, Japan, Laos, South Korea and Thailand. *Eurobracon yokahamae* is redescribed and illustrated for comparative purposes. The two species are separable mainly on colouration, but differ markedly based on their mitochondrial gene sequences (cytochrome c oxidase I, cytochrome b and 16S rDNA). The slower-evolving nuclear 28S rDNA and elongation factor 1-alpha did not differentiate *E. bhaskarai* **sp. nov.** from *E. yokahamae*, but consistently split *Eurobracon* into two species groups.

Keywords

16S, COI, cytochrome b, DNA sequences, Japan, mitochondrial genes, molecular analysis, Oriental, parasitoid wasp

Introduction

Some of the largest braconid parasitoid wasps belong to the braconine genus *Euurobracon* Ashmead, 1900, which is distributed from the East Palaearctic (China, Japan, Korea), throughout the Oriental region (India, Sri Lanka and South East Asia) and reaches the Australasian region (Papua New Guinea) (Quicke 1989a). Female body length reaches 21 mm and their ovipositors can be up to 18.8 cm long. The genus comprised a total of 14 described species (Li et al. 2016; Yu et al. 2016), of which 11 were included in the revision by Quicke (1989a) and three more from China that were added by Li et al. (2016). Despite its wide distribution, only four species have been recorded from Indonesia: *E. cephalotes* (Smith, 1858) (Java, Sumatra and N. Mollucas), *E. forticornis* (Cameron, 1905) (Sumatra and N. Mollucas), *E. impossibilis* (Dalla Torre, 1898) (N. Mollucas), and *E. denticephalus* Quicke, 1989 (Irian Jaya). However, *E. interstitialis* Quicke, 1989 which is known from Sarawak and Sabah on Borneo Island must surely also occur in that country. Of these, only *E. cephalotes* has previously been recorded from Java (Yu et al. 2016).

By far the best-known species is *E. yokahamae* which is relatively common in Japan and has a remarkably long ovipositor. Despite its impressive size we present the first molecular data for this species. *Euurobracon yokahamae* has been recorded in the literature as parasitising two species of cerambycid beetles, *Batocera lineolata* Chevrolat, 1852 (Watanabe 1934; repeated in Shenefelt 1978) and of the pupa of *Neocerambyx raddei* Blessig & Solsky, 1872 (syn. *Massicus raddei* (Blessig & Solsky, 1872)) (Kaga et al. 2018; Cao et al. 2020). However, Kaga et al. (2018) strongly infer that the record from *Batocera* is incorrect because the beetle's ecology makes this unsuitable to be a host. *Euurobracon yokahamae* adults overwinter in wood (e.g., *Quercus serrata* and *Castanea crenata*). Kaga et al. (2018) noted that oviposition occurs by inserting the ovipositor into cracks in the wood and suggest that it is highly unlikely that they lay eggs directly on the host. The sex ratio is approximately one for specimens extracted from wood prior to emergence but that of individuals collected/observed in the field is markedly female-biased, with males being rare. This might be due to males being short-lived and/or being less conspicuous. In Japan, *E. yokahamae* adults are observed in the fields from late spring to early summer (late April to early June).

Here we describe a new species from West Java (Indonesia), *E. bhaskarai* Quicke sp. nov., and differentiate it from the closely related *E. yokahamae* on the basis of colour pattern, morphology and DNA sequence data for three mitochondrial genes.

Material and methods

Materials

Terminology follows van Achterberg (1988) except for wing venation nomenclature which follows Sharkey and Wharton (1997); see also figure 2.2 in Quicke (2015) for comparison of wing venation naming systems. Specimens of *E. bhaskarai* sp. nov. were photographed using a Leica M205 C microscope. Images were prepared by image stacking using Leica Application Suite (LAS).

Abbreviations

CUMZ	Entomological Museum, Chulalongkorn University, Bangkok;
KPM-NK	Kanagawa Prefectural Museum of Natural History, Japan;
MZB	Museum Zoologicum Bogoriense (Zoological Museum), Indonesian Institute of Sciences, Bogor, Indonesia.

Molecular methods

DNA sequences were generated for the barcoding region of cytochrome oxidase c subunit 1 (COI), cytochrome b (cytb), 16S rDNA (16S), elongation factor 1-alpha (EF-1 α), and the D2-D3 expansion region of 28S rDNA (28S) for four specimens of *E. bhaskarai* Quicke sp. nov., five specimens of *E. yokahamae* (deposited in KPM-NK), and one each of *E. breviterebrae* (deposited in KPM-NK), and *E. cephalotes* (deposited in CUMZ). An additional COI barcode for *E. breviterebrae* was obtained from GenBank.

A combined barcoding and phylogenetic rapid bootstrap tree was generated using the maximum likelihood program RAxML (Stamatakis 2014). Combined sequences from two species of the putatively closely related Afrotropical genus *Archibracon* Saussure, (1890) 1892, (Quicke 1989b) were used to root the tree.

Gene sequences are deposited on GenBank and accession numbers are given in Table 1.

Results

Molecular analysis

No intraspecific variation was present in any of the gene fragments. All genes recovered the phylogeny: ((*bhaskarai* sp. nov. + *yokahamae*) (*cephalotes* + *breviterebrae*)) (Fig. 1). All mitochondrial genes separated *E. bhaskarai* sp. nov. from *E. yokahamae* with high bootstrap support (96–100%). The two species differed by 16 bases in the CO1 gene (2.5%), by 13 bases in the cytb gene (3.37%) and by 10 indels in the 16S gene (2.37%).

Table 1. GenBank accession numbers for newly generated sequences.

Taxon	BOLD process ID	GenBank accession numbers				
		COI	cytb	16S	28S	EF-1 α
<i>Archibracon</i> sp.	BBTH2575-21	OM950937	OM950960	OM952149	OM950949	–
<i>E. bhaskarai</i> sp. nov.	BBTH2844-21	OM950947	OM950970	OM952159	OM950958	OM950980
<i>E. bhaskarai</i> sp. nov.	BBTH2843-21	OM950940	OM950963	OM952152	OM950951	OM950974
<i>E. bhaskarai</i> sp. nov.	BBTH2841-21	OM950939	OM950962	OM952151	OM950950	OM950973
<i>E. bhaskarai</i> sp. nov.	BBTH2678-21	OM950944	OM950967	OM952156	OM950955	OM950977
<i>E. bhaskarai</i> sp. nov.	BBTH2840-21	OM950948	OM950971	OM952160	OM950959	OM950981
<i>E. breviterebrae</i>	BBTH2845-21	OM950942	OM950965	OM952154	OM950953	OM950975
<i>E. cephalotes</i>	BBTH2676-21	OM950943	OM950966	OM952155	OM950954	OM950976
<i>E. yokahamae</i>	BBTH2842-21	OM950938	OM950961	OM952150	–	OM950972
<i>E. yokahamae</i>	BBTH2839-21	OM950941	OM950964	OM952153	OM950952	–
<i>E. yokahamae</i>	BBTH2677-21	OM950945	OM950968	OM952157	OM950956	OM950978
<i>E. yokahamae</i>	BBTH2846-21	OM950946	OM950969	OM952158	OM950957	OM950979

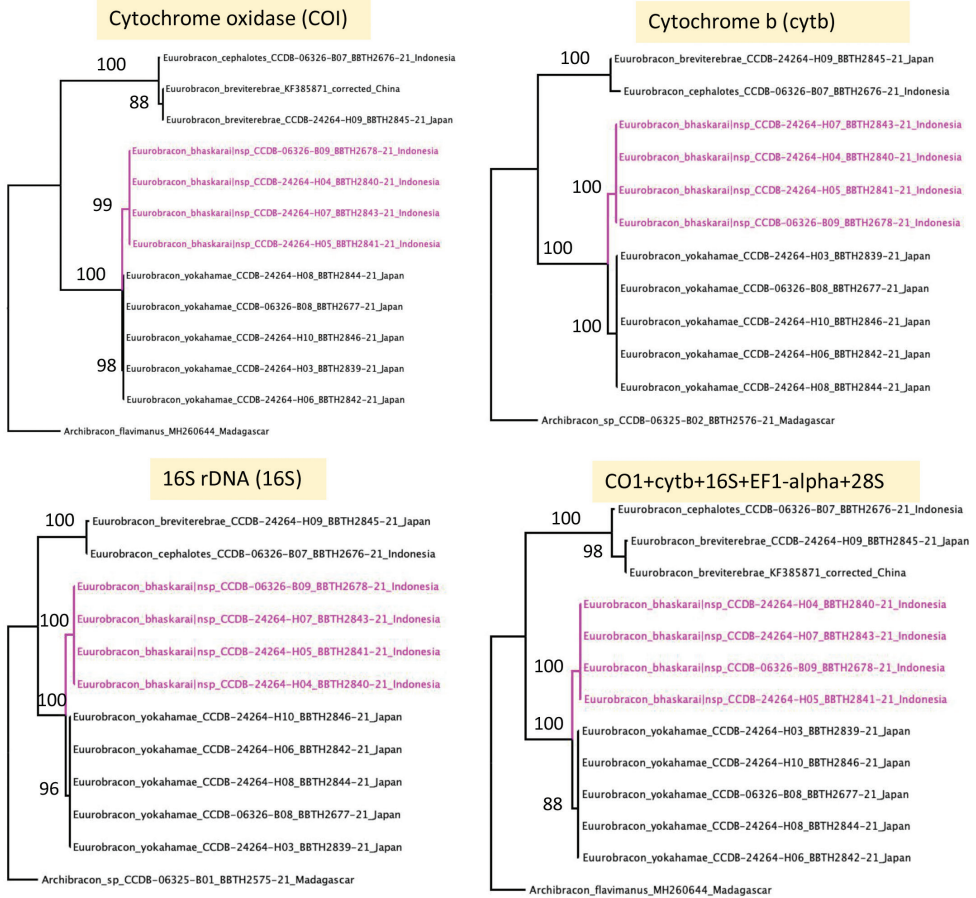


Figure 1. Maximum likelihood bootstrap trees of all available *Euurobracon* sequences rooted with a representative of the putatively closely related Afrotropical genus *Archibracon* Saussure. Individual trees are shown for cytochrome oxidase (COI), cytochrome b (cytb) and 16S rDNA (16S).

The 28S gene and EF-1 α did not differentiate *E. bhaskarai* sp. nov. from *E. yokahamae*, but consistently split *Euurobracon* into two species groups (Fig. 1), the differences in 28S between these groups being entirely indels.

Taxonomy

Euurobracon Ashmead, 1900

Euurobracon Ashmead, 1900: 140. Type species: *Bracon penetrator* Smith, 1877 not Smith, 1863.

Delmira Cameron, 1900: 87. Type species: *Delmira triplagiata* Cameron [Synonymized by Baltazar 1961.]

Exobracon Szépligeti, 1902: 45. Type species: *Bracon quadriceps* Smith, 1861 not Smith, 1858. [Synonymized by Roman 1913.]

Lissobracon Cameron, 1905:103. Type species: *Lissobracon forticornis* Cameron [Synonymized by Roman 1913.]

Diagnosis. Scapus subglobose, shorter ventrally than dorsally in lateral aspect; face flat, clypeus not separated from face by a ridge or carina; propodeum smooth medio-posteriorly (Fig. 7); fore wing vein 3RSa of fore wing $2.5\text{--}3.4 \times$ vein 2RS (Figs 2, 8); fore wing vein 1cu-a strongly postfurcal and curved (except *E. interstitialis*), vein 1CUb $3.0\text{--}4.6 \times$ 1CUa (Figs 6, 12); hind wing vein 1r-m much longer than SC+R1 (Figs 6, 12); hind wing vein 1r-m short longitudinal (Fig. 12) to shortly transverse (Fig. 6); surroundings of vein cu-a of hind wing setose; metasoma smooth and shiny, first tergite with smooth, polished, convex median area bordered laterally by pair of distinct furrows, with at most weak indication of rounded, dorsal carina anteriorly, without dorsolateral carinae; second metasomal tergite smooth, with at most a weak medio-anterior pair of short converging grooves but without mid-basal triangular area; second suture smooth; fifth and sixth tergites largely exposed and smooth; hypopygium large, reaching or projecting beyond apex of metasoma; ovipositor strongly exerted; dorsal valve of ovipositor with small pre-apical nodus.

The adult rectum is unique among braconids in having a large number (>12) of small rectal pads, compared with four in other genera (Quicke et al. 1999).

***Euurobracon bhaskarai* Quicke, sp. nov.**

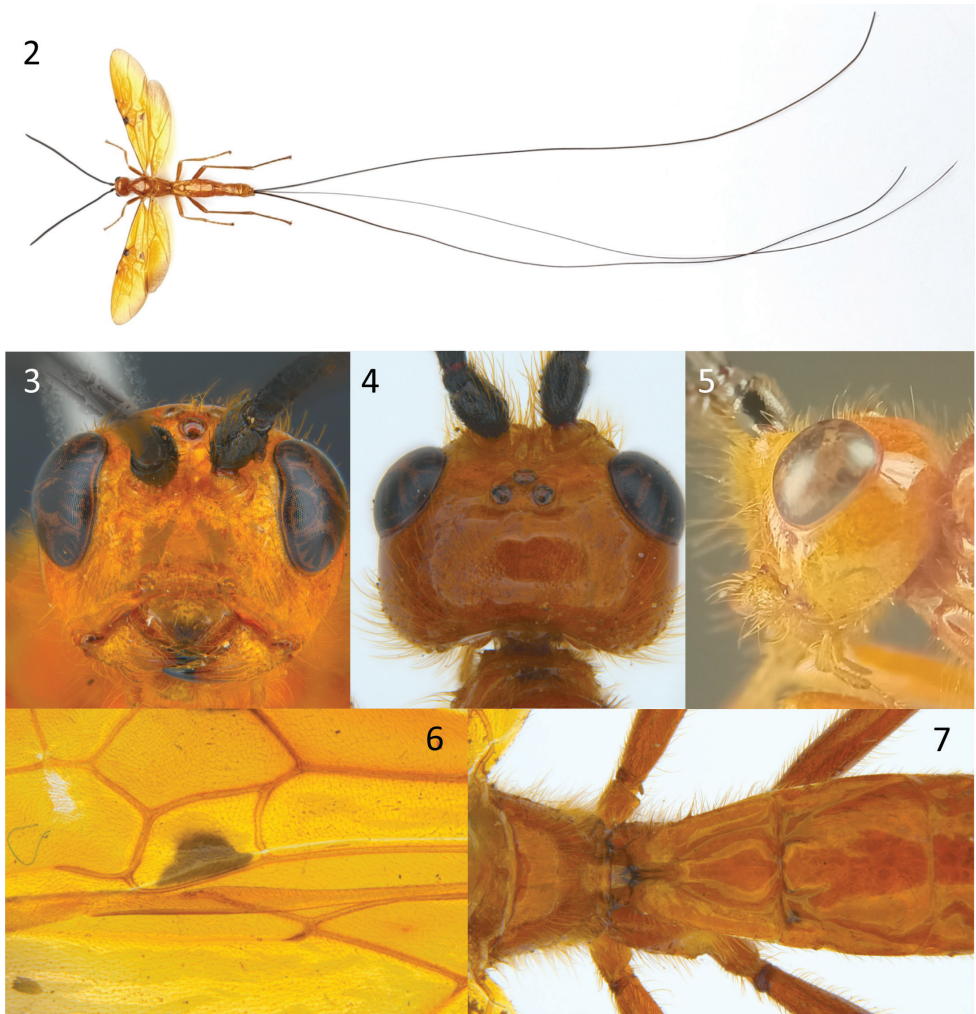
<http://zoobank.org/D6533B79-844D-43DA-B6E3-66CC88BB8C19>

Figs 2–7

Type material. *Holotype* ♀, INDONESIA, West Java, nr Mt Halimun, ii.2021, local collector, DNA voucher CCDB-24624-H04 (MZB). *Paratypes*: 3 ♀, same data as holotype (1 MZB, DNA voucher CCDB-6326-B09; 2 CUMZ, DNA vouchers CCDB-24624-H05, CCDB-24624-H07).

Diagnosis. Body largely orange-yellow; wings largely yellow, fore wing with greyish margin narrowly infusate, a small dark brown mark at apex of pterostigma, a dark brown patch around the confluence of veins 1RS, 1-M and (RS+M)a, and a brown patch at the posterior part of the 1st subdiscal cell; hind wing vein R (or RSa) interstitial or short transverse; 2nd metasomal tergite without transverse groove at approximately midlength; ovipositor more than $4 \times$ longer than body. In addition, apex of hind wing basal cell with a small elongate sclerome in the membrane at approximately midlength of 1r-m.

The new species is morphologically very similar *E. yokahamae*, the only other predominantly yellow species with very long ovipositor. Nearly all specimens of *E. yokahamae* have hind wing vein R longitudinal (i.e., vein RSa arising from R distal to 1r-m); very rarely it is interstitial. In *E. bhaskarai* sp. nov. vein RSa is short but distinctly transverse or occasionally interstitial. The most conspicuous difference is in the extent



Figures 2–7. *Euurobracon bhaskarai* Quicke sp. nov., ♀, holotype **2** habitus, dorsal view **3** head, anterior view **4** head, dorsal view **5** head, lateral view **6** medial part of fore and hind wings **7** propodeum and metasomal tergites 1 and 2, dorsal view.

of the dark markings of the fore wing. There is some variation in wing colour pattern in female *E. yokahamae* and this was illustrated by Sonan (1932), but this does not include restriction of the fore wing grey pattern to a faint narrow margin with just three small brown spots as in the new species. In addition, in the distal part of hind wing basal cell there is a small thickening of the cell membrane creating a tiny sclerome which is absent in *E. yokahamae*. The antennal flagellum of the four available specimens of the new species is parallel-sided whereas in *E. yokahamae* it is distinctly widened distally.

Description. Length of body 19.5–23.5 mm, of fore wing 18.7–20.0 mm, of antenna 16.6–18.0 mm and of ovipositor, 97–123 mm. **Head.** Antenna with 70–71

flagellomeres, more or less parallel-sided. Terminal flagellomere tapering progressively to a point and distinctly acuminate, approximately $1.5 \times$ longer than basally wide. Median flagellomeres transverse, $1.5 \times$ wider than long. Length of first flagellomere: second flagellomere: third flagellomere = 1.45: 1.1; 1.0, the latter being more or less quadrate. Width of head: width of face: height of eye (measured at level of antennal socket) = 2.5: 1.45: 1.0. Dorsal half of clypeus densely long setose. Face densely long setose except for a small median triangular area above the clypeus. Inter-tentorial distance $1.25 \times$ tentorio-ocular distance. Frons sparsely setose. Head widest behind eyes; length of head behind eye $1.1 \times$ length of eye in dorsal view. Malar space $0.9 \times$ longer than basal width of mandible. Minimum length of malar space located at above inner articulation of mandible. Shortest length of mandible $1.2 \times$ longer than basal width of mandible. **Mesosoma.** Mesosoma $1.75 \times$ longer than high. Middle lobe of mesoscutum often largely moderately densely setose laterally. Notauli present anteriorly only. Anterior margin of propodeum without a deep medial emargination. Propodeal spiracle elongate, ca $2.0 \times$ longer than maximum width. **Wings.** Fore wing vein 1cu-a far postfurcal, vein 1CUb $3.3 \times$ 1CUa. Forewing vein 2CUa only weakly and gradually expanded posteriorly. Vein (RS+M)a $1.0\text{--}1.1 \times$ length of 1-M. Forewing vein m-cu straight, $2.0 \times$ longer than (RS+M)b. Lengths of fore wing veins r-rs: 3RSa: 3RSb = 1.0: 5.5: 6.0. Lengths of fore wing veins 2RS: 3RSa: rs-m = 1.0: 2.75: 1.1. Hindwing vein 1r-m approximately $1.3 \times$ longer than R1 before it reaches wing margin hind wing vein R marginally longitudinal, interstitial or marginally transverse (i.e., with very short vein rs-m). **Legs.** Length of fore femur: tibia: tarsus = 1.0: 1.0: 1.25. Anterolateral aspect of fore tibia more or less densely clothed with slightly thickened setae. Fore basitarsus $4.3 \times$ longer than maximally deep. Length of hind femur: tibia: basitarsus = 1.0: 1.4: 1.2. Hind femur $6.0 \times$ longer than maximum depth in lateral view. Hind tibia $12.5 \times$ longer than maximum depth in lateral view. Hind basitarsus $8.3 \times$ longer than deep. **Metasoma.** First tergite $1.2 \times$ longer than maximally wide. Second tergite smooth, $1.2\text{--}1.35 \times$ wider than long, without any trace of median transverse groove or furrow. Second + third metasomal tergites $1.3\text{--}1.4 \times$ longer than maximally wide. Ovipositor long, $5.2\text{--}6.2 \times$ forewing, $5.0\text{--}5.3 \times$ longer than body. **Coloration.** Antenna black. Head, including stemmaticum, and body uniformly ferruginous-yellow (orange-yellow), usually with few black marks as follows: posterior margin of propodeum, medio-anterior of tergite 1, anterolateral part and longitudinal sublateral grooves of tergite 2, anterolateral part of tergite 3, posterior margins of tergites 3–5. Wings largely yellow, narrowly weakly infusate distally and postero-distally, with dark brown marks at apex of pterostigma, around junction of veins 1RS, 1-M and (RS+M)a but excluding parastigma, and posterior part of first subdiscal cell, membrane. Fore and mid legs ferruginous-yellow except apex of hind tibia and basal three hind tarsomeres which are piceous. Ovipositor sheaths black.

Male. Unknown.

Etymology. Named after Mr Edy Bhaskara, friend of the first author, who lives on the island where the new species was collected.

Biology. Unknown.

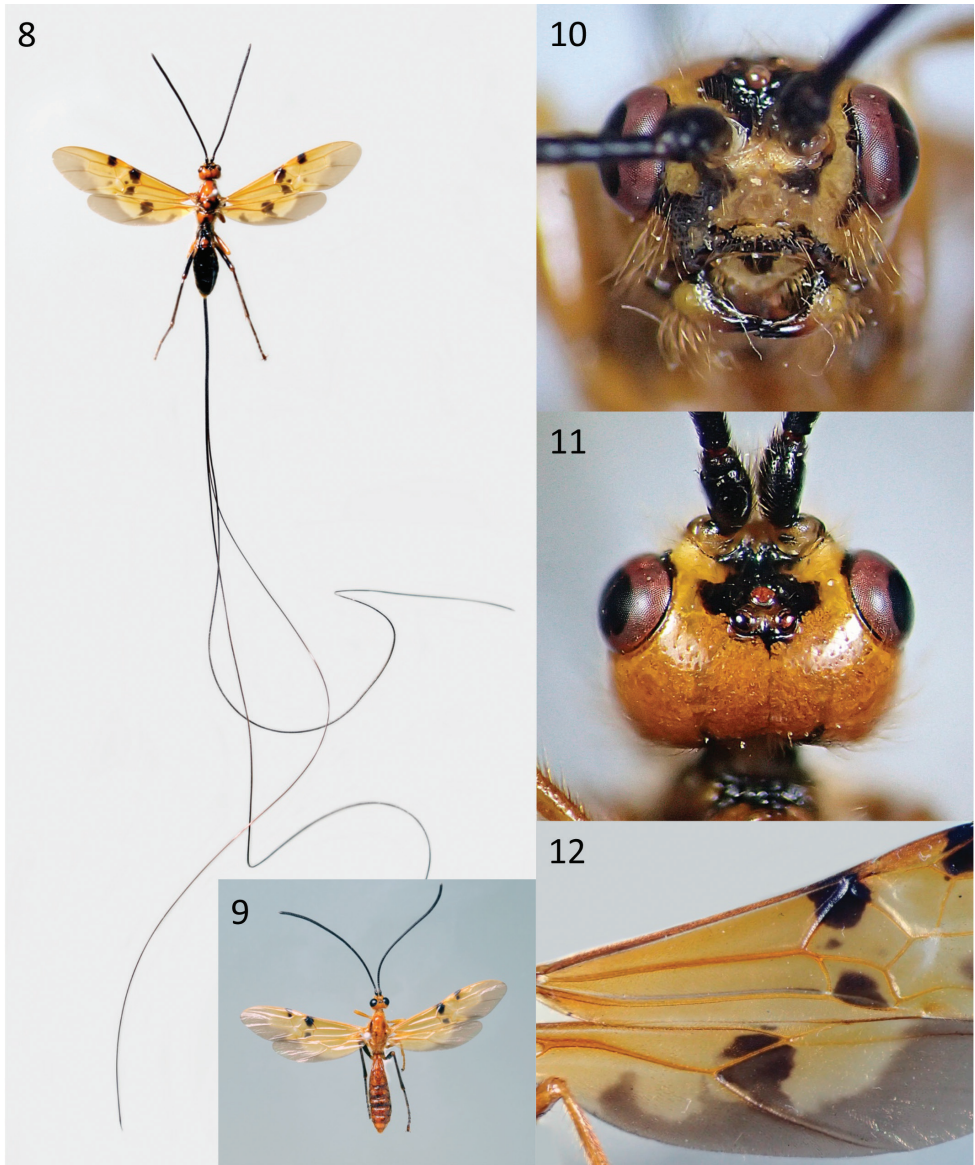
***Euurobracon yokahamae* (Dalla Torre, 1898)**

Figs 8–12

Material examined. JAPAN, Honshu, KPM-NK62083, ♀, Kanagawa Pref., Yokohama City, Aoba-Ku, Jike, 9.v.2017; KPM-NK62090, ♀, Kanagawa Pref., Yokohama City, Midori-Ku, Mihomachi, 11.v.2017; KPM-NK55278, ♀, Kanagawa Pref., Sagami-hara City, Midori-Ku, Magino, 20.v.2019, H. Karube leg.; KPM-NK51571, ♀, Kanagawa Pref., Aikawa Town, Mimase, 2.v.2017, H. Karube leg.; KPM-NK62092, ♀, Kanagawa Pref., Aikawa Town, Sumida, 12.v.2017, H. Fujita leg.; KPM-NK51570, ♀, Kanagawa Pref., Hiratsuka C., Kisawa, 1.v.2017, H. Karube leg.; KPM-NK47713, ♀, Kanagawa Pref., Oiso Town, Nishikoiso, 12.v.2017; KPM-NK55279, ♀, Kanagawa Pref., Nakai Town, Zoushiki, 7.v.2019, K. Watanabe leg.; KPM-NK62086, ♀, Kanagawa Pref., Hadano City, Horikawa, 6.i.2016 (from dead tree), K. Suzuki leg.; KPM-NK47711, ♀, Kanagawa Pref., Hadano City, Mt. Koubou-yama, 19.v.2017, R. Kaga leg.; KPM-NK69393, ♂, same locality, 30.v.2018 (host coll.), 13.vii.2018 (em.), R. Kaga et al. leg.; KPM-NK69395, 69389, 69405, 1 ♀ & 2 ♂, Kanagawa Pref., Hadano City, Mt. Koubou-yama, 30.v.2018 (host coll.), 14. VII. 2018 (em.), R. Kaga et al. leg.; KPM-NK69402, 69403, 2 ♂, Kanagawa Pref., Hadano City, Mt. Koubou-yama, 30.v.2018 (host coll.), 18.vii.2018 (em.), R. Kaga et al. leg.; KPM-NK62085, ♀, Kanagawa Pref., Ooi Town, Yamada, 11.v.2017, H. Karube leg.; KPM-NK62379, ♂, Kanagawa Pref., Minamiashigara City, Iwahara, 7.x.2015 (from dead tree), K. Suzuki leg.; KPM-NK47708, ♀, Kanagawa Pref., Minamiashigara City, Tsukahara, 11.v.2017, H. Karube leg.; KPM-NK62089, ♀, Shizuoka Pref., Fukuroi City, Tsurugaikae, 5.v.2017, H. Karube leg.; KPM-NK55276, ♀, Yamanashi Pref., Nirasaki City, Hosaka Town, Mitsuzawa, 11.v.2018, H. Fujita leg.; KPM-NK55277, ♀, Gifu Pref., Ena City, Okasezawa, 11.v.2019, H. Karube leg.

Description. We update the description of this species proposed by Quicke (1989a) based on examination of the above material, including males.

Females: Length of body 14.5–21.5 mm, of forewing 15.5–23.0 mm, and of ovipositor 85–204 mm. **Head.** Antenna with 65–77 flagellomeres (the number of articles is approximately proportional to the body length), distinctly widening distally to approximately $1.2 \times$ width near base. Terminal flagellomere tapering progressively to a point and distinctly acuminate, approximately $1.5 \times$ longer than basally wide. Median flagellomeres transverse, $1.5 \times$ wider than long. Lengths of first flagellomere: second flagellomere: third flagellomere = 2.0: 1.65: 1.8–2.0. First flagellomere more or less parallel-sided except for slight basal flare, the latter being more or less quadrate. Head widest across eyes, 0.7 and 0.7–1.1 \times longer than maximum width of eye and of gena in dorsal view, respectively. Width of head: width of face (measured at height of antennal socket): height of eye = 2.7: 1.6: 1.0. Length of head behind eye 1.0–1.5 \times length of eye in dorsal view. Maximum width of gena 1.0–1.4 \times longer than maximum width of eye in lateral view. Dorsal half of clypeus densely long setose. Face densely long setose except for a small median triangular area immediately above the clypeus. Malar space 0.8–1.15 \times longer than basal width of mandible. Minimum length of malar space located at above inner articulation of mandible. Shortest length of mandible 1.1–1.3 \times



Figures 8–12. *Euurobracon yokahamae* **8** ♀ habitus, dorsal view **9** ♂ habitus, dorsal view **10** ♀ head, anterior view **11** ♀ head, dorsal view **12** ♀ basal two-thirds of fore and hind wings.

longer than basal width of mandible. Shortest distance between eyes $0.55\text{--}0.6 \times$ longer than maximum width of head in frontal view. Frons largely densely short setose except for median area sparsely setose. POL: diameter of posterior ocellus: shortest distance between posterior ocellus and eye = $0.45\text{--}0.9$: 1.0 : $2.5\text{--}2.7$. Occiput moderately densely setose. **Mesosoma.** Mesosoma $1.6\text{--}1.7 \times$ longer than high. Middle lobe of mesoscutum

often largely moderately densely setose. Notauli present, ending posteriorly near centre of mesoscutum. Anterior margin of propodeum without a deep medial emargination. Propodeal spiracle elongate, ca $2.0 \times$ longer than maximum wide. **Wings.** Fore wing vein 1cu-a far postfurcal, vein 1CUB $3.0\text{--}4.6 \times$ 1CUa vein. Forewing vein 2CUa usually only weakly and gradually expanded posteriorly. Lengths of fore wing veins r-rs: 3RSa: 3RSb = 1.0: 4.3–4.8: 6.1–6.5. Vein (RS+M)a $1.0\text{--}1.1 \times$ length of 1-M. Forewing vein m-cu straight, $1.6\text{--}2.2 \times$ longer than (RS+M)b. Lengths of forewing veins 2RS: 3RSa: rs-m = 2.0: 2.1–2.3: 0.9–0.95. Hindwing vein 1r-m approximately $1.55 \times$ longer than R1 before it reaches wing margin. Hindwing vein R usually longitudinal, rarely interstitial. **Legs.** Lengths of fore femur: tibia: tarsus = 1.0: 1.0–1.15: 1.1–1.12. Anterolateral aspect of fore tibia more or less densely clothed with slightly thickened setae. Fore basitarsus $4.3\text{--}4.5 \times$ longer than maximally deep. Lengths of hind femur: tibia: basitarsus = 1.0: 1.5: 1.5–1.75. Hind femur $5.0\text{--}5.8 \times$ longer than maximum depth in lateral view. Hind tibia $9.5\text{--}11.0 \times$ longer than maximum depth in lateral view. Hind basitarsus $7.7 \times$ longer than deep. **Metasoma.** First metasomal tergite $0.98\text{--}1.24 \times$ longer than maximally wide (generally shorter in length for larger specimens); dorsal carinae relatively close together, broadly rounded ridges rather than lamelliform carinae; raised median area with or without a mid-longitudinal groove. Second metasomal tergite largely glabrous $1.25\text{--}1.43 \times$ wider than long, without a distinct transverse median groove on either side of the midline, with a pair of sublateral oblique furrows. Third metasomal tergite with distinct anterolateral areas, without a pair of sub-medial transverse grooves or pits. Second + third metasomal tergites $1.1\text{--}1.3 \times$ longer than maximally wide. Ovipositor long, $5.55\text{--}9.3 \times$ forewing length [$5.0\text{--}14.0$ in Quicke (1989a)] though generally between 6.0 and $9.0 \times$ fore wing; $5.85\text{--}9.5 \times$ longer than body. Apex of lower valve of ovipositor with five teeth. Approximately distal 0.1 of lower valve of ovipositor with rough surface laterally (and also ventrally except for teeth). **Coloration.** The additional materials completely agree with the character states of coloration proposed by Quicke (1989a) which is reproduced below. Antenna and ovipositor sheath black. Body usually largely or entirely ferruginous-yellow (somewhat paler in the Indian specimens), sometimes with piceous markings especially on the metasomal tergites, propodeum, metanotum, mesopleuron and propodeum. Fore and middle legs ferruginous-yellow, hind legs usually black or dark piceous but entirely yellow in specimens from India, Laos and Thailand. Wings yellow with a somewhat variable brown pattern (Sonan, 1932), the distinctive features being: a dark mark at the parastigma and at the apex of the pterostigma of the forewing; usually a dark mark in the first subdiscal cell of the forewing; a pale grey-brown at the apex of the forewing, extending and darkening slightly along the postero-distal part of the wing margin; hindwing with a grey-brown apical region which extends along the posterior wing margin and is produced into the base of the submarginal cell and again into the discal+subdiscal cells.

Males: Similar to female. Length of first flagellomere: second flagellomere: third flagellomere = 2.0: 1.1–1.3: 1.4–1.55. Head $1.1\text{--}1.15 \times$ longer than maximum width of gena in dorsal view. Eye relatively larger than in female, maximum width of gena $0.5\text{--}0.6 \times$ longer than maximum width of eye in lateral view. Shortest distance between eyes $0.25\text{--}0.3 \times$ longer than maximum width of head in frontal view. Face slightly narrower

than female, 0.43–0.7 × longer than maximum width. Ocelli larger than female. POL distinctly longer than shortest distance between posterior ocellus and eye. POL: diameter of posterior ocellus: shortest distance between posterior ocellus and eye = 0.5–0.6: 1.0: 0.3–0.5. Malar space (minimum length) 2.0 × longer than basal width of mandible. Minimum length of malar space located at above outer articulation of mandible. Length of hind femur: tibia: basitarsus = 1.0: 1.55–1.8: 1.35–1.6. First metasomal tergite slenderer than female, 1.25–1.4 × longer than maximum width. Second and third metasomal tergites usually with slight transverse depression. **Male genitalia.** Basal ring V-shaped, its dorsal part narrow and linear. Digitus large and triangular, with three minute tubercles at apex. Apex of paramere not projecting beyond apex of aedeagus, densely setose. Dorsal surface of aedeagus largely flat subapically. Ventral side of aedeagus with lamella-like expansion. Described in detail and illustrated by SEM in Quicke (1988).

Distribution. Japan, Korea, China, Taiwan, Laos, Thailand and India (Yu et al. 2016).

Biology. See Introduction.

Remarks. A set of eight figures showing the range of variation of forewing markings found in the East Palearctic population was provided by Sonan (1932). Quicke (1989a) classified this species into its own, monotypic, *E. yokahamae* species group which is recognizable from all other *Euurobracon* spp. by its interstitial or longitudinal hindwing vein 2-SC+R in combination with predominantly yellow or red-yellow coloration.

Discussion

In general, even among parasitoid wasps, large and brightly coloured species, have often already been described, and indeed, not uncommonly have one or more synonyms (Jones et al. 2009, 2011; Quicke 2012). Most of the undescribed diversity occurs among the smaller and less spectacular groups. Nevertheless, in South-east Asia, and adjacent southern China, many such new species are being described. Members of the genus *Euurobracon* are, despite their large body size and often impressive ovipositors, almost certainly vastly under-recorded in South-east Asia.

Acknowledgements

We are very grateful to Paul D.N. Hebert, Suresh Naik and Ramya Manjunath at the Centre for Biodiversity Genomics, University of Guelph for sequencing these specimens and for archiving the data. We also extend our sincere thanks to Histocenter (Thailand) Co. Ltd. for the loan of the Leica photomicroscopy system. Michael Geiser (Natural History Museum, London) kindly explored and clarified the name and authorship of a recorded host of *Euurobracon*. DLJQ was supported by the award of a Senior Postdoctoral Fellowship from the Rachadaphiseksomphot Fund, Graduate School, Chulalongkorn University. BAB was supported by Rachadaphiseksomphot Fund (RCU_F_64_006_23) and RSPG Chula. Finally, we thank our three very careful referees for their useful comments and corrections.

References

- Cao L-M, van Achterberg C, Tang Y-L, Wang X-Y, Yang ZQ (2020) Revision of parasitoids of *Massicus raddei* (Blessig & Solsky) (Coleoptera Cerambycidae) in China, with one new species and genus. *Zootaxa* 4881(1): 104–130. <https://doi.org/10.11646/zootaxa.4881.1.7>
- Jones OR, Purvis A, Baumgart E, Quicke DLJ (2009) Using taxonomic revision data to estimate the geographic and taxonomic distribution of undescribed species richness in the Braconidae (Hymenoptera: Ichneumonoidea). *Insect Conservation and Diversity* 2(3): 204–212. <https://doi.org/10.1111/j.1752-4598.2009.00057.x>
- Jones OR, Purvis A, Quicke DLJ (2011) Latitudinal gradients in taxonomic overdescription rate affect macroecological inferences using species list data. *Ecography* 35(4): 333–340. <https://doi.org/10.1111/j.1600-0587.2011.06956.x>
- Kaga R, Kawashima I, Karube H (2018) Notes on the life history of the parasitoid wasp, *Euurobracon yokahamae* (Dalla Torre, 1898) (Insecta: Hymenoptera: Braconidae), with special reference to the natural host insect. *Kanagawa Kenritsu Hakubutsukan Kenkyu Hokoku, Shizen Kagaku* 47: 59–66. [In Japanese, with English abstract]
- Li Y, He JH, Chen X-X (2016) The genus *Euurobracon* Ashmead (Hymenoptera, Braconidae, Braconinae) in China, with description of three new species. *Zootaxa* 4132(3): 383–392. <https://doi.org/10.11646/zootaxa.4132.3.6>
- Quicke DLJ (1988) Inter-generic variation in the male genitalia of the Braconinae (Insecta, Hymenoptera, Braconidae). *Zoologica Scripta* 17(4): 399–409. <https://doi.org/10.1111/j.1463-6409.1988.tb00115.x>
- Quicke DLJ (1989a) The Indo-Australian and E. Palaearctic braconine genus *Euurobracon* (Hymenoptera: Braconidae: Braconinae). *Journal of Natural History* 23(4): 775–802. <https://doi.org/10.1080/00222938900770411>
- Quicke DLJ (1989b) Parasitic braconine wasps of the genus *Archibracon* (Hymenoptera: Braconidae). *Journal of Natural History* 23(1): 29–70. <https://doi.org/10.1080/00222938900770031>
- Quicke DLJ (2012) We know too little about parasitoid wasp distributions to draw any conclusions about latitudinal trends in species richness, body size and biology. *PLoS ONE* 7(2): e32101. <https://doi.org/10.1371/journal.pone.0032101>
- Quicke DLJ (2015) *Biology, Systematics, Evolution and Ecology of Braconid and Ichneumonid Parasitoid Wasps*. Wiley Blackwell, Chichester, 681 pp. <https://doi.org/10.1002/9781118907085>
- Quicke DLJ, Basibuyuk HH, Fitton MG, Rasnitsyn AP (1999) Morphological, palaeontological and molecular aspects of ichneumonoid phylogeny (Hymenoptera, Insecta). *Zoologica Scripta* 28(1–2): 175–202. <https://doi.org/10.1046/j.1463-6409.1999.00005.x>
- Sharkey MJ, Wharton RA (1997) Morphology and terminology. In Wharton RA, Marsh PM, Sharkey MJ (Eds) *Identification Manual to the New World Genera of Braconidae*. Special Publication of the International Society of Hymenopterists 1: 19–37. Washington, D.C.
- Shenefelt RD (1978) Braconidae 10. Braconinae, Gnathobraconinae, Mesostoinae, Pseudodicrogeniinae, Telengainae, Ypsistocerinae, plus Braconidae in general, major groups, unplaced genera and species. *Hymenopterorum Catalogus* 15: 1425–1872. [nova editio]
- Sonan J (1932) Notes on the braconid-fly, *Iphiaulax (Euurobracon) penetrator* Smith (Hym.). *Kontyu* 7: 115–123. [In Japanese.]

- Stamatakis A (2014) RAxML version 8: A tool for phylogenetic analysis and post-analysis of large phylogenies. *Bioinformatics* (Oxford, England) 30(9): 1312–1313. <https://doi.org/10.1093/bioinformatics/btu033>
- van Achterberg C (1988) Revision of the subfamily Blacinae Foerster (Hymenoptera: Braconidae). *Zoologische Verhandelingen* 249: 1–324.
- Watanabe C (1934) Notes on Braconidae of Japan V. *Eurobracon*. *Insecta Matsumurana* 9: 19–23.
- Yu DS, van Achterberg C, Horstmann K (2016) Taxapad 2016. Ichneumonoidea 2015 (Biological and Taxonomical Information), Taxapad Interactive Catalogue Database on Flash-drive.

On eleven species of jumping spiders from Xishuangbanna, China (Araneae, Salticidae)

Cheng Wang¹, Shuqiang Li²

1 Guizhou Provincial Key Laboratory for Biodiversity Conservation and Utilization in the Fanjing Mountain Region, Tongren University, Tongren, Guizhou 554300, China **2** Institute of Zoology, Chinese Academy of Sciences, Beijing 100101, China

Corresponding author: Shuqiang Li (lisq@ioz.ac.cn)

Academic editor: Ingi Agnarsson | Received 28 February 2022 | Accepted 25 July 2022 | Published 8 August 2022

<https://zoobank.org/28FBF607-95F2-4E60-AE38-7439D84DE527>

Citation: Wang C, Li S (2022) On eleven species of jumping spiders from Xishuangbanna, China (Araneae, Salticidae). ZooKeys 1116: 85–119. <https://doi.org/10.3897/zookeys.1116.82858>

Abstract

One new genus and eight new species from Xishuangbanna, China are described and diagnosed: *Bocusoides zhaii* **gen. nov.** and **sp. nov.**, *Euochin mii* **sp. nov.** (♂♀), *E. tangi* **sp. nov.** (♀), *Eupoia logunovi* **sp. nov.** (♂♀), *Indomarengo wengnan* **sp. nov.** (♀), *Laufeia zhangae* **sp. nov.** (♂♀), *Simaetha huigang* **sp. nov.** (♂♀), and *Synagelides cheni* **sp. nov.** (♀). The unknown sexes of three endemic species, *Chalcovietnamicus lii* (Lei & Peng, 2010) **comb. nov.** (ex *Chalcoscirtus* Bertkau, 1880), *Indomarengo yui* Wang & Li, 2020, and *Rhene triapophyses* Peng, 1995 are described for the first time.

Keywords

Morphology, new combination, new genus, new species, Southeast Asia, taxonomy

Introduction

As a result of a series of taxonomic studies and biodiversity surveys conducted over the last three decades, knowledge of the salticid fauna from Xishuangbanna, China has increased considerably (Li 2020; Lin and Li 2020; Hong et al. 2022). To date, the list of salticids from Xishuangbanna, including the eight new species described here, comprises at least 145 species, which is more than the number of species in several adjacent countries and regions (Logunov 2021; Wang and Li 2021; WSC 2022). However, there is no doubt that new records and species will be discovered in this biodiversity

hotspot and the list of species will be increased further because most area of this region remains insufficiently surveyed (Wang et al 2020; Li et al 2021; Yao et al 2021).

In the current study, eight species collected from Xishuangbanna are recognized as new to science, and the unknown sexes of three endemic species are also described.

Materials and methods

Specimens were collected by fogging and sieving leaf litter in the tropical rainforest of Xishuangbanna, China. All specimens are preserved in 75% ethanol and are deposited in the Institute of Zoology, Chinese Academy of Sciences (IZCAS) in Beijing, China. Methods follow Wang and Li (2021).

All measurements are given in millimeters. Leg measurements are given as: total length (femur, patella + tibia, metatarsus, tarsus). References to figures in the cited papers are listed in lowercase type (fig. or figs); figures in this paper are noted with an initial capital (Fig. or Figs). Abbreviations used in the text and figures are as follows: **AERW** anterior eye row width; **AME** anterior median eye; **ALE** anterior lateral eye; **AG** accessory gland; **AR** atrial ridge; **AS** anterior chamber of spermatheca; **At** atrium; **CD** copulatory duct; **CO** copulatory opening; **CP** cymbial process; **DTA** dorsal tibial apophysis; **E** embolus; **ED** embolic disc; **ET** embolic tooth; **EFL** eye field length; **FD** fertilization duct; **H** epigynal hood; **MA** median apophysis; **MP** median plate; **MS** median septum; **PERW** posterior eye row width; **PL** posterior lobe; **PLE** posterior lateral eye; **PS** posterior chamber of spermatheca; **RFA** retrolateral femoral apophysis; **RPA** retrolateral patellar apophysis; **RTA** retrolateral tibial apophysis; **S** spermatheca; **SD** sperm duct; **TA** terminal apophysis; **TF** tibial flange; **TmA** terminal apophysis of embolic division; **VTA** ventral tibial apophysis.

Taxonomy

Family Salticidae Blackwall, 1841

Genus *Bocusoides* gen. nov.

<https://zoobank.org/4805E7A8-886F-4F82-9134-EF0390496619>

Type species. *Bocusoides zhai* sp. nov. from China.

Etymology. The generic name is the combination of “oides”, meaning “having the form of”, and the similar genus name *Bocus*; gender masculine.

Diagnosis. *Bocusoides* gen. nov. can be easily distinguished from other genera of Myrmarachnina, except *Bocus* Peckham & Peckham, 1892, by having an elongated carapace with an obvious postocular constriction and an anteriorly broadened sternum. It can be distinguished from *Bocus* by the following: 1) male cheliceral paturon abruptly broadened at base (Fig. 2C–E, G; Deeleman-Reinhold and Floren 2003: fig. 9) versus gradually broadened from the base to the middle part in *Bocus* (Wanless 1978a: fig. 1C, 2B); 2) carapacial postocular constriction narrower, about 1/2

the carapacial width (Fig. 2C, F; Deeleman-Reinhold and Floren 2003: fig. 9) versus broader, about 2/3 the carapacial width in *Bocus* (Wanless 1978a: figs 1A, 2A); 3) pedical with conical, dorsal process (Fig. 2D; Deeleman-Reinhold and Floren 2003: fig. 11) versus absent in *Bocus* (Wanless 1978a: figs 1H, 2D); 4) leg formula 4123 versus 4132 in *Bocus* (see the description by Wanless 1978a); 5) male abdomen not constricted (Fig. 2C; Deeleman-Reinhold and Floren 2003: fig. 9) versus constricted at anterior 1/3 in *Bocus* (Wanless 1978a: figs 1A, 2A); 6) male palp with short tibia, which is wider than long and with filiform embolus with proximal disc (Fig. 1D; Deeleman-Reinhold and Floren 2003: fig. 13) versus tibia longer, at least as long as wide, and flat embolus without proximal disc in *Bocus* (Wanless 1978a: fig. 3A, E); 7) epigyne with distally circled copulatory ducts, elongated spermathecae, and elongated, arched fertilization ducts (Fig. 2A, B; Deeleman-Reinhold and Floren 2003: fig. 17) versus copulatory ducts not circled, spermathecae spherical, and fertilization ducts ordinary in *Bocus* (Wanless 1978a: fig. 1G).

Description. Medium-sized, ant-like spiders. Carapace elongated. Pedicel short, with dorsal, conical process. Chelicerae well developed and with paturon abruptly broadened at base in males. Endites longer than wide, distally bearing dense, dark setae. Labium slightly darker than endites. Sternum irregular, anteriorly broadened. Legs elongated, with 11 and five ventral spines on tibiae and metatarsi I, respectively. Abdomen oval, not constricted; dorsum with white guanine patches or yellow-silver spots at the lateral sides of anterior half, and alternate dark and paler transverse bands posteriorly, entirely covered by scutum in males; venter dark-brown.

Palp: tibia wider than long, with tapered, short retrolateral apophysis and triangular flange; cymbium flat, setose, with an apical spine; bulb flat and almost round, with tapered sperm duct extending along the submargin; embolus twice coiled, the first forming a broad, flat circle, the second with an elongated, lamellar disc followed by filiform remainder.

Epigyne: with posteriorly located hood; atria paired, oval, medially located, with arched lateral ridges; copulatory openings hidden; copulatory ducts membranous at origin, followed by sclerotized portion ascending obliquely, distally coiled four circles, which are encircling or lateral to the elongated spermathecae; fertilization ducts slender, arched, originating from the anterior portions of spermathecae.

Composition. The genus currently includes the type species and *B. angusticollis* (Deeleman-Reinhold & Floren, 2003) comb. nov.

***Bocusoides zhaoi* sp. nov.**

<https://zoobank.org/C17F2855-F271-40D6-9137-DDDC0C2F1E0F>

Figs 1, 2

Type material. *Holotype* ♂ (IZCAS-Ar42904), CHINA: Yunnan: Xishuangbanna, Mengla County, Menglun Town, Xishuangbanna National Nature Reserve, 200 m east of Lvshilin, artificial forest (21°57.95'N, 101°12.30'E, ca 780 m alt.), 13.viii.2011, Q. Zhao leg. *Paratypes* 2♂7♀ (IZCAS-Ar42905–42913), same data as holotype; 1♂2♀ (IZCAS-Ar42914–42916), 55 km from Xishuangbanna National Nature Re-

serve, secondary forest (21°57.99'N, 101°12.17'E, ca 840 m alt.), 18.viii.2011, Q. Zhao leg.

Etymology. The specific name is a patronym in honor of Qingyuan Zhao, the collector of this new species; noun (name) in genitive case.

Diagnosis. *Bocusoides zhaoi* sp. nov. closely resembles *B. angusticollis* comb. nov. from Borneo in having a similar habitus and copulatory organs, but it can be easily distinguished by the following: 1) width of embolic disc greater than largest diameter of visible sperm duct (Fig. 1D) versus less than 1/2 in *B. angusticollis* (Deeleman-Reinhold and Floren 2003: fig. 13); 2) RTA curved inward distally in ventral view (Fig. 1D) versus curved retrolaterally in *B. angusticollis* (Deeleman-Reinhold and Floren 2003: fig. 13); 3) tibial flange about 1/4 RTA length in dorsal view (Fig. 1E) versus more than 1/2 in *B. angusticollis* (Deeleman-Reinhold and Floren 2003: fig. 14); 4) male chelicerae with three distal promarginal teeth that are almost equal in size, and female chelicerae with six promarginal teeth (Fig. 2G, H) versus male chelicerae include a basal denticle among the three distal promarginal teeth and female chelicerae with only three promarginal teeth in *B. angusticollis* (see the description by Deeleman-Reinhold and Floren 2003); 5) copulatory ducts partially encircle spermathecae (Fig. 2B) versus copulatory ducts lateral to spermathecae in *B. angusticollis* (Deeleman-Reinhold and Floren 2003: fig. 17).

Description. Male (Figs 1, 2C–E, G). Total length 5.00. Carapace 2.68 long, 1.23 wide. Abdomen 2.00 long, 1.23 wide. Clypeus 0.03 high. Eye sizes and inter-distances: AME 0.37, ALE 0.19, PLE 0.17, AERW 1.06, PERW 1.06, EFL 0.89. Legs: I 4.88 (1.45, 1.98, 0.90, 0.55), II 4.15 (1.30, 1.60, 0.80, 0.45), III 4.96 (1.55, 1.68, 1.23, 0.50), IV 6.52 (2.13, 2.23, 1.63, 0.53). Carapace elongated, yellow to yellow-brown, covered with dark brown setae at anterior margin, elevated cephalic region and sloped thorax separated by deep constriction. Pedicel short, with dorsal, conical process. Chelicerae broad, with five promarginal and six retromarginal teeth. Endites longer than wide, bearing dense, dark setae distally. Labium slightly darker than endites. Sternum elongated, irregular, about 2.5 times longer than wide. Legs yellow to dark brown, with 11 and five ventral spines on tibiae and metatarsi I, respectively. Abdomen suboval, dorsum with yellow-sliver spots separated by a longitudinal, central, vein-shaped, brown band anteromedially, followed by alternate dark and dark yellow transverse bands, entirely covered by scutum; venter dark brown.

Palp (Fig. 1A–E): tibia wider than long in ventral view, with short, triangular flange, tapered retrolateral apophysis slightly curved into an S-shape at distal half, pointed apically; cymbium flat, setose, with apical bristle; bulb flat, almost round, with tapered sperm duct; embolus twice coiled, the first forming a broad, flat circle, the second with elongated, lamellar disc followed by filiform remainder coiling about 360° and reaching cymbial tip distally.

Female (Fig. 2A, B, F, H). Total length 5.59. Carapace 2.68 long, 1.09 wide. Abdomen 2.46 long, 1.50 wide. Clypeus 0.03 high. Eye sizes and inter-distances: AME 0.38, ALE 0.19, PLE 0.17, AERW 1.06, PERW 1.05, EFL 0.83. Legs: I 3.81 (1.18, 1.53, 0.65, 0.45), II 3.33 (1.05, 1.30, 0.60, 0.38), III 4.23 (1.35, 1.43, 1.00, 0.45), IV 5.69 (1.80, 1.98, 1.43, 0.48). Habitus similar to that of male except with

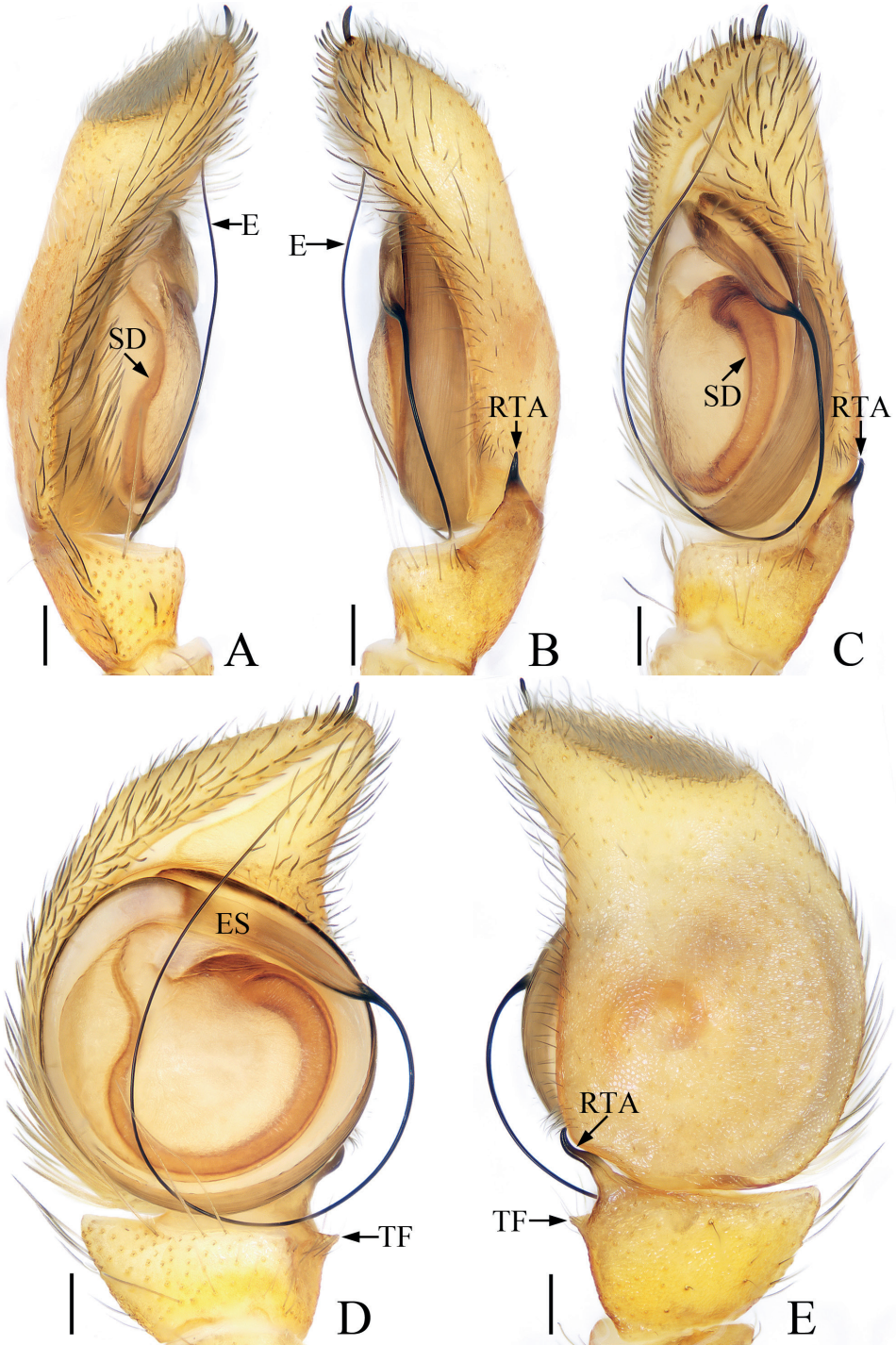


Figure 1. *Bocusoides zhaii* sp. nov., male holotype palp **A** prolateral **B** retrolateral **C** ventro-lateral **D** ventral **E** dorsal. Scale bars: 0.1.

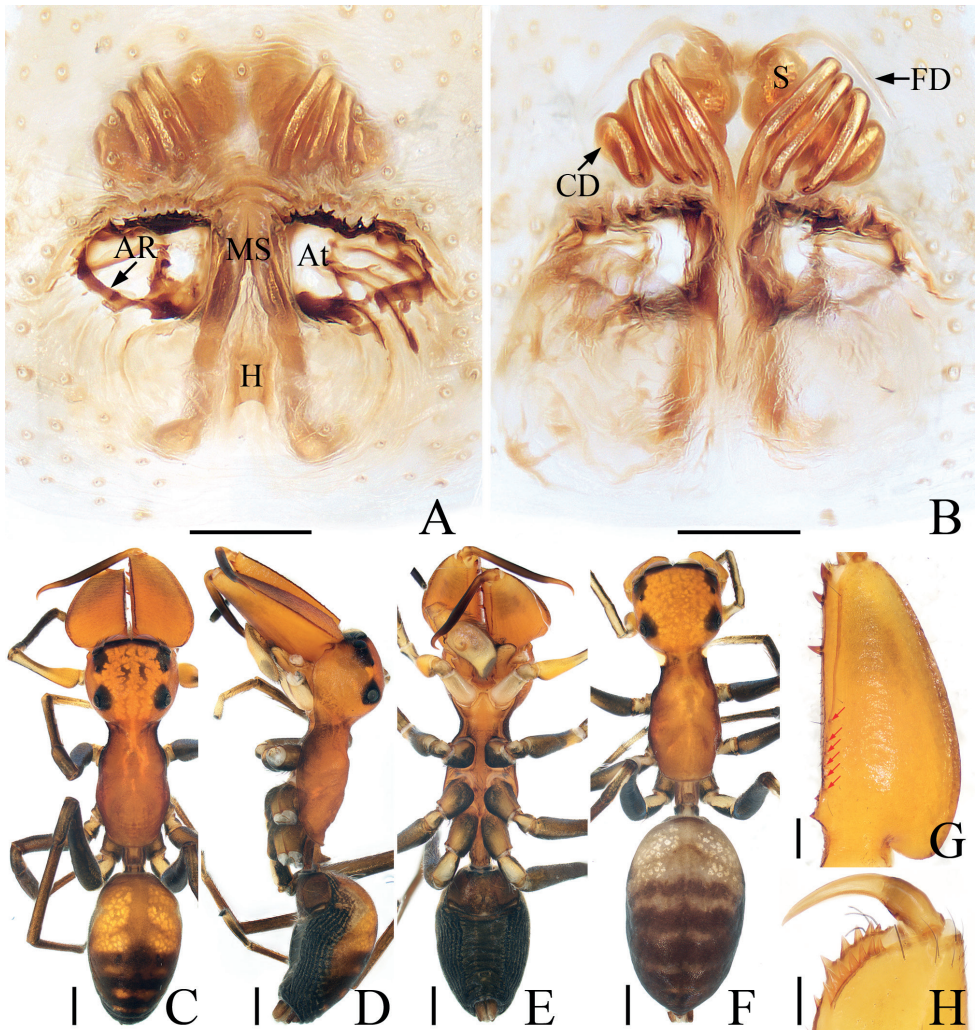


Figure 2. *Bocusoides zhaoi* sp. nov., male holotype and female paratype **A** epigyne, ventral **B** vulva, dorsal **C** male holotype habitus, dorsal **D** ditto, lateral **E** ditto, ventral **F** female paratype habitus, dorsal **G** holotype chelicera, posterior **H** female paratype chelicera, posterior. Scale bars: 0.1 (**A, B, G, H**); 0.5 (**C–F**).

less-developed chelicerae with six promarginal and seven retromarginal teeth, a pair of white spots on the lateral margins of carapace constriction, without scutum on dorsum of abdomen.

Epigyne (Fig. 2A, B): slightly longer than wide, with tube-shaped, posteriorly located hood; atria paired, oval, extending transversely, with arched lateral ridges; copulatory openings hidden; copulatory ducts membranous at origin, followed by sclerotized portion ascending obliquely, coiled four times distally; spermathecae elongated, partly encircled by copulatory ducts; fertilization ducts slender, arched, originating from the anterior portions of spermathecae.

Distribution. Known only from the type locality in Yunnan, China.

Genus *Chalcovietnamicus* Marusik, 1991

Type species. *Chalcoscirtus vietnamensis* Żabka, 1985 from Vietnam by subsequent designation.

***Chalcovietnamicus lii* (Lei & Peng, 2010) comb. nov.**

Figs 3, 4

Chalcoscirtus lii Lei and Peng 2010: 67, fig. 1A–C (female holotype, not examined).

Material examined. 1♂1♀ (IZCAS-Ar42917–42918), CHINA: Yunnan: Xishuangbanna, Mengla County, Menglun Town, Menglun Nature Reserve, Xishuangbanna Tropical Botanical Garden, 1 site in Mafengzhai (21°53.49'N, 101°17.40'E, ca 520 m alt.), 29.iv.2019, C. Wang leg.

Diagnosis. The male of this species closely resembles that of *C. vietnamensis* (Żabka, 1985) from Vietnam in having a similar palp, but it can be distinguished by the following: 1) embolus with small, semicircular lamellar process (Fig. 3B)

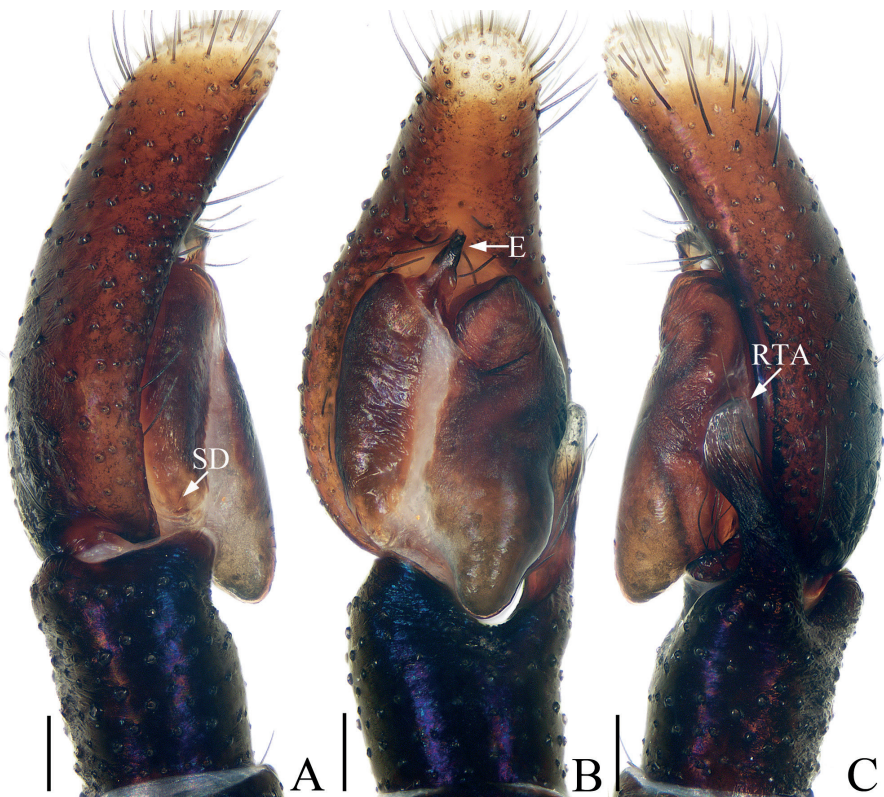


Figure 3. *Chalcovietnamicus lii* comb. nov., male palp **A** prolateral **B** ventral **C** retrolateral. Scale bars: 0.1.

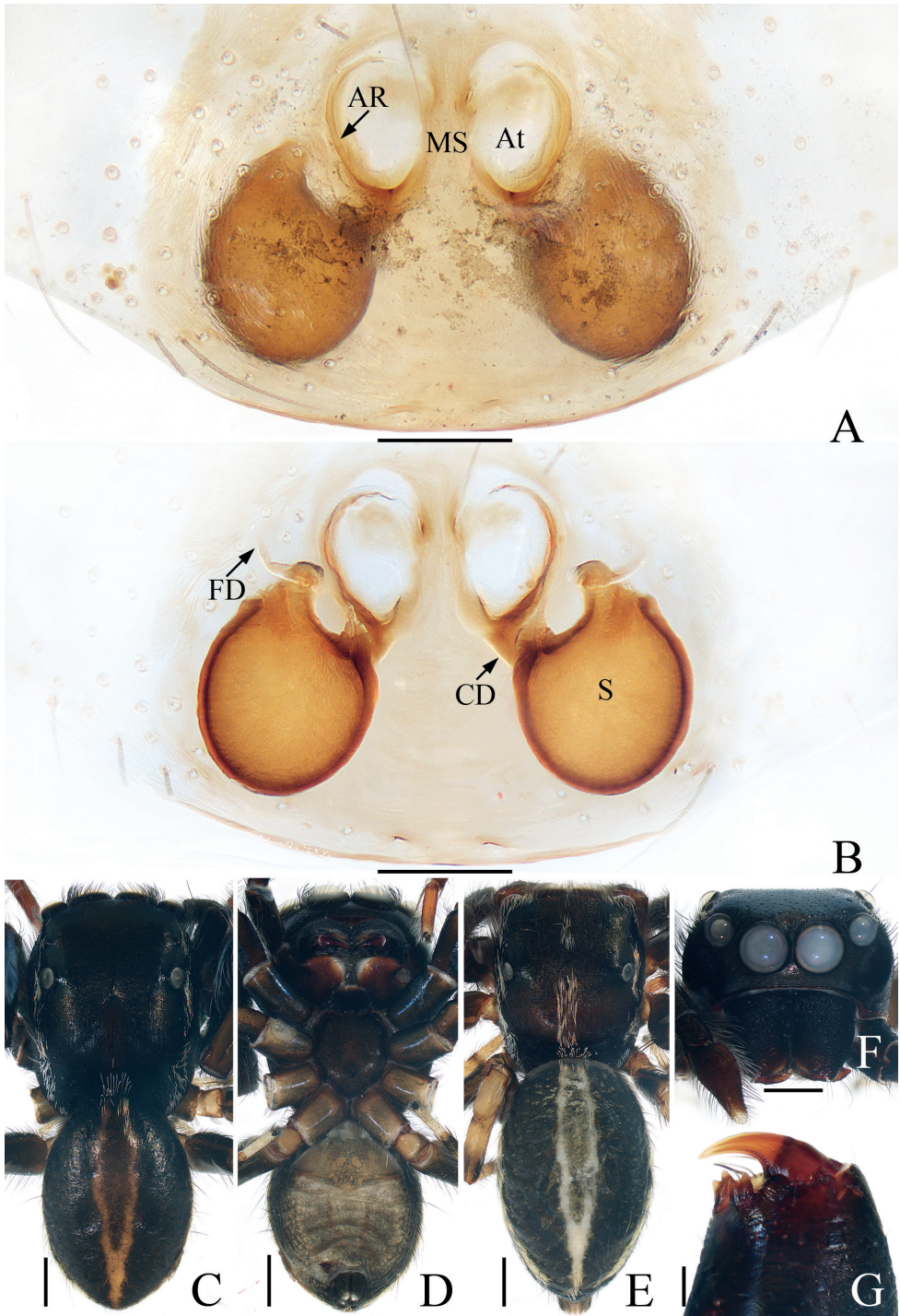


Figure 4. *Chalcovietnamicus lii* comb. nov. **A** epigyne, ventral **B** vulva, dorsal **C** male habitus, dorsal **D** ditto, ventral **E** female habitus, dorsal **F** male carapace, frontal **G** male chelicera, posterior. Scale bars: 0.1 (**A, B, G**); 0.5 (**C-F**).

versus with a larger, subtriangular process in *C. vietnamensis* (Žabka 1985: fig. 71); 2) RTA broadened and extending anteriorly at distal half (Fig. 3C) versus somewhat tapered, extending antero-prolaterally in *C. vietnamensis* (Žabka 1985: fig. 72). The female of this species resembles that of *Chalcoscirtus parvulus* Marusik, 1991 from Greece, Turkey, Kazakhstan, Iran, and Central Asia in having paired, oval atria and straight, short copulatory ducts, but it can be easily distinguished by the following: 1) spermathecae separated by more than 2/3 their width (Fig. 4A, B) versus touching in *C. parvulus* (Logunov and Marusik 1999: fig. 93); 2) abdomen dorsally with a longitudinal, fusiform stripe across entire surface (Fig. 4E) versus with a pair of bars posteriorly in *C. parvulus* (Logunov and Marusik 1999: fig. 91).

Description. Male (Figs 3, 4C, D, F, G). Total length 4.23. Carapace 2.30 long, 1.77 wide. Abdomen 2.24 long, 1.53 wide. Clypeus 0.11 high. Eye sizes and inter-distances: AME 0.49, ALE 0.31, PLE 0.25, AERW 1.50, PERW 1.53, EFL 1.27. Legs: I 6.71 (2.00, 2.95, 1.23, 0.53), II 5.03 (1.53, 2.00, 1.05, 0.45), III 4.21 (1.33, 1.48, 0.95, 0.45), IV 4.46 (1.40, 1.60, 1.01, 0.45). Carapace dark brown, bearing bilateral white and antero-marginal dark setae. Fovea dark, longitudinal, bar-shaped. Chelicerae red-brown to dark, with two promarginal teeth and one retromarginal fissidental tooth with two cusps. Endites paler than chelicerae, with pale ental margins bearing dark, thin setae. Labium dark. Sternum colored as labium, almost heart-shaped, bearing dark setae. Legs I longest, dark brown except tarsi red-brown, with three and two pairs of ventral spines on tibia and metatarsi, respectively; rest of legs yellow, with dark brown femora. Abdomen suboval, dorsum dark brown, with longitudinal, yellow to dark brown fusiform stripe across entire surface, cluster of antero-marginal white setae; venter brown, with pair of rufous, oblique stripes medially, covered with dark, thin setae.

Palp (Fig. 3A–C): tibia thick, slightly longer than wide; retrolateral tibial apophysis narrowed medially, broadened, extending anteriorly at distal half; cymbium almost two times longer than wide, gradually narrowed at distal half in ventral view; bulb suboval, with sperm duct sinuous retrolaterally; embolus short, originating from antero-prolateral portion of bulb, blunt apically, with small, semicircular lamellar process at base.

Female (Fig. 4A, B, E). Described by Lei and Peng (2010).

Distribution. Known only from the type locality in Yunnan, China.

Genus *Euochin* Prószyński, 2018

Type species. *Euophrys atrata* Song & Chai, 1992 from China by original designation.

Euochin mii sp. nov.

<https://zoobank.org/CEFDA51B-09E0-455C-8454-1FD0423DC48B>

Figs 5, 6

Type material. Holotype ♂ (IZCAS-Ar42919), CHINA: Yunnan: Xishuangbanna, Mengla County, Xiaolongha Village, Xishuangbanna National Nature Reserve,

seasonal rainforest (21°24.24'N, 101°36.27'E, ca 710 m alt.), 17.xi.2013, Q. Zhao and Z. Chen leg. *Paratypes* 1♂6♀ (IZCAS-Ar42920–42926), same data as holotype; 1♂2♀ (IZCAS-Ar42927–42929), same locality and collectors, 21.xi.2013.

Etymology. The species is named after Prof. Xiaoqi Mi, who helped us greatly with this research; noun (name) in genitive case.

Diagnosis. *Euochin mii* sp. nov. resembles that of *E. subwanyan* (Wang & Li, 2020) from China in having a tapered embolus, straight retrolateral tibial apophysis and similarly sized, paired atria, but it differs by the following: 1) embolus forming a disc at base (Fig. 5C) versus indistinct in *E. subwanyan* (Wang and Li 2020a: fig. 5C), 2) copulatory ducts about 1/7 diameter of spermatheca and curved anteromedially (Fig. 5C) versus about 1/4 diameter of spermatheca and twisted entirely in *E. subwanyan* (Wang and Li 2020a: fig. 6C). The female also closely resembles *E. luzonica* Logunov, 2020 from Philippines in having thin copulatory ducts and large, spherical spermathecae, but it can be easily distinguished by the distance between the atrium and epigastric furrow, which is about 2/5 the spermathecal diameter (Fig. 6) but less than 1/10 the diameter in *E. luzonica* (Logunov 2020: fig. 15).

Description. Male (Figs 5, 6C, D, F, G). Total length 2.87. Carapace 1.64 long, 1.23 wide. Abdomen 1.28 long, 0.94 wide. Clypeus 0.08 high. Eye sizes and inter-distances: AME 0.39, ALE 0.27, PLE 0.22, AERW 1.26, PERW 1.09, EFL 0.72. Legs: I 3.73 (1.15, 1.43, 0.70, 0.45), II 2.91 (0.93, 1.00, 0.55, 0.43), III 3.41 (1.15, 1.05, 0.78, 0.43), IV 3.51 (1.10, 1.13, 0.85, 0.43). Carapace dark brown, with longitudinal, yellow area and dark radial lines on thorax, bearing dense, bilateral, white setae and sparse, golden, thin setae, denser at eye base. Fovea dark red, longitudinal. Chelicerae orange to dark brown, with two promarginal teeth and one retromarginal tooth. Endites orange to dark, white entally at tip, broadened distally. Labium almost linguiform, with several dark setae distally. Sternum dark brown, heart-shaped. Legs dark brown except middle 1/2 of metatarsi and tarsi pale or pale yellow. Abdomen suboval, dorsum rufous, dotted, with a subtrapeziform yellow patch at anterior margin, pair of transverse yellow stripes medially, two large, irregular, pale markings posteriorly; venter dark brown, with four dotted lines.

Palp (Fig. 5A–D): tibia short, about 3 times wider than long in ventral view, with tapered, straight retrolateral tibial apophysis about 1.5 times longer than tibia; cymbium about 1.8 times longer than wide in ventral view; bulb swollen, with strongly curved sperm duct; embolus forming a disc at base, followed by tapered, knife-shaped portion, coiled into about 1/4 circle, and pointed apically.

Female (Fig. 6A, B, E). Total length 3.15. Carapace 1.59 long, 1.18 wide. Abdomen 1.67 long, 1.28 wide. Clypeus 0.08 high. Eye sizes and inter-distances: AME 0.38, ALE 0.25, PLE 0.22, AERW 1.19, PERW 1.08, EFL 0.72. Legs: I 2.76 (0.88, 1.05, 0.48, 0.35), II 2.46 (0.75, 0.88, 0.48, 0.35), III 3.18 (1.03, 1.15, 0.65, 0.35), IV 3.21 (1.00, 1.08, 0.78, 0.35). Habitus similar to that of male except with pale yellow legs and a distinct inverted triangular, yellow area across entire surface of thorax.



Figure 5. *Euochin mii* sp. nov., male holotype palp **A** prolateral **B** retrolateral **C** ventral **D** dorsal. Scale bars: 0.1.

Epigyne (Fig. 6A, B): atria oval, paired; copulatory openings anteriorly located, close to each other; copulatory ducts thin, strongly curved before descending posteriorly to connect with median part of ental sides of spermathecae; spermathecae almost spherical, touching; fertilization ducts lamellar, transversely extending, originating from anterior portions of spermathecae.

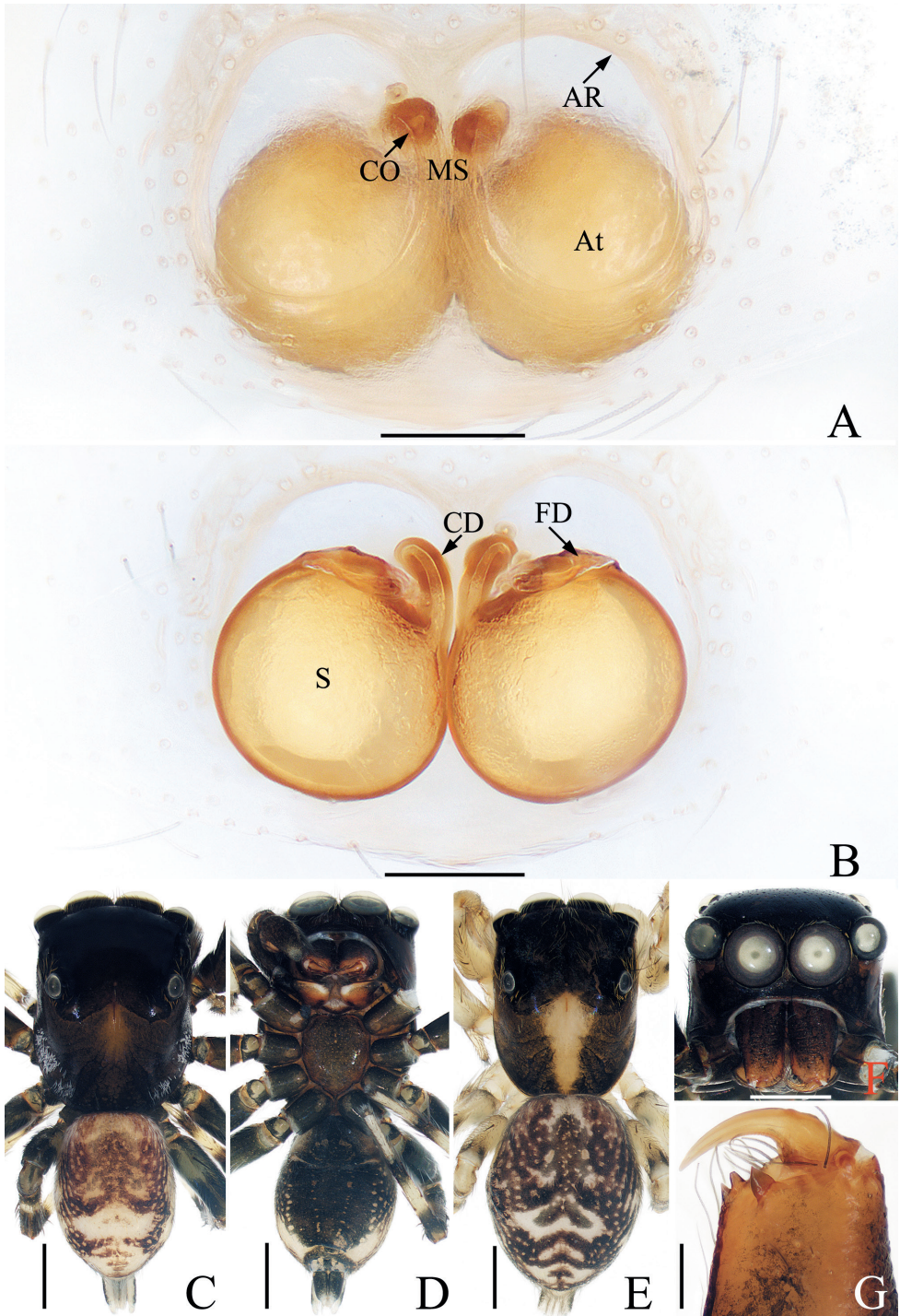


Figure 6. *Euochin mii* sp. nov., male holotype and female paratype **A** epigyne, ventral **B** vulva, dorsal **C** male holotype habitus, dorsal **D** ditto, ventral **E** female paratype habitus, dorsal **F** holotype carapace, frontal **G** holotype chelicera, posterior. Scale bars: 0.1 (**A**, **B**, **G**); 0.5 (**C**–**F**).

Distribution. Known only from the type locality in Yunnan, China.

Comments. Wang and Li (2021) mentioned that the generic position of *Euochin yaoi* Wang & Li, 2021 may need further confirmation. This is true for the new species and the following one as well for the same reasons.

***Euochin tangi* sp. nov.**

<https://zoobank.org/1BEE50AF-BF19-4FA2-8292-DAA5F3923486>

Fig. 7

Type material. *Holotype* ♀ (IZCAS-Ar42930), CHINA: Yunnan: Xishuangbanna, Mengla County, Xiaolongha Village, Xishuangbanna Biodiversity Conservation Corridor, ravine rainforest (21°24.25'N, 101°36.32'E, ca 760 m alt.), 16.xi.2013, Q. Zhao and Z. Chen leg. *Paratype* 1♀ (IZCAS-Ar42931), same data as holotype.

Etymology. The specific name is a patronym in honor of the late Guo Tang, a major collector of spiders from Xishuangbanna; noun (name) in genitive case.

Diagnosis. The new species can be easily distinguished from other congeners by the presence of anteromedial accessory glands of the copulatory ducts, and the long (longer than spermathecae) and medially fold copulatory ducts (Fig. 7A–C), which lack accessory glands of the copulatory ducts, and have short (shorter than spermathecae) and not fold copulatory ducts in others (see Metzner 2022).

Description. Female (Fig. 7). Total length 3.82. Carapace 1.76 long, 1.41 wide. Abdomen 1.99 long, 1.48 wide. Clypeus 0.07 high. Eye sizes and inter-distances: AME 0.47, ALE 0.30, PLE 0.25, AERW 1.48, PERW 1.33, EFL 0.88. Legs: I 3.51 (1.10, 1.38, 0.63, 0.40), II 3.01 (0.95, 1.15, 0.53, 0.38), III 3.79 (1.25, 1.28, 0.83, 0.43), IV 4.07 (1.25, 1.38, 1.01, 0.43). Carapace yellow to dark brown, with pair of bilateral yellow bands and longitudinal, an irregular yellow band extending from the center of eye field to posterior margin, covered with dark and golden setae. Fovea thin, red-brown, longitudinal. Chelicerae yellow, with two promarginal teeth and one retromarginal fissidental tooth. Endites paler than chelicerae, bearing dense, dark setae at ental margins. Labium dark brown. Sternum pale to yellow, covered with brown, thin setae. Legs pale to yellow. Abdomen suboval, dorsum gray-brown to dark brown, dotted, with a longitudinal, irregular gray band anteriorly followed by two pairs of muscle depressions, then several herringbone and arched stripes, as well as several pairs of irregular gray patches laterally; venter pale yellow, with irregular dark brown patches posteromedially.

Epigyne (Fig. 7A–C): slightly wider than long; atria oval, paired; copulatory openings slit-like, beneath the anterior margin of median septum; copulatory ducts thick, posteriorly extending at origin, then curving bilaterally before folding, obliquely extending posteriorly to connect with anterior ental portions of spermathecae, with short accessory glands anteriorly; spermathecae subspherical, touching; fertilization ducts lamellar, originating from anterolateral portions of spermathecae.

Male. Unknown.

Distribution. Known only from the type locality in Yunnan, China.

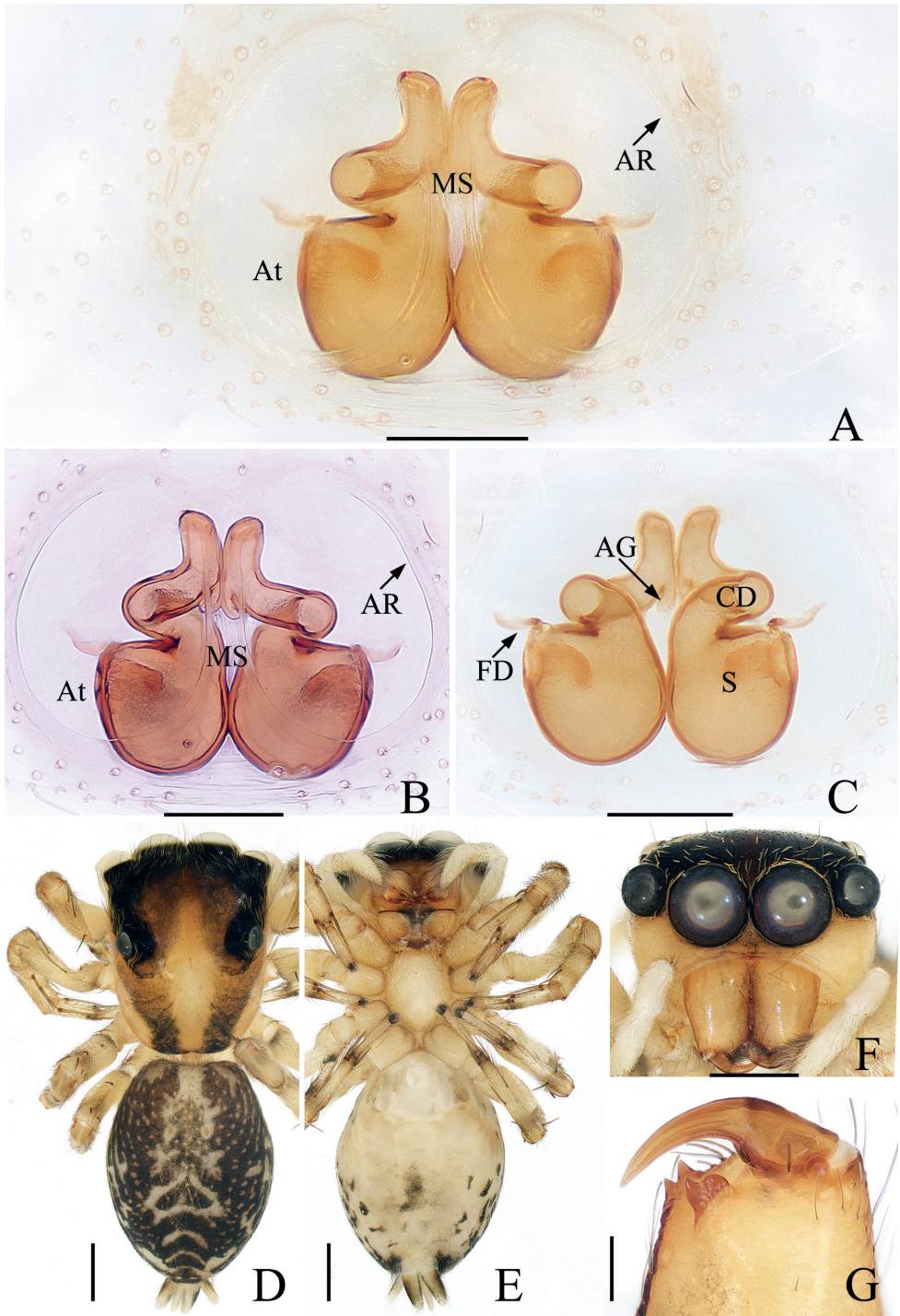


Figure 7. *Euochin tangi* sp. nov., female holotype **A, B** epigyne, ventral **C** vulva, dorsal **D** habitus, dorsal **E** ditto, ventral **F** carapace, frontal **G** chelicera, posterior. Scale bars: 0.1 (**A–C, G**); 0.5 (**D–F**).

Genus *Eupoa* Żabka, 1985

Type species. *Eupoa prima* Żabka, 1985 from Vietnam by original designation.

***Eupoa logunovi* sp. nov.**

<https://zoobank.org/62C86F4D-CA74-4620-9C7A-8BCD97156B91>

Figs 8, 9

Type material. *Holotype* ♂ (IZCAS-Ar42932), CHINA: Yunnan: Xishuangbanna, Mengla County, Xiaolongha Village, Xishuangbanna Biodiversity Conservation Corridor, ravine rainforest (21°24.25'N, 101°36.32'E, 760 ± 20 m alt.), 16.xi.2013, Q. Zhao and Z. Chen leg. *Paratypes* 1♂1♀ (IZCAS-Ar42933–42934), same data as holotype.

Etymology. The specific name is a patronym in honor of Dmitri V. Logunov, who contributed significantly to the taxonomy of the genus *Eupoa*; noun (name) in genitive case.

Diagnosis. *Eupoa logunovi* sp. nov. can be easily distinguished from other congeners by the long, twisted retrolateral femoral apophysis (longer than the tibia), which is absent or shorter than the tibia in others (see Metzner 2022). The female of this species resembles that of *E. prima* Żabka, 1985 from Vietnam in having very long copulatory ducts, but it can be easily distinguished by the presence of a concave septum (Fig. 9A) versus absent in *E. prima* (Żabka 1985: figs 167, 168), and by copulatory ducts that are connected to the baso-inner portions of spermathecae (Fig. 9B), whereas in *E. prima* they are lateral to the spermathecae (Żabka 1985: fig. 169).

Description. Male (Figs 8, 9C, E–H). Total length 2.02. Carapace 1.02 long, 0.91 wide. Abdomen 0.96 long, 0.74 wide. Clypeus 0.07 high. Eye sizes and inter-distances: AME 0.29, ALE 0.21, PLE 0.13, AERW 0.94, PERW 0.85, EFL 0.53. Legs: I 1.89 (0.60, 0.68, 0.38, 0.23), II 1.61 (0.53, 0.55, 0.30, 0.23), III 1.61 (0.50, 0.50, 0.38, 0.23), IV 2.28 (0.75, 0.80, 0.48, 0.25). Carapace yellow to dark brown, steeply sloped at posterior margin, with an inverted subtriangular yellow area extending from middle of eye field to posterior margin, bearing sparse setae at eye base. Fovea indistinct. Chelicerae pale to yellow, with two promarginal and four retromarginal teeth. Endites colored as chelicerae. Labium slightly darker than endites. Sternum almost heart-shaped, paler medially, covered with thin, brown setae. Legs yellow, with three pairs of ventral spines on metatarsi and tibiae I, respectively. Abdomen suboval, dorsum dark, somewhat mingled with blue, with longitudinal, central, narrow yellow stripe across nearly the entire surface; venter pale, setose, without markings.

Palp (Fig. 8A–D): femur about 2.5 times longer than wide in retrolateral view, with tapered, S-shaped retrolateral apophysis twisted into pointed tip; patella slightly wider than femur, with spiraled retrolateral apophysis; tibia wider than long, with strongly sclerotized, tapered ventral apophysis extending posteriorly to blunt end and squarish retrolateral apophysis; cymbium setose; bulb swollen, oval; median apophysis transversely extending in ventral view, forming small hook distally; terminal apophysis lamellar, extending antero-retrolaterally, with blunt tip; embolus filiform, coiled into circle distally, tip extending beyond cymbial tip.

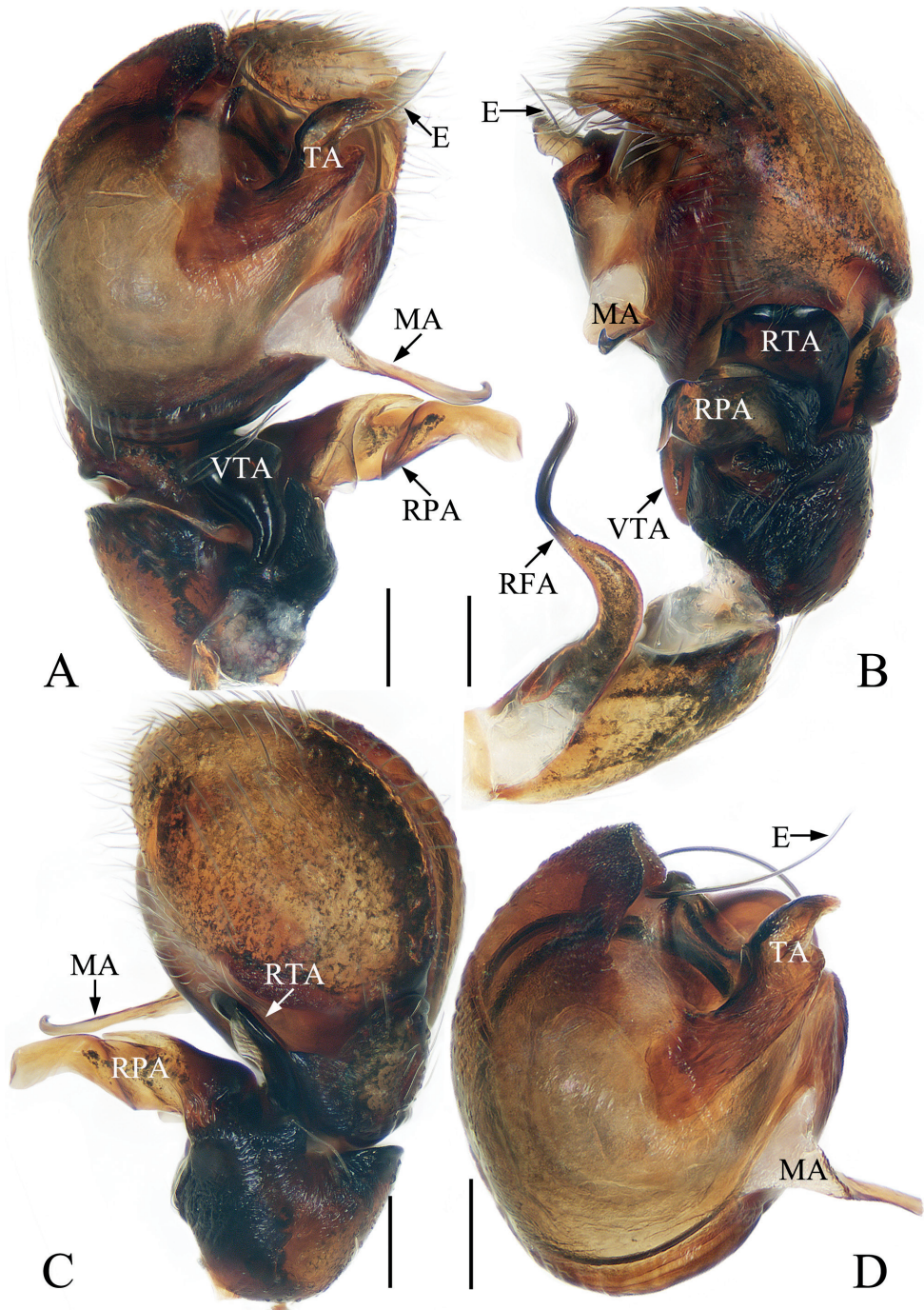


Figure 8. *Eupoia logunovi* sp. nov., male holotype palp **A** ventral **B** retrolateral **C** dorsal **D** bulb, ventral. Scale bars: 0.1.

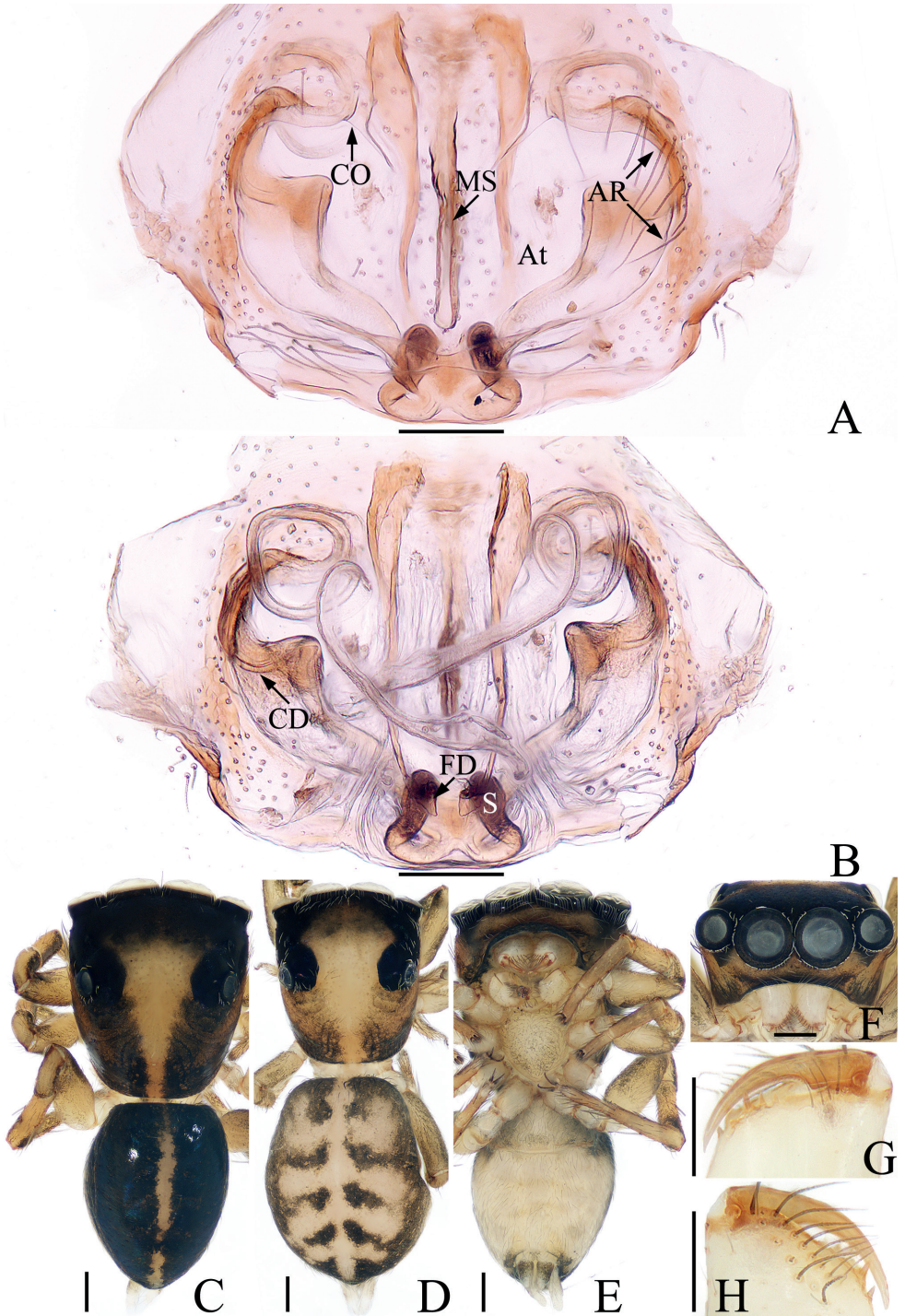


Figure 9. *Eupoa logunovi* sp. nov., male holotype and female paratype **A** epigyne, ventral **B** vulva, dorsal **C** male holotype habitus, dorsal **D** female paratype habitus, dorsal **E** holotype habitus, ventral **F** holotype carapace, frontal **G** holotype chelicera, posterior **H** ditto, anterior. Scale bars: 0.1 (**A, B, G, H**); 0.2 (**C-F**).

Female. (Fig. 9A, B, D). Total length 2.20. Carapace 0.95 long, 0.82 wide. Abdomen 1.18 long, 0.94 wide. Clypeus 0.08 high. Eye sizes and inter-distances: AME 0.27, ALE 0.19, PLE 0.13, AERW 0.86, PERW 0.79, EFL 0.52. Legs: I 1.94 (0.60, 0.73, 0.38, 0.23), II 1.59 (0.48, 0.58, 0.30, 0.23), III 1.61 (0.50, 0.50, 0.38, 0.23), IV 2.46 (0.78, 0.90, 0.53, 0.25). Habitus similar to that of male except paler, with four distinct yellow bands on dorsum of abdomen.

Epigyne (Fig. 9A, B): wider than long; atrium large, suboval separated by concave septum, with pair of arched anterolateral ridges and U-shaped posterior ridge; copulatory openings anteriorly located; copulatory ducts membranous at origin, and then leading to lateral, twisted, sclerotized portions that descend obliquely and connect to the base of elongated spermathecae; fertilization ducts triangular, originating from anterior portion of spermathecae.

Distribution. Known only from the type locality in Yunnan, China.

Genus *Indomarengo* Benjamin, 2004

Type species. *Indomarengo sarawakensis* Benjamin, 2004 from Indonesia by original designation.

Indomarengo wengnan sp. nov.

<https://zoobank.org/6FF5D3FD-D2AA-4F2F-9795-9A396EFA1F25>

Fig. 10

Type material. *Holotype* ♀ (IZCAS-Ar42935), CHINA: Yunnan: Xishuangbanna, Jinghong City, Meng'a Township, Wengnan Village, secondary forest (22°05.00'N, 100°22.22'E, 1137 ± 12 m alt.), 25.xii.2012, Q. Zhao and Z. Chen leg.

Etymology. The specific name is derived from the name of the type locality and is a noun in apposition.

Diagnosis. *Indomarengo wengnan* sp. nov. resembles that of *I. yui* Wang & Li, 2020 from China in having a similar habitus and L-shaped spermathecae, but it can be easily distinguished by the following: 1) atria separated from each other by more than their width (Fig. 10A–D) versus almost touching in *I. yui* (Fig. 11A–C); 2) copulatory ducts not coiled (Fig. 10A–D) versus distally coiled in *I. yui* (Fig. 11A–C). The species is also similar to *Tauala elongatus* Peng & Li, 2002 from China in the general habitus and the paired, separated atria, but it differs by the absence of accessory glands of the copulatory ducts and L-shaped spermathecae (Fig. 10A–D), whereas in *T. elongatus* the glands of the copulatory ducts are present and the spermathecae are tube-shaped (Peng and Li 2002: fig. 20).

Description. Female (Fig. 10A–J). Total length 3.55. Carapace 1.38 long, 0.79 wide. Abdomen 2.03 long, 0.82 wide. Clypeus almost invisible. Eye sizes and inter-distances: AME 0.29, ALE 0.13, PLE 0.11, AERW 0.73, PERW 0.77, EFL 0.51. Legs: I 2.66 (0.70, 1.13, 0.63, 0.20), II 1.68 (0.50, 0.63, 0.35, 0.20), III 1.59 (0.48, 0.53, 0.38, 0.20), IV 2.23 (0.68, 0.85, 0.50, 0.20). Carapace flat, covered with thin

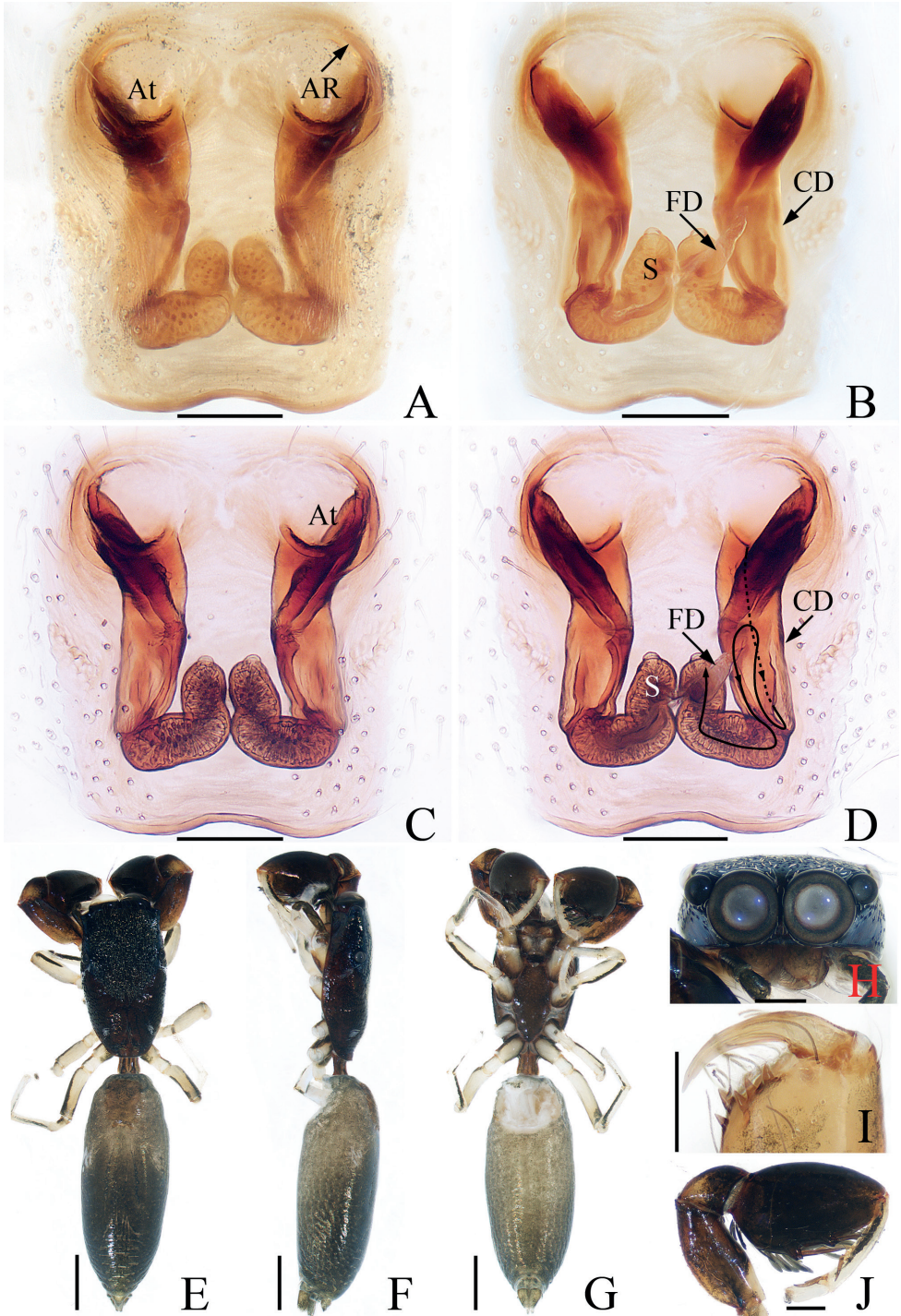


Figure 10. *Indomarengo wengnan* sp. nov., female holotype **A, C** epigyne, ventral **B, D** vulva, dorsal **E** habitus, dorsal **F** ditto, lateral **G** ditto, ventral **H** carapace, frontal **I** chelicera, posterior **J** leg I, prolateral. Scale bars: 0.1 (**A-D, G**); 0.5 (**E-G**); 0.2 (**H, J**).

setae anteromedially, bearing four clusters of white scales with two posterolateral to AMEs and two posterolaterally located on thorax. Chelicerae with two promarginal and three retromarginal teeth. Endites longer than wide, pale the ental sides. Labium dark. Sternum elongated, almost fusiform. Legs I strongest, with enlarged tibia bearing cluster of leaf-like scales and five spines ventrally, others pale, with dark brown stripes laterally on femora and tibia. Abdomen elongated, dorsum brown to dark brown, with subtrapezoid sclerite near anterior margin and pair of indistinct white patches of setae laterally on anterior 1/3; venter gray-brown, without distinct markings.

Epigyne (Fig. 10A–D): longer than wide; atria paired, almost round, separated from each other by more than their diameter, with pair of semicircular anterolateral atrial ridges; copulatory ducts flat, broad, extending posteriorly along longitudinal axis at anterior half, before contrary extending and leading to the slender parts that slightly curved medially and connected to lateral part of spermathecae; spermathecae prominent, L-shaped, with hemispherical processes at anterior margins; fertilization ducts originating from middle of longitudinally extending portions of spermathecae.

Male. Unknown.

Distribution. Known only from the type locality in Yunnan, China.

Comments. According to the morphological characters, the new species and *I. yui* are similar to *I. thomsoni* (Wanless, 1978) and *Philates chelififer* (Simon, 1900) in having an elongated, flat body, a specific form of the copulatory ducts, and prominent spermathecae, which are absent in the type species of *Indomarengo* and *Philates* Simon, 1900, but both may not be monophyletic and need further revision. We provisionally place our two species in *Indomarengo*.

Indomarengo yui Wang & Li, 2020

Fig. 11

Indomarengo yui Wang & Li, 2020b: 51, figs 5A–D, 6A–E (male holotype, examined).

Material examined. 1♂1♀ (IZCAS-Ar42936–42937), CHINA: Yunnan: Xishuangbanna, Mengla County, Huigang Village, Xilu habitat restoration area, seasonal rainforest (21°37.05'N, 101°35.27'E, 760 ± 25 m alt.), 12.xii.2012, Q. Zhao and Z. Chen leg.; 1♀ (IZCAS-Ar42938), Menglun Nature Reserve, secondary tropical forest, around garbage dump (21°54.17'N, 101°16.87'E, ca 610 m alt.), 31.xii.2018, Z. Bai et al. leg.

Diagnosis. The male was thoroughly diagnosed by Wang and Li (2020b). The female resembles that of *I. thomsoni* (Wanless, 1978) from Borneo in having a similar epigyne, but it can be easily distinguished by the paired atria and L-shaped spermathecae (Fig. 11A–C), whereas there is a single atrium and irregular spermathecae in *I. thomsoni* (Wanless 1978b: fig. 8B, D, E). The species also resembles *Philates chelififer* from Indonesia, but it can be easily distinguished by having the abdomen with pair of round patches and a transverse band anteriorly (Fig. 11E), which are absent in *P. chelififer*, and by the L-shaped spermathecae (Fig. 11C), which are almost U-shaped in *P. chelififer* (Benjamin 2004: fig. 26C).

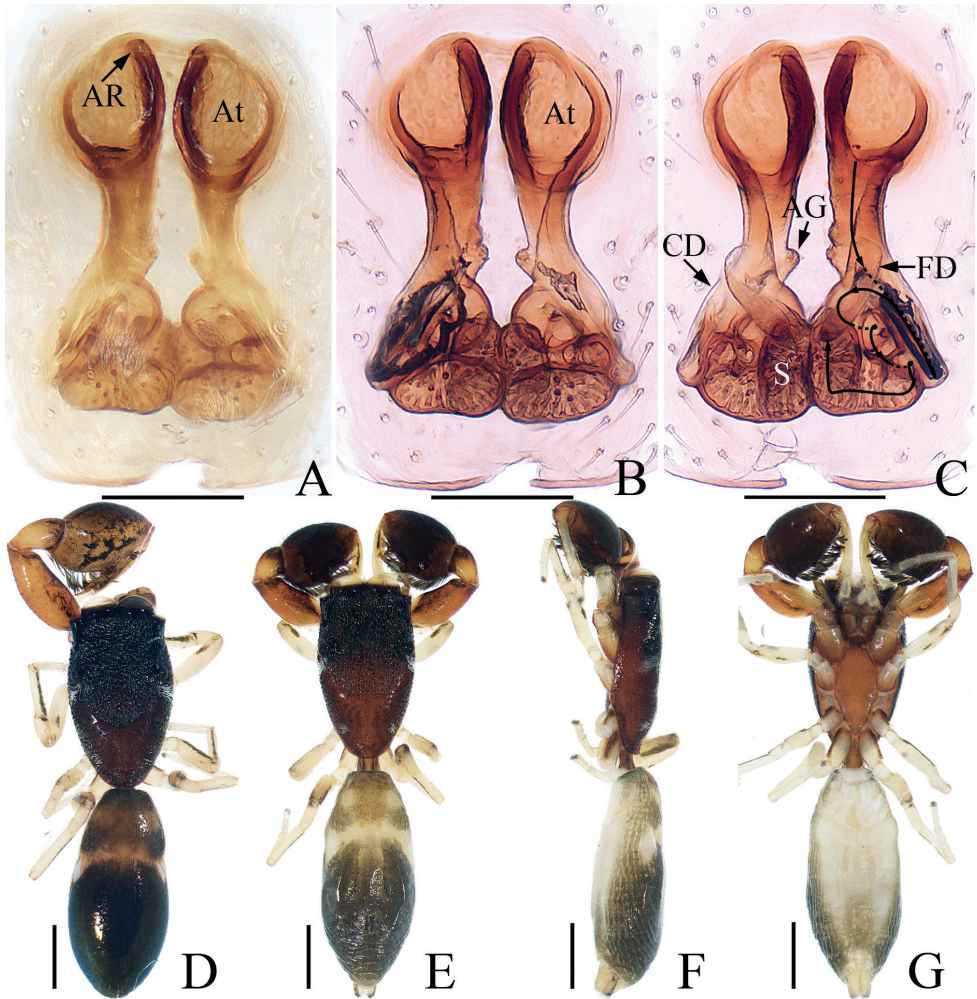


Figure 11. *Indomarengo yui* **A, B** epigyne, ventral **C** vulva, dorsal **D** male habitus, dorsal **E** female habitus, dorsal **F** ditto, lateral **G** ditto, ventral. Scale bars: 0.1 (**A-C**); 0.5 (**D-G**).

Description. Male (Fig. 11D). See Wang and Li (2020b).

Female (Fig. 11A–C, E–G). Total length 3.20. Carapace 1.20 long, 0.79 wide. Abdomen 1.73 long, 0.76 wide. Clypeus almost invisible. Eye sizes and inter-distances: AME 0.28, ALE 0.12, PLE 0.11, AERW 0.73, PERW 0.78, EFL 0.51. Legs: I 2.48 (0.68, 1.05, 0.55, 0.20), II 1.57 (0.48, 0.58, 0.33, 0.18), III 1.51 (0.48, 0.50, 0.35, 0.18), IV 2.07 (0.64, 0.80, 0.45, 0.18). Carapace flat, red-brown to dark, covered with thin setae, bearing four clusters of white scales. Chelicerae, endites, labium, sternum, and legs similar to that of male. Abdomen elongated, dorsum brown to dark brown, with subtrapezoid sclerite, pair of round pale patches near anterior margin, followed by transverse pale band bearing pair of white patches at lateral margins; venter pale.

Epigyne (Fig. 11A–C): longer than wide, with arched atrial ridge anteriorly; atria paired, oval, nearly touching; copulatory openings located at base of atria; copulatory ducts posterolaterally extending before returning to the middle part, then continuing, coiled into two semicircles, connecting to the lateral sides of spermathecae; spermathecae prominent, almost L-shaped, with small, hemispheric processes at anterior margins; fertilization ducts originating from anterior portions of longitudinal extensions of spermathecae.

Distribution. Known only from the type locality in Yunnan, China.

Genus *Laufeia* Simon, 1889

Type species. *Laufeia aenea* Simon, 1889 from Japan by original designation.

Laufeia zhangae sp. nov.

<https://zoobank.org/27C8FE88-B067-4B7B-A496-E9B377518ECA>
Figs 12, 13

Laufeia squamata Logunov & Jäger, 2015: 355, figs 33–36 (♂, mismatched).

Type material. *Holotype* ♂ (IZCAS-Ar42939), CHINA: Yunnan: Xishuangbanna, Jihong City, Mengyang Township, seasonal forest (22°09.77'N, 100°52.55'E, 860 ± 30 m alt.), 22.xii.2012, Q. Zhao and Z. Chen leg. *Paratypes* 1♂ (IZCAS-Ar42940), Menglun Township, 55 km from Xishuangbanna National Nature Reserve, artificial *Ficus microcarpa* forest (21°54.97'N, 100°16.05'E, ca 610 m alt.), 21.viii.2011, Q. Zhao leg.; 1♀ (IZCAS-Ar42941), 55 km from Xishuangbanna National Nature Reserve, seasonal rainforest (21°57.70'N, 101°12.52'E, 670 ± 30 m alt.), Q. Zhao and Z. Chen leg.; 1♀ (IZCAS-Ar42942), Mengyang Township, seasonal rainforest off Baihuashan tunnel (22°09.53'N, 101°55.21'E, 860 ± 12 m alt.), 16. xii.2012, Q. Zhao and Z. Chen leg.

Etymology. The species name is a patronym in honor of Ms Junxia Zhang, who has contributed greatly to the taxonomy of jumping spiders worldwide; noun (name) in genitive case.

Diagnosis. *Laufeia zhangae* sp. nov. closely resembles *L. aenea* Simon, 1889 from China, Korea, and Japan in general habitus and copulatory organs, but it can be easily distinguished by the following: 1) embolus lacks a branched projection (Fig. 12C) versus branched projection present in *L. aenea* (Ikeda 1998: fig. 6); 2) tibia with a subtriangular ventral apophysis (Fig. 12C) versus ventral apophysis indistinct in *L. aenea* (Ikeda 1998: fig. 6); 3) copulatory openings slit-like (Fig. 13A) versus openings oval in *L. aenea* (Ikeda 1998: fig. 7); 4) copulatory ducts with proximal conical accessory glands (Fig. 13B) versus glands indistinct in *L. aenea* (Ikeda 1998: fig. 8).

Description. **Male** (Figs 12, 13C, D, F, G). Total length 3.56. Carapace 1.83 long, 1.39 wide. Abdomen 1.92 long, 1.31 wide. Clypeus 0.03 high. Eye sizes and inter-

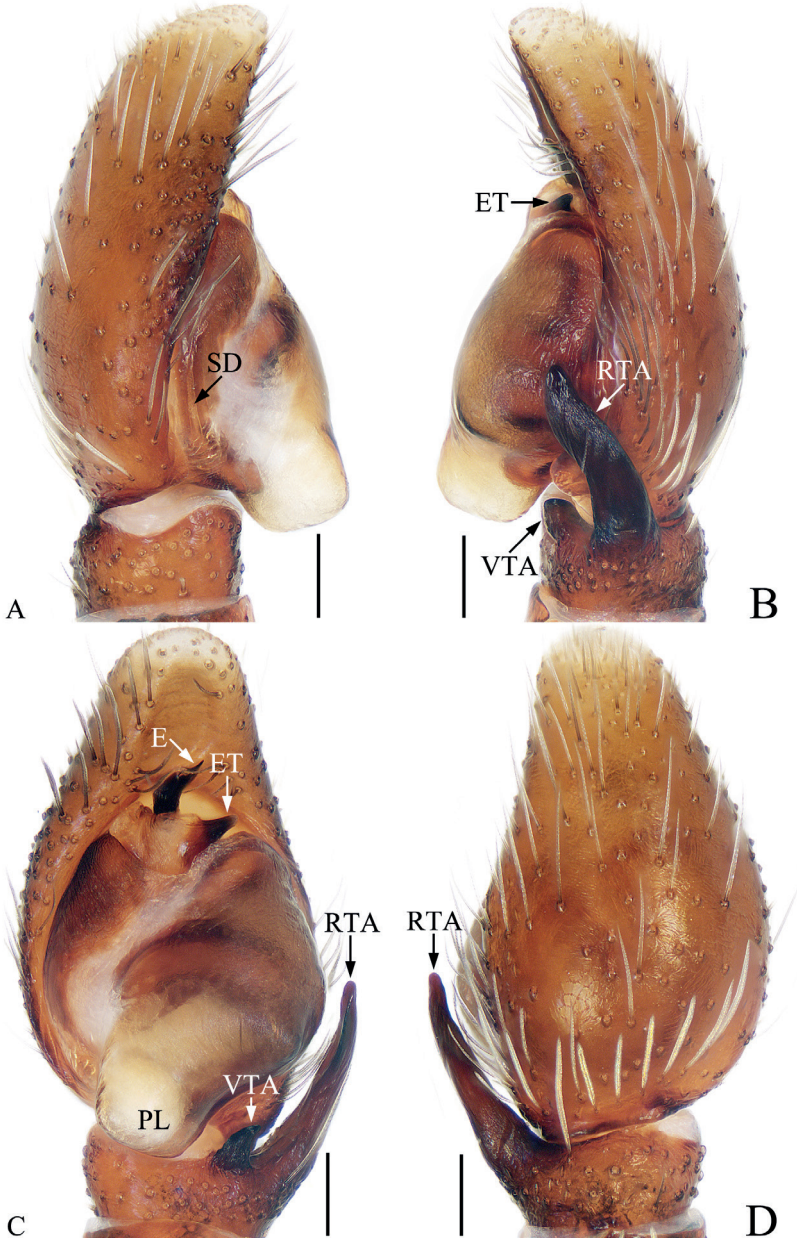


Figure 12. *Laufeia zhangae* sp. nov., male holotype palp **A** prolateral **B** retrolateral **C** ventral **D** dorsal. Scale bars: 0.1.

distances: AME 0.36, ALE 0.25, PLE 0.22, AERW 1.18, PERW 0.88, EFL 0.78. Legs: I 3.61 (1.13, 1.50, 0.58, 0.40), II 2.96 (0.90, 1.13, 0.53, 0.40), III 2.96 (0.95, 1.08, 0.53, 0.40), IV 3.01 (0.90, 1.13, 0.58, 0.40). Carapace squarish, red-brown to dark brown, covered with dense, white setae, and golden setae on anterior eye bases and clypeus. Fovea dark, longitudinal. Chelicerae dark red to dark, with two promarginal

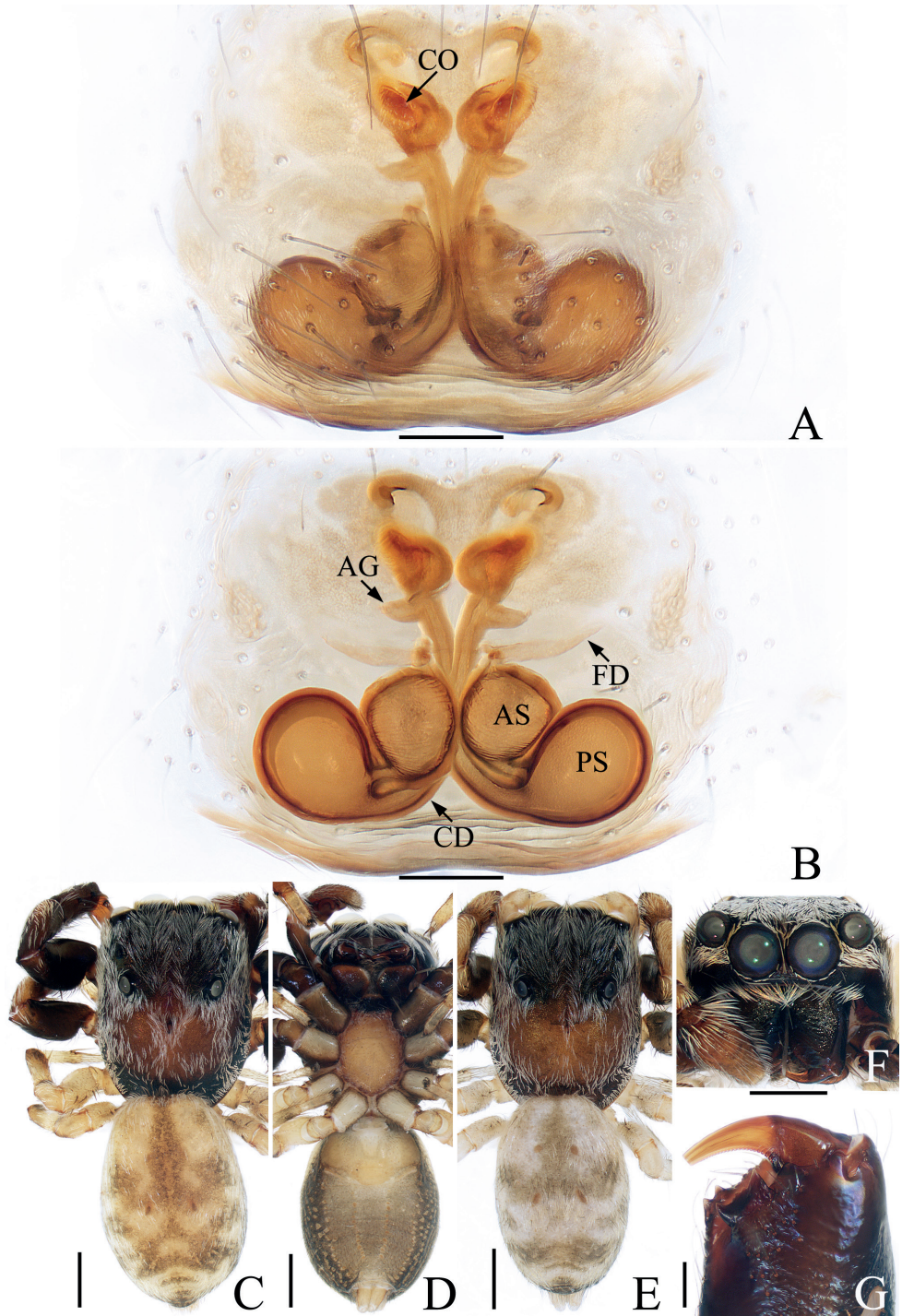


Figure 13. *Laufeia zhangae* sp. nov., male holotype and female paratype **A** epigyne, ventral **B** vulva, dorsal **C** male holotype habitus, dorsal **D** ditto, ventral **E** female paratype habitus, dorsal **F** holotype carapace, frontal **G** holotype chelicera, posterior. Scale bars: 0.1 (**A**, **B**, **G**); 0.5 (**C**–**F**).

teeth and one retromarginal fissidental tooth with two cusps. Endites red-brown to dark, broadened distally, bearing dense, dark setae at ental margins. Labium dark, almost linguiform. Sternum yellow, covered with pale, thin setae. Legs pale yellow to dark brown. Abdomen suboval, with large, irregular, dark brown patch and two pairs of muscle depressions, covered with short, white, thin setae; venter brown to dark brown, dotted laterally, with pair of dotted lines medially.

Palp (Fig. 12A–D): tibia short, about 1.5 times wider than long in retrolateral view, with strongly sclerotized, subtriangular ventral apophysis pointed apically, and tapered retrolateral apophysis slightly curved, extending antero-prolaterally to a blunt tip in retrolateral view; cymbium about 1.7 times longer than wide in ventral view, with sparse, long, white scales at dorsum of proximal portion; bulb longer than wide, with subtrapezoid posterior lobe; embolus strongly sclerotized, short, curved towards retrolateral side distally, with a pointed tip directed towards about 1:00 position, and a tapered, blunt basal tooth.

Female (Fig. 13A, B, E). Total length 3.15. Carapace 1.67 long, 1.26 wide. Abdomen 1.64 long, 1.13 wide. Clypeus 0.03 high. Eye sizes and inter-distances: AME 0.33, ALE 0.23, PLE 0.19, AERW 1.05, PERW 0.87, EFL 0.69. Legs: I 2.66 (0.83, 1.20, 0.38, 0.25), II 2.36 (0.78, 0.95, 0.38, 0.25), III 2.60 (0.85, 0.95, 0.50, 0.30), IV 2.89 (0.88, 1.10, 0.58, 0.33). Habitus similar to that of male except paler.

Epigyne (Fig. 13A, B): wider than long, with pair of shallow hoods anteriorly; copulatory openings anteriorly located, slit-like; copulatory ducts swollen at origin, extending posteriorly to connect with the base of ental sides of posterior chambers of spermathecae, with proximal, conical accessory glands; spermathecae divided into two sub-spherical chambers; fertilization ducts anterior to anterior chamber of spermathecae, extended transversely.

Distribution. China (Yunnan), Vietnam.

Genus *Rhene* Thorell, 1869

Type species. *Rhanis flavigera* C. L. Koch, 1846 from Indonesia by original designation.

Rhene triapophysys Peng, 1995

Figs 14, 15

Rhene triapophysys Peng, 1995: 35, figs 1–5 (male holotype, not examined); Peng 2020: 395, fig. 288a–c.

Material examined. 1♂3♀ (IZCAS-Ar42943–42946), CHINA: Yunnan, Xishuangbanna, Mengla County, Menglun Town, Xishuangbanna Tropical Botanical Garden, Yulinjiegou (21°55.05'N, 101°16.24'E, ca 570 m alt.), 19.xii.2018, X. Mi et al. leg.; 1♂1♀ (IZCAS-Ar42947–42948), 1 site in Mafengzhai (21°53.45'N, 101°17.40'E, ca 543 m alt.), 29.ix.2019, Y. Tong et al. leg.

Diagnosis. *Rhene triapophyses* Peng, 1995 closely resembles that of *R. setipes* Żabka, 1985 from China, Vietnam and Japan in the general shape of the habitus and copulatory organs, but it differs in the following: 1) embolic division includes two terminal apophyses (Fig. 14B) versus only one terminal apophysis in *R. setipes* (Żabka 1985: fig. 563); 2) anteromedially, retrolateral tibial apophysis extending antero-retrolaterally (Fig. 14C) versus extending antero-prolaterally in *R. setipes* (Żabka 1985: fig. 564); 3) female almost indistinguishable from *R. setipes* except in the form of the copulatory ducts and atria (Fig. 15A–C vs Tanikawa 1993: figs 10, 11).

Description. Male (Figs 14, 15D, E, G–I). Total length 4.07. Carapace 1.93 long, 1.90 wide. Abdomen 2.30 long, 1.83 wide. Clypeus 0.08 high. Eye sizes and inter-distances: AME 0.42, ALE 0.22, PLE 0.20, AERW 1.43, PERW 1.87, EFL 1.24. Legs: I 4.66 (1.63, 1.85, 0.68, 0.50), II 3.19 (1.08, 1.13, 0.58, 0.40), III 2.98 (1.00, 0.98, 0.60, 0.40), IV 3.88 (1.33, 1.40, 0.75, 0.40). Carapace red-brown to dark brown, almost hexagonal, with large, irregular dark brown patch at center of eye field, covered with dense setae. Fovea indistinct. Chelicerae red-brown, with two promarginal teeth and one retromarginal tooth, the paturon covered by papillae, with distinct incision on anterior surface. Endites typical, bearing dark setae entally. Labium darker than endites. Sternum almost oval, bearing pale, thin setae. Legs I strongest, with enlarged femora, two pairs of ventral spines on tibia and three ventral spines on metatarsi, other legs yellow to dark brown, with slightly enlarged femora. Abdomen suboval, dorsum red-brown, yellow posteriorly, with an irregular, longitudinal dark patch anteromedially followed by a broad, transverse, dark brown band, covered with short, pale white, thin setae and wholly covered by large scutum; venter brown, with a pair of longitudinal, dark stripes medially.

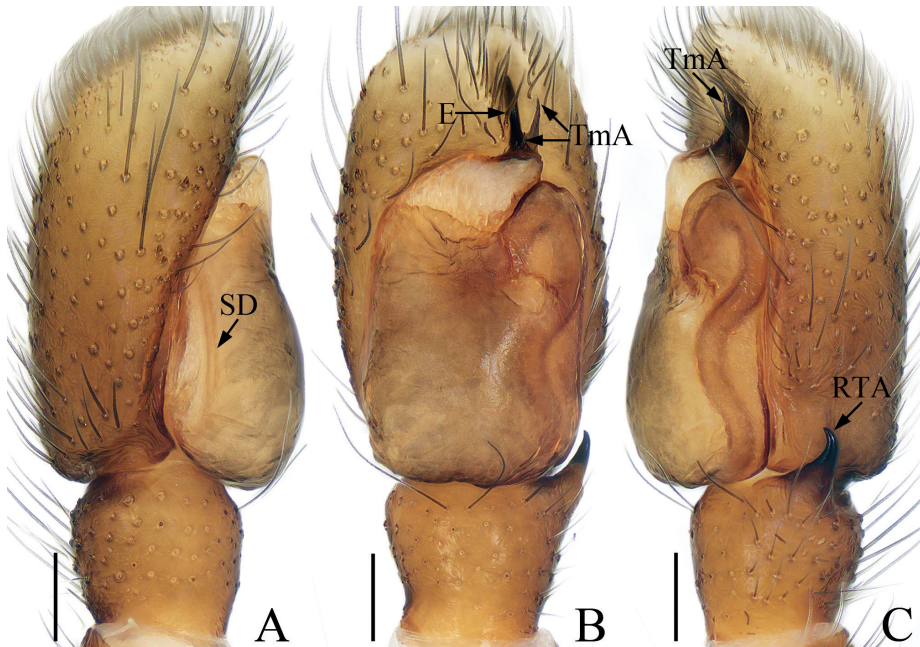


Figure 14. *Rhene triapophyses*, male palp **A** prolateral **B** ventral **C** retrolateral. Scale bars: 0.1.

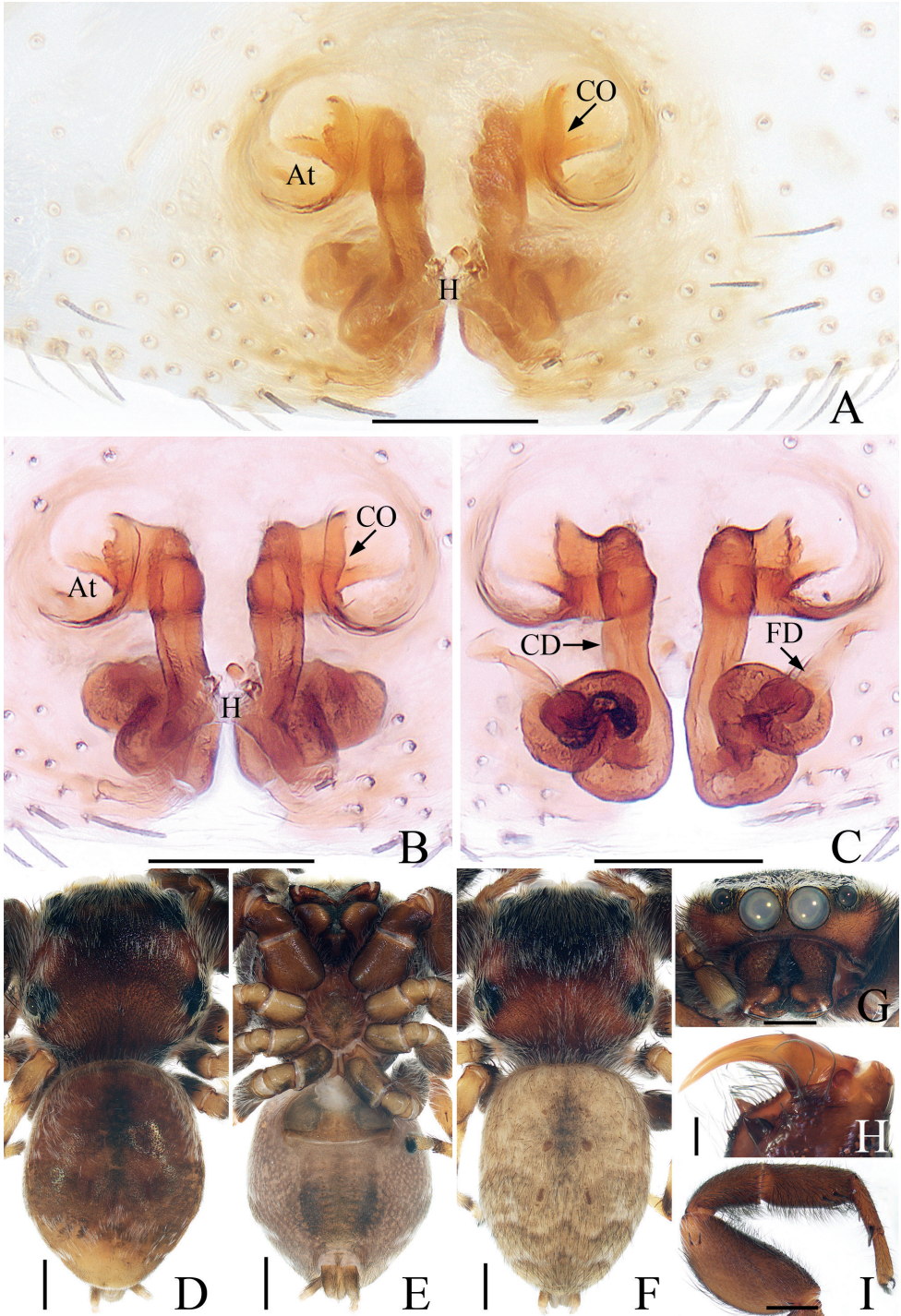


Figure 15. *Rhene triapophyses* **A, B** epigyne, ventral **C** vulva, dorsal **D** male habitus, dorsal **E** ditto, ventral **F** female habitus, dorsal **G** male carapace, frontal **H** male chelicera, posterior **I** male leg I, prolateral. Scale bars: 0.1 (**A-C, H**); 0.5 (**D-F, I**); 0.2 (**G**).

Palp (Fig. 14A–D): tibia almost as long as wide, with tapered retrolateral apophysis distally curved inward to a pointed tip; cymbium about 1.5 times longer than wide; bulb slightly swollen posteromedially, with tapered sperm duct, sinuous retrolaterally; embolus originating from middle of anterior margin of bulb, bar-shaped, blunt apically, division with two spiny apophyses.

Female (Fig. 15A–C, F). Total length 4.32. Carapace 2.04 long, 1.96 wide. Abdomen 2.50 long, 1.86 wide. Clypeus 0.08 high. Eye sizes and inter-distances: AME 0.40, ALE 0.22, PLE 0.20, AERW 1.43, PERW 1.96, EFL 1.29. Legs: I 4.00 (1.45, 1.55, 0.55, 0.45), II 3.13 (1.08, 1.15, 0.50, 0.40), III 3.08 (1.03, 1.05, 0.60, 0.40), IV 4.09 (1.33, 1.53, 0.83, 0.40). Habitus similar to that of male except paler and without dorsal scutum on abdomen.

Epigyne (Fig. 15A–C): wider than long, with broad posterior hood distant from epigastric furrow; atria paired, oval, separated from each other by slightly more than width of epigynal hood; copulatory ducts long, transversely extending before curving 90° then descending posteriorly, continuing into an S-shaped coil; spermathecae indistinct; fertilization ducts lamellar, extending anterolaterally.

Distribution. China (Yunnan).

Comments. The male of the new material is almost identical with the holotype in palpal and cheliceral structure except detail difference in the length of the apophyses of embolic division. Moreover, material studied in this paper were collected from the same locality as holotype in Menglun County, Xishuangbanna, China.

Genus *Simaetha* Thorell, 1881

Type species. *Simaetha thoracica* Thorell, 1881 from Australia by original designation.

Simaetha huigang sp. nov.

<https://zoobank.org/C45C3830-6985-49C1-B781-9FF7B7EFB63C>

Figs 16, 17

Type material. *Holotype* ♂ (IZCAS-Ar42949), CHINA: Yunnan: Xishuangbanna, Mengla County, Huigang Village, Xilu habitat restoration area, seasonal rainforest (21°37.05'N, 101°35.27'E, 764 ± 25 m alt.), 12.xii.2012, Q. Zhao and Z. Chen leg. *Paratypes* 1 ♀ (IZCAS-Ar42950), same data as holotype; 1 ♂ (IZCAS-Ar42951), Menglun Town, Menglun Nature Reserve, 2 site of Leprosy Village (21°53.59'N, 101°17.30'E, ca 550 m alt.), 4.v.2019, Y. Tong et al. leg; 1 ♂ 1 ♀ (IZCAS-Ar42952–42953), Xiaolongha Village, diversity conservation corridor of Xishuangbanna National Nature Reserve, seasonal rainforest (21°24.19'N, 101°37.03'E, 657 ± 15 m alt.), 29.xi.2012, Q. Zhao and Z. Chen leg.

Etymology. The species name is a noun in apposition derived from the holotype locality.

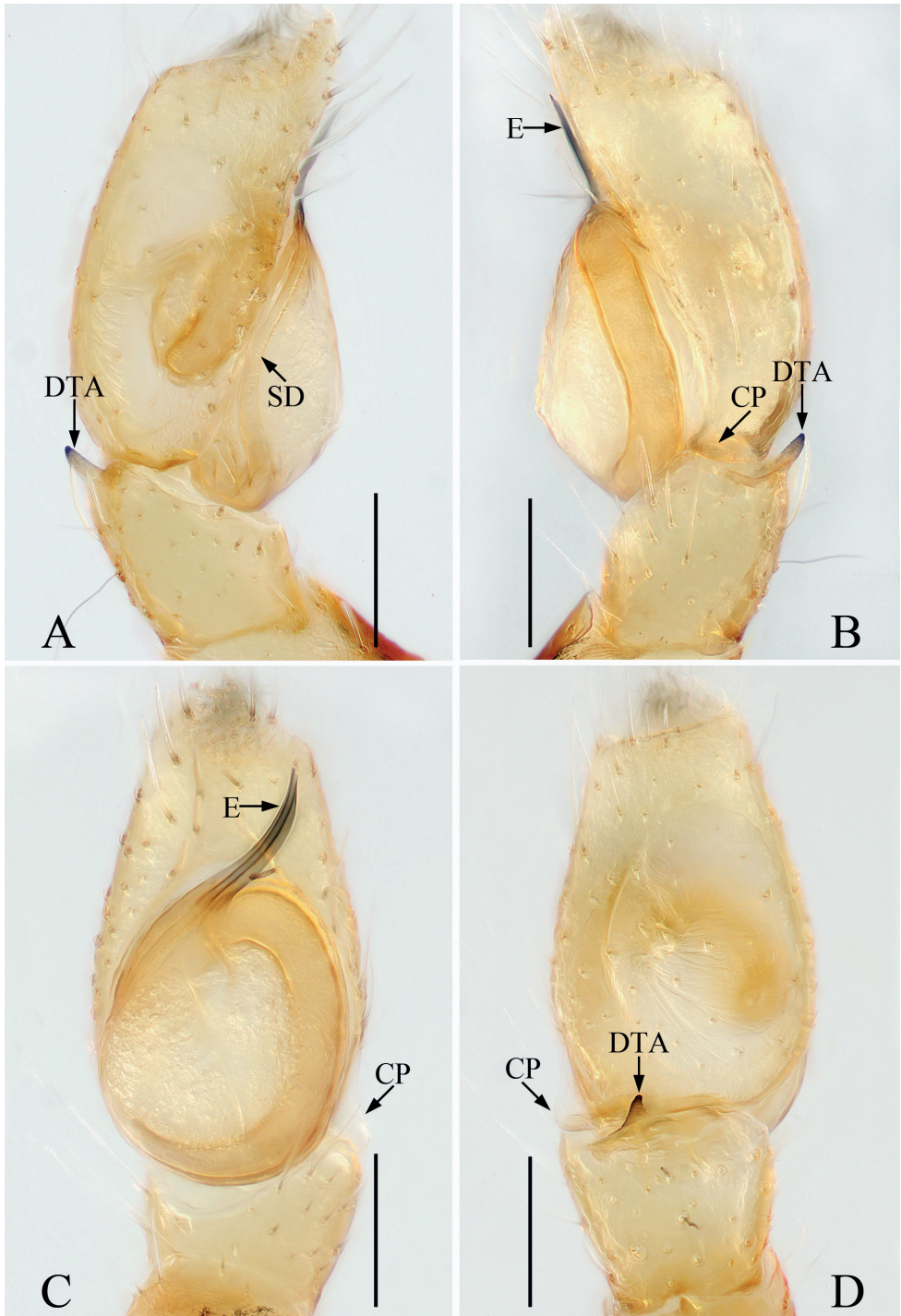


Figure 16. *Simaetha huigang* sp. nov., male holotype palp **A** prolateral **B** retrolateral **C** ventral **D** dorsal. Scale bars: 0.1.

Diagnosis. *Simaetha huigang* sp. nov. closely resembles *S. cheni* from China in the general shape of the habitus and copulatory organs, but it differs in the following: 1) dorsal tibial apophysis less than 1/4 tibial length in retrolateral view (Fig. 16B) versus more than 1/2 tibial length in *S. cheni* (Wang and Li 2021: fig. 18C); 2) cheliceral paturon lacks process (Fig. 17F, G) versus process present mediolaterally on anterior surface in *S. cheni* (Wang and Li 2021: fig. 19G, H); 3) epigynal hood almost as long as posterior chamber of spermathecae (Fig. 17A, B) versus less than 1/2 length of posterior chamber of spermathecae in *S. cheni* (Wang and Li 2021: fig. 19A–C).

Description. Male (Figs 16, 17C, D, F, G). Total length 2.77. Carapace 1.36 long, 1.11 wide. Abdomen 1.60 long, 1.17 wide. Clypeus 0.02 high. Eye sizes and inter-distances: AME 0.32, ALE 0.17, PLE 0.15, AERW 0.92, PERW 1.04, EFL 0.75. Legs: I 2.96 (1.00, 1.20, 0.43, 0.33), II 2.11 (0.68, 0.73, 0.40, 0.30), III 1.93 (0.65, 0.60, 0.40, 0.28), IV 2.41 (0.85, 0.83, 0.43, 0.30). Carapace red-brown to dark, squarish, slightly narrowed at anterior half, covered with dense setae and scales. Fovea indistinct. Chelicerae yellow-brown, with two promarginal and one retromarginal fissidental tooth with two cusps. Endites longer than wide, bearing dense setae at ental margins. Labium darker than endites. Sternum 1.5 times longer than wide, covered by pale, long, thin setae. Legs I strongest, covered with pale and blue scales on enlarged femora and tibiae, with two pairs of spines on tibiae and metatarsi, respectively; other legs yellow to dark. Abdomen oval, the dorsum with a large, irregular dark band followed by a broad, transverse, yellow band, entirely covered by large scutum, bearing short, pale, thin setae; venter dark brown, laterally with pair of longitudinal, pale setal stripes.

Palp (Fig. 16A–D): tibia wider than long in ventral view, with short, straight, lamellar dorsal apophysis slightly pointed apically; cymbium about 1.8 times longer than wide, with lamellar, proximal retrolateral process; bulb almost round, with sperm duct extending along submargin; embolus flat, about 1/2 the bulb length, originating from antero-prolateral portion of bulb, slightly curved medially, blunt apically.

Female (Fig. 17A, B, E). Total length 2.99. Carapace 1.32 long, 1.02 wide. Abdomen 1.70 long, 1.09 wide. Clypeus 0.02 high. Eye sizes and inter-distances: AME 0.30, ALE 0.16, PLE 0.15, AERW 0.91, PERW 1.02, EFL 0.67. Legs: I 2.19 (0.73, 0.73, 0.43, 0.30), II 1.70 (0.55, 0.60, 0.30, 0.25), III 1.64 (0.53, 0.53, 0.33, 0.25), IV 2.23 (0.78, 0.80, 0.40, 0.25). Habitus similar to that of male except paler.

Epigyne (Fig. 17A, B): wider than long, with large, central, bell-shaped hood almost equal in length to posterior chamber of spermathecae; copulatory openings lateral to base of hood, slit-like; copulatory ducts thick, connected with anterior portions of anterior chambers of spermathecae; spermathecae divided into two chambers, anterior chamber oval, extending posteriorly, posterior chamber almost spherical, separated from each other by 1/4 their diameter; fertilization ducts originating from anterior portions of posterior chamber of spermathecae, extending anterolaterally.

Distribution. Known only from the type locality in Yunnan, China.

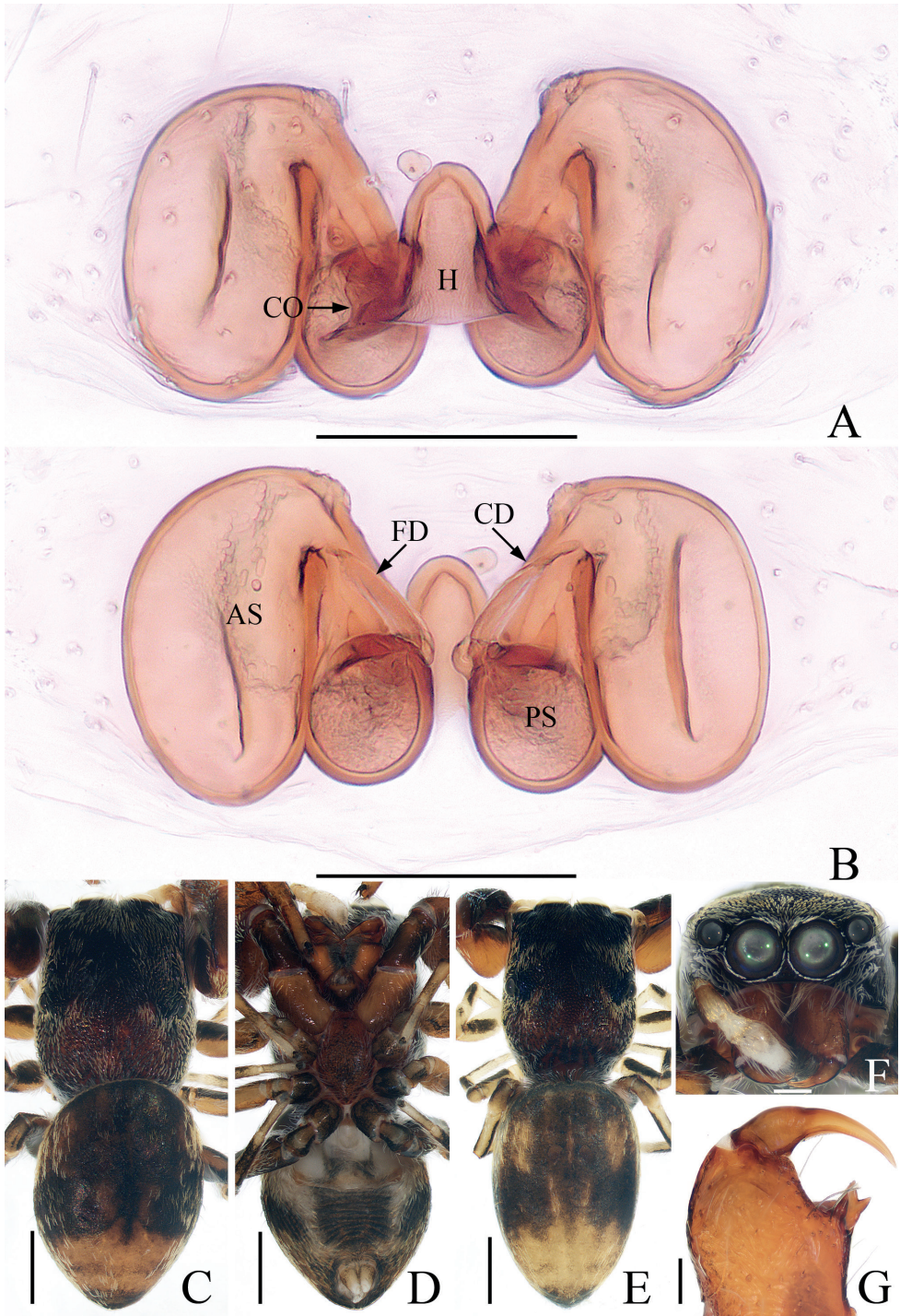


Figure 17. *Simaetha huigang* sp. nov., male holotype and female paratype **A** epigyne, ventral **B** vulva, dorsal **C** male holotype habitus, dorsal **D** ditto, ventral **E** female paratype habitus, dorsal **F** holotype carapace, frontal **G** holotype chelicera, anterior. Scale bars: 0.1 (**A, B, G**); 0.5 (**C-E**); 0.2 (**F**).

Genus *Synagelides* Strand, 1906

Type species. *Synagelides agoriformis* Strand, 1906 from Japan by original designation.

Synagelides cheni sp. nov.

<https://zoobank.org/D1842C11-3FDF-44AC-AA58-271BEBAF31F2>

Fig. 18

Type material. *Holotype* ♀ (IZCAS-Ar42954), CHINA: Yunnan: Xishuangbanna, Mengla County, Menglun Township, 55 kilometers from Xishuangbanna National Nature Reserve, ravine rainforest (21°57.68'N, 101°12.03'E, 718 ± 11 m alt.), 12.xi.2013, Q. Zhao and Z. Chen leg. *Paratype* 1 ♀ (IZCAS-Ar42955), same data as holotype.

Etymology. The specific name is a patronym in honor of Zhigang Chen, one of the collectors of the new species; noun (name) in genitive case.

Diagnosis. *Synagelides cheni* sp. nov. resembles that of *S. tangi* Liu, Chen, Xu & Peng, 2017 from China in having anteriorly located, paired, arched atrial ridges and a centrally located epigynal hood, but it can be easily distinguished by the following: 1) atrial ridges occupying nearly entire anterior 1/2 of epigyne (Fig. 18 A, B) versus occupying about anterior 1/3 of the epigyne in *S. tangi* (Liu et al. 2017: figs 4C, D, 5E, F); 2) epigynal hood about three times wider than long (Fig. 18A) versus about as long as wide in *S. tangi* (Liu et al. 2017: figs 4C, 5E).

Description. Female (Fig. 18). Total length 4.38. Carapace 2.04 long, 1.46 wide. Abdomen 2.33 long, 1.28 wide. Clypeus 0.05 high. Eye sizes and inter-distances: AME 0.50, ALE 0.31, PLE 0.29, AERW 1.48, PERW 1.45, EFL 1.14. Legs: I 3.74 (1.58, 1.28, 0.55, 0.33), II 3.56 (1.10, 1.33, 0.75, 0.38), III 3.71 (1.10, 1.30, 0.93, 0.38), IV 5.13 (1.45, 1.98, 1.25, 0.45). Carapace stippled, yellow to dark, covered with dark and pale setae. Fovea oval, hollow. Chelicerae yellow, with two promarginal teeth and one retromarginal fissidental tooth with two cusps. Endites slightly paler than chelicerae. Labium dark yellow, bearing several dark setae at distally. Sternum yellow, almost shield-like. Legs pale to yellow, with four and two pairs of ventral spines on metatarsi and tibiae I, respectively. Abdomen elongated, dorsum dark brown, with two pairs of muscle depressions medially, two wavy, transverse dark stripes and two transverse dotted lines posteriorly; venter pale, with longitudinal, gray-brown stripe anteromedially.

Epigyne (Fig. 18A, B): slightly longer than wide, with pair of arched atrial ridges occupying nearly entire anterior half, subtrapezoid median plate bearing an inverted boat-shaped hood about three times wider than long; copulatory openings small, situated at base of atrial ridges; copulatory ducts descending, forming C-shape, terminally with transversely extending, bar-shaped accessory glands; spermathecae almost L-shaped, with spherical lateral and oval ental portions; fertilization ducts lamellar, originating from anterior margins of ental portions of spermathecae, extending transversely.

Male. Unknown.

Distribution. Known only from the type locality in Yunnan, China.

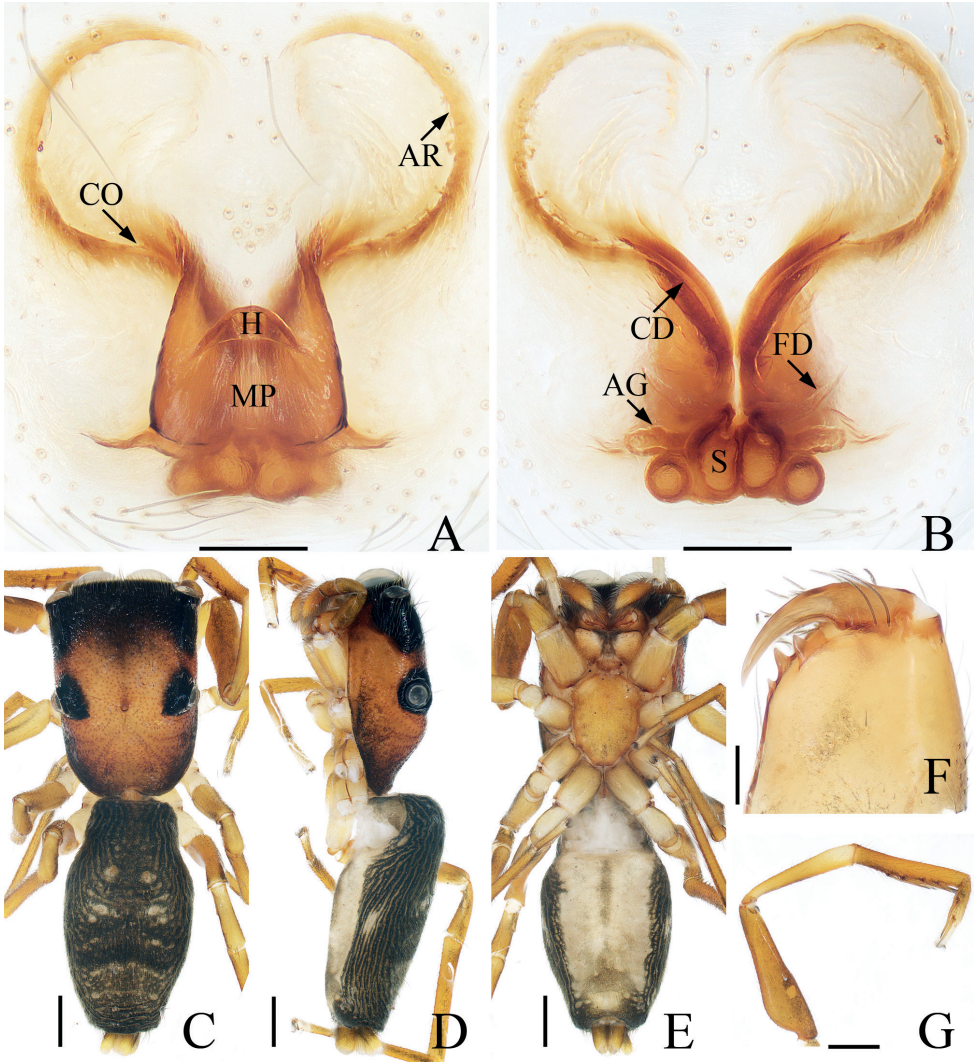


Figure 18. *Synagelides cheni* sp. nov., female holotype **A** epigyne, ventral **B** vulva, dorsal **C** habitus, dorsal **D** ditto, lateral **E** ditto, ventral **F** chelicera, posterior **G** leg I, prolateral. Scale bars: 0.1 (**A, B, F**); 0.5 (**C–E, G**).

Acknowledgements

The manuscript benefited greatly from comments by Ingi Agnarsson (Burlington, USA), Dmitri V. Logunov (Manchester, UK), Junxia Zhang (Baoding, China), and Yanfeng Tong (Shenyang, China). Sarah Crews (San Francisco, USA) and Robert Forsyth (Kamloops, Canada) checked the English of the manuscript. Guo Zheng, Guo Tang, Qingyuan Zhao, Zhiyuan Yao, Yanfeng Tong, Hao Yu, Zhigang Chen, and Zilong Bai helped with fieldwork. This research was supported by the National Natural

Science Foundation of China (NSFC-31972869, 31660609), the Science and Technology Project Foundation of Guizhou Province ([2020]1Z014), and the Doctoral Research Foundation of Tongren University (trxyDH2102).

References

- Benjamin SP (2004) Taxonomic revision and phylogenetic hypothesis for the jumping spider subfamily Ballinae (Araneae, Salticidae). *Zoological Journal of the Linnean Society* 142(1): 1–82. <https://doi.org/10.1111/j.1096-3642.2004.00123.x>
- Deeleman-Reinhold CL, Floren A (2003) Some remarkable, new or little-known pluridentate salticid spiders from Bornean tree canopy (Araneae: Salticidae). *Bulletin of the British Arachnological Society* 12: 335–344.
- Hong D, Zhuang W, Zhu M, Ma K, Wang X, Huang D, Zhang Y, Ren G, Bu W, Cai W, Ren D, Yang D, Liang A, Bai F, Zhang R, Lei F, Li S, Kong H, Cai L, Dai Y, Zhu C, Yang Q, Chen J, Sha Z, Jiang J, Che J, Wu D, Li J, Wang Q, Wei X, Bai M, Liu X, Chen X, Qiao G (2022) Positioning taxonomic research for the future. *Zoological Systematics* 47(3): 185–187. <https://doi.org/10.11865/zs.2022301>
- Ikeda H (1998) Spiders of the genus *Laufeia* (Araneae: Salticidae) from Japan. *Acta Arachnologica* 47(1): 37–43. <https://doi.org/10.2476/asjaa.47.37>
- Lei H, Peng XJ (2010) Two new jumping spiders of the genus *Chalcoscirtus* from China (Araneae: Salticidae). *Acta Arachnologica Sinica* 19(2): 66–69.
- Li S (2020) Spider taxonomy for an advanced China. *Zoological Systematics* 45(2): 73–77. <https://doi.org/10.11865/zs.202011>
- Li J, Yan X, Lin Y, Li S, Chen H (2021) Challenging Wallacean and Linnean shortfalls: *Ectosticta* spiders (Araneae, Hypochilidae) from China. *Zoological Research* 42(6): 791–794. <https://doi.org/10.24272/j.issn.2095-8137.2021.212>
- Lin YJ, Li S (2020) Two new genera and eight new species of jumping spiders (Araneae, Salticidae) from Xishuangbanna, Yunnan, China. *ZooKeys* 952: 95–128. <https://doi.org/10.3897/zookeys.952.51849>
- Liu K, Chen ZW, Xu X, Peng XJ (2017) Three new species of *Synagelides* Strand, 1906 from China (Araneae: Salticidae). *Zootaxa* 4350(2): 291–300. <https://doi.org/10.11646/zootaxa.4350.2.5>
- Logunov DV (2020) New and poorly known leaf-litter dwelling jumping spiders from South-East Asia (Araneae: Salticidae: Euophryini and Tisanibini). *Arachnology* 18(6): 521–562. <https://doi.org/10.13156/arac.2020.18.6.521>
- Logunov DV (2021) Jumping spiders (Araneae: Salticidae) of the Na Hang Nature Reserve, Tuyen Quang Province, Vietnam. *Arachnology* 18(9): 1021–1055. <https://doi.org/10.13156/arac.2021.18.9.1021>
- Logunov DV, Jäger P (2015) Spiders from Vietnam (Arachnida: Aranei): new species and records. *Russian Entomological Journal* 24(4): 343–363. <https://doi.org/10.15298/ruse-ntj.24.4.09>

- Logunov DV, Marusik YM (1999) A brief review of the genus *Chalcoscirtus* Bertkau, 1880 in the faunas of Central Asia and the Caucasus (Aranei: Salticidae). *Arthropoda Selecta* 7: 205–226.
- Metzner H (2022) Jumping Spiders (Arachnida: Araneae: Salticidae) of the World. <https://www.jumping-spiders.com> [Accessed on: 10 May 2022]
- Peng XJ (2020) *Fauna Sinica, Invertebrata* 53, Arachnida: Araneae: Salticidae. Science Press, Beijing, 612 pp.
- Peng XJ, Li S (2002) Four new and two newly recorded species of Taiwanese jumping spiders (Araneae: Salticidae) deposited in the United States. *Zoological Studies* 41: 337–345.
- Tanikawa A (1993) Two newly recorded spiders from Japan, *Bavia sexpunctata* (Doleschall, 1859) and *Rhene setipes* Żabka, 1985 (Araneae: Salticidae). *Acta Arachnologica* 42(1): 13–19. <https://doi.org/10.2476/asjaa.42.13>
- Wang C, Li S (2020a) On eight species of jumping spiders from Xishuangbanna, Yunnan, China (Araneae, Salticidae). *ZooKeys* 909: 25–57. <https://doi.org/10.3897/zookeys.909.47137>
- Wang C, Li S (2020b) Seven new species of jumping spiders (Araneae, Salticidae) from Xishuangbanna, China. *ZooKeys* 968: 43–69. <https://doi.org/10.3897/zookeys.968.55047>
- Wang C, Li S (2021) On ten species of jumping spiders from Xishuangbanna, China (Araneae, Salticidae). *ZooKeys* 1062: 123–155. <https://doi.org/10.3897/zookeys.1062.72531>
- Wang C, Li S, Zhu W (2020) Taxonomic notes on Leptonetidae (Arachnida, Araneae) from China, with descriptions of one new genus and eight new species. *Zoological Research* 41(6): 684–704. <https://doi.org/10.24272/j.issn.2095-8137.2020.214>
- Wanless FR (1978a) A revision of the spider genus *Bocus* Simon (Araneae: Salticidae). *Bulletin of the British Museum, Natural History. Zoology* 33: 239–244. <https://doi.org/10.5962/bhl.part.28737>
- Wanless FR (1978b) A revision of the spider genus *Marengo* (Araneae: Salticidae). *Bulletin of the British Museum, Natural History. Zoology* 33: 259–278. <https://doi.org/10.5962/p.28739>
- WSC (2022) World Spider Catalog. Version 23.0. Natural History Museum Bern. [Accessed on: 16 February 2022] <https://doi.org/10.24436/2>
- Yao Z, Wang X, Li S (2021) Tip of the iceberg: Species diversity of *Pholcus* spiders (Araneae, Pholcidae) in Changbai Mountains, Northeast China. *Zoological Research* 42(3): 267–271. <https://doi.org/10.24272/j.issn.2095-8137.2021.037>
- Żabka M (1985) Systematic and zoogeographic study on the family Salticidae (Araneae) from Viet-Nam. *Annales Zoologici, Warszawa* 39: 197–485.

A new species of *Sinopoda* from China, with first description of the male of *S. wuyiensis* Liu, 2021 (Araneae, Sparassidae)

Yang Zhong^{1,2,3,4}, Meng-Yun Zeng¹, Chao-Lan Gu¹,
Hui-Liang Yu^{3,4}, Jing-Yuan Yang^{3,4}

1 School of Nuclear Technology and Chemistry & Biology, Hubei University of Science and Technology, Xianning 437100, Hubei, China **2** Hubei Key Laboratory of Radiation Chemistry and Functional Materials, Hubei University of Science and Technology, Xianning 437100, Hubei, China **3** Shennongjia National Park Administration, Shennongjia 442421, Hubei, China **4** Hubei Province Key Laboratory of Conservation Biology for Shennongjia Golden Monkey, Shennongjia 442421, Hubei, China

Corresponding authors: Yang Zhong (hubeispider@aliyun.com), Jing-Yuan Yang (snjbhq@163.com)

Academic editor: Gergin Blagoev | Received 13 April 2022 | Accepted 18 July 2022 | Published 9 August 2022

<https://zoobank.org/83FFFD94-67F9-47CE-A7E8-5D1B05F3FEF9>

Citation: Zhong Y, Zeng M-Y, Gu C-L, Yu H-L, Yang J-Y (2022) A new species of *Sinopoda* from China, with first description of the male of *S. wuyiensis* Liu, 2021 (Araneae, Sparassidae). ZooKeys 1116: 121–132. <https://doi.org/10.3897/zookeys.1116.85303>

Abstract

One new species of the genus *Sinopoda* Jäger, 1999, *S. muyuensis* **sp. nov.** (♂, ♀), is described and figured from the Shennongjia Forestry District, Hubei Province, China. In addition, the male of *Sinopoda wuyiensis* Liu, 2021 is described for the first time from the Wuyishan National Nature Reserve, Fujian Province, China.

Keywords

Biodiversity, Fujian, Hubei, huntsman spiders, taxonomy

Introduction

The genus *Sinopoda* was established by Jäger (1999). As currently recognised, it comprises 137 species, of which 71 species were recorded from China, representing 51.8% of the global species [World Spider Catalog (WSC) 2022]. The genus has been reported from East Asia (85 species in China, Japan, and Korea), Southeast Asia (50 species in Brunei, Indonesia, Laos, Malaysia, Myanmar, Thailand, and Vietnam) and South Asia (a single species in India) (Zhang et al. 2021).

We have found two *Sinopoda* species present in collections from China in the past year. The discovery of one of these species, *Sinopoda muyuensis* sp. nov. from Hubei represents the first record of this species in Shennongjia Forestry District. Furthermore, specimens of *Sinopoda wuyiensis* Liu, 2021 from Fujian have allowed us to provide the first description of the male of the species.

Materials and methods

Specimens were examined and measured with an Olympus SZX7 stereomicroscope. Positions of tegular appendages are given according to clock positions, based on the left palp in ventral view. Male and female copulatory organs were examined and illustrated after dissection from the spider bodies; vulvae were cleared in a warm 10% potassium hydroxide (KOH) solution. All photographs were captured with a KUY NICE industrial digital camera (20.0 megapixels) mounted on an Olympus CX43 dissecting microscope, and assembled using Helicon Focus 3.10.3 image stacking software. Photographic images were then edited using Adobe Photoshop CC 2018. All measurements were obtained using an Olympus SZX7 stereomicroscope and are given in millimetres (mm).

Leg measurements are shown as: total length (femur, patella, tibia, metatarsus, tarsus). Number of macrosetae is listed for each segment in the following order: prolateral, dorsal, retrolateral, ventral (in femora and patellae ventral spines are absent and fourth digit is omitted in the setation formula). Abbreviations used in the text and figures are given below: **AB** = anterior bands, **ALE** = anterior lateral eye, **AME** = anterior median eye, **AW** = anterior width of carapace, **C** = conductor, **CH** = clypeus height, **dRTA** = dorsal branch of RTA, **E** = embolus, **EA** = embolic apophysis, **FD** = fertilization duct, **FE** = femur, **GA** = glandular appendage, **LL** = lateral lobes, **LS** = lobal septum, **MS** = membranous sac, **Mt** = metatarsus, **OL** = opisthosoma length, **OW** = opisthosoma width, **Pa** = patella, **PI** = posterior incision of LL, **PL** = carapace length, **PLE** = posterior lateral eyes, **PME** = posterior median eyes, **Pp** = palp or palpus, **PP** = posterior part of spermathecae, **PW** = carapace width, **RTA** = retrolateral tibial apophysis, **SP** = spermophor, **SS** = slit sensillum, **ST** = subtegulum, **T** = tegulum, **Ta** = tarsus, **Ti** = tibia. I, II, III, IV—legs I to IV, **TP** = tegular protrusion, **vRTA** = ventral branch of RTA, **HUST** = School of Nuclear Technology and Chemistry and Biology, Hubei University of Science and Technology, Xianning, Hubei, China.

Taxonomy

Family Sparassidae Bertkau, 1872

Subfamily Heteropodinae Thorell, 1873

Genus *Sinopoda* Jäger, 1999

Type species. *Sarotes forcipatus* Karsch, 1881

Diagnosis. See Jäger (1999), Liu et al. (2008), Zhang et al. (2015), and Grall and Jäger (2020).

Composition. Within the genus *Sinopoda*, five groups were established by Jäger and Ono (2000), Grall and Jäger (2020) and Zhang et al. (2021): *S. anguina*-group (*S. anguina* Liu, Li & Jäger, 2008, *S. bifurca* Grall & Jäger, 2020, *S. bispina* Grall & Jäger, 2020, *S. fornicata* Liu, Li & Jäger, 2008, *S. improcera* Zhong et al., 2019, *S. lata* Zhong et al., 2019, *S. longicymbialis* Grall & Jäger, 2020, *S. mamillata* Zhong, Cao & Liu, 2017, *S. nanphagu* Grall & Jäger, 2020, *S. phiset* Grall & Jäger, 2020, *S. rotunda* Grall & Jäger, 2020 and *S. tuber* Grall & Jäger, 2020); *S. chiangmaiensis*-group (*S. chiangmaiensis* Grall & Jäger, 2020, *S. lot* Grall & Jäger, 2020 and *S. phathai* Grall & Jäger, 2020); *S. globosa*-group (*S. globosa* Zhang, Zhang & Zhang, 2015, *S. longiducta* Zhang, Zhang & Zhang, 2015, *S. mi* Chen & Zhu, 2009, *S. ovata* Zhong et al., 2019, *S. triangula* Liu, Li & Jäger, 2008 and *S. yaanensis* Zhong et al., 2019); *S. tumefacta*-group (*S. crassa* Liu, Li & Jäger, 2008, *S. debiscens* Zhong et al., 2019, *S. erromena* Zhong et al., 2019, *S. tumefacta* Zhong et al., 2019, *S. yanlingensis* Zhong et al., 2019 and *S. yaojingensis* Liu, Li & Jäger, 2008); *S. okinawana*-group [*S. forcipata* (Karsch, 1881), *S. cochlearia* Zhang, Zhang & Zhang, 2015, *S. derivata* Jäger & Ono, 2002, *S. fasciculata* Jäger Gao & Fei, 2002, *S. guangyuanensis* Zhong et al., 2018, *S. hamata* (Fox, 1937), *S. koreana* (Paik, 1968), *S. okinawana* Jäger & Ono, 2000, *S. tanikawai* Jäger & Ono, 2000, *S. wangi* Song & Zhu, 1999]. Ninety-six other species have not yet been grouped.

***Sinopoda muyuensis* sp. nov.**

<https://zoobank.org/4BCEBD12-8C2A-44EA-9180-DDE1FB4ACD39>

Figs 1, 2, 4A, B, E–H, 5A, B, 6

Type material. **Holotype:** ♂ (HUST 0003), **CHINA: Hubei:** Shennongjia Forestry District, Muyu Town, Guanmenshan Scenic Area; 31.45°N, 110.40°E; alt. 1200 m; 10.XII.2021; Y. Zhong leg. **Paratypes** (HUST): 2♂, 3♀, same data as holotype.

Etymology. ‘Muyu’ refers to the type locality of this species, Muyu Town.

Diagnosis. The male of *Sinopoda muyuensis* sp. nov. resembles *S. angulata* Jäger, Gao & Fei, 2002 (Zhu et al. 2020: figs 1A–C, 2A–C) and *S. yichangensis* Zhu, Zhong & Yang, 2020 (Zhu et al. 2020: figs 4A–C, 5A–C; Gong and Zhong 2021: figs 2A–C) in having the embolus distally filiform, as long as the embolic apophysis, and RTA arising subdistally from tibia, but the new species can be separated from *S. angulata* by the posterior margins of the embolic apophysis being distinctly humped (smooth in

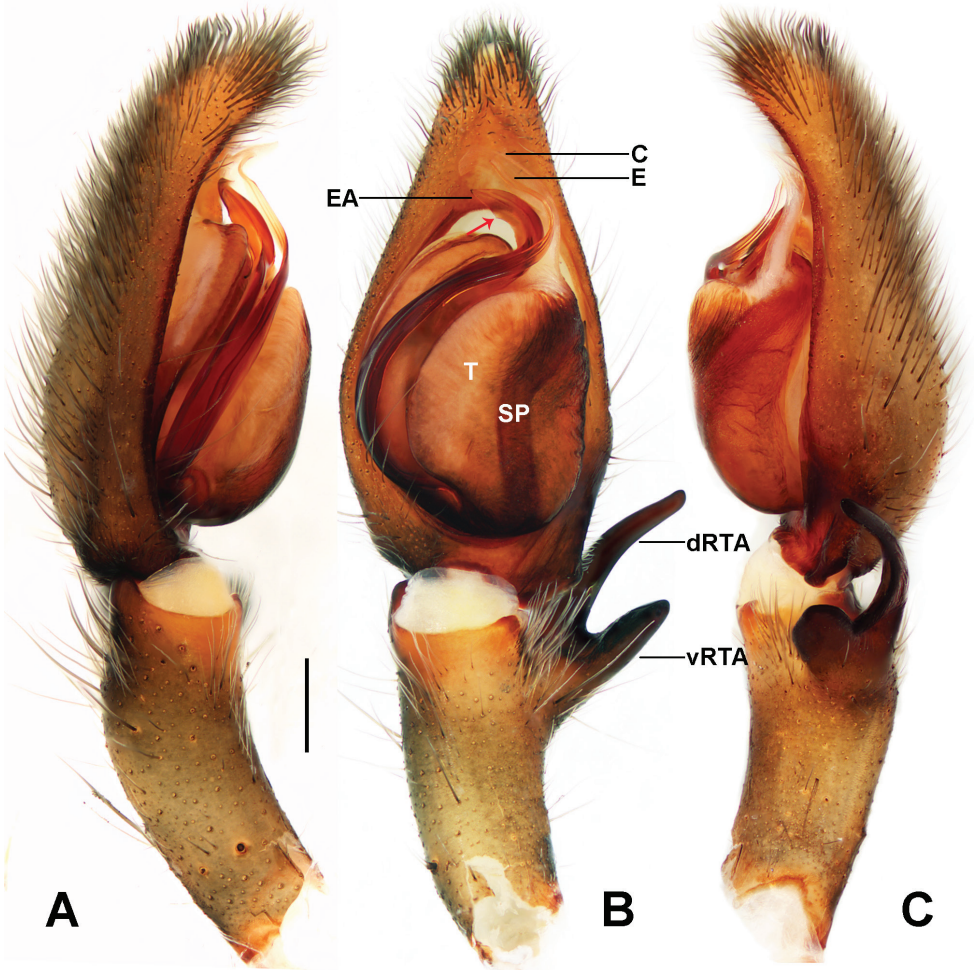


Figure 1. *Sinopoda muyuensis* sp. nov., holotype male **A–C** palp, left (**A** prolateral view **B** ventral view **C** retrolateral view). Abbreviations: C – conductor, dRTA – dorsal branch of RTA, E – embolus, EA – embolic apophysis, SP – spermophore, T – tegulum, vRTA – ventral branch of RTA. Red arrow: embolic apophysis projection. Scale bar: 0.5 mm.

S. angulata); from *S. yichangensis* by the tip of embolic apophysis with a pointed end (blunt in *S. yichangensis*). Females are similar to those of *S. angulata* (Zhu et al. 2020: fig. 2D, E) in having the epigyne with a lobal septum $\sim 1/4$ of the epigynal width, posterior part of the spermathecae considerably larger than the glandular projection, and the angle of the diverging internal duct system $\sim 80^\circ$, but distinguished by the vulva with its internal duct system not touching (touching along the median line in *S. angulata*); glandular appendages extending into the median half of the internal duct system (anterior half in *S. angulata*); ends of internal duct system nearly straight in dorsal view (bent at 180° in *S. angulata*) (Figs 1, 2).

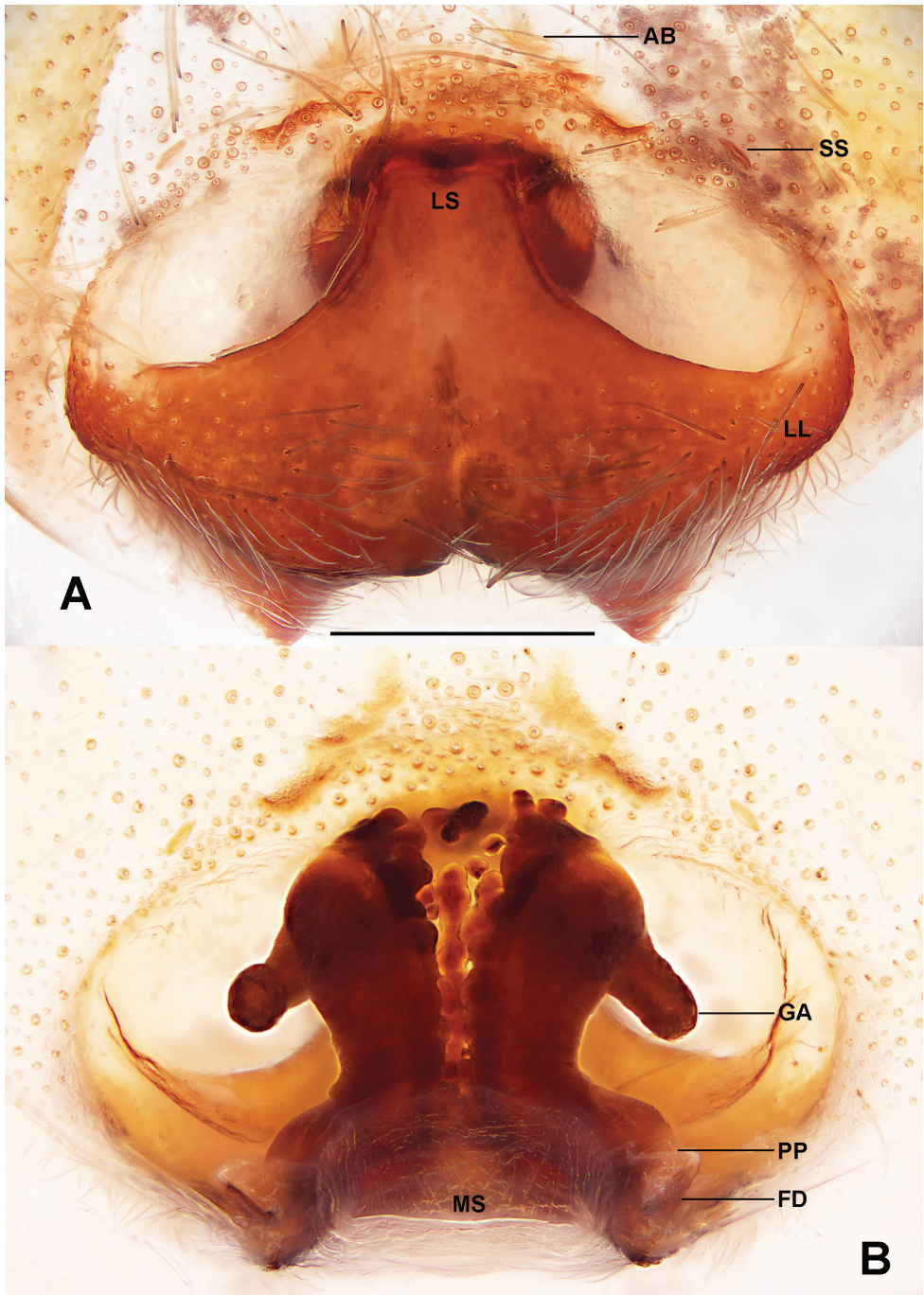


Figure 2. *Sinopoda muyuensis* sp. nov., paratype female **A** epigyne **B** vulva (**A** ventral view **B** dorsal view). Abbreviations: AB – anterior bands, FD – fertilisation duct, GA – glandular appendage, LL – lateral lobes, LS – lobal septum, MS – membranous sac, PP – posterior part of spermathecae, SS – slit sensillum. Scale bar: 0.5 mm.

Description. Male. PL 5.3, PW 4.7, AW 2.5, OL 5.8, OW 3.9. Eyes: AME 0.19, ALE 0.31, PME 0.22, PLE 0.32, AME–AME 0.20, AME–ALE 0.16, PME–PME 0.28, PME–PLE 0.36, AME–PME 0.38, ALE–PLE 0.25, CH AME 0.19, CH ALE 0.26. Setation: Palp: 131, 101, 1100; Fe: I–III 323, IV 321; Pa: I–IV 101; Ti: I–IV 2326; Mt: I–II 1014, III 2026, IV 3036. Measurements of palp and legs: Palp 6.8 (2.4, 1.3, 1.3, –, 1.8), I 17.6 (4.4, 1.4, 5.5, 4.9, 1.4), II 19.1 (5.6, 1.7, 6.5, 3.9, 1.4), III 15.7 (4.9, 1.5, 4.8, 3.3, 1.2), IV 15.9 (5.3, 1.5, 4.8, 3.3, 1.0). Leg formula: II-I-IV-III. Cheliceral furrow with three anterior and four posterior teeth, and with ~ 36 denticles (Fig. 4A). Carapace yellowish brown dorsally, with yellow transversal stripe posteriorly, with shallow fovea and radial furrows. Chelicerae deep reddish brown. Sternum yellow with brown margin. Endites and labium deep yellowish brown, with margin deep brown. Legs yellowish brown, covered by short spines. Opisthosoma yellowish brown dorsally, with three pairs of dark patches laterally. Opisthosoma uniformly yellowish brown with some brown patches ventrally (Fig. 4E, F).

Palp as in Fig. 1. Cymbium distinctly longer than tibia. Embolus S-shaped, arising from tegulum at nearly the 6-o' clock-position in ventral view. Conductor arising at 12- to 1-o' clock-position from tegulum. RTA arising mesially to distally from tibia, with distinct brush of stiff setae. dRTA slender, finger-shaped, vRTA roughly rectangular in retrolateral view.

Female. PL 5.7, PW 4.8, AW 3.1, OL 5.9, OW 3.9. Eyes: AME 0.16, ALE 0.25, PME 0.18, PLE 0.25, AME–AME 0.27, AME–ALE 0.09, PME–PME 0.33, PME–PLE 0.35, AME–PME 0.32, ALE–PLE 0.28, CH AME 0.20, CH ALE 0.25. Setation: Palp: 131, 101, 2026, 1014; Fe: I–III 323, IV 321; Pa: I–IV 000; Ti: I–III 2026, IV 2024; Mt: I–II 1014, III 2026, IV 3036. Measurements of palp and legs: Palp 5.8 (1.9, 0.8, 1.3, –, 1.8), I 14.6 (4.5, 2.4, 4.1, 2.3, 1.3), II 16.9 (5.2, 2.4, 4.1, 3.8, 1.4), III 13.2 (4.4, 2.0, 3.0, 2.6, 1.2), IV 14.2 (4.7, 1.8, 3.4, 3.0, 1.3). Leg formula: II-I-IV-III. Cheliceral furrow with three anterior and four posterior teeth, and with ~ 45 denticles (Fig. 4B).

Copulatory organ as in Fig. 2. Epigynal field wider than long, with short anterior bands and one slit sensillum on each side close to the epigynal field. Lateral lobes fused, with some fusion bubbles along median line. Fertilisation ducts arising posterolaterally. Membranous sac between fertilisation ducts almost rectangular.

Colouration in ethanol as in males, but generally slightly darker, Opisthosoma brown dorsally (Fig. 4G, H).

Distribution. Known only from the type locality (Fig. 6).

***Sinopoda wuyiensis* Liu, 2021**

Figs 3, 4C, D, I–L, 5C, 6

Sinopoda wuyiensis Liu, in Zhang et al. 2021: 20, fig. 9A–D (holotype female from Wuyishan National Nature Reserve, Fujian Province, deposited in College of Life Science, Hubei University LJ-202002-ZY, examined)

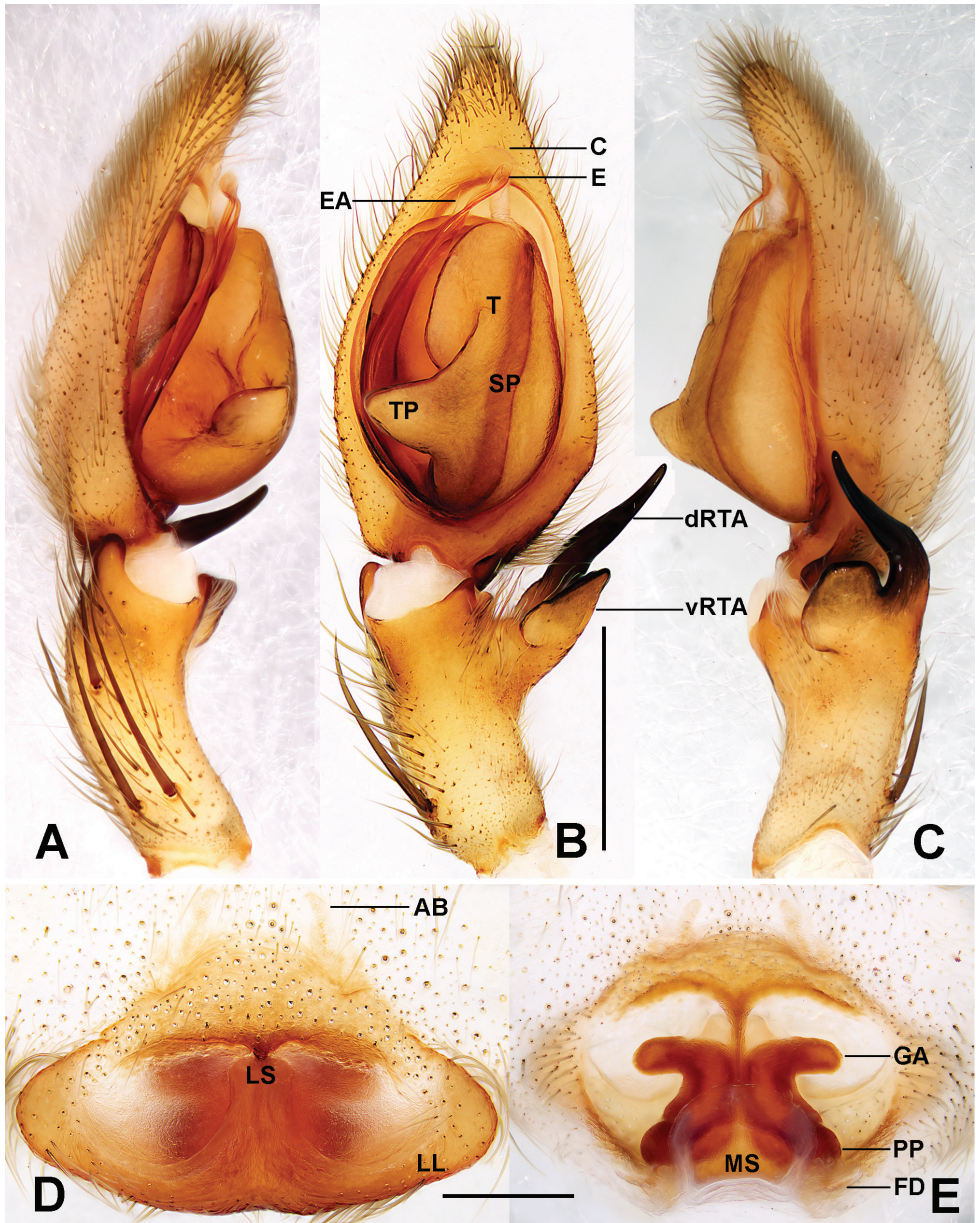


Figure 3. *Sinopoda wuyiensis* Liu, 2021 **A–C** palp, left, ventral view **D** epigyne **E** vulva (**A** prolateral view **B, D** ventral view **C** retrolateral view **E** dorsal view). Abbreviations: AB – anterior bands, C – conductor, dRTA – dorsal branch of RTA, E – embolus, EA – embolic apophysis, FD – fertilisation duct, GA – glandular appendage, LL – lateral lobes, LS – lobal septum, MS – membranous sac, PP – posterior part of spermathecae, SP – spermophore, T – tegulum, TP – tegular protrusion, vRTA – ventral branch of RTA. Scale bars: 0.5 mm.

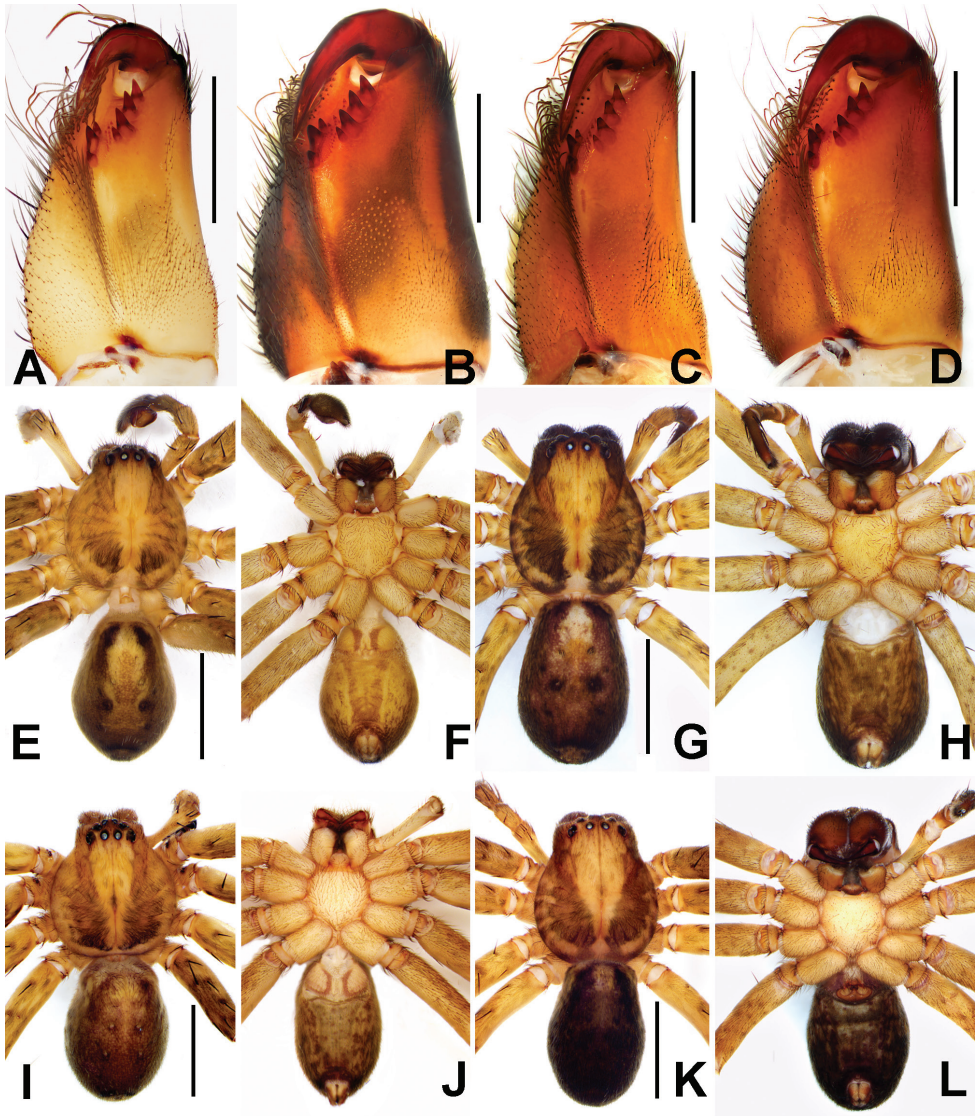


Figure 4. **A, B** cheliceral dentition of *Sinopoda muyuensis* sp. nov. **C, D** cheliceral dentition of *Sinopoda wuyiensis* Liu, 2021 **E–H** habitus of *Sinopoda muyuensis* sp. nov. **I–L** habitus of *Sinopoda wuyiensis* Liu, 2021 (**A, C, F, J** male, ventral view **E, I** male, dorsal view **B, D, H, L** female, ventral view **G, K** female, dorsal view). Scale bars: 0.5 mm (**A–D**); 5 mm (**E–L**).

Material examined. 3♂, 4♀ (HUST 0004), **CHINA: Fujian:** Wuyishan National Reserve, Guadun Village; 27.58°N, 117.48°E; 16.XI.2021; Y. Zhong leg.

Diagnosis. Males of *S. wuyiensis* can be distinguished from other *Sinopoda* species by the combination of the following characters: bases of the tegulum with a distinct sub-triangular protrusion, embolic apophysis reduced, distinctly narrower and shorter

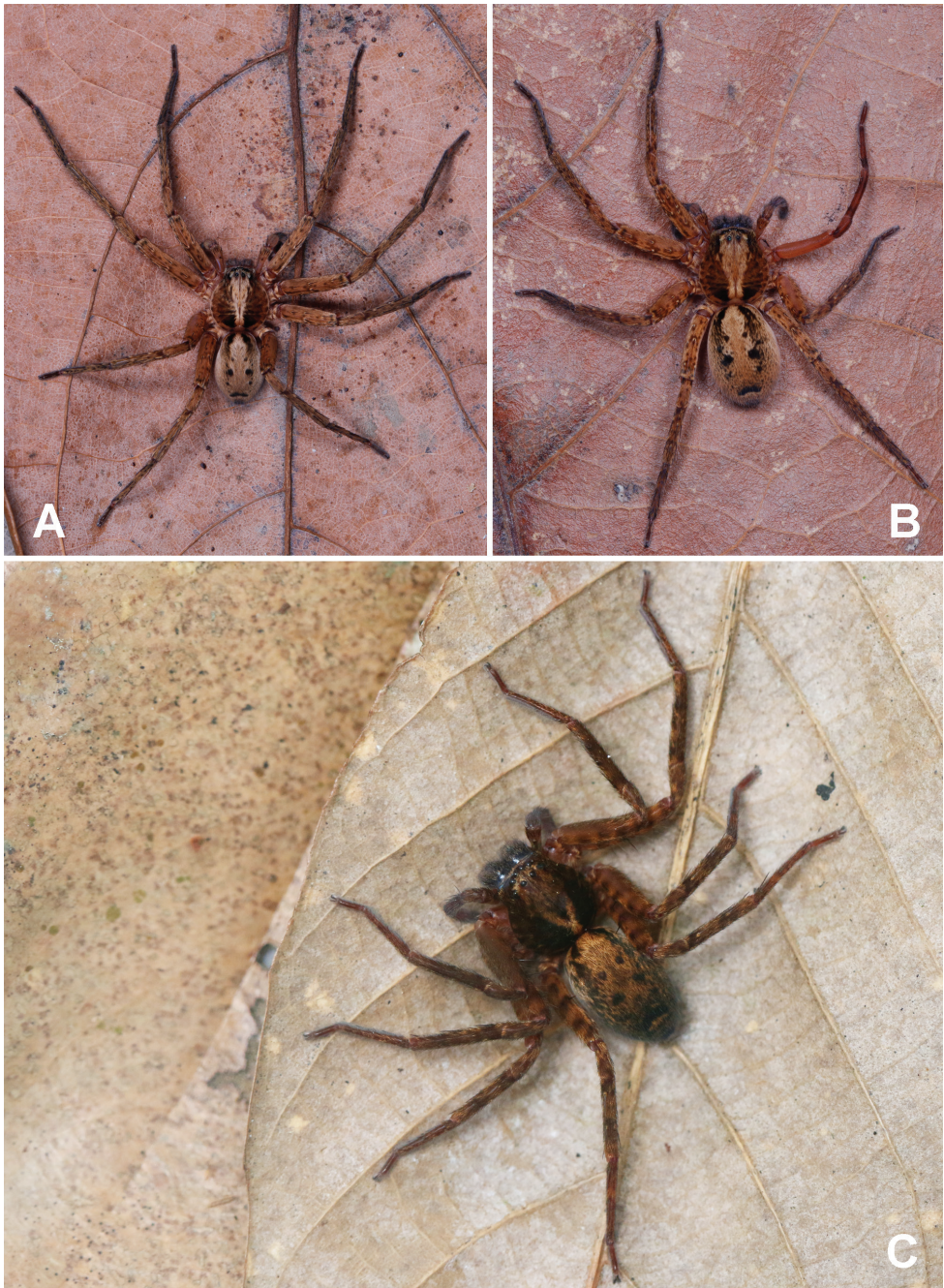


Figure 5. **A, B** Photograph of living *Sinopoda muyuensis* sp. nov. **C** photograph of living *Sinopoda wuyiensis* Liu, 2021 **A** male **B, C** female.

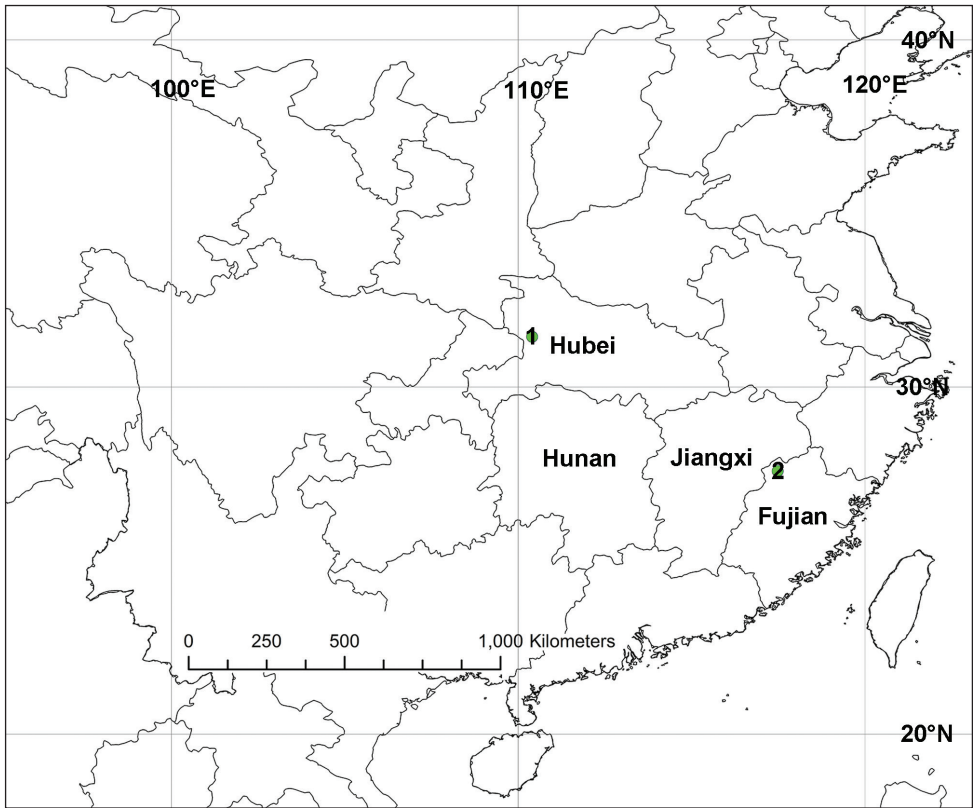


Figure 6. Distribution records of *Sinopoda* species in China **1** *Sinopoda muyuensis* sp. nov. **2** *Sinopoda wuyiensis* Liu, 2021.

than the embolus, and the dRTA about twice as long as the vRTA in ventral view. Females of *S. wuyiensis* may be recognised by the following combination of characters: epigynal field almost fusiform, lateral lobes fused without visible seam, with their anterior and posterior margins almost parallel, and glandular appendages laterad, as wide as posterior part of spermathecae (Fig. 3).

Description. Male. PL 4.5, PW 4.3, AW 2.5, OL 5.3, OW 3.0. Eyes: AME 0.18, ALE 0.28, PME 0.26, PLE 0.31, AME–AME 0.24, AME–ALE 0.10, PME–PME 0.24, PME–PLE 0.28, AME–PME 0.33, ALE–PLE 0.23, CH AME 0.10, CH ALE 0.14. Setation: Palp: 131, 101, 1021; Fe: I–III 323, IV 321; Pa: I–IV 000; Ti: I–IV 2226; Mt: I 1014, II 2024, III–IV 3036. Measurements of palp and legs: Palp 6.4 (1.9, 1.2, 1.4, –, 1.9), I 18.8 (5.1, 2.2, 5.5, 4.7, 1.3), II 21.9 (6.0, 2.2, 6.2, 5.9, 1.6), III 16.8 (5.1, 2.0, 4.6, 3.6, 1.5), IV 18.3 (4.6, 2.1, 5.1, 4.9, 1.6). Leg formula: II–I–IV–III. Cheliceral furrow with three anterior and four posterior teeth, and with ~ 38 denticles (Fig. 4C). Carapace deep yellowish brown dorsally, laterally and posteriorly with dark brown U-shaped pattern, with shallow fovea and radial furrows. Chelicerae deep reddish brown. Sternum yellow with brown margin. Endites and labium deep yellow.

lowish brown, with margin deep brown. Legs deep yellowish brown, covered by short spines. Opisthosoma brown dorsally, median part with four brown dots, posteriorly dark brown. Opisthosoma uniformly greyish brown with some brown patches ventrally (Fig. 4I, J).

Palp as in Fig. 3A–C. Cymbium $\sim 2\times$ longer than tibia in ventral view. Embolus slightly curved, arising from tegulum at nearly the 6-o' clock-position in ventral view. Conductor curving distally, arising at 12- to 1-o'clock-position from tegulum. Spermophore almost straight. RTA arising mesially to distally from tibia, with distinct brush of stiff setae. vRTA wider than dRTA, dRTA long, in ventral view proximal part wide and tip tapering.

Female. PL 5.4, PW 4.7, AW 3.0, OL 5.3, OW 3.6. Eyes: AME 0.21, ALE 0.33, PME 0.21, PLE 0.39, AME–AME 0.26, AME–ALE 0.07, PME–PME 0.33, PME–PLE 0.46, AME–PME 0.35, ALE–PLE 0.25, CH AME 0.15, CH ALE 0.20. Setation: Palp: 131, 101, 2121 1014; Fe: I–III 323, IV 321; Pa: I–IV 000; Ti: I–III 2026, IV 2226; Mt: I–II 1014, III 2024, IV 3036. Measurements of palp and legs: Palp 5.8 (2.0, 0.6, 1.0, –, 2.2), I 15.7 (4.7, 1.7, 4.1, 3.6, 1.6), II 16.2 (4.8, 1.8, 4.5, 3.7, 1.4), III 13.9 (4.4, 1.9, 3.5, 3.0, 1.1), IV 15.1 (4.4, 1.9, 4.1, 3.6, 1.1). Leg formula: II-I-IV-III. Colouration in ethanol as in males, but opisthosoma distinctly darker dorsally and ventrally (Fig. 4K, L; see Zhang et al. (2021) for others described).

Distribution. Known only from the type locality (Fig. 6).

Acknowledgements

The manuscript benefitted greatly from comments by Gergin Blagoev, Galina N. Azarkina, Tamas Szuts, and İlhan Coşar. We thank Guofei Ma (Shennongjia National Park Administration), Jiangwei Zheng (HUST), Han Dong (HUST), and Wei Wang (HUST) for assistance in collecting specimens. This study was financially supported by the National Natural Sciences Foundation of China (32000303), Technology Innovation Project of Hubei Province (2019AC161): Biodiversity research, monitoring and demonstration in Shennongjia National Park, Hubei Province Key Laboratory of Conservation Biology for Shennongjia Golden Monkey Foundation (No. SNJKL2021003), and the program of Hubei University of Science and Technology (2021ZX12).

References

- Gong LJ, Zhong Y (2021) First description of the female of *Sinopoda yichangensis* Zhu, Zhong & Yang, 2020 (Araneae, Sparassidae). *ZooKeys* 1067: 93–100. <https://doi.org/10.3897/zookeys.1067.72419>
- Grall E, Jäger P (2020) Forty-seven new species of *Sinopoda* from Asia with a considerable extension of the distribution range to the south and description of a new species group

- (Sparassidae: Heteropodinae). *Zootaxa* 4797(1): 1–101. <https://doi.org/10.11646/zootaxa.4797.1.1>
- Jäger P (1999) *Sinopoda*, a new genus of Heteropodinae (Araneae, Sparassidae) from Asia. *The Journal of Arachnology* 27: 19–24.
- Jäger P, Ono H (2000) Sparassidae of Japan. I. New species of *olios*, *Heteropoda*, and *Sinopoda* with notes on some known species (Araneae: Sparassidae: Sparassinae and Heteropodinae). *Acta Arachnologica* 49: 41–60. <https://doi.org/10.2476/asjaa.49.41>
- Liu J, Li SQ, Jäger P (2008) New cave-dwelling huntsman spider species of the genus *Sinopoda* (Araneae: Sparassidae) from southern China. *Zootaxa* 1857(1): 1–20. <https://doi.org/10.11646/zootaxa.1857.1.1>
- World Spider Catalog WSC (2022) World Spider Catalog, version 23.0. Natural History Museum, Bern. <https://doi.org/10.24436/2> [accessed on 27 July 2022]
- Zhang BS, Zhang ZS, Zhang F (2015) Three new *Sinopoda* species (Araneae: Sparassidae) from southern China. *Zootaxa* 3974(1): 59–75. <https://doi.org/10.11646/zootaxa.3974.1.4>
- Zhang H, Zhong Y, Zhu Y, Agnarsson I, Liu J (2021) A molecular phylogeny of the Chinese *Sinopoda* spiders (Sparassidae, Heteropodinae): implications for taxonomy. *PeerJ* 9: e11775. [26 pp] <https://doi.org/10.7717/peerj.11775>
- Zhu Y, Zhong Y, Yang TB (2020) One new species of the genus *Sinopoda* from Hubei Province, with description of the male of *Sinopoda angulata* (Araneae, Sparassidae). *Biodiversity Data Journal* 8: e55377. <https://doi.org/10.3897/BDJ.8.e55377>

Two new species of *Metapocyrtus* (*Orthocyrtus*) Heller, 1912 (Coleoptera, Curculionidae, Entiminae) from southern Mindanao, Philippines, with ecological notes

Analyn A. Cabras¹, Rizalyn Cudera², Joelyn Mamon², Milton Norman D. Medina¹

1 *Coleoptera Research Center, Institute of Biodiversity and Environment, University of Mindanao, Davao City, 8000, Philippines* **2** *Sultan Kudarat State University, EJC Montilla, Tacurong City, Sultan Kudarat, 9800, Philippines*

Corresponding author: Analyn A. Cabras (ann.cabras24@umindanao.edu.ph)

Academic editor: M. Alonso-Zarazaga | Received 7 March 2022 | Accepted 21 July 2022 | Published 9 August 2022

<https://zoobank.org/B64BD37A-BF91-400E-9404-5727884C20C3>

Citation: Cabras AA, Cudera R, Mamon J, Medina MND (2022) Two new species of *Metapocyrtus* (*Orthocyrtus*) Heller, 1912 (Coleoptera, Curculionidae, Entiminae) from southern Mindanao, Philippines, with ecological notes. ZooKeys 1116: 133–147. <https://doi.org/10.3897/zookeys.1116.83236>

Abstract

Two new species of the genus *Metapocyrtus* Heller, 1912, subgenus *Orthocyrtus* Heller, 1912 are described and illustrated from southern Mindanao, Philippines: *M. (O.) melibengoy* **sp. nov.** and *M. (O.) flomlok* **sp. nov.** Another two species were transferred from the subgenus *Artapocyrtus* Heller, 1912 to *Orthocyrtus*, namely, *M. (O.) willietorresi* Cabras & Medina, 2018 and *M. (O.) villalobosae* Patano et al., 2021. Ecological notes are provided.

Keywords

Biodiversity, change of placement, Cotabato, new species, taxonomy, weevils

Introduction

Members of the subgenus *Orthocyrtus* Heller, 1912 (genus *Metapocyrtus* Heller, 1912) are among the most notable of the tribe Pachyrhynchini for their conspicuously large size. The subgenus is currently recognized as endemic to the Philippines and

is distributed all over the archipelago. Up to the present, the subgeneric division of *Metapocyrtus* is uncertain and badly needs revision. However, members of *Orthocyrtus* have distinct and stable characters that distinguish them from other subgenera: 1) large species, with a few exceptions; 2) rostrum of medium length, dorsally straight, mostly in a plane with the front (exceptionally slightly concave) and at the base, the sides are rectangularly declined; 3) female, with a few exceptions, without any secondary sexual structural characters aside from a stouter form, and similar to the male; (Schultze 1925; Cabras et al. 2018). The biology and ecology of the genus remain understudied; however, members of the subgenus can be found in a range of habitats which include lowland coconut farmlands, mid-elevation between 300–800 m in mixed secondary forest, as well as old-growth primary and secondary forests (Cabras et al. 2018; Cabras and Medina 2019; Cabras et al. 2021a, b).

In the past two years, two species belonging to *Orthocyrtus* were collected from southern Mindanao and found to be new to science. In this paper, the two new species are described and illustrated. Short notes on their ecology are provided. Another two species from the subgenus *Artapocyrtus* Heller, 1912 were transferred to *Orthocyrtus*, namely, *M. (O.) willietorresi* Cabras & Medina, 2018 and *M. (O.) villalobosae* Patano et al., 2021.

Materials and methods

The specimens deposited in the University of Mindanao Coleoptera Research Center were collected by sheet beating and handpicking and killed in vials with ethyl acetate. Morphological characters were observed under Luxeo 4D and Nikon SMZ745T stereomicroscopes. The treatment of the genitals follows Yoshitake (2011). Anatomical parts of the female genitalia are not illustrated as very little of the chitinous structures are used to identify and characterize different species of Pachyrhynchini (Cabras et al. 2021a). Images of the habitus were taken using a Nikon D5300 digital camera with a Sigma 18–250 macro lens. Images were stacked and processed using a licensed version of Helicon Focus 6.7.0, then contrast adjusted in Photoshop CS6 Portable software. Label data are indicated verbatim.

Abbreviations and symbols mentioned in this paper are abbreviated as follows:

/	different lines;
//	different labels;
LB	body length, from the apical margin of pronotum to the apex of elytra;
LR	length of rostrum;
LP	pronotal length, from the base to apex along the midline;
LE	elytral length, from the level of the basal margins to the apex of elytra;
WR	maximum width across the rostrum;
WP	maximum width across the pronotum;
WE	maximum width across the elytra.

Comparative materials and specimens used in the study are deposited in the following institutional collections:

- PNM** Philippine National Museum of Natural History, Manila, Philippines;
SKSUABC Sultan Kudarat State University ACCESS Biological Collection, Tacurong, Philippines;
SMTD Senckenberg Natural History Collections, Dresden, Germany;
UMCRC University of Mindanao Coleoptera Research Center, Davao City Philippines.

Taxonomy

Metapocyrtus (Orthocyrthus) melibengoy Cabras & Medina, sp. nov.

<https://zoobank.org/D82A7BCD-3E58-441F-B651-CBAF006469CB>

Figs 1–4

Type material. *Holotype* (Figs 1, 3), male: Philippines - Mindanao / Lake Holon / South Cotabato / October, 2021 / coll. Cabras (typed on white card) // HOLOTYPE male / *Metapocyrtus (Orthocyrthus) melibengoy* / CABRAS & MEDINA, 2022 (typed on red card). Presently in UMCRC, will be deposited in PNM. *Paratypes* (2♂♂, 3♀♀): same data as holotype; all in UMCRC; (3♀♀): Philippines - Mindanao / Lake Holon / South Cotabato / October, 2021 / coll. Mamon, all in SKSUABC. All paratypes with additional red label: PARATYPE / *Metapocyrtus (Orthocyrthus) melibengoy* / CABRAS & MEDINA, 2022.

Diagnosis. *Metapocyrtus (Orthocyrthus) melibengoy* sp. nov. is related to *Metapocyrtus (Orthocyrthus) lanusinus* Schultz, 1922 but differs in its pronotal and elytral scaly markings. *Metapocyrtus (Orthocyrthus) melibengoy* sp. nov. has two small spots on each side of the disc of its pronotum, and each elytron with one small subbasal spot near the suture, one median stripe from the suture to the lateral side, two subapical spots, a short post-median stripe at stria III, and a long stripe along the lateral margin, confluent with the post-median stripe.

Description. Male. Dimensions: LB: 9.2–10.4 mm (holotype 10 mm). LR: 2.0–2.5 mm (2.0 mm). WR: 1.4–1.7 mm (1.4 mm). LP: 3.1–3.6 mm (3.1 mm). WP: 3.6–4.0 mm (3.6 mm). LE: 6.1–6.8 mm (6.1 mm). WE: 5.5–5.7 mm (5.7 mm). *N* = 3.

Integument black. Body surface, rostrum, head, and underside moderately shiny. **Head** finely punctured on dorsum with sparse and very minute pubescence, dorsal surface with a scaly patch of metallic pale-yellow ochre and turquoise round scales near the transverse groove; lateroventral side below the eye with a semi-elliptical scaly patch of metallic pale-yellow-ochre and turquoise round scales interspersed with adpressed metallic bluish piliform scales; forehead between eyes slightly depressed; eyes medium-sized and feebly convex. **Rostrum** weakly rugose and coarsely punctured on basal 2/3 and finely punctured on apical third, longer than wide (LR/WR:2/1.4mm), dorsum covered with sub-adpressed brownish setae, with large subelongate scaly patch of overlapping light-yellow-ochre, turquoise and bluish round scales on basal half, lateral sur-

face with minute subadpressed brownish setae interspersed with long suberect whitish setae, ventral surface with long suberect whitish setae; transverse basal groove distinct; longitudinal groove along midline distinct and forms a shallow concavity; dorsum almost flattish dorsally and apex weakly convex; lateral sides with moderately widened apicad. Antennal scape and funicle almost the same length, scape reaching slightly behind the hind margin of eye, covered with subadpressed fine light-colored setae, and funicle with suberect brownish setae. Funicular segments I and II are almost of the same length, three times longer than wide; segments III–VII nearly as long as wide; club sub-ellipsoidal, nearly 3 times longer than wide. **Prothorax** subglobular, wider than long (LP/WP:3.1/3.6 mm), finely punctured with minute pubescence, widest at middle, weakly convex on dorsal surface, dorsal contour highest point on basal $\frac{1}{4}$. Prothorax with the following scaly markings of metallic, light-yellow ochre and turquoise, round scales: a) stripe at the anterior margin, b) two small subcircular spots on each side of discs, c) stripe at the posterior margin, and d) slightly broader stripe before the coxa confluent with the anterior and posterior marginal stripes. **Elytra** ovate (LE/WE:6.1/5.7 mm), moderately wider and nearly twice longer than prothorax (WE/WP: 5.7/3.6 mm, LE/LP: 6.1/3.1 mm), distinctly and randomly punctured with very minute pubescence, dorsum strongly convex, dorsal contour highest before the middle, lateral contour evenly arcuate, widest at middle, apex quite rounded with sparse, white, fine setae. Each elytron with the following scaly markings of pale-yellow-ochre, turquoise and bluish round scales: a) one subbasal spot between stria II and III, b) one median interrupted stripe from suture towards but not reaching lateral margin, c) two subapical spots on dorsolateral surface, d) a short longitudinal post-median stripe at stria III, and e) one long stripe along lateral margin from base to apex, interrupted before middle. Post-median, and lateral marginal stripe confluent at the apex. **Legs** with moderately clavate femora. Femora black covered with subadpressed bluish piliform scales which tend to get longer towards apex and with yellow-ochre, turquoise and bluish oval scales near apical margin. Tibiae covered with suberect long white setae, weakly serrate along inner edge with few protruding teeth. Fore tibiae and midtibiae bear a mucro at apex. Tarsomeres pubescent. Forecoxae covered with colored piliform scales and with pale-yellow-ochre to bluish round scales; mesocoxae and metacoxae covered with setae. Mesoventrite covered with light-colored setae and with light-yellow and turquoise round scales on distal ends. Metaventrite densely covered with white setae and with light-yellow ochre and turquoise elliptical scales on distal ends. Ventrite I slightly depressed on disc, densely covered with white setae and with light-yellow to turquoise elliptical scales towards lateral margin. Ventrite II to V sparsely covered with whitish setae. Ventrite V flattened, apical half finely densely punctured, with minute setae.

Male aedeagus as shown in Figs 9–11.

Female. Dimensions: LB: 11.8–13.0 mm: LR: 2.3–2.5 mm: WR: 1.9–2.0 mm. LP: 3.5–4.0 mm. WP: 4.0–4.6 mm. LE: 8.0–9.0 mm. WE: 6.0–7.0 mm. $N = 5$.

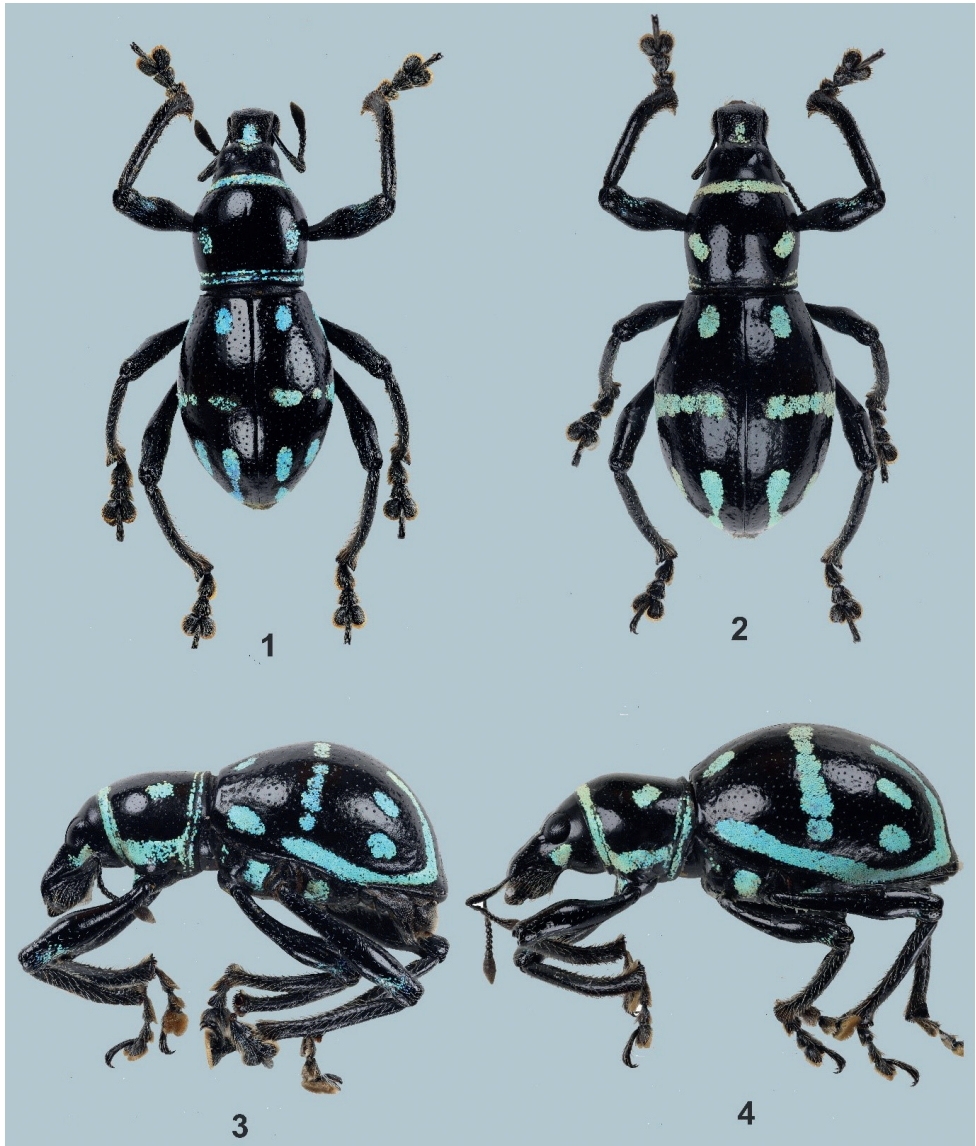
Habitus as shown in Figs 2 and 4.

Females differ from males in the following: a) pronotum slightly wider, and longer than in male; b) base of pronotum slightly widened on sides, c) elytra longer and mod-

erately wider, lateral contour widest before the middle; and d) ventrite I slightly convex on disc. Otherwise, the female is similar to the male.

Etymology. The new species is named after its type locality, Mt. Melibengoy, which is the local name of Mt. Parker.

Distribution. *Metapocyrtus (Orthocyrtus) melibengoy* sp. nov. is known from Tboli Municipality, South Cotabato.



Figures 1–4. *Metapocyrtus (Orthocyrtus) melibengoy* sp. nov. **1** male holotype, dorsal view **2** female, dorsal view **3** male, lateral view **4** female, lateral view.

***Metapocyrtus (Orthocyrtus) flomlok* Cabras & Medina, sp. nov.**

<https://zoobank.org/184E0A42-5491-49CC-9B9B-BBE85A79CBE1>

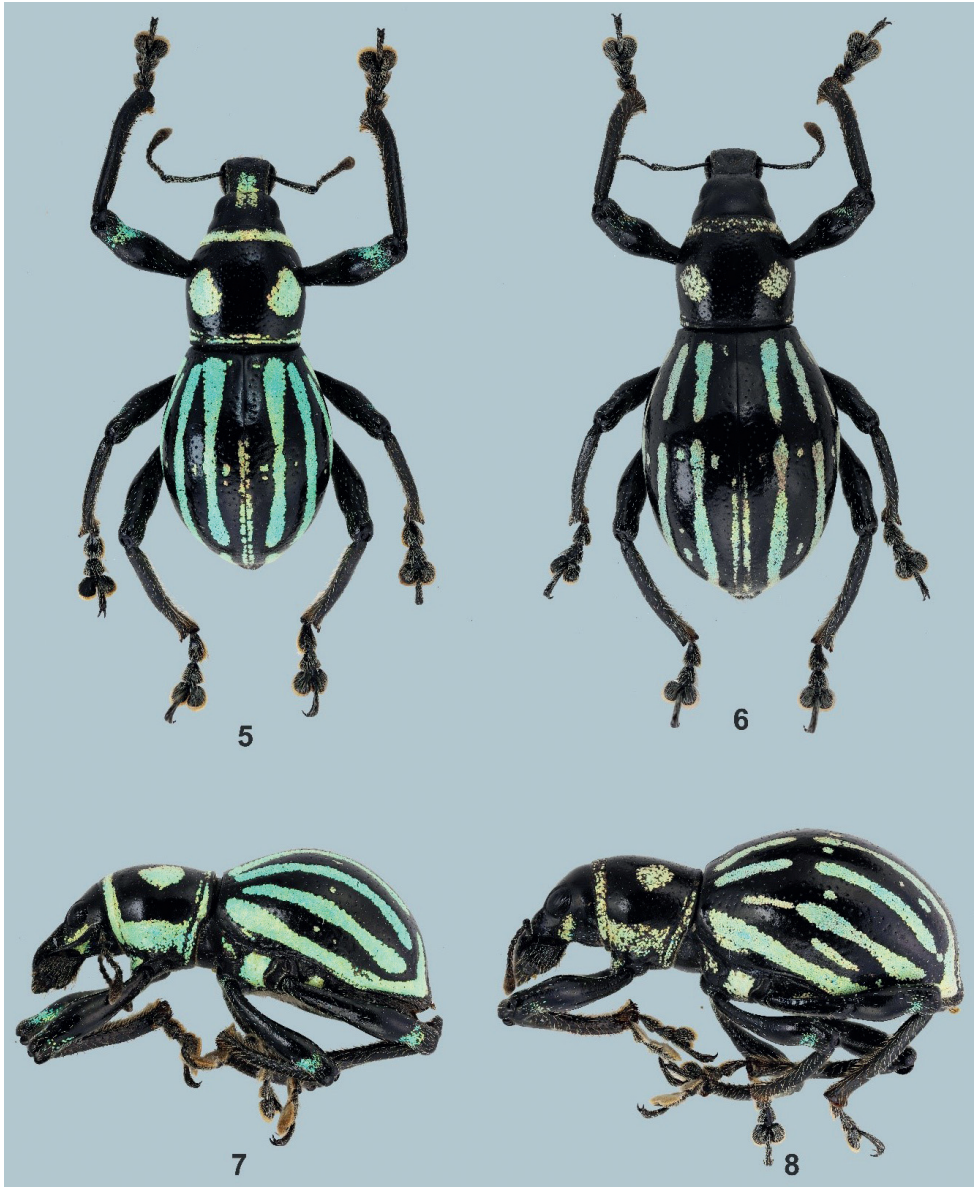
Figs 5–8

Type material. *Holotype* (Figs 5, 7), male: Philippines - Mindanao / Polomolok / South Cotabato / October, 2021 / coll. Cabras (typed on white card) // HOLOTYPE male / *Metapocyrtus (Orthocyrtus) flomlok* / CABRAS & MEDINA, 2021 (typed on red card). Presently in UMCRC, will be deposited in National Museum of Natural History (PNMNH) under the National Museum of the Philippines. *Paratypes* (2♂♂, 2♀♀): same data as holotype; all in UMCRC. All paratypes with additional red label: PARATYPE / *Metapocyrtus (Orthocyrtus) flomlok* / CABRAS & MEDINA, 2021.

Diagnosis. *Metapocyrtus (Orthocyrtus) flomlok* sp. nov. is closely related to *Metapocyrtus (Orthocyrtus) lanusinus* Schultz, 1922 but differs in the following: shorter and stouter body, pronotal scaly marks of two huge round spots on each side of disc, distinct and continuous thick longitudinal stripes from the base to the apex of the elytra, and the stouter and shorter aedeagal body. Meanwhile, *M. (O.) lanusinus* has a thin transverse band at mid-length, and elytral marks having four interrupted longitudinal stripes distinctly short and oftentimes with short spots in between each longitudinal stripe in the mid-length.

Description. Male. Dimensions: LB: 11.0–11.5 mm (holotype 11.0 mm). LR: 2.1–2.3 mm (2.1 mm). WR: 1.8–2.0 mm (1.8 mm). LP: 3.8–4.0 mm (3.8 mm). WP: 4.4–4.7 mm (4.4 mm). LE: 7.0–7.4 mm (7.0 mm). WE: 6.0–6.5 mm (6.0 mm). *N* = 3.

Integument black. Body surface, rostrum, head, and underside with weak luster. **Head** finely punctured on dorsum with sparse and very minute setae, frons covered with metallic golden orange, round scales, lateroventral parts below the eye with a semi-elliptical scaly patch of pale-yellow and turquoise round scales, latero-ventral parts with adpressed metallic bluish piliform scales, forehead between eyes nearly flattish. Eyes medium-sized and feebly convex. **Rostrum** coarsely rugose on basal 2/3 and finely punctured on apical third, slightly longer than wide (LR/WR:2.1/1.8 mm), dorsum with sparse and adpressed brownish setae, lateral surface with sparse minute subadpressed bluish piliform scales interspersed with brownish and whitish, long suberect setae especially towards the apical margin, ventral surface with long suberect whitish setae; transverse basal groove distinct; longitudinal groove along midline distinct and forms a shallow concavity filled with metallic golden orange with a tinge of green, round scales; dorsum almost flattish dorsally and apex weakly convex; lateral sides with strongly expanded apicad. Antennal scape and funicle of almost the same length, scape reaching the hind margin of eye, covered with subadpressed metallic fine light-colored hairs, and funicle with suberect brownish hairs. Funicular segments I and II almost of the same length, three times longer than wide; segments III–VII nearly as long as wide; club sub-ellipsoidal, nearly 3 times longer than wide. **Prothorax** subglobular, wider than long (LP/WP:3.8/4.4 mm), finely punctured especially near anterior margin, widest before middle, weakly convex on dorsal surface, dorsal contour highest point before the middle. Prothorax with



Figures 5–8. *Metapocyrtus (Orthocyrtes) flomlok* sp. nov. **5** male holotype, dorsal view **6** female, dorsal view **7** male, lateral view **8** female, lateral view.

the following scaly markings of metallic, light-yellow and turquoise round scales: a) thin stripe at the anterior margin, b) two large subcircular spots on each side of disc, c) thin stripe at the posterior margin, and d) slightly broader stripe before the coxa confluent with the anterior and posterior marginal bands. *Elytra* ovate (LE/WE:7.0/6.0 mm), slightly wider and moderately longer than prothorax (WE/WP:

6.0/4.4 mm, LE/LP: 7.0/3.8 mm), finely and distinctly punctured with very minute pubescence, strongly convex, dorsal contour highest before the middle, lateral contour evenly arcuate, widest at middle, apex rounded with sparse, colored, fine setae. Each elytron with the following scaly markings of pale-yellow-ochre, turquoise and bluish round scales: a) three continuous longitudinal scaly stripes from basal margin towards apex of the elytron, b) one long stripe along lateral margin from base to apex, c) one premedian longitudinal stripe along suture, and d) very minute and at times negligible spots in the middle of each scaly stripe at the median portion. **Legs** with moderately clavate femora. Femora black covered with subadpressed light blue and turquoise piliform scales and turquoise elliptical scales near the apical margin. Tibiae covered with suberect long white setae, weakly serrate along inner edge with few protruding teeth. Fore and midtibiae bear a mucro at apex. Tarsomeres pubescent. Forecoxae covered with colored piliform scales and with turquoise elliptical scales; mesocoxae and metacoxae covered with setae. Mesoventrite covered with light-colored setae and with turquoise round scales on distal ends. Metaventrite sparsely covered with light-colored piliform scales and with turquoise round scales on distal ends. Ventrite I slightly depressed on disc, covered with light-colored piliform scales and with light-yellow to turquoise round scales towards lateral margin. Ventrite II to V sparsely covered with whitish setae and piliform scales which tends to get denser at distal ends. Ventrite V flattened, apical half finely coarsely rugose, with minute setae. Male aedeagus as shown in Figs 12–14.

Female. Dimensions: LB: 12.0–12.7 mm: LR: 2.0–2.1 mm: WR: 1.7–1.8 mm. LP: 3.6–3.8 mm. WP: 3.6–3.8 mm. LE: 7.8–8.0 mm. WE: 7.2–7.5 mm. *N* = 2.

Habitus as shown in Figs 6 and 8. Females differ from males in the following: a) base of pronotum slightly widened on sides, b) elytra longer and moderately wider, lateral contour widest before the middle, c) the three stripes from base to apex in the elytra are interrupted before the middle, and d) ventrite I slightly convex on disc. Otherwise female similar to the male.

Etymology. The new species is named after “*flomlok*” the old B’laan name of its type locality Polomolok. The term *flomlok* means hunting ground due to the abundance of wildlife in the area prior to the settlement of lowlanders and agricultural companies.

Distribution. *Metapocyrtus (Orthocyrtus) flomlok* sp. nov. is known from Polomolok Municipality, South Cotabato.

***Metapocyrtus (Orthocyrtus) willietorresi* Cabras & Medina, 2019**

Metapocyrtus (Artapocyrtus) willietorresi Cabras & Medina, 2019: 186

Type locality. Mt. Apo Natural Park, Davao del Sur.

Type depository. UMCRC.

Material examined. Male: Philippines - Mindanao / Kapatagan / Davao del Sur / December, 2021 / coll. LC (typed on white card). Presently in UMCRC.

Remarks. Cabras and Medina (2019) placed the species under the subgenus *Artapocyrtus*. However, based on additional materials and further evidence, the authors obviously made some errors, and the species should be placed in the subgenus *Orthocyrtus* based on the characters mentioned by Cabras et al. (2018). In addition, Cabras and Medina (2019) described the species based on two specimens from Mt. Apo and declared it a new species due to the uniqueness of its elytral and pronotal markings consisting of circular patterns. The shape of the aedeagus of the newly acquired materials (Figs 15–17) further confirms membership of the species in *Orthocyrtus* and its relationship to the *Orthocyrtus lanusinus* species group. One of the defining characteristics of *Orthocyrtus* is the shape of its rostrum. Figs 18–21 show the dorsal view of the different species of *Orthocyrtus* mentioned in this paper.

***Metapocyrtus (Orthocyrtus) villalobosae* Patano, Amoroso, Mohagan, Guiang & Yap, 2021**

Metapocyrtus (Artapocyrtus) villalobosae Patano et al., 2021: 284

Type locality. Mount Kabunulan, Hamiguitan Range, Surop, Governor Generoso, Davao Oriental, 6°27'44.29"N, 126°10'18.15"E, 400 m a.s.l.

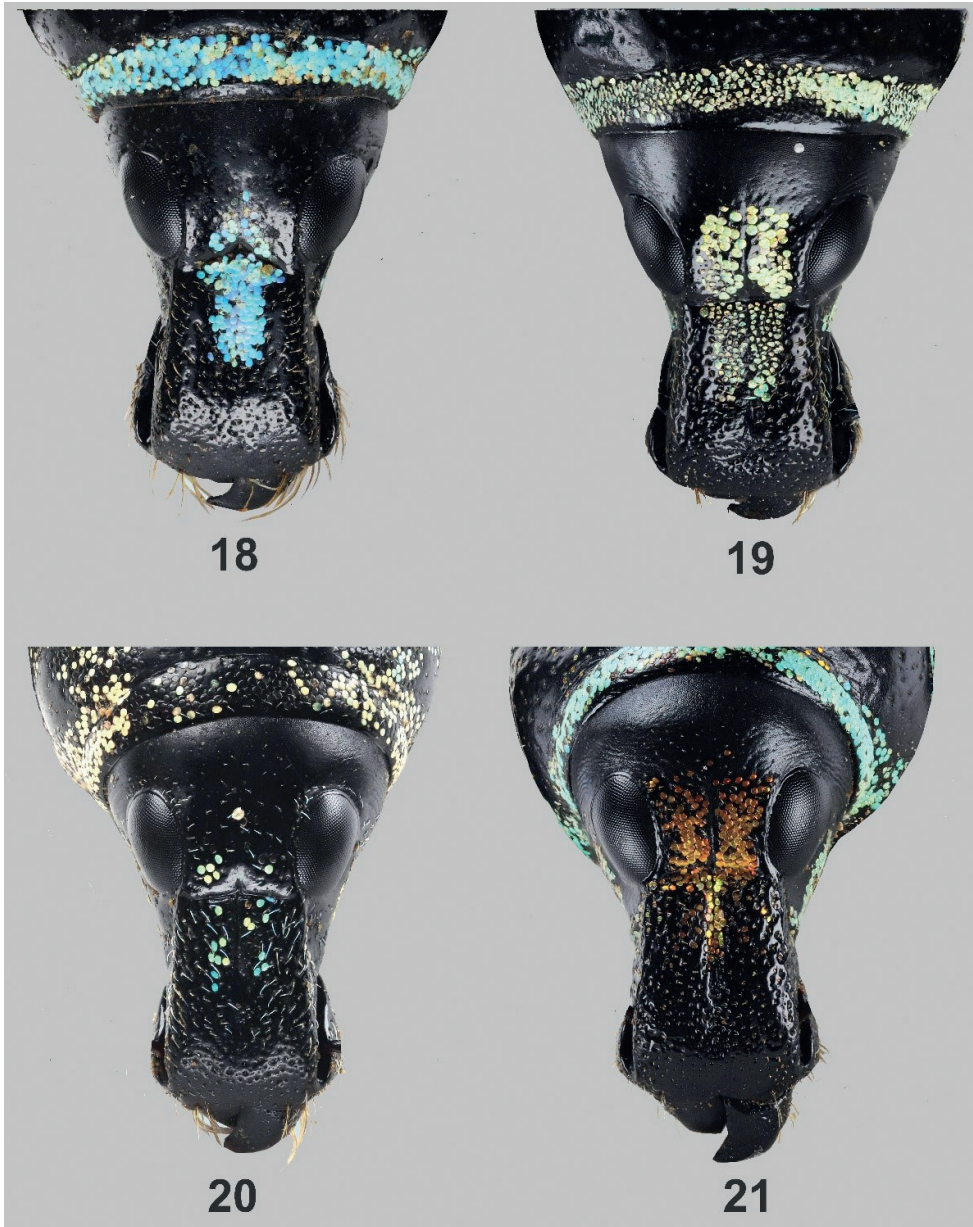
Type depository. CMUZS.

Material examined. 4♂♂, 2♀♀: Philippines - Mindanao / San Isidro / Oriental / December, 2021 / coll. LC (typed on white card). Presently in UMCRC.

Remarks. Patano et al. (2021) recently described a new species *Metapocyrtus (Artapocyrtus) villalobosae* under the subgenus *Artapocyrtus* based on four specimens collected at Mount Kabunulan, Hamiguitan Range in Governor Generoso, Davao Oriental at an elevation of 400 m. Based on the images of the male and female habitus described in the original paper (Patano et al. 2021: 285, fig. 3) with a size ranging from 13.2–14.5 mm and a holotype of 14.5 mm, it doubtlessly belongs to *Orthocyrtus* based on its size, shape of the rostrum, as well as the general shape of the male and female habitus. In 2021, specimens that appeared to belong to *Metapocyrtus (Artapocyrtus) villalobosae* from San Isidro, Davao Oriental, which is part of the range of Mt. Hamiguitan, were donated to UMCRC. Upon examination, the said specimens were found to be very similar to the male holotype, and female paratype in the paper of Patano et al. (2021). The only difference is the short longitudinal subbasal stripes which we believe are simply part of the variability of the species. We believe it was wrongly placed in the subgenus *Artapocyrtus* and thus, we are proposing that it be transferred to the subgenus *Orthocyrtus* based on the characters mentioned by Cabras et al. (2018) including the shape of its rostrum (Fig. 21). Furthermore, while the species elytral patterns may have a superficial resemblance to *M. (Sclerocyrtus) chamissoi* Schultze, 1925, it is actually more closely related to *M. (Orthocyrtus) davaoensis* Cabras, Medina & Bollino, 2021 described from Davao City and Bukidnon. The general habitus of the male and female, the elytral and pronotal patterns as well as the genitalia are also



Figures 9–17. Male genitalia of *Orthocyrthus* sp. **9–11** *Metapocyrthus (Orthocyrthus) melibengoy* sp. nov. **12–14** *Metapocyrthus (Orthocyrthus) flomlok* sp. nov. **15–17** *Metapocyrthus (Orthocyrthus) willietorresi* **9, 12, 15** aedeagus in lateral view **10, 13, 16** idem in dorsal view **11, 14, 17** sternite IX in dorsal view.



Figures 18–21. Dorsal view of *Orthocyrtes* spp. rostrums **18** *M. (O.) melibengoy* sp. nov. **19** *M. (O.) flomlok* sp. nov. **20** *M. (O.) willietorresi* **21** *M. (O.) villalobosae*.

very similar. Molecular data and/or eversion of the endophallus in the near future can be used in delineating the *davaoensis* species group which seems to have a widespread form and distribution throughout Mindanao. Eversion of the endophallus in the tribe Pachyrhynchini is quite challenging to accomplish and needs a lot of specimens as mentioned by Bollino and Sandel (2017) and Cabras et al. (2018).

Key to species of *Metapocyrtus* (*Orthocyrtus*)

- 1 Pronotum coarsely punctured with a transverse scaly stripe in the entire width in the middle; elytra coarsely striate punctate, striae beset with golden yellow and reddish scales..... *M. (O.) villalobosae* Patano et al. 2021
- Pronotum subglabrous or finely punctured without a transverse stripe; elytra finely punctate, striae with fine setae..... 2
- 2 Prothorax as long as wide with subcircular scaly rings on each side of disc; each elytron with two circular scaly rings on basal, medial and apical parts...
..... *M. (O.) willietorresi* Cabras & Medina, 2018
- Prothorax wider than long with scaly spot on each side of disc; elytra with spots or longitudinal scaly stripes from basal margin towards apex..... 3
- 3 Pronotum with small scaly spots on each side of disc; elytra ovate with sub-basal and subapical spots and an interrupted median stripe and a short longitudinal post-median stripe at stria III..... *M. (O.) melibengoy* sp.nov.
- Pronotum with large round scaly spot on each side of disc; elytra strongly ovate with thick longitudinal scaly stripes from basal margin towards apex..... *M. (O.) flomlok* sp.nov.

Notes on the habitat of *Metapocyrtus* (*Orthocyrtus*) *melibengoy* sp. nov. and *Metapocyrtus* (*Orthocyrtus*) *flomlok* sp. nov.

Metapocyrtus (*Orthocyrtus*) *melibengoy* sp. nov. was collected from forest vegetation along the Salacafe trail leading to Lake Holon, at an elevation of 1200 m (Fig. 22). Lake Holon is a caldera of Mt. Parker, a potentially active stratovolcano in southern Mindanao. The specimens were collected on leaves of a *Melastoma* sp. (Melastomataceae), *Piper aduncum* (Piperaceae), and *Cyathea* spp. (Cyatheaceae) in a partially open area of the trail. The area where the specimens were collected, roughly 9 km from the Barangay Salacafe, serves as the receiving area. The trail to Lake Holon is quite open, with various species of ferns, grasses, and shrubs, and an abundance of pitcher plants and other angiosperms. On the initial ascent to the lake, the trail is quite open with some portions having been converted into farmlands planted with *Zea mays* ssp. *Mays* (Poaceae), *Coffea* spp. (Rubiaceae), and *Musa textilis* (Musaceae).

As for *Metapocyrtus* (*Orthocyrtus*) *flomlok* sp. nov., it was collected in an open and quite degraded area in Polomolok, South Cotabato, near a pineapple plantation at an elevation of 1021 m. The new species was collected on a slope near a small creek with pristine waters (Fig. 23). It was found on the leaves of buyo-buyo (*Piper aduncum*) and avocado (*Persea americana*). During personal correspondence with Stan Cabigas, he mentioned and showed photos of the same species from Mt. Matutum together with its possible model/mimic - *Pachyrhynchus gilvamaculatus* Yoshitake, 2016. Thus, we believe that the population near the pineapple plantation is the remnant population that survived the degradation of the forested habitats and conversion of land in Polomolok. A similar scenario has been observed with *M. (Orthocyrtus) davaoensis* described based

on a limited number of specimens near the lowland of Carmen, Davao City. In our recent surveys of the higher elevation and more forested part of Carmen, a huge thriving population of *M. (O.) davaoensis* was found.



Figures 22–23. Habitats of *Orthocyrthus* spp. **22** *M. (O.) melibengoy* sp. nov. in Mt. Parker, T’boli, South Cotabato **23** *M. (O.) flomlok* sp. nov. in Polomolok, South Cotabato.

Discussion

The genus *Metapocyrtus* is one of the most taxonomically complex genera of the tribe Pachyrhynchini. The genus is characterized by mimicry with other members of Pachyrhynchini (i.e., *Pachyrhynchus* Germar, 1824, *Trichomacrocyrtes* Yoshitake, 2018, *Eumacrocyrtes* Schultzze, 1923) as well as other weevil groups (i.e., *Alcidodes* Marshall, 1939, *Eupyrigops* Berg, 1898, *Polycatus* Heller, 1912, *Calidiopsis* Heller, 1913), and even with the family Cerambycidae as exemplified by the genus *Doliops* Waterhouse, 1841. For the genus *Metapocyrtus*, elytral patterns alone or color variation of the scaly markings should not be used as a basis in delineating species since intersubgeneric mimicry among its members as well as color polymorphism is quite a common occurrence (Schultzze 1925; Cabras et al. 2021a). In addition, the shape and general profile of the rostrum, pronotum, and body should be considered in identifying species and not only the elytral patterns. Two almost identical species, in terms of elytral patterns or coloration, could turn out to be two species from different subgenera or even tribes. Such mistakes seem common in the Philippines as evidenced by several online materials as well as specimens housed in some museums, and collections that are erroneously identified.

Another problem with this genus is the subgeneric delineation which remains unresolved and requires a thorough revision. As for the subgenus *Orthocyrtes*, the large body size, shape of its rostrum, and body make this taxon quite straightforward to identify. Despite recent publications on this subgenus, many species remain unknown and some species may even be cryptic; only eversion of the endophallus or molecular data could help in species delineation. However, because of the unabated loss of forest cover in the Philippines due to illegal logging, conversion of forest lands for commercial or agricultural purposes, as well as mining activities, these species are at a high risk of extinction. Thus, discoveries of new species and research on species biology, ecology, and threats are very important as they may provide the International Union of Conservation of Nature Red List and local stakeholders with evidence to be used for their assessment and conservation initiatives.

Acknowledgements

We express our gratitude to the University of Mindanao; to DENR for the Gratuitous Permit, Kim Jumawan, and Amy Ponce for the help in the collection; the Department of Science and Technology - National Research Council of the Philippines (DOST-NRCP), for the funding, and DOLE-Philippines for facilitating the biodiversity assessments in their farms in Polomolok; Dr. Arvids Barševskis from DUBC, Latvia; Dr. Hiraku Yoshitake from Institute for Agro-Environmental Sciences, NARO (NIAES), Tsukuba, Japan; Dr. Klaus-Dieter Klass and Olaf Jäger from Senckenberg Natural History Collections, Dresden, Germany for their assistance during the first and last author's visit. We are also grateful to Dr. Dave Waldien for reviewing the English text.

References

- Bollino M, Sandel F (2017) Two new taxa of the Subgenus *Artapocyrtus* Heller, 1912, Genus *Metapocyrtus* Heller, 1912 from the Philippines (Coleoptera, Curculionidae, Entiminae, Pachyrhynchini). *Baltic Journal of Coleopterology* 17(1): 1–14.
- Bollino M, Medina MN, Cabras AA (2020) Three new *Metapocyrtus* Heller, 1912 (Curculionidae, Entiminae, Pachyrhynchini) from Mindanao Island, Philippines. *Journal of Tropical Coleopterology* 1(1): 26–38.
- Cabras A, Medina MN (2019) *Metapocyrtus ginalopezae* sp.n., a new *Orthocyrthus* from Davao de Oro. *Baltic Journal of Coleopterology* 19(2): 205–2011.
- Cabras A, Medina MN, Bollino M (2018) A new species of the subgenus *Orthocyrthus* Heller, 1912, genus *Metapocyrtus* Heller, 1912 (Coleoptera, Curculionidae, Entiminae, Pachyrhynchini) from Mindanao, with notes on its ecology. *Baltic Journal of Coleopterology* 18(1): 39–46.
- Cabras A, Medina MN, Bollino M (2021a) Two new species of the genus *Metapocyrtus* Heller, 1912 (Coleoptera, Curculionidae, Entiminae, Pachyrhynchini), subgenus *Orthocyrthus* Heller, 1912, from Mindanao Island, Philippines. *ZooKeys* 1029: 139–154. <https://doi.org/10.3897/zookeys.1029.63023>
- Cabras A, Villanueva RJ, Medina MN (2021b) A New Species of *Metapocyrtus* Heller, 1912 (Coleoptera, Curculionidae, Entiminae) from Mindanao Island, Philippines. *Journal of Tropical Coleopterology* 2(1): 35–41.
- Patano R, Amoroso V, Mohagan A, Guiang MM, Yap S (2021) Two new species of the genus *Metapocyrtus* Heller, 1912 (Coleoptera: Curculionidae: Entiminae), from Mindanao Island and an updated checklist of *Metapocyrtus* species in the Philippines. *The Raffles Bulletin of Zoology* 69: 282–303.
- Schultze W (1925) A monograph of the pachyrhynchid group of the Brachyderinae, Curculionidae: Part III. The genera *Apocyrtdius* Heller and *Metapocyrtus* Heller. *Philippine Journal of Science* 26: 131–310.
- Yoshitake H (2011) A new species of the subgenus *Artapocyrtus* of the genus *Metapocyrtus* (Coleoptera: Curculionidae: Entiminae) from Mindanao, the Philippines. *Esakia* 50: 115–119. <https://doi.org/10.5109/19404>

Revision of the family Milacidae from Switzerland (Mollusca, Eupulmonata, Parmacelloidea)

Vivianne M. Schallenberg^{1,2}, René Heim^{3,4}, Ulrich E. Schneppat⁵,
Peter Müller⁶, Jörg Rüetschi⁷, Eike Neubert^{1,2}

1 Natural History Museum Bern, Bernastrasse 15, CH-3005 Bern, Switzerland **2** Institute of Ecology and Evolution, University of Bern, CH-3012 Bern, Switzerland **3** St.-Karli-Strasse 32c, CH-6004 Lucerne, Switzerland **4** Natur Museum Lucerne, Kasernenplatz 6, CH-6003 Lucerne, Switzerland **5** Sennereiweg 8, CH-7074 Churwalden-Malix, Switzerland **6** Witikonstrasse 180, CH-8053 Zurich, Switzerland **7** Malakologische Untersuchungen, Weidweg 42, CH-3032 Hinterkappelen, Switzerland

Corresponding author: Eike Neubert (eike.neubert@nmbe.ch)

Academic editor: Menno Schilthuizen | Received 25 February 2022 | Accepted 8 July 2022 | Published 9 August 2022

<https://zoobank.org/8A3C95DA-976E-4419-8122-C54098768B4B>

Citation: Schallenberg VM, Heim R, Schneppat UE, Müller P, Rüetschi J, Neubert E (2022) Revision of the family Milacidae from Switzerland (Mollusca, Eupulmonata, Parmacelloidea). ZooKeys 1116: 149–179. <https://doi.org/10.3897/zookeys.1116.82762>

Abstract

In this work, the presence of species of the slug family Milacidae in Switzerland was investigated by using the barcoding marker cytochrome c oxidase subunit I (COI) as well as traits of the body and the genital organs. Currently, three species of *Tandonia* living in Switzerland in established populations could be reported, i.e., *T. rustica*, *T. budapestensis*, and *T. nigra*. The three records of *Milax gagates* were re-investigated, but only for one of these records could the identification be reconfirmed. This species has currently no established and thriving population in Switzerland. For all species recorded, detailed descriptions of body morphology, genital anatomy, and distribution data are provided based on the investigated Swiss animals. An unknown pale colour morph of a *Tandonia* sp. from Canton Ticino could be identified as *T. nigra*, and the barcodes of *T. nigra* specimens were submitted to GenBank for the first time. The identity of the Italian and Austrian populations of *T. nigra* from the Bergamasque Alps and north Tirol is evaluated. Observations on details of the morphology of the genital organs in *T. rustica* vs. *T. kusceri* are discussed.

Keywords

barcoding, colour variation, distribution records, genital organs, *Milax*, slugs, *Tandonia*

Introduction

The family Milacidae Ellis, 1926 currently comprises two genera with 14 extant species in *Milax* Gray, 1855, and 29 extant species in *Tandonia* Lessona & Pollonera, 1882 (MolluscaBase, accessed on 28 December 2021). The last comprehensive revision of the family was published by Wiktor (1987). The family is distributed in Europe with the Balkan peninsula as the area of highest species richness. In Switzerland, the family is represented by only four species (Bank and Neubert 2017). These species were listed in the Red List for continental molluscs of Switzerland, and their conservation status was assessed (Rüetschi et al. 2012). According to these lists (Rüetschi et al. 2012; Bank and Neubert 2017), the following milacid species are known from Switzerland: *Milax gagates* (Draparnaud, 1801), *Tandonia budapestensis* (Hazay, 1880), *Tandonia rustica* (Millet, 1843), and *Tandonia nigra* (C. Pfeiffer, 1894).

Tandonia rustica is a rarely discovered but widespread taxon in the country; it is a nocturnal species strictly confined to beech forests on limestone talus (pers. obs.). The species is also recorded from the Italian Alps ranging from Canton Ticino to Lake Garda and from many locations in the Piemontese Alps in Valle di Susa (Wiktor 1987; Gavetti et al. 2008; pers. obs.). In contrast, *T. nigra* is considered to represent a rather local alpine species with a smaller distribution area. The type locality of this species is the summit of Monte Generoso in Canton Ticino close to Lugano. According to Wiktor (1987), the species is also recorded from the Austrian Alps in North Tirol, and the recent Red List assessment by the International Union for Conservation of Nature (IUCN) records a distribution from the Italian Alps ranging from the Canton Ticino to Lake Garda (Nardi 2017). The identity of these Austrian and Italian records is discussed below. In the last years, one of the authors (P. Müller) observed a form of a small *Tandonia* species in Val Cürta on the southwestern slope of the Monte Generoso, which differed from the black *T. nigra* from the summit by a grey to beige body colour and an elongate very slim penial papilla.

The aim of this paper is to verify the correct identification of the *Tandonia* species from Switzerland in general, and to specifically investigate the status of the grey to beige *Tandonia* specimens from lower altitudes of Monte Generoso. We compared our genetic data with a few species recorded in GenBank by Liberto et al. 2012; Rowson et al. 2014a; Korábek et al. 2016; Turóci et al. 2020 and other unpublished data to corroborate our identifications. Since the results of the COI analysis produced well-supported data, we decided not to analyse further markers. Our aim was to characterise species with a simple marker, and not to reveal phylogenetic relationships of the clades detected, which would have required a much deeper research approach with a sampling that exceeds our current possibilities.

Materials and methods

Specimens

Most investigated specimens were freshly collected during field trips in Switzerland, Italy, Republic of San Marino, and France. If possible and necessary, juveniles were

kept alive until they reached adulthood. To complete and increase the genetic data set also previously inventoried specimens of the Natural History Museum Bern (NMBE) were included in this study. Detailed sampling locations, voucher numbers and the GenBank accession numbers of the sequenced specimens are shown in Suppl. material 1: Table S1. All records in this study will be uploaded to the map server of the Centre Suisse de Cartographie de la Faune (CSCF) and will be displayed on the respective species distribution maps (<https://lep.usn.ch/cartof/>).

Husbandry of live slugs and their preservation

Juvenile and subadult slugs were kept individually in 0.2 L polypropylene boxes (Rondo 4, Rotho Kunststoff AG, Switzerland) perforated with a hot needle for air exchange. The boxes were stored in a wine refrigerator at 16 °C, the bottom was carpeted with several layers of moistened paper towels. Nutrition was provided in form of slices of champignon, cucumber, and high protein cat feed pellets. The slugs were checked and weighed once per week with replacement of the paper towel and food. The maturity was checked by evaluation of the genital pore: fully adult animals have a visible and clearly open pore. All captured adult specimens were photographed alive, and tissue samples and body measurements were taken before preservation. For preservation, the animals were relaxed and killed in sparkling water for ~ 30 min. The dead animals were placed on kitchen paper and frozen in the freezer for several hours. After that they were thawed in cold water and additional slime was removed by placing the specimens into ethanol. The animals were transferred into 96% ethanol, and, for proper body cavity preservation, 96% ethanol was injected through the sole tip into the body cavity with a 1 mL syringe using a fine needle (Terumo Corporation, Philippines). After 24 h, the slugs were transferred in 80% ethanol. The following day, the ethanol was exchanged, and the specimens were stored in the fridge at 5 °C awaiting DNA extraction and dissection. This procedure properly maintains the soft tissue for anatomical studies and keeps the DNA intact for the genetic investigation.

Morphological and anatomical analysis

All specimens used for live body measurements were fully adult specimen from the collection of R. Heim. The following measurements were taken:

Live weight (**lw**) was taken with a digital scale to 0.01 g weekly. The last measured weight before preservation of each specimen was taken for calculation. In the analysis the weights were rounded up to 0.5 g.

Total length (**tl**) was measured with a metal ruler from specimens in full stretch when crawling to 1 mm. Starting from the front to the outermost extension of the posterior sole or dorsum.

Sole width (**sw**) was measured from the crawling specimen on a sheet of glass with a ruler or a calliper to 0.5 mm. The widest extension was usually at mid of the sole.

The ratio of mantle length (**ml**) / total length (**tl**) is given because it might be an additional character for species differentiation.

Number of tubercle rows (**tr**) were counted on the freshly preserved animals with a dissection needle under a binocular. Starting from the first tr at the slit of the pneumostome along the posterior edge of the mantle to the last tr at the keel. Counting was done twice, back and forth. If not clearly countable, the two closest numbers were indicated. In the analysis the lowest and highest counts of our specimens were taken.

Before dissection of selected specimens, photographs of the preserved animals were made in dorsal, lateral (left and right), and ventral position. The dissection of the slug genitalia was performed under a binocular (Leica MZ6) using thin forceps (Dumont 0.5; 3.5) and micro scissors. For the anatomical pictures, the genital organs were detached from the body, spread on a wax bed, and properly pinned with minutia pins to visualize and investigate the structures. Additionally, the inner structures of penis, epiphallus and vagina were shown. Pictures were taken with a Leica DVM6 microscope camera (Leica Camera, Wetzlar, Germany) using the image-processing program FIJI for scaling (Schindelin et al. 2012). The distribution map of the investigated species (Fig. 1) was created using QGIS software v3.20.3-Odense (QGIS.org, 2022. QGIS Geographic Information System. QGIS Association. <http://www.qgis.org>).

Molecular analysis

The total DNA extraction was performed following the manufacturers protocol of the Qiagen Blood and Tissue Kit using the QIAcube extraction robot (Qiagen; Hilden, Germany). Approximately 0.5 cm² of mantle tissue was cut, cleaned with a sterilized scalpel (Schreiber GmbH, Germany) from superficial slime, and placed in 180 µL ATL buffer and 20 µL proteinase K. For small specimen, an additional snippet from the foot or body wall was added to the digestion mix in order to yield enough DNA for sequencing. The tissue was then incubated for 4 h at 56 °C and 40 rpm in a thermo shaker (Labnet, Vortemp 56, witec AG, Littau, Switzerland). After digestion the QIAcube extraction robot did the DNA extraction following the standard protocol 430 (DNeasy Blood Tissue and Rodent tails Standard). The extracted DNA samples were then stored in a -80 °C freezer for long-term storage.

In this study, the sequences of the mitochondrially encoded barcoding marker cytochrome c oxidase I (**COI**) was investigated. For the COI PCR mixture 3 µL of DNA template in 12.5 µL GoTaq G2 HotStart Green Master Mix (Promega M7423), 7.5 µL ddH₂O, 1 µL of the established Folmer primers LCO1490 and HCO2198 (Folmer et al. 1994) were used. The PCR cycle was set as following: 3 min at 94 °C, followed by 40 cycles of 1 min at 95 °C, 1 min at 47 °C and 1 min at 72 °C and for the last step, the final elongation 10 min at 72 °C. The PCR products were controlled using gel electrophoresis. PCR products with a visible, single band with the desired length were sent to LGC (LGC Genomics Berlin, Germany) for purification and Sanger sequencing. For each specimen, the forward and reverse sequence were aligned using the software package Geneious v. 9.1.8 (Biomatters Ltd) and the consensus sequence was extracted. Finally, the consensus sequence was trimmed to the 655 bp used in further analysis.

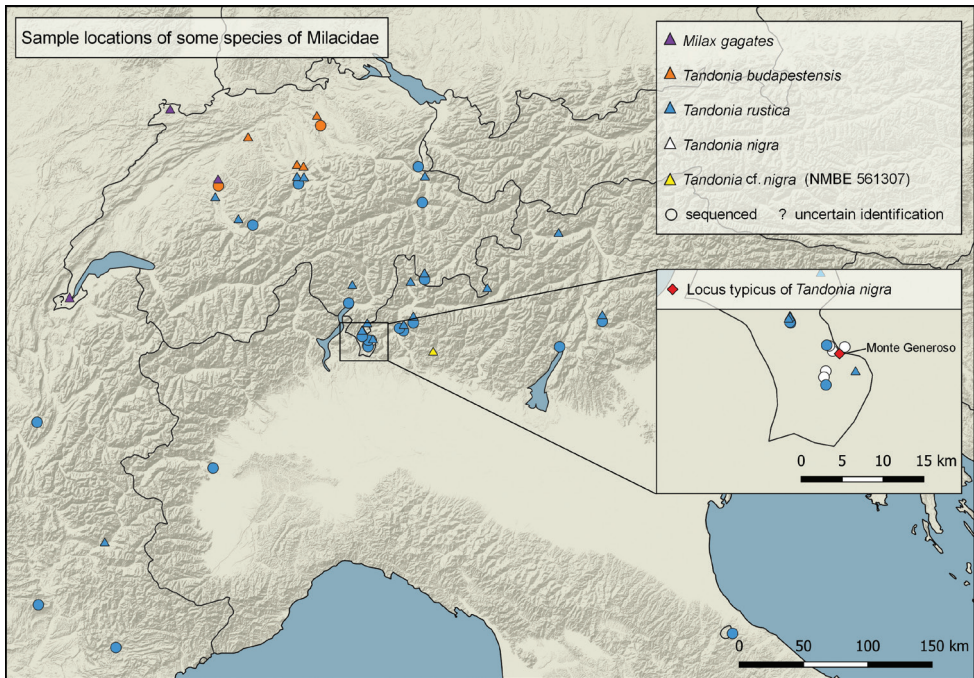


Figure 1. Distribution map of collected specimens.

Phylogenetic analysis

For the phylogenetic analyses, sequence KT371419 from GenBank (*Oxychilus draparnaudi* (H. Beck, 1837)) was included as outgroup. Additionally, 34 sequences were downloaded from GenBank comprising *Tandonia budapestensis*, *Tandonia rustica*, *Tandonia kusceri* (H. Wagner, 1931), *Tandonia sowerbyi* (A. Férussac, 1823) and *Tandonia cristata* (Kaleniczenko, 1851). The sequences were included into the phylogenetic analysis to obtain a better overview of the genus *Tandonia* and to compare our results to those of Rowson et al. (2014a). The included species and their accession numbers are listed in the Suppl. material 1: Table S1.

For sequence processing, alignments and calculation of trees, the software package Geneious v. 9.1.8 (Biomatters Ltd) was used. The protein-coding gene fragment of COI was defined in three data blocks, with each codon position as separate subset.

To calculate the ML interference, the RAxML plug-in for Geneious (Stamatakis 2006) was implemented, using the Geneious plug-in with rapid bootstrapping setting, the search for the best scoring ML tree, the nucleotide model GTR CAT I and 2000 bootstrapping replicates.

With the same alignment data, a second maximum likelihood tree was calculated using the IQ Tree web tool (<http://iqtree.cibiv.univie.ac.at/>) (Trifinopoulos et al. 2016), using the default settings for the input data and the substitution model set to auto detect. The branch support analysis was set to ultrafast with 1000 bootstrap alignment and performing a SH-aLRT branch test (Guindon et al. 2010) with a 1000 replicates.

Bayesian Inference (**BI**) was performed using Mr. Bayes v3.2.6 × 64 (Huelsenbeck and Ronquist 2001; Ronquist and Huelsenbeck 2003; Altekar et al. 2004) through the HPC cluster from the University of Bern (<http://www.id.unibe.ch/hpc>). For the data set, the nucleotide model was set 4 by 4, and we applied a mixed model search. The Monte Carlo Markov Chain (MCMC) parameter was set as follows: starting with four chains and four separate runs for 15 million generations with the temperature set to 0.2. The tree sampling frequency was set to 1000 with a burn in of 25%.

Species delimitation analysis

Species partitions analysis was performed on the Assemble Species by Automatic Partitioning (**ASAP**) web tool (<https://bioinfo.mnhn.fr/abi/public/asap/asapweb.html>) (Puillandre et al. 2021), using the Kimura (K80) (Kimura 1980) substitution model with the default settings for the transition/transversion rate ratio (ts/tv) = 2 and the standard advanced options for 5 best partition suggestions for 71 available COI sequences.

Abbreviations

ad	adult
ASAP	Assemble Species by Automatic Partitioning
BI	Bayesian Interference
BS	Bootstrap support
COI	cytochrome c oxidase subunit I
CSCF	Centre Suisse de Cartographie de la Faune (Neuchâtel, Switzerland)
gp	genital pore
HNHM	Hungarian Natural History Museum, Budapest
IUCN	International Union for Conservation of Nature
juv	juvenile
lw	live weight
MHNG	Muséum d'histoire naturelle de la Ville de Genève
ml	mantle length
ML	maximum likelihood
nc	not countable
NMB	Natural History Museum Basel
NMBE	Natural History Museum Bern
NMLU	Natur-Museum Luzern
NMW	National Museum of Wales, Cardiff
PCR	Polymerase Chain Reaction
SMNS	State Museum of Natural History Stuttgart
sw	sole width
tl	total length
tr	tubercle rows
ZMH	Zoological Museum Hamburg

Results

The results of the genetic analysis based on COI are summarised in Fig. 2. The tree is based on the topology of RaxML, which was confirmed by IQTree and Bayesian Interference. Interpretation of Bootstrap values for RaxML and IQ Tree: 70 to 80 = moderate support; 80 to 90 = well supported; > 90 = high support and for the Bayesian posterior probabilities values: > 0.95 = significant support. This tree does not reflect relationship of species as only six out of 29 currently accepted species are included (<https://molluscabase.org/aphia.php?p=taxdetails&id=819994> on 28 December 2021); the selection of taxa mainly followed the availability of COI sequences.

Tandonia nigra appears as a rather well supported clade within the selected group. The three highlighted sequences originate from topotypic specimens from the top of Monte Generoso. All other populations investigated were collected from a narrow range at lower altitudes on the mountain and contain all the different colour morphs. Despite their differing body colour (Fig. 8), there is almost no variation in the COI

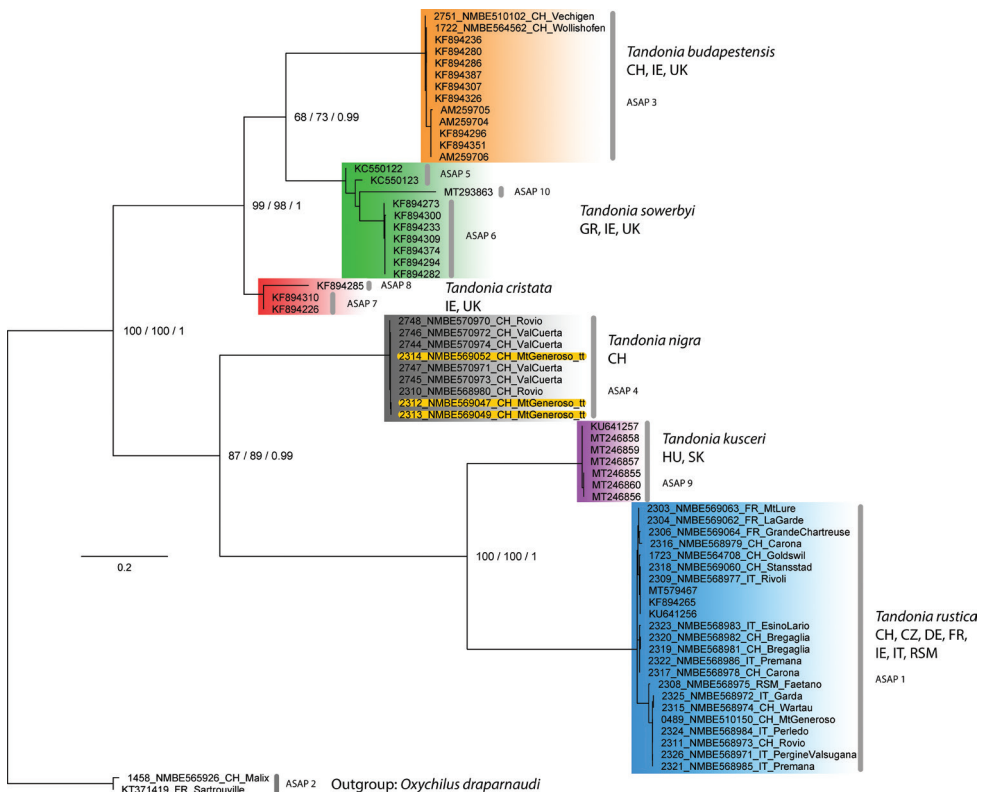


Figure 2. Phylogenetic tree of some species of the genus *Tandonia* based on COI. Numbers at the nodes record support values for RaxML/IQTree/BI. Sequences published in GenBank are named with their accession number; new sequences obtained are named as following: Lab number, museums voucher number, country, and approximate locality. The grey vertical bars indicate the best score for species delimitation calculated with ASAP.

sequences of these specimens observable. Furthermore, the genetic clades of *T. rustica* and *T. kusceri* are clearly separated and well supported.

The best two ASAP scores support the existence of ten different clades as visualized in Fig. 2 with the grey bars labelled with numbers from 1 to 10. This gives 3 subclades in the *T. sowerbyi* clade and two for the *T. cristata* clade. The third best score however supports the concept of seven different clades in the same way, as the clades in Fig. 2 are coloured.

Taxonomy

Milacidae Ellis, 1926

Diagnostic features. Horse-shoe shaped groove on the mantle; pneumostome post-medial; keel connecting sole tip and mantle; sole tripartite, central sole field with V-shaped wrinkles, only visible in preserved animals (Wiktor 1987).

Tandonia Lessona & Pollonera, 1882

Diagnostic features. No stimulatory organ in the atrium, accessory glands opening into the vagina (Wiktor 1987).

Tandonia rustica (Millet, 1843)

Figs 1, 3, 7A–D

Limax rustica Millet, 1843, Magasin de Zoologie, ser. 2, 5: 1, plate 63, fig. 1 [nord de l'Anjou, à la Bouillant, commune de la Chapelle-Hullin, ainsi qu'à Thorigné, etc.].

Type specimens. Probably does not exist, after Wiktor (1987: 286). See also remarks.

Differential diagnosis. Epiphallus more than twice as long as the penis (almost the same length in *T. nigra* and *T. budapestensis*); dark stripe above the pneumostome and on the opposite side of the mantle (missing in *T. nigra* and *T. budapestensis*); penial papilla short, blunt, with flap-like lobes around the central porus (short and blunt but folded in *T. nigra*; elongated with a stalk in *T. budapestensis*).

Description. Colouration. Many fully adult specimens ($n = 56$) were studied from six different Swiss Cantons (Bern, St Gallen, Grisons, Ticino, Obwalden, Nidwalden) as well as from five regions in Italy (Bolzano, Sondrio, Torino, Lecco, Trento), from the Republic of San Marino and from two Departments of France (Alpes de Haute Provence, Isère).

The general pigmentation of Swiss specimens varies from a warm reddish brown to dark reddish or chestnut brown to very dark brown without any reddish brown hue. This pigmentation normally is not fading downwards to the fringe of the sole. How-

ever, in some cases in the less dark pigmented populations in Switzerland, little fading downwards can be observed (Fig. 7A). The mantle is of the same colour as the dorsum, except for the surrounding of the pneumostome, which usually is paler. Many specimens investigated are markedly darker when compared to Wiktor (1973, 1987) and Rowson et al. (2014b). The darkest specimens were found in southern Switzerland (Ticino, Grisons - Val Bregaglia), and in the southwest bordering areas to Italy and France (Fig. 7B). Specimens from Central Switzerland (Lucerne, Nidwalden, Obwalden), northern and eastern Grisons, St. Gallen, and the eastern border area in Italy (Bolzano, Trento) are of a markedly lighter, pale reddish brown pigmentation (Fig. 7A, C, D).

The whole slug is covered with small black spots on dorsum, flanks, and mantle, but not on the keel. The characteristic black streaks above the pneumostome and on the same location on the left side of the mantle can vary greatly in size and form. Even though all our investigated specimens had spots and the characteristic streaks on the mantle, in some specimens they are almost invisible because of the overall dark pigmentation (Fig. 7B). Additionally spots in darker specimen may be much larger and sometimes irregularly jagged and elongated to streaks.

Head, neck and ommatophores are dark brown, while the tentacles are slightly paler. In many cases, the black pigmented ommatophoran retractor is clearly visible through the integument.

The keel is commonly paler in colour than the dorsum. Rarely the general pigmentation of the keel matches the dorsal colour, this occurs especially in darker specimens.

The tripartite sole in pale coloured slugs is creamy yellowish, while darker slugs have a pale yellowish brown sole. Many darker coloured specimens have a hue of greyish black at the posterior outer margins of the lateral sole fields formed by very little black dots. Isolated single greyish black spots may occur along the outer edge of the sole.

Mantle structure. The pneumostome is positioned at 2/3 of mantle length, well posterior of the centre of the mantle. The pneumostome is not surrounded by a distinct ring-like structure, like it is the case in *T. nigra*. The "slit" of the pneumostome in all specimens does not end in the lumen of the pneumostome but runs anteriorly to at least the dorsal edge of pneumostome. In living individuals, the mantle surface is completely smooth besides the horseshoe-shaped sinus groove. The sinus groove is completely developed in all specimens in our series, and it reaches at both sides almost the posterior end of the mantle. In the dark specimens it needs magnification to see it clearly. The posterior margin of the mantle is not tightly attached to the integument and in living and contracted animals smoothly rounded. The posterior free mantle flap covers the anterior integument-tubercles as well as the openings of the postpallial or Wiktor's pocket organ.

Postpallial pocket organ. In all specimens examined, the posterior part of the mantle covered two slit-like openings, the postpallial pocket organ, which was first detected and described by Schnepf et al. (2011) for *Tandonia totevi* (Wiktor 1975).

Integument structures. The number of tr ($n = 52$; tr 12/13-tr 19, \emptyset tr 15) does not vary much in our specimens, and there is no significant variation between populations. The surface texture and the width of tubercles in live specimens vary from fully

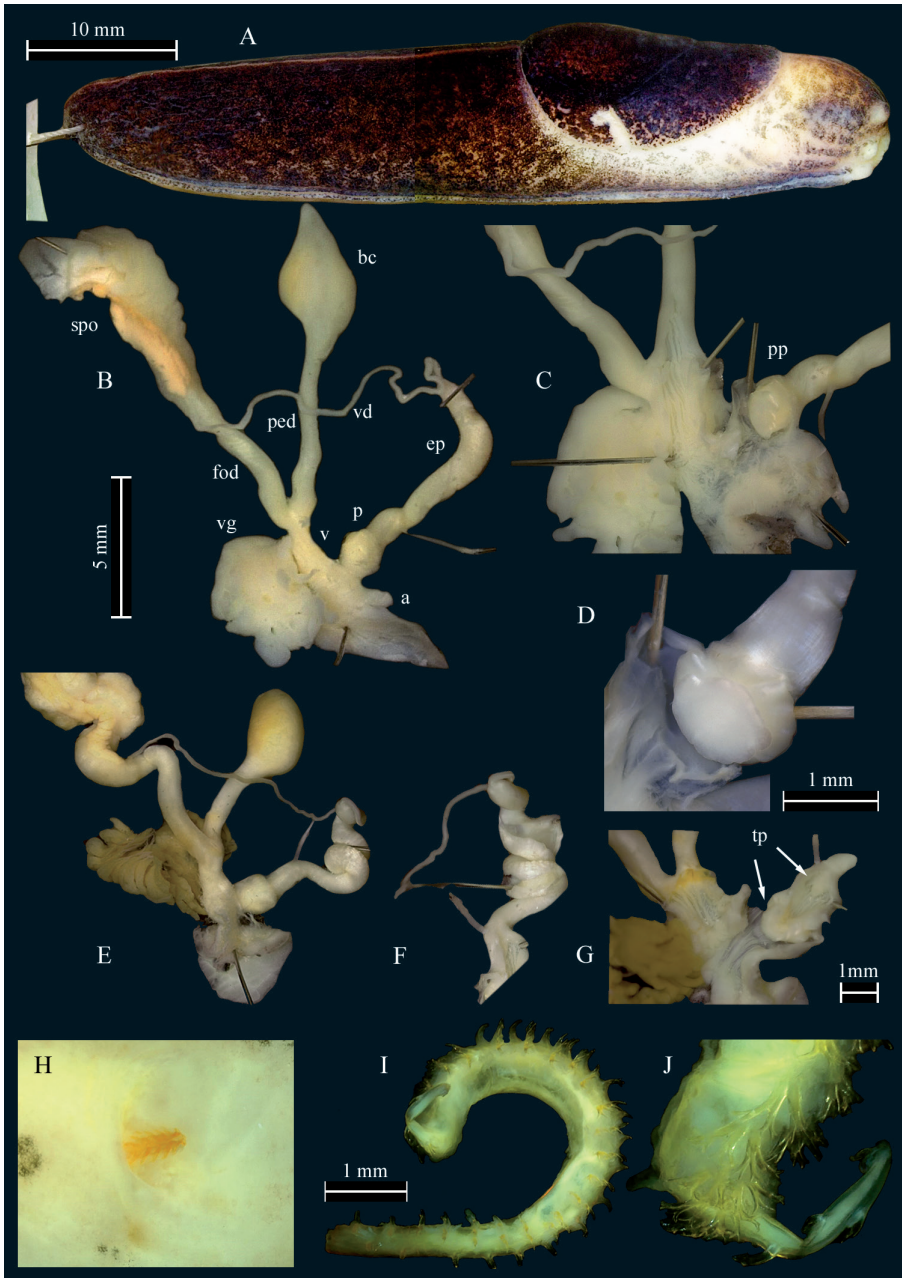


Figure 3. *Tandonia rustica*. **A–C** sequenced specimen NMBE 568973, Rovio, Sovaglia **A** preserved animal **B** situs of genitalia **C** distal genitalia showing anatomical details **D** penis papillae of sequenced specimen NMBE 568978, Carona **E–G** sequenced specimen NMBE 564708, Goldswil **E** situs of genitalia **F** distorted epiphallus **G** details of lumina of vagina, atrium and penis, arrows pointing at the “twin papillae” (tp) **H–J** spermatophore of specimen NMBE 571414, Orselina **H** genital pore with piece of spermatophore **I, J** largest part of the three pieces **J** detail of surface covering spines. Abbreviations: a = atrium; bc = bursa copulatrix; ep = epiphallus; fod = free oviduct; p = penis; ped = pedunculus; pp = penial papilla; spo = spermooviduct; tp = “twin papillae”; v = vagina; vd = vas deferens; vg = vaginal gland.

straight to torn, depending on their body position. All tr from head to the 7th–9th row posterior to the pneumostome are entirely flat, smooth, wide, and remain so from the head and flank to the peripodial tubercle. The remaining tr reaching to the keel are somewhat crenulated, but are also wide, flat, and lacking ridges. Crenulations can only be seen under magnification. The tubercle rows may be long and undivided down to the peripodial tubercle, especially the ones below the lateral mantle edge. The more dorsal rows usually are divided in several tubercle compartments.

The keel is extended from the posterior margin of the mantle to the end of the dorsum. In some specimens, the keel was observed to be even slightly extending over the fringe of the sole, like a very little terminal thorn or knob. The keel has always an entirely smooth surface structure and is therefore clearly discernible from the crenulated neighbouring dorsal tubercles. Live and preserved specimens do not differ in the extension of the keel and its structure.

Sole structure. The outermost edge or seam of the sole is separated from the dorsum by a longitudinal fold, the peripodial tubercle, which begins left and right of the mouth-flaps and runs posterior around the body. The peripodial tubercle together with the peripodial groove clearly separate the seam of the sole at its outermost posterior end, where the sole is rounded and not pointed. In the central field of the sole, many V-shaped transverse wrinkles exist, which are invisible in animal crawling on a pane of glass but are well visible in preserved specimens.

Mucus. The mucus lacks any pigmentation on body, mantle and sole and is extremely sticky. When irritated, some of the animals produced defensive mucus of white to yellowish greenish colour on dorsum, flanks, and mantle, but this could only rarely be observed.

Measurements. lw ($n = 56$): 1.5–6 g, \emptyset 3 g; tl ($n = 56$): 52–92 mm, \emptyset 69 mm; ml ($n = 50$): 18–33 mm, \emptyset 23 mm; sw ($n = 47$): 5–10 mm, \emptyset 7.3 mm. Ratio of tl/ml ranges from ca. 52/18 mm to ca. 92/33 mm; \emptyset ml is 1/3 of tl.

Genital organs. Atrium very short and tubular; penis short, with a distal bulb harbouring the penial papilla and a second bulb consisting of the papilla basis marking the boundary to the epiphallus, interior penial walls simple; penis papilla ornamented, apex of papilla with a row of curved crests encircling the complete papilla giving it a flower like appearance (Fig. 3C, F); penis retractor muscle inserting at the epiphallus/penis boundary; epiphallus externally with smooth surface, consistent in diameter, reaching up to 4 times the length of the penis.

Vagina twice the length of the penis, separated from the atrium by a sphincter; accessory glands entering close to the boundary of atrium and vagina; accessory glands digitiform or sac-like, either beige, brown or bright rusty red coloured; vaginal lumen with elongated, waved folds pointing towards the oviduct and the pedunculus of the bursa copulatrix; pedunculus somewhat longer than the vesicle; vesicle may be pointed or rounded.

Spermatophore. A spermatophore was found in a single specimen, broken into three parts (NMBE 571414, Ticino, Orselina, 14 February 2020). One part still stuck in the lumen of the genital pore of the slug, length 0.2 cm; it is completely covered with simple spines (Fig. 3H). The other two parts were found embedded in the vesicle

in a white, fibrous mass; digestion had already started. The smaller part is 0.35 cm long, curved and covered with undivided and, further on, bifurcated spines laterally. The largest part of the spermatophore is ~ 0.9 cm long and curled (visualized in Fig. 3I, J). Its outer surface is covered on the entire length with bifurcated spines. This is the first record of the spermatophore of this species.

Distribution. Our own distribution records are mainly limited to Switzerland, France, northern Italy, and the Republic of San Marino. The species itself is frequently recorded from the western alpine arc, but also from a wide range in Great Britain, Ireland, The Netherlands, Belgium, Luxemburg, France, Germany, Austria, Poland, Czech Republic, Slovakia, and Hungary (Wiktor 1987; Gavetti et al. 2008; Rowson 2017). Reports for Romania are likely misidentifications with *T. kusceri*. Old reports for Bulgaria are shown to be wrong identifications of the very common *T. kusceri* (pers. obs.).

Habitat. This species is confined to beech forests on limestone talus.

Remarks. As original name of this species, Wiktor (1987) referenced a “*Limax marginatus rusticus* Millet, 1843”, which is wrong. In his text, Millet states “Je l’ai rencontrée au nord de l’Anjou, à la Bouillant, commune de la Chapelle-Hullin, ainsi qu’à Thorigné, etc.”. These localities can be found in the larger surrounding north of Angers, Region Pays de la Loire, Département Maine-et-Loire, thus we consider this area the “type area” of *L. rusticus*. A neotype should be selected from one of the mentioned places to unambiguously fix the use of this name.

When it comes to morphology Wiktor (1987) mentioned 18–19 tr, which is higher than most of our counts, but still in the range of our data. Comparing the exterior of living and preserved specimens with the description by Wiktor (1987: 286) and Rowson et al (2014b), many differences were found. No specimens of generally “white or white creamy” pigmentation, nor those of “pinkish or violetish” hues could be recorded by us in Switzerland and bordering areas. Most specimens investigated are explicitly darker than described by Wiktor (1987) and Rowson et al (2014b) indicating a much higher intraspecific variability of the species in other areas of distribution. Colour morphs exclude each other’s following the geographical pattern as described above. In Wiktor (1987: figs 196, 197), the pneumostome is positioned on the left side of the body, which most probably is an error or a sinistral specimen.

Regarding the genital anatomy we found genetically identified *T. rustica* (NMBE 564708, NMBE 568978), which show a very similar anatomy to *T. kusceri* with a long (in one specimen) coiled epiphallus and in both a round bursa copulatrix (Fig. 3E, F). For the coiled epiphallus it might be a sexually active specimen, very probably after the ejection of the spermatophore. Even though the characters of *T. rustica* and *T. kusceri* seem to meet, the two species can be distinguished by their habitat. *Tandonia kusceri* usually is found in disturbed, synanthropic habitats, whereas *T. rustica* is usually found in untouched more natural woodland habitats.

Wiktor (1973) and Likharev and Wiktor (1980) report a long stem of the penial papilla, an observation we could not reproduce. Later, Wiktor (1987) reported a slightly reduced length, but even this reduction does not fit to our results. In all our dissected

specimen, we had a bulky papilla tightly attached to the constriction of the epiphallus and therefore without a stem.

Gerhardt (1940) observed the copulation behaviour of the species in his laboratory; however, he did not illustrate the spermatophore. He observed the first copulation on 17 November 1938 followed by two copulations on the 4 December 1938. His specimens were collected near Porto d'Ischia, Isola d'Ischia, Italy. It remains unclear whether these specimens were *T. rustica*; later research on the island yielded no specimens of this species. In case Gerhardt's determination was correct, the data of the observed copulation and those from our collection with the spermatophore found on 14 February 2020 indicate that this species probably mates during the winter season, a period where malacological research activity is rather low.

***Tandonia nigra* (C. Pfeiffer, 1894)**

Figs 4, 5, 7C, D, 8

Amalia nigra C. Pfeiffer, 1894, *Nachrichtsblatt der Deutschen Malakozoologischen Gesellschaft*, 26: 68 [Gipfel des Mte. Generoso (1695 m.)].

Type specimen. *Holotype* SMF 107558.

Differential diagnosis. Torus with spikes inside the vagina, epiphallus with a field of nodes on the surface; for other character states, refer to the paragraph under *T. rustica*.

Description. Colouration. The animals at the type locality are dark blackish brown coloured with the dorsum almost black (Figs 4, 8B, C). In lower altitudes of the mountain, animals were dark grey (Fig. 8A) to almost white in colour, with the mantle and dorsum finely blotched (Fig. 8D, E). Two animals also had a light greyish cream ground colouration, one with darker small grey blotches all over the body (Fig. 8F).

The mantle generally matches the dorsal colour. For the topotypic specimen, dots at the edges of the mantle are lacking. However, in light colour morphs, the mantle appears slightly darker than the dorsum because of the accumulated dots and blotches. In many of these specimens the highest density is along the sinus groove.

For the topotypical colour morph the flanks are pigmented as the dorsum, but with a narrow, paler greyish stripe just above the edge of the sole with little blackish grey dots and stripes. This also refers to the flanks below the edge of mantle. In the light colour morphs, the dorsum and flanks are covered by very fine dark dots on the top of the tubercles (not along the groove lines; not a reticulation). This pigmentation pattern is found from the dorsum down to the edge of the sole. Some larger, irregularly scattered black spots more posterior on dorsum and flanks add to this remarkable colouration. The flanks below the mantle lack this dark pigmentation and are of a paler colour than the rest.

Neck and head in the dark colour morphs are black as are the ommatophores. The ommatophores are somewhat translucent, and the black ommatophoran retractor can be seen through the integument. No black dotting on the ommatophores is visible.

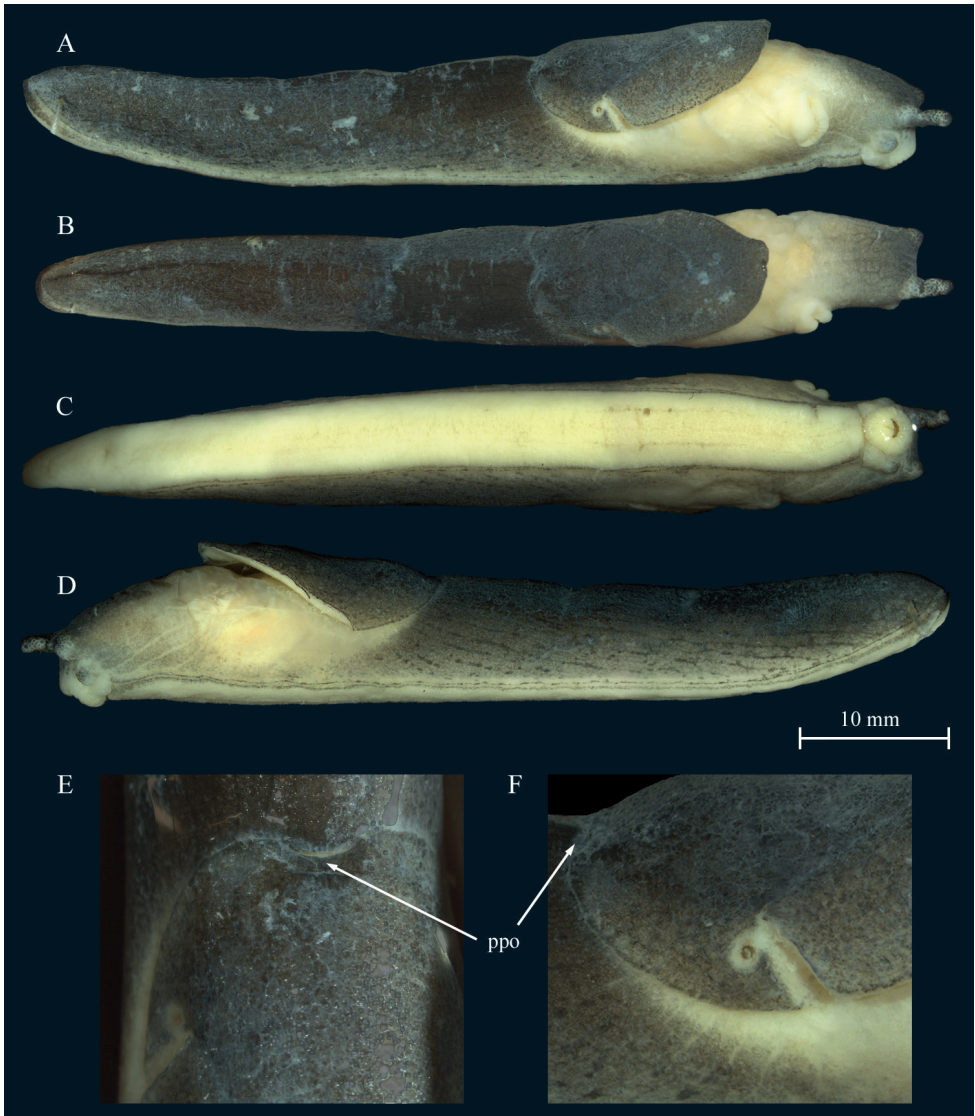


Figure 4. *Tandonia nigra*. **A–F** sequenced topotype NMBE 569047, Monte Generoso, Rovio, Calvagnone, 1.650 m alt **A** lateral view right **B** dorsal view **C** ventral view **D** lateral view left **E** dorsal view showing the postpallial pocket organ (indicated with arrows) **F** lateral right view of mantle with pneumostome. Abbreviation: ppo = postpallial pocket organ.

The tentacles are black. In the light colour morphs, the head, neck and the ommatophores are always darker if compared to the body colour.

The keel is of the same colour as the body and thus difficult to see in a crawling animal.

The sole is uniformly creamy yellowish grey in all specimens. In one topotypic specimen, the posterior ends of the lateral sole fields are pigmented with dark grey

dots. In two other specimens, the seam of the sole is pale grey with irregularly dispersed, small black dots.

Mantle structures. The pneumostome is positioned on the right side, at ca. $\frac{3}{4}$ of mantle length, well posteriorly of the middle of the mantle, surrounded by a narrow and almost invisible ring-like structure (Fig. 4F). The visibility of surface structures in living animals strongly depends on the age of the specimen, its condition, and the general air humidity when it is observed. The surface of mantle, besides the sinus groove, can be totally smooth (high temperature/humidity and high production of mucus) or very finely crenulated, or a stage between; the sinus groove is completely visible, often accentuated by a dark pigmentation, reaching almost the end of the posterior mantle edge. The slit of the pneumostome runs anteriorly to at least the dorsal edge of pneumostome. The posterior margin of the mantle is not tightly attached to the integument. The posterior free mantle flap covers the anterior integument-tubercles (Fig. 4A) as well as the slit-like transverse openings of the postpallial pocket organ (Fig. 4E). The posterior mantle edge is markedly indented (curved).

Postpallial pocket organ. As in *Tandonia rustica*.

Integument structures. The number of tr of integument, from the slit of pneumostome to the keel does not vary much ($n = 3$; the topotypes only); from tr 15–17). The surface texture and the width of tubercles in live specimens vary depending on their position on the body. The tr do not appear to be strongly divided in several compartments, only few compartments exist. The tr are all finely crenulated, but also can appear to be totally smooth. In all specimens, the keel extends from the posterior margin of the mantle to the end of the dorsum and is entirely smooth. It is not erected, but evenly rounded, sometimes almost flat and not exposed over the dorsal tr.

Sole structure. As in *Tandonia rustica*.

Measurements. lw ($n = 3$): 1.35–2.5 g, \emptyset 1.85 g; tl ($n = 2$): 46 mm and 70 mm; ml ($n = 2$): 17 mm and 22 mm; sw ($n = 2$): 4.5 mm and 5 mm.

Ratio of tl/ml ranges from ca. 46/17 mm to 70/22 mm; \emptyset ml being a little more than $\frac{1}{3}$ of tl.

Mucus. The mucus is transparent on body, mantle and sole, and sticky. So far, no coloured defensive mucus was observed.

Genital organs. Atrium short; penis tubular, constricted in the middle; interior penial wall with a prominent transversely oriented fold; distal to the fold a simple penis papilla (Fig. 5B, C); papilla base slightly swollen; penis and epiphallus equal in length and diameter, divided by a constriction, where penis retractor muscle inserts; epiphallus surface with nodular structures primarily on its proximal end.

Vagina shorter than penis; accessory glands entering distally on vagina, close to pedunculus and oviduct, formed by a broad truncus with bundles of tubuli attached; the vaginal walls richly covered with folds forming a zig zag pattern; a prominent torus with a row of acute conical spikes running through the vagina from atrium almost reaching the branching point of the pedunculus of the bursa copulatrix (Fig. 5D, E); pedunculus shorter than vesicle; vesicle elongated, rounded at the tip; oviduct slim and long.

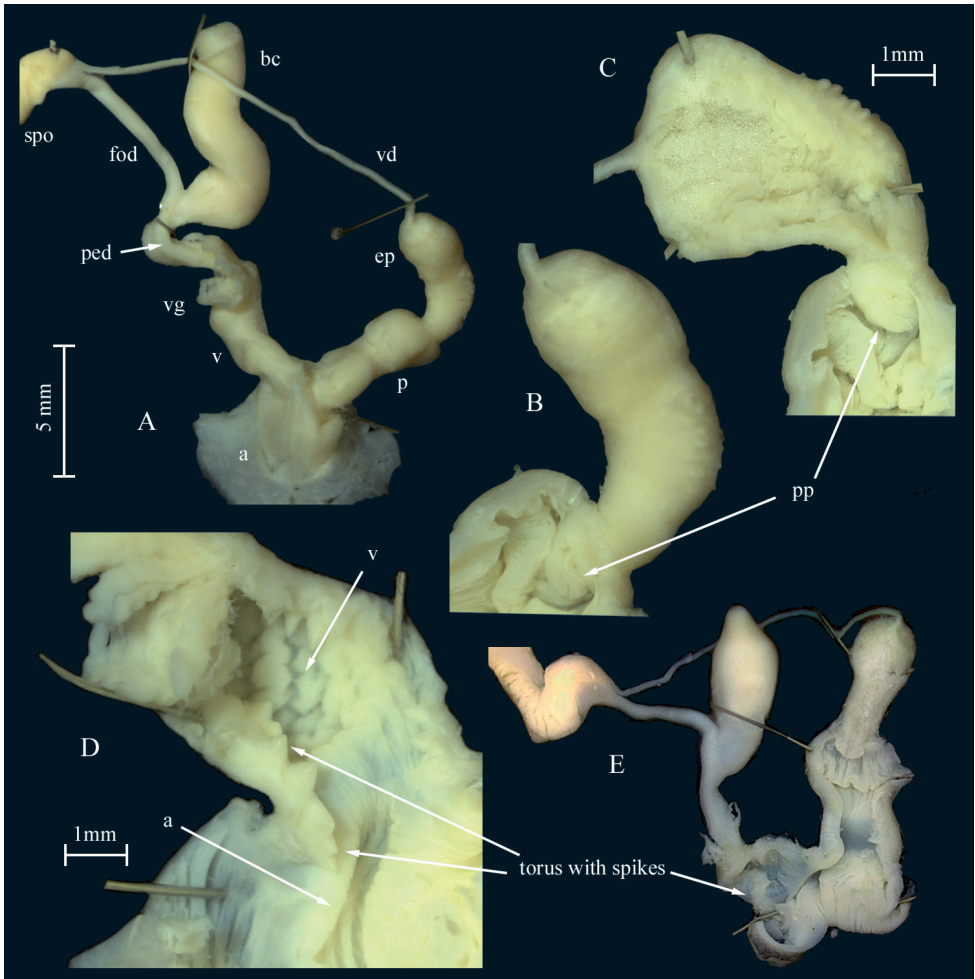


Figure 5. *Tandonia nigra*. **A–D** sequenced topotype NMBE 569047, genital organs **A** situs of genitalia **B** penis with epiphallus showing the granulation on the epiphallial surface and the penis papilla **C** epiphallus opened to show the transparent globuli **D** vagina opened showing the torus with the row of spikes **E** sequenced specimen NMBE 568980, situs of genitalia. Abbreviations: a = atrium; bc = bursa copulatrix; ep = epiphallus; fod = free oviduct; p = penis; ped = pedunculus; pp = penial papilla; spo = spermo-viduct; v = vagina; vd = vas deferens; vg = vaginal gland.

Spermatophore. No spermatophore found in our specimens. It was described and figured by Regteren Altena (1953: fig. 7).

Distribution. *Tandonia nigra* is a rarely found species in Switzerland, and all locally constricted to the Sottoceneri, which is the southern part of the Canton of Ticino, including the districts Lugano and Mendrisio. Our series is very small ($n = 9$). All specimens are from Canton Ticino, from a very restricted area around the Monte Generoso only, including the type locality ($n = 3$). For more information refer to chapters Remarks and Discussion.

Habitat. In the summit region of Monte Generoso, *T. nigra* lives in crevice-rich limestone rocks, which are sparsely vegetated. Under dry weather conditions *T. nigra* is rarely found active on the surface, it is hidden in rock crevices, at least during the day. In the summit region, only very dark-coloured animals have been observed so far. In lower altitudes, *T. nigra* is so far recorded in semi-natural deciduous forests. These are various mixed deciduous forests with beech, hop hornbeam, lime, field maple, ash, hazel, common whitebeam, and manna ash (i.e., southern alpine toothwort beech forest, *Cardamino-Fagetum cyclametosum*, hop hornbeam forest, *Orno-Ostryon*). All habitats are relatively shady. At higher altitudes, these forests are relatively dry, at lower altitudes they tend to be fresh to moist. For the snails, retreat sites with a certain soil cover and air humidity are important. In autumn 2021, however, two animals could be observed crawling during the day in relatively high humidity on a crack-rich, largely dry retaining wall. The first wall was on a mortared garden retaining wall on a natural road, the other on a dry stone wall along a road. Both walls are situated in semi-shade and are only exposed to sunlight for a few hours a day. In the forest, *T. nigra* is found under stones, amongst fallen leaves, in rock crevices and on dead wood. During several hikes in the summit region, only single animals were observed in humid conditions and during sunrise.

So far, all records in Switzerland originate from areas with a good calcium supply. The altitudinal range of its habitats spans from 435 m near Rovio to the highest point at 1700 m.

Life history. There are almost no observations on the biology of the species published. *Tandonia nigra* feeds on fallen leaves, but possibly also on lichens and detritus. Mating behaviour and reproduction mode are not yet described. A specimen with spermatophore was collected on 30 July 1948 (Regteren Altena 1953). We conclude that the copulation season for *T. nigra* is in July.

Remarks. The author of this species is Karl Ludwig Pfeiffer (1874–1952), who usually published under the name Karl L. Pfeiffer = K. L. Pfeiffer (Zilch 1972).

The most remarkable new finding is the presence of several/additional colour morphs in *T. nigra*. Pfeiffer's (1894) sketchy description of the "small and slim" single specimen (most probably a juvenile) he had collected in autumn 1893, is rather uninformative. Nonetheless, he described a few interesting details concerning the colouration: "almost entirely deep black, only towards the sole somewhat lighter, with two longitudinal black lines leaving a very fine yellow line between". The "very fine yellow line" describes the peripodial groove, the first black line a stripe (peripodial fold) just above the yellow line, the second black line must be the edge of the sole. In our topotypes ($n = 3$) such a fine yellow line was missing in two specimens, while in the other one the line was creamy white. The extremely fine black lines are in fact not visible by the bare eye only. Pfeiffer found "the keel as black as the dorsum and mantle". Wiktor (1987) mentioned that "Pfeiffer thought it can be a melanistic form of *T. rustica*", but Pfeiffer (1894) did not mention *T. rustica* at all. Wiktor described the colouration based on a single topotypic specimen (Rijksmuseum Leiden no. 988), which also had been examined by Regteren Altena in 1953. This specimen was differing in some respects from the original description by Pfeiffer: "Mantle at first sight uniformly black,

in fact at its edges very dense black dots on dirty creamy ground, visible however only in magnification”. The differences in these descriptions already indicated that for this species some intraspecific variation can be expected.

Our recent research on the new additional colour morphs of *T. nigra* at the lower altitudes of Mt. Generoso at Mendrisio, Val Cürta (PM), and from the surrounding of Rovio (pers. comm. K. Lassauer 2020) has confirmed this impression. These pale creamy specimens were first thought to belong to a different, potentially new species, but our genetic assessment evidenced that these are just colour morphs of *T. nigra*. The penis papilla in some pale colour morphs was less fleshy and bulgy than the topotypic adult specimens. The difference in the penis papilla of some lighter colour morphs might be due to their subadult stage. Concerning the anatomy, the nodular structure on the epiphallus has been visible in fully adult but also in subadult specimens. In some cases, the lumen of the epiphallus was filled with transparent, tiny globuli (Fig. 5C) of unknown function.

In each of the Swiss specimens examined, the posterior end of mantle is markedly indented, as it was already described by Pfeiffer (1894). Pfeiffer (1894) found nine tr on both sides of the body. Most probably he counted the number of tr between keel and the edge of the sole, i.e., at mid of the dorsum downwards to the edge of the sole. Wiktor (1987) reported 13 tr from the single specimen examined by him. This result also does not compare to our counts in the topotypes. The tr can also be totally smooth as already reported by Pfeiffer (1894). The high number of tr will always allow differentiating *T. nigra* from *T. budapestensis*, but not necessarily from juvenile *T. rustica* if not taking pigmentation into account. Concluding, the main intraspecific variability can be found in the body pigmentation as well as in the number of tr on the body. Given the few specimens investigated so far, essentially more research is required to cover all variants in this species.

For a rather long period, *T. nigra*, was thought to constitute an endemic species for Switzerland, or it was omitted as a member of the Swiss Fauna (Forcart 1942). Quite recently, Rähle (1997) identified a population of a small black *Tandonia* species from Valle Brembilla, Bergamo, Italy (coll. SMNS) as *T. nigra*. Forcart (1959) identified a sample (NMB 06166a) from Austria, north Tirol as *Milax simrothi* Hesse 1923, which subsequently was corrected by Wiktor (1987) to *T. nigra*. We received a specimen identified by G. Nardi as *T. nigra* from Italy, Laxolo, Valle Brembilla, Bergamo (NMBE 561307), which is almost identical with Rähle’s locality. As a result, Nardi (2017) shaped the distribution area of *T. nigra* over a rather wide range in northern Italy. We tried to re-assess the identity of these specimens.

Unfortunately, it was impossible to extract DNA from the specimen from Laxolo (NMBE 561307), and the preservation state of the animal was poor. As a result, there is no genetic evidence that this is the same species as *T. nigra*. It shares some details with the topotypic Swiss specimens, particularly the presence of the penial papilla, the vaginal torus with the spiked papillae, and the epiphallial node field. However, Rähle (1997) found major differences in the genital organs: He did not find a penial papilla (large and well developed in our specimens), and the accessory glands in his specimen

were restricted to some unbranched tubes situated around the distal end of the vagina (large, branched bundles of tubuli in our specimens). This is astonishing as both specimens originate from the same locality. Revision of the Austrian sample (NMB 06166a) failed because of its bad preservation status.

Since its description, eight malacologists (CSCF mapserver, May 2022) have recorded this species from the summit of Mt. Generoso. New sites were found by two malacologists from 2005–2021. Given the doubts in identification of the non-Swiss populations, the question whether this is an endemic species for Switzerland or not is not finally answered.

***Tandonia budapestensis* (Hazay, 1880)**

Figs 6, 7E, F

Amalia budapestensis Hazay, 1880, Malakozoologische Blätter, Neue Folge. 3: 37, pl. 1, fig. 1 [Budapest, Festungsberg im königlichen Garten].

Type specimens. Not researched and not mentioned by Wiktor (1987); probably lost.

Diagnosis. Sole with a dark central field; for other character states, refer to the paragraph under *T. rustica*.

Description. Colouration. Living Swiss specimens ($n = 10$) show a dark rusty-brown to dark chocolate-brown colour on dorsum and flanks to the fringe of the sole. The flanks below the mantle are somewhat paler dark brown grey. Dorsum and flanks, if not unicolourous, may show small black spots and stripes concentrated along the tubercle groves. This can be observed only under magnification and in good light.

The mantle sometimes can be darker than the dorsum because of many black dots and irregular black marbling.

The ommatophores are almost black-brown, but sometimes little translucent in good light, so the black ommatophoran retractor can be seen through the integument. The tentacles are of the same colour.

The colour of the keel ranges from dark brown to rusty orange in its full length.

The sole is grey to dark blackish grey, with the central field sometimes being almost black. In all three sole fields, many black, irregularly jagged spots (chromatophores?) exist, which can be seen only under magnification.

Mantle structures. The pneumostome is positioned on the right side of the body at 2/3 of mantle length, well posteriorly of the middle of the mantle.

Postpallial pocket organ. As in *Tandonia rustica*.

Integument structures. The number of tr on the integument, counted from the slit of pneumostome to the keel ($n = 7$; tr 9/10-tr 12, \emptyset tr 10/11). The low number of tr allows in almost all cases to differentiate *T. budapestensis* from small and dark *T. rustica*. Wiktor (1987) found 9–11 tr, which fits to the variation we found in Swiss specimens. The surface texture and the width of tubercles in live specimens vary somewhat depending on their position on the body. The tr are all more or less finely crenulated.

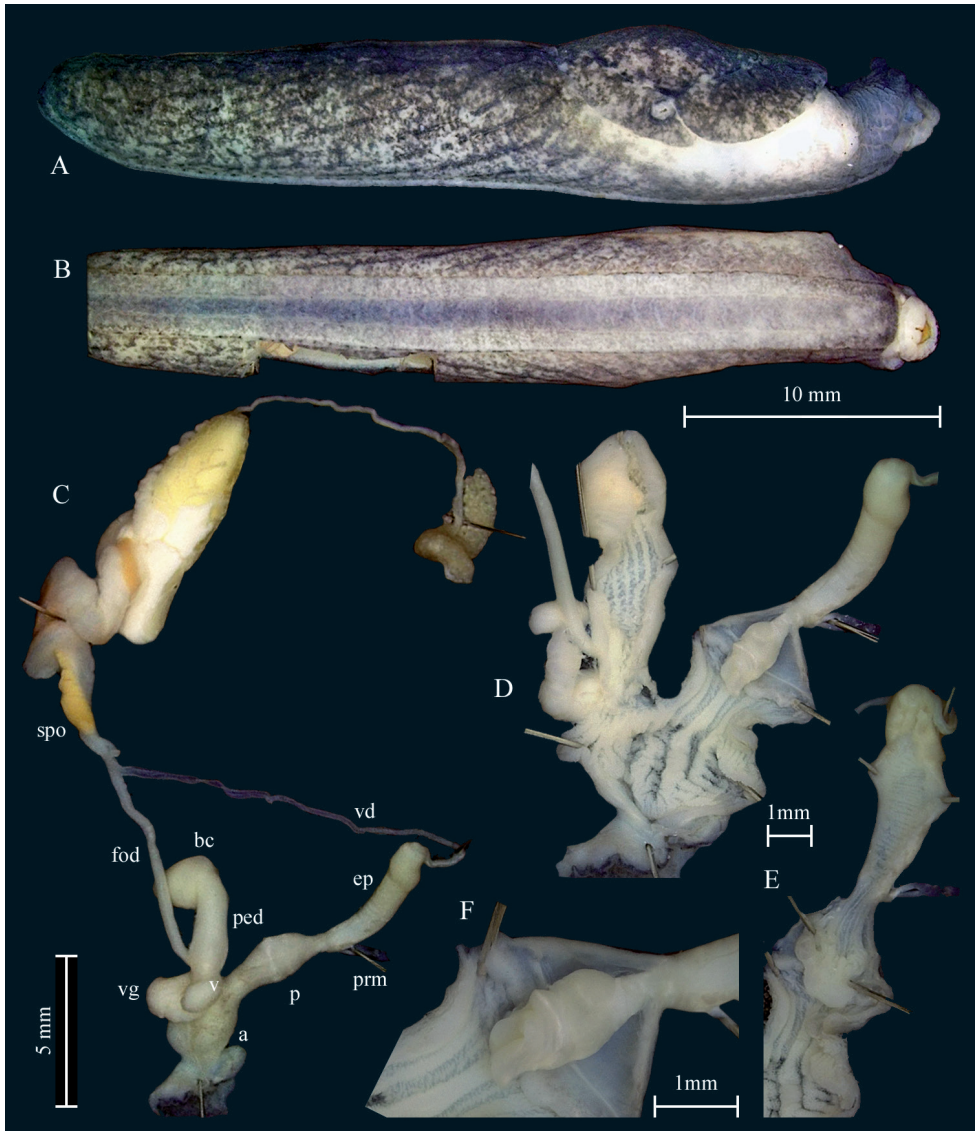


Figure 6. *Tandonia budapestensis*. Sequenced specimen NMBE 564562, Zurich, Wollishofen. **A** lateral right view **B** ventral view **C** situs of genitalia **D** distal genitalia opened to show inner structures **E** opened penis papilla and epiphallus **F** penial papilla. Abbreviations: a = atrium; bc = bursa copulatrix; ep = epiphallus; fod = free oviduct; p = penis; ped = pedunculus; prm = penis retractor muscle; spo = spermoviduct; v = vagina; vd = vas deferens; vg = vaginal gland.

Caused by the low number of tr, they are comparatively wide and obviously wider than in *T. rustica*. All tr are divided in several compartments.

In all specimens, the keel extends from the posterior margin of the mantle to the end of the dorsum. It is not projecting but evenly rounded, sometimes almost flat and not much exposed over the dorsal tr. It is entirely smooth.



Figure 7. Living specimens of *Tandonia*. **A, B** *Tandonia rustica* **A** sequenced specimen NMBE 568974, Wartau, Trübbach **B** sequenced specimen NMBE 568973, Rovio, Sovaglia **C, D** *Tandonia rustica* (two mottled specimens) meeting a pale colour morph specimen of *Tandonia nigra*, Val Cürta, Mt. Generoso **E, F** *Tandonia budapestensis* **E** NMBE 571881, Roggwil, **F** NMBE 571882, Meggen.

Sole structure. The sole structure is similar as in *Tandonia rustica*, but the colouration is not uniform and has a dark central field.

Measurements. lw ($n = 8$): 0.4–1.28 g; \emptyset 0.78 g; tl ($n = 8$): 24.6–62 mm, \emptyset 40 mm; ml ($n = 8$): 7–19 mm, \emptyset 12 mm; sw ($n = 8$): 2.5–6 mm, \emptyset 3.7 mm.

Ratio of tl/ml ranges from 24/7 mm to ca. 62/19 mm; \emptyset ml is little more than 1/3 of tl.

Mucus. The mucus lacks any pigmentation on body, mantle and sole, but is extremely sticky. In a few cases mucus of little pale-orange colour may occur in Swiss specimens.

Genital organs. Atrium wide, spherical shaped; atrium wall covered with folds; penis bulged in the centre; penial walls with long folds ending at muscular ring; penis papilla large, simple oval fold around the opening; papilla basis long, distally shrinking in diameter; penis/epiphallus boundary marked with constriction, where penis retractor muscle inserts; epiphallus matching penis in length; epiphallus surface smooth with apical part kinked.

The vagina is extremely short, separated from the atrium by a muscular ring; accessory glands sac-like attached at centre of the vagina; vaginal walls simple; pedunculus of bursa copulatrix large in diameter, longish vesicle; pedunculus wall with longitudinal internal folds showing a zig zag pattern; oviduct slim and long.

Spermatophore. The spermatophore was described and illustrated by Wiktor (1987: figs 114, 115).

Distribution. *Tandonia budapestensis* is an introduced species and not commonly found in Switzerland. Our series are small ($n = 10$), and all originate from Cantons Bern, Lucerne, and Zurich. It is rather strictly nocturnal, but occasionally occurs under very wet weather conditions also during the day (pers. obs.). It is a quite inconspicuous slug, and thus only rarely found. The relatively few records at CSCF hardly reflect the state of occurrence in the country, and it is assumed that the species is widely overlooked by Swiss malacologists. It is apparently a lowland species and has not yet reached higher altitudes. This coincides with observations on this species in Bulgaria.

Habitat. All Swiss specimen were exclusively found in urban areas (anthropogenic habitats) in house gardens, along an old city wall, and close to a small brook with trees and shrubs. The population along the old city wall of Lucerne was checked several times over the years and seems to be stable.

Remarks. We found some Bulgarian specimens ranging from unicoloured yellow to almost completely black. Such colour morphs might be expected in the future in Switzerland, too.

Milax Gray, 1855

Diagnostic features. Atrial accessory glands present, atrium with internal stimulator (Wiktor 1987).

Milax gagates (Draparnaud, 1801)

Limax gagates Draparnaud, 1801, Tableau des mollusques terrestres et fluviatiles de la France: 100 [presumably near Montpellier fide Wiktor 1987: 202].

Type specimens. Not investigated and probably do not exist; not mentioned by Wiktor (1987).

Swiss specimens examined. NMBE 510286, Bern, Vechigen, in a garden, July 1970, leg. M. Wüthrich; other record: NMBE 561736, Jura, Porrentruy, in a garden, August 1985, leg. Rüetschi (specimen dried up).

Description. Colouration. Wiktor (1987) describes *M. gagates* as uniformly greyish to blackish, except for the flanks being lighter and always lacking spots. However, our specimen from Vechigen has a beige basic colouration with grey-brown blurred dots covering the mantle and dorsal part of the slug. On the flanks, mainly the longitudinal tubercles are coloured by small brown dots, which results in a rather striped than reticulated appearance (Fig. 9A, B).

The mantle has the same colouration as the dorsum. Above the pneumostome, along the horseshoe-shaped sinus groove, is a prominent grey band.

The neck and head have a darker colouration compared to the body and are uniformly grey coloured without dots.

The keel is also beige, but lighter coloured compared to the rest of the body.

According to Wiktor (1987), the sole varies from grey to blackish, with darker lateral zones and lighter central zone. In the Swiss specimen, the sole shows the same colour as the body, but small, brown-grey dots are spread over the whole sole with a strong accumulation in the central zone. Thus, it seems that the lateral zones are lighter if compared to the central one (see Fig. 9C).

Mantle structure. The pneumostome is positioned slightly posteriorly to the centre of the mantle. The sinus groove is well visible in this preserved specimen.

Postpallial pocket organ. As described in *T. rustica*.

Integument structure. The tr are not countable, most likely because of the preservation of the specimen. The tubercles are large, similar to *T. budapestensis*, and not small as in *T. nigra* and *T. rustica*.

The keel is elevated over the neighbouring tubercles only close to the mantle, and flattens towards the posterior end.

Sole structure. The sole structure is like in the described *Tandonia* species (see *T. rustica*), but instead of a uniform colouration, the sole is lighter on the lateral zones and more pigmented on the central zone.

Measurements. The measurements were done on the preserved specimen NMBE 510286. tl = 30.8 mm; sw = 4.1 mm; ml = 9.8 mm. This results in a ml/tl ratio of $\sim 1/3$.

Genital organs. Atrium short, spherical; accessory atrial glands are attached centrally to the atrium with several coiled tubules (Fig. 9E, arrow); inside the atrium, a short, pointed but flat stimulator (Fig. 9F, arrow) existing; penis rather long with a constriction in the middle; distal bulb containing penial papilla; penis retractor muscle attached at penis-epiphallus boundary; epiphallus tubular, widened distally; vas deferens entering asymmetrically on epiphallus.

Vagina shorter than penis; pedunculus broad and equal in length to vesicle; vesicle wider than pedunculus, spherical; female oviduct slender and long.

Spermatophore. The spermatophore was illustrated and described by Wiktor (1987: fig. 72).

Distribution. This species is widespread in the western Palearctic, in Portugal and parts of Spain, France, United Kingdom, etc. (see Wiktor 1987: map 3). Many of the existing populations are considered to be introductions; the original distribution remains unknown. Meanwhile, the species reached an almost global distribution.



Figure 8. Colour variations of *Tandonia nigra*. **A** greyish morph from Rovio, waterfall at Botto, NMBE 568980 **B, C** toptype from summit area; NMBE 569047 **D** Mendrisio, Val Cürta, NMBE 570972 **E** Capolago, Val Cürta, NMBE 570971 **F** Rovio, Sasso Piatto, NMBE 570974.

Remarks. The specimen from Vechigen is provisionally identified as *M. gagates*. The single animal depicted in Fig. 9 shows the general anatomical character states of this species; however, in our animal, the penis is considerably longer than in the specimen illustrated by Wiktor (1987: fig. 68). A comparison with all other *Milax* species yields no match; the only species, which might be present in the area is *M. nigricans*. This species differs by having a short epiphallus, and long tubules connecting the atrial glands with the atrium. Another potentially reliable distinctive character state can be found in the atrial stimulator: With only a few spines in *M. gagates*, and with lots of spines in *M. nigricans* (see Wiktor 1987; Hutchinson and Reise 2013). However, the stimulator

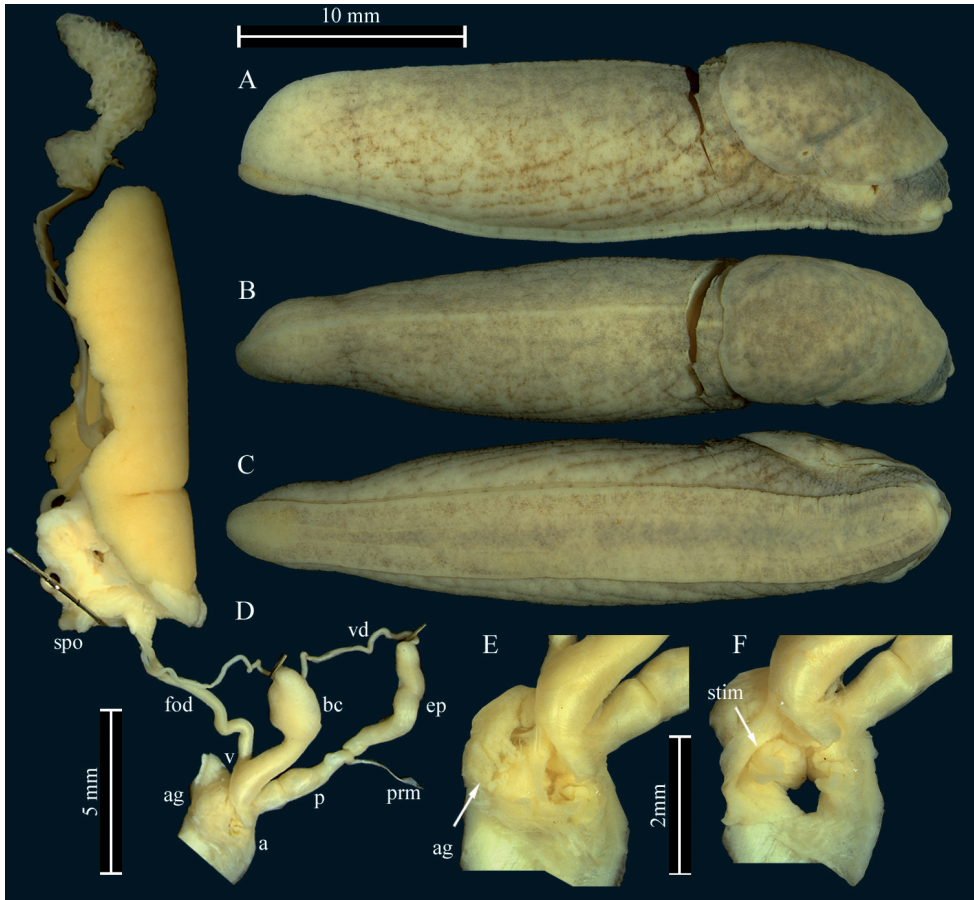


Figure 9. Anatomy of *Milax gagates*. **A–F** NMBE 510286 **A** lateral view right **B** dorsal view **C** ventral view **D** situs of genitalia **E** accessory atrial glands attached with coiled tubules on atrium **F** stimulator inside the atrium. Abbreviations: a = atrium; ag = atrial gland; bc = bursa copulatrix; ep = epiphallus; fod = free oviduct; p = penis; ped = pedunculus; prm = penis retractor muscle; spo = spermoviduct; stim = stimulator; v = vagina; vd = vas deferens.

in our specimen was completely reduced and no detailed structures were discernible. Unfortunately, no DNA could be extracted from the rather old specimen from Vechigen.

The very small specimen from Porrentruy was not only completely dried up and completely bleached but turned out to be a young juvenile without any sign of a genital pore. In fact, juvenile specimens cannot be determined on species level from exterior characters, when genital anatomy is not developed. For this reason, we suggest considering this record as *Milax* sp. rather than *M. gagates*.

Finally, there is a specimen housed in the collection of the Muséum d'histoire naturelle de la Ville de Genève, which had been identified as *M. gagates* (MHNG-MOLL-138933, Geneva, November 1968). The specimen was already dissected prior to our investigation and damaged. The investigation of its genital organs yielded no definite result on its specific identity; it certainly is a species from the Milacidae.

Discussion

In this study we discuss four species of Milacidae recorded from Switzerland. Three are widely distributed in Europe like *T. rustica*, *M. gagates*, and *T. budapestensis*, while *T. nigra* is considered to be a small range endemic species for the Central Alps. Regardless, the group is badly underreported in Switzerland, and some of the information provided here is new to science (e.g., finding the first spermatophore for *T. rustica*). Usually, the descriptive details provided here are taken from Swiss specimens investigated by the authors; hence, other colour morphs of the respective species may occur elsewhere. A general character analysis embracing specimens from the entire distribution area of a species must be postponed.

Comparing the anatomical character states between *T. rustica* and *T. kusceri*, some discrepancies can be found between our results and those of other authors (Wiktor 1987; Korábek et al. 2016; Turóci et al. 2020) who claim that *T. rustica* is characterised by a pointed vesicle of the bursa copulatrix and a straight epiphallus threefold the length of the penis (Wiktor 1987: 288). In contrast, *T. kusceri* is considered to have a rounded vesicle and a heavily coiled epiphallus 5–6 times the length of the penis (Wiktor 1987: 259). Our sequenced specimens (Fig. 3) unambiguously cluster with all *T. rustica* samples from alpine areas of Switzerland, France, and Italy. Our Fig. 3A–C displays the classical *rustica* conditions in the morphology of its genital organs. This is contrasted by a specimen from Goldswil (NMBE 564708), which resembles the *kusceri* conditions. These observations raise the question of the reliability of such character states, which ideally should be based on investigation of topotypic specimens. Is the shape of the vesicle a fixed trait? Functioning as a receptor of the spermatophore one can expect that the form of this organ may vary according to 1) the maturity of the individual, 2) the form of the spermatophore, and 3) the actual sexual stage the animal reached at the moment of preservation (pre-mating, spermatophore intact inside the vesicle, or spermatophore already digested). Therefore, some variability of the shape should be conceded. For example, Turóci et al. (2020: fig. 7) illustrated a rounded elongate vesicle for *T. rustica*, and the claimed “apically pointed” trait is not visible for us. Obviously, the shape of the vesicle undergoes some variation, and thus cannot strictly be used for species discrimination. It remains to be investigated on how many specimens Wiktor based his firm statement for *T. rustica* (his specimen(s) came from Poland); a comparative study based on several animals from several populations should be performed to clarify this. Similarly, the shape of the epiphallus may depend on the maturity status of the specimen. A coiled epiphallus may be found shortly after the ejection of the (often coiled) spermatophore, and probably explains the differences in our specimens depicted in Fig. 3A–C and Fig. 3E–G. Wiktor (1987: 243, fig. 132) provided a sketched drawing of the penis-epiphallus boundary, where he found two papillae in a row for *T. cristata* (Kaleniczenko, 1851). Here, the penial retractor attaches at a constriction of the “epiphallus”, which is internally accompanied by a first papilla, and then followed by a second papilla pointing into the atrium. Browsing through his anatomical drawings and the position of the papillae, it seems as if some species have a “twin” system, and others have only a distal papilla. Our Fig. 3G shows

exactly such a twin case in a specimen, which genetically turns out to be *T. rustica* (see arrows). Obviously, we are far from understanding the morphological details of the male copulatory system of *Tandonia* species, so many more traits await detection and evaluation as to whether they are suitable for species recognition or not. Finally, it must be noted that our use of the names *T. rustica* and *T. kusceri* needs to be corroborated by inclusion of topotypic specimens in future studies. There are no genetic nor detailed morphological data available for animals from Angers (*T. rustica*) nor from Niş (*T. kusceri*), which is prerequisite for the correct application of the names to a biological entity. The fact is that there are two genetically separated clades as proven by Korábek et al. (2016) and Turóci et al. (2020), and which could be confirmed by our study.

We could show that the small and dark specimens of *Tandonia* species from the Alps east of the Monte Generoso, from Monte Baldo, the Bergamasque Alps, north Tirol in Austria, and elsewhere are still in need of a very careful revision. Here, a genetic investigation is pending targeting at taxa such as *T. simrothi* (Hesse, 1923), eventually also *T. baldensis* (Simroth, 1910). Wiktor and Milani (1995) and Nardi (2011) recorded *T. simrothi* from the area of Brescia and further east and northeast, indicating the potential confusion of these species with *T. nigra* as both species are small in size and usually overall darkly pigmented. The newly described brighter colour morphs in *T. nigra* indicate that such a survey should not be restricted to “small and black species”. Otherwise, we potentially overlook existing biodiversity. In fact, Switzerland still has a high responsibility for *T. nigra*, which may be a true endemic of the Mt. Generoso area.

Tandonia budapestensis, an invasive species, was first recorded for Switzerland in 1934 (Forcart 1942; NMB no. 4580a & b). This species can easily be detected and identified. It is known as a potential pest species, but fortunately, records for Switzerland are extremely rare. This might be explained by a bias because malacologists rarely investigate synanthropic sites, and thus the recording has a methodologically biased gap. We consider this species as still significantly underreported for Switzerland, and probably also elsewhere.

Milax gagates is also considered an introduced species and was recorded only three times for Switzerland. Each time, only a single specimen was found. Probably this species is introduced to Switzerland from time to time (Rüetschi et al. 2012); however, as far as we know, no permanent population has been established in the country so far.

For future research we recommend following the preservation procedures for slugs as described above. Perfect samples should be accompanied by photographs taken in the field. Juvenile and subadult specimens should be raised until reaching maturity prior to preservation.

Barcoding and species delimitation such as ASAP can be helpful tools when it comes to the question of species identification, abundance, and distribution. In this study, we found that many characters which were thought to be diagnostic for a specific species have been shown to be intraspecific variables. In some cases, this variability of one or more characters may even overlap with other species, as it is the case for the anatomy of *T. rustica* and *T. kusceri*. In this specific case, a genetic study can help to distinguish those species.

Acknowledgements

We are grateful to Marianne Cornu, Zurich, and Monika Cornu, St. Gallen, for support during field collections; to Regula Cornu, Chur for long lasting and ongoing support in field collection and consistent support and assistance in the laboratory and collection; Katja Lassauer, and Christian Roggenmoser, Lucerne for their collections and ongoing enthusiasm. Special thanks go to Guisepe Nardi for his support with specimens from Italy, and Ira Richling, Stuttgart, for information on a specimen of *T. nigra* dissected by the late W. Rähle. Further we thank Emmanuel Tardy (MHNG) and Urs Wüest (NMB) for the loan of the respective Milacidae species. René Heim supported the project financially and provided most specimens from his private collection, which are now housed at NMBE. This study was partly supported by the Bundesamt für Umwelt Bern (BAFU) under the contract No. 110010344/8T30/00.5147.PZ/0006.

References

- Altekar G, Dwarkadas S, Huelsenbeck J, Ronquist F (2004) Parallel Metropolis coupled Markov chain Monte Carlo for Bayesian phylogenetic inference. *Bioinformatics* 20(3): 407–415. <https://doi.org/10.1093/bioinformatics/btg427>
- Bank RA, Neubert E (2017) MolluscaBase. Checklist of the land and freshwater Gastropoda of Europe, 170 pp. www.molluscabase.org [accessed on 28 December 2021]
- Beck H (1837–1838) Index molluscorum praesentis aevi musei principis augustissimi Christiani Frederici, 124 pp. [Hafniae [Copenhagen]. Pp. 1–100 [1837]; 101–124 [1838]; Appendix: 1–8 [June 1837]].
- Draparnaud J-P-R (1801) Tableau des Mollusques de la France. Montpellier [Renaud]; Paris [Bossange, Masson et Besson], 116 pp.
- Férussac A (1819–1832) Tome deuxième, première partie Histoire naturelle générale et particulière des mollusques terrestres et fluviatiles tant des espèces que l'on trouve aujourd'hui vivantes, que des dépouilles fossiles de celles qui n'existent plus; classés d'après les caractères essentiels que présentent ces animaux et leurs coquilles. J.-B. Baillière, Paris, Livraison 1: [3 pp. = dedication], i-xvi (= Préface) (6-III-1819); livr. 2: 1–16 (5-VI-1819); 3: 17–56 (10-VII-1819); 4: 57–72 (18-IX-1819); 5: 73–96 (4-XII-1819); 7: 97–128 (17-VI-1820); 9: xvi pp. (= Explication des planches du premier volume) (6-IV-1821); 17: v pp. (= Explication des planches supplémentaires et de celles qui ne font pas partie du premier volume) (2-XI-1822); 19/21: 96a-z, 96alpha-lambda (27-IX-1823); 22/27: iv pp. (= Explication des planches des livraisons XXII, XXIII, XXIV, XXV, XXVI et XXVII) (4-VIII-1832) pp. [Note: continued by G.-P. Deshayes (1839–1851)]
- Folmer O, Black M, Hoeh W, Lutz R, Vrijenhoek R (1994) DNA primers for amplification of mitochondrial cytochrome c oxidase subunit I from diverse metazoan invertebrates. *Molecular Marine Biology and Biotechnology* 3(5): 294–299.
- Forcart L (1942) Die Verbreitung der Limaciden und Milaciden in der Schweiz. *Archiv für Molluskenkunde* 74(2/3): 114–119.
- Forcart L (1959) *Milax simrothi* Hesse in Nordtirol. *Archiv für Molluskenkunde* 88(4/6): 195.

- Gavetti E, Birindelli S, Bodon M, Manganelli G (2008) Molluschi terrestri e d'acqua dolce della Valle di Susa. Monografie Museo Regionale di Scienze Naturali 44: 1–273.
- Gerhardt U (1940) Neue biologische Nacktschneckenstudien. -. Zeitschrift für Morphologie und Ökologie der Tiere 36(4): 557–580. <https://doi.org/10.1007/BF01260999>
- Guindon S, Dufayard J-F, Lefort V, Anisimova M, Hordijk W, Gascuel O (2010) New Algorithms and Methods to Estimate Maximum-Likelihood Phylogenies: Assessing the Performance of PhyML 3.0. Systematic Biology 59(3): 307–321. <https://doi.org/10.1093/sysbio/syq010>
- Hazay J (1880) Die Molluskenfauna von Budapest. Malakozoologische Blätter, Neue Folge 3: 1–69, 160–183, Taf. 1–9.
- Hesse P (1923) Kritische Fragmente XXV-XXXVII. Archiv für Molluskenkunde 55: 193–198.
- Huelsenbeck JP, Ronquist F (2001) MRBAYES: Bayesian inference of phylogenetic trees. Bioinformatics 17(8): 754–755. <https://doi.org/10.1093/bioinformatics/17.8.754>
- Hutchinson JMC, Reise H (2013) A persisting population of an introduced slug, *Milax nigricans*, in Dunkirk, France. Mitteilungen der deutschen malakozoologischen Gesellschaft 89: 35–38.
- Kaleniczenko J (1851) Description d'un nouveau genre de Limaces de la Russie méridionale. Bulletin de la Société Impériale des Naturalistes de Moscou 24: 215–228.
- Kimura M (1980) A simple method for estimating evolutionary rates of base substitutions through comparative studies of nucleotide sequences. Journal of Molecular Evolution 16(2): 111–120. <https://doi.org/10.1007/BF01731581>
- Korábek O, Čejka T, Juříčková L (2016) *Tandonia kusceri* (Pulmonata: Milacidae), a slug new for Slovakia. Malacologica Bohemoslovaca 15: 3–8. <https://doi.org/10.5817/MaB2016-15-3>
- Liberto F, Giglio S, Colomba MS, Sparacio I (2012) New and little known land snails from Sicily (Mollusca Gastropoda). Biodiversity Journal 3: 201–228.
- Likharev IM, Wiktor A (1980) Slizni fauny SSSR i sopredelnykh stran (Gastropoda terrestria nuda) [The Fauna of Slugs of the USSR and adjacent Countries (Gastropoda terrestria nuda)]. In: Fauna SSSR, Molljuskii III, 5 [= N.S. 122] Leningrad (Nauka), 1–437. [pl. 1]
- Millet PA (1843) Description de plusieurs espèces nouvelles de Mollusques de France. Magasin de Zoologie ser. 2, 5: 1–4. [pls 63–64]
- Nardi G (2011) Nuove segnalazioni di limacce per la malacofauna bresciana (Gastropoda: Arionidae, Milacidae, Limacidae, Agriolimacidae). Bolletino Malacologico 47: 9–22.
- Nardi G (2017) *Tandonia nigra*. The IUCN Red List of Threatened Species 2017: e.T21385A85575878.
- Pfeiffer C (1894) Kleine Reiseergebnisse. Nachrichtenblatt der Deutschen Malakozoologischen Gesellschaft 26: 68–71.
- Puillandre N, Brouillet S, Achaz G (2021) ASAP: Assemble species by automatic partitioning. Molecular Ecology Resources 21(2): 609–620. <https://doi.org/10.1111/1755-0998.13281>
- Rähle W (1997) Ein Fund von *Tandonia nigra* (Carl Pfeiffer 1894) in den Bergamasker Alpen (Alpi Orobiche, Norditalien) (Gastropoda: Pulmonata: Milacidae). Mitteilungen der deutschen malakozoologischen Gesellschaft 60: 5–10.
- Regteren Altena CO van (1953) Notes sur les limaces. 1. A propos de *Milax niger* (Carl Pfeiffer, 1894). Basteria 17(3): 43–48.
- Ronquist F, Huelsenbeck JP (2003) MrBayes 3: Bayesian phylogenetic inference under mixed models. Bioinformatics 19(12): 1572–1574. <https://doi.org/10.1093/bioinformatics/btg180>

- Rowson B (2017) *Tandonia rustica*. The IUCN Red List of Threatened Species 2017: e.T171361A1325060.
- Rowson B, Anderson R, Turner JA, Symondson WOC (2014a) The slugs of Britain and Ireland: Undetected and undescribed species increase a well-studied, economically important fauna by more than 20%. PLoS ONE 9(4): e91907. <https://doi.org/10.1371/journal.pone.0091907>
- Rowson B, Turner JA, Anderson R, Symondson WOC (2014b) The Slugs of Britain and Ireland: Identification, understanding and control. Field Studies Council, Telford, UK, 136 pp. [ISBN 978-1-908819-13-0]
- Rüetschi J, Stucki P, Müller P, Vicentini H, Claude F (2012) 1216 Rote Liste Weichtiere (Schnecken und Muscheln). Gefährdete Arten der Schweiz Stand 2010. BAFU & CSCF, Bern, 148 pp.
- Schindelin J, Arganda-Carreras I, Frise E, Kaynig V, Longair M, Pietzsch T, Preibisch S, Rueden C, Saalfeld S, Schmid B, Tinevez J-Y, White DJ, Hartenstein V, Eliceiri K, Tomancak P, Cardona A (2012) Fiji: An open-source platform for biological-image analysis. Nature Methods 9(7): 676–682. <https://doi.org/10.1038/nmeth.2019>
- Schneppat UE, Georgiev DG, Dedov IK, Wondrak G, Knechtle F (2011) *Tandonia totevi* (Wiktor, 1975) (Pulmonata: Milacidae) in Bulgaria and north eastern Greece. Folia Malacologica 19(4): 225–248. <https://doi.org/10.2478/v10125-011-0025-4>
- Stamatakis A (2006) RAxML-VI-HPC: Maximum likelihood-based phylogenetic analyses with thousands of taxa and mixed models. Bioinformatics 22(21): 2688–2690. <https://doi.org/10.1093/bioinformatics/btl446>
- Trifinopoulos J, Nguyen L-T, von Haeseler A, Minh BQ (2016) W-IQ-TREE: A fast online phylogenetic tool for maximum likelihood analysis. Nucleic Acids Research 44(W1): W232–W235. <https://doi.org/10.1093/nar/gkw256>
- Turóci Á, Fehér Z, Krízsik V, Páll-Gergely B (2020) Two new alien slugs, *Krynickyllus melanocephalus* Kaleniczenko, 1851 and *Tandonia kusceri* (H. Wagner, 1931), are already widespread in Hungary. Acta Zoologica Academiae Scientiarum Hungaricae 66(3): 265–282. <https://doi.org/10.17109/AZH.66.3.265.2020>
- Wagner H (1931) Diagnosen neuer Limaciden aus dem Naturhistorischen Museum in Wien. Zoologischer Anzeiger 95: 194–202.
- Wiktor A (1973) Die Nachtschnecken Polens. Monografie Fauny Polski 1: 1–182. [40 pls]
- Wiktor A (1975) New slug species (Pulmonata: Milacidae and Limacidae) from the Balkan Peninsula. Annales Zoologici 33: 77–91.
- Wiktor A (1987) Milacidae (Gastropoda, Pulmonata) - systematic monograph. Annales Zoologici 41: 153–319.
- Wiktor A, Milani N (1995) Contribution to the knowledge of two scarcely known Alpine slugs, *Tandonia simrothi* (Hesse, 1923) and *Deroceras planarioides* (Simroth, 1910) (Gastropoda: Pulmonata: Milacidae et Agriolimacidae). Malakologische Abhandlungen Staatliches Museum für Tierkunde Dresden 17: 151–160.
- Zilch A (1972) Zur Geschichte der deutschen Malakozoologie, IX. Zur Konchylien-Sammlung von K. L. Pfeiffer. Mitteilungen der Deutschen Malakozoologischen Gesellschaft 22: 324–326.

Supplementary material I

Table S1

Authors: Vivianne M. Schallenberg, René Heim, Ulrich E. Schneppat, Peter Müller, Jörg Rüetschi, Eike Neubert

Data type: excel file

Explanation note: Genetically and/or morphologically investigated specimens.

Copyright notice: This dataset is made available under the Open Database License (<http://opendatacommons.org/licenses/odbl/1.0/>). The Open Database License (ODbL) is a license agreement intended to allow users to freely share, modify, and use this Dataset while maintaining this same freedom for others, provided that the original source and author(s) are credited.

Link: <https://doi.org/10.3897/zookeys.1116.82762.suppl1>

